Designing Reactive Distillation Processes with Improved Efficiency

economy, exergy loss and responsiveness

Designing Reactive Distillation Processes with Improved Efficiency

economy, exergy loss and responsiveness

Proefschrift

ter verkrijging van de graad van doctor
aan de Technische Universiteit Delft,
op gezag van de Rector Magnificus prof. dr. ir. J. T. Fokkema,
voorzitter van het College voor Promoties,
in het openbaar te verdedigen op maandag 14 november 2005 om 13:00 uur
door

Cristhian Paúl ALMEIDA-RIVERA

Ingeniero Químico
(Escuela Politécnica Nacional, Ecuador)
Scheikundig ingenieur
geboren te Quito, Ecuador

Dit proefschrift is goedgekeurd door de promotor:
Prof. ir. J. Grievink

Samenstelling promotiecommissie:

Rector Magnificus	Voorzitter
Prof. ir. J. Grievink	Technische Universiteit Delft, promotor
Prof. dr. G. Frens	Technische Universiteit Delft
Prof. ir. G. J. Harmsen	Technische Universiteit Delft/Shell Chemicals
Prof. dr. F. Kapteijn	Technische Universiteit Delft
Prof. dr. ir. H. van den Berg	Twente Universiteit
dr. A. C. Dimian	Universiteit van Amsterdam
Prof. dr. ir. A. I. Stankiewicz	Technische Universiteit Delft/DSM
Prof. dr. ir. P. J. Jansens	Technische Universiteit Delft (reserve lid)

Published by Cristhian P. Almeida-Rivera, Delft

ISBN 9-090200-37-1 / 9789090200378

Keywords: process systems engineering, reactive distillation, conceptual process design, multiechelon design approach, life-span inspired design methodology, residue curve mapping, multilevel approach, dynamic optimization, singularity theory, dynamic simulation, non-equilibrium thermodynamics, exergy, responsiveness

Printed by PrintPartners Ipskamp in the Netherlands

Dedicated to
my daughter Lucía and
my wife Paty

Contents

Contents

List of Figures

List of Figures

List of Tables

List of Tables

List of Explanatory Notes

"With the possible exception of the equator, everything begins somewhere."

Peter Robert Fleming, writer (1907-1971)

1 Introduction

The conceptual design of reactive distillation processes is investigated in this PhD thesis. The motivation for this research came from taking a sustainable life-span perspective on conceptual design, in which economics and potential losses over the process life span were taken into consideration. The technological and scientific scenarios used in this research are described in this chapter. First, the drivers for change in the current dynamic environment of chemical processing industry are identified. Then the reactive distillation processing is introduced. The generalities of this process together with its technical challenges in design and operation are addressed. The scientific setting of conceptual design in process systems engineering, with an emphasis on the key challenges in the design of reactive distillation is addressed. The scope of this thesis is then introduced, together with a statement of the scientific questions dealt with in the thesis. The chapter is concluded with a thesis outline and a concise description of the scientific novelty of this research.

1.1 A Changing Environment for the Chemical Process Industry

The chemical process industry is subject to a rapidly changing environment, characterized by slim profit margins and fierce competitiveness. Rapid changes are not exclusively found in the demands of society for new, high quality, safe, clean and environmentally benign products (Herder, 1999), they can be found in the dynamics of business operations, which include global operations, competition and strategic alliances mapping, among others.

Being able to operate at reduced costs with increasingly shorter time-to-market times is the common denominator of successful companies, however, attaining this performance level is not a straightforward or trivial issue. Success is dependant on coping effectively with dynamic environments and short process development and design times. Taking into account life span considerations of products and processes is becoming essential for development and production activities. Special attention needs to be paid the potential losses of resources over the process life span. Since these resources differ in nature, for example they can be capital, raw materials, labor, energy. Implementing this life-span aspect is a challenge for the chemical industry. Moreover, manufacturing excellence practice needs to be pursued, with a stress on the paramount importance of stretching profit margins, while maintaining safety procedures. In addition, society is increasingly demanding sustainable processes and products. It is no longer innovative to say that the chemical industry needs to take into account biospheres sustainability. Closely related to sustainable development, risk minimization, another process aspect, must also be taken into consideration. In today's world, processes and products must be safe for their complete life span. Major incidents such as Flixborough (1974) with 28 casualties and Bhopal (1984) with 4000+ casualties may irreversibly affect society's perception of the chemical industry and should be a thing of the past.

Addressing all these process aspects, given the underlying aim of coping effectively with the dynamic environment of short process development and design times, has resulted in a wide set of technical responses. Examples of these responses include advanced process control strategies and real-time optimization. Special attention is paid to the synthesis of novel unit operations that can integrate several functions and units to give substantial increases in process and plant efficiency (Grossman and Westerberg, 2000; Stankiewicz and Moulijn, 2002). These operations are conventionally referred to as hybrid and intensified units, respectively and are characterized by reduced costs and process complexity. Reactive distillation is an example of such an operation.

1.2 Reactive Distillation Potential

1.2.1 Main Features and Successful Stories

Reactive distillation is a hybrid operation that combines two of the key tasks in chemical engineering, reaction and separation. The first patents for this processing route appeared in the 1920s, *cf.* Backhaus (1921*a*,*b*,*c*), but little was done with it before the 1980s Malone and Doherty (2000); Agreda and Partin (1984) when reactive distillation gained increasing attention as an alternative process that could be used instead of the conventional sequence chemical reaction-distillation.

The RD synthesis of methyl acetate by Eastman Chemicals is considered to be the textbook example of a task integration-based process synthesis (Stankiewicz and Moulijn, 2002; Stankiewicz, 2003, 2001; Li and Kraslawski, 2004; Siirola, 1996*a*) (see figure 1.1).

Using this example one can qualitatively assess the inherent value of this processing strategy. The process costs are substantially reduced ($\sim$ 80%) by the elimination of units and the possibility of heat integration. Using task integration-based synthesis the conventional process, consisting of 11 different steps and involving 28 major pieces of

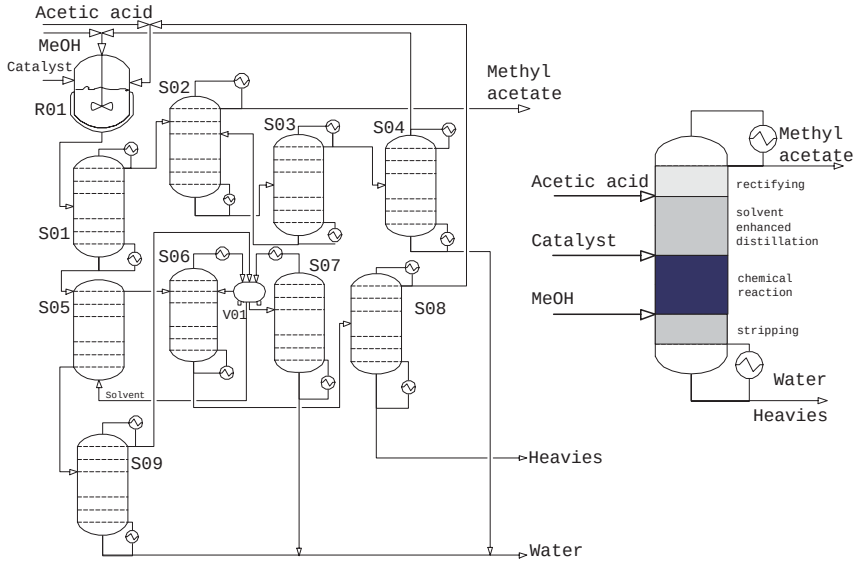

Figure 1.1. Schematic representation of the conventional process for the synthesis of methyl acetate (left) and the highly task-integrated RD unit (right). **Legend**: R01: reactor; S01: splitter; S02: extractive distillation; S03: solvent recovery; S04: MeOH recovery; S05: extractor; S06: azeotropic column; S07,S09: flash columns; S08: color column; V01: decanter

equipment, is effectively replaced by a highly task-integrated RD unit.

The last decades have seen a significant increase in the number of experimentally research studies dealing with RD applications. For example, Doherty and Malone (2001) (see table 10.5) state more than 60 RD systems have been studied, with the synthesis of methyl *t*-butyl ether (MTBE) and ethyl *t*-butyl ether (ETBE) gaining considerable attention. Taking an industrial perspective Stankiewicz (2003) lists the following processes as potential candidates for RD technology: (*i*) decomposition of ethers to high purity olefins; (*ii*) dimerization; (*iii*) alkylation of aromatics and aliphatics (*e.g.* ethylbenzene from ethylene and benzene, cumene from propylene and benzene); (*iv*) hydroisomerizations; (*v*) hydrolyses; (*vi*) dehydrations of ethers to alcohols; (*vii*) oxidative dehydrogenations; (*viii*) carbonylations (*e.g.* *n*-butanol from propylene and syngas); and (*ix*) C_1 chemistry reactions (*e.g.* methylal from formaldehyde and methanol). Recently, in the frame of fine chemicals technology Omota *et al.* (2001, 2003) propose an innovative RD process for the esterification reaction of fatty acids. The feasibility of this process is firstly suggested using a smart combination of thermodynamic analysis and computer simulation (Omota *et al.*, 2003). Secondly, the proposed design methodology is successfully applied to a representative esterification reaction in the kinetic regime (Omota *et al.*, 2001).

Process development, design and operation of RD processes are highly complex tasks. The potential benefits of this intensified process come with significant complexity in process development and design. The nonlinear coupling of reactions, transport phenomena and phase equilibria can give rise to highly system-dependent features, possibly leading to the presence of reactive azeotropes and/or the occurrence of steady-state multiplicities (*cf.* section §2.9). Furthermore, the number of design decision variables for such an integrated unit is much higher than the overall design degrees of freedom of separate reaction and separation units. As industrial relevance requires that design issues are not separated from the context of process development and plant operations, a life-span perspective was adopted for the research presented in this thesis.

1.2.2 Technical Challenges in the Process Design and Operation of Reactive Distillation

A generalized applicability of RD technology is a key challenge for the process-oriented community. Operational applicability is seen as strategic goal coupled with the development of (conceptual) design methodologies that can be used to support the RD decision making process. Thus, the process systems engineering community is expected to provide tools and supporting methods that can be used to faster develop and better operation of RD processes. Designing chemical process involves the joint consideration of process unit development and design programs (*cf.* section §4.5) and these are key

challenges in RD process design.

A topic that is emerging as a challenge in the RD arena, is that, due to its system-dependency, RD processing is strongly limited by its reduced operation window (P,T). This feasibility domain, which is determined by the overlapping area between feasible reaction and distillation conditions (Schembecker and Tlatlik, 2003), spans a small region of the P-T space. On top of these two an additional window could be imposed by the equipment and material feasibility. In this context and within the development program, the key challenges for the RD community include: (*i*) the introduction of novel and more selective catalysts; (*ii*) the design of more effective and functional packing structures (*e.g.* super X-pack (Stankiewicz, 2003)); and (*iii*) finding new applications. The first two challenges are strongly driven by the need to expand the RD operational window beyond the current bounds for a given application.

1.3 Significance of Conceptual Design in Process Systems Engineering

1.3.1 Scientific Setting of Conceptual Design in Process Systems Engineering

Since its introduction, process systems engineering (PSE) has been used effectively by chemical engineers to assist the development of chemical engineering. In tying science to engineering PSE provides engineers with the systematic design and operation methods, tools that they require to successfully face the challenges of today's chemical-oriented industry (Grossman and Westerberg, 2000).

At the highest level of aggregation and regardless of length scale (*i.e.* from micro-scale to industrial-scale) the field of PSE discipline relies strongly on engineers being able to identify production systems. For the particular case of chemical engineering, a production system is defined as a purposeful sequence of physical, chemical and biological transformations used to implement a certain function (Marquardt, 2004). A production system is characterized by its function, deliberate delimitation of its boundaries within the environment, its internal network structure and its physical behavior and performance. These production systems are used to transform raw materials into product materials characterized by different chemical identities, compositions, morphologies and shapes. From a PSE perspective the most remarkable feature of a system is its ability to be decomposed or aggregated in a goal-oriented manner to generate smaller or larger systems (Frass, 2005). Evidently, the level of scrutiny is very much linked to the trade-off between complexity and transparency.

At a lower level of aggregation a system comprises the above mentioned sequence of transformations or processes. Thus, a process can be regarded as a realization of a

system and is made up of an interacting set of physical, chemical or biological transformations, that are used to bring about changes in the states of matter. These states can be chemical and biological composition, thermodynamic phases, a morphological structure and electrical and magnetic properties.

Going one level down in the aggregation scale gives us the chemical plant. This is no more than the physical chemical process system. It is a man-made system, a chemical plant, in which processes are conducted and controlled to produce valuable products in a sustainable and profitable way. The conceptual process design (CPD) is made at the following level of reduced aggregation. In the remainder of this section particular attention is given to CPD in the context of PSE.

Since its introduction, CPD has been defined in a wide variety of ways. CPD and PSE activities are rooted in the concept of unit operations and the various definitions of CPD are basically process unit-inspired. The definition of CPD given by Douglas (1988) is regarded as the one which extracts the essence of this activity. Thus, CPD is defined as the task of finding the *best* process flowsheet, in terms of selecting the process units and interconnections among these units and estimating the optimum design conditions (Goel, 2004). The *best* process is regarded as the one that allows for an economical, safe and environmental responsible conversion of specific feed stream(s) into specific product(s).

Although this CDP definition might suggest a straight-forward and viable activity, the art of process design is complicated by the nontrivial tasks of (Grievink, 2003): (*i*) identifying and sequencing the physical and chemical tasks; (*ii*) selecting feasible types of unit operations to perform these tasks; (*iii*) finding ranges of operating conditions per unit operation; (*iv*) establishing connectivity between units with respect to mass and energy streams; (*v*) selecting suitable equipment options and dimensioning; and (*vi*) control of process operations.

Moreover, the design activity increases in complexity due to the combinatorial explosion of options. This combination of many degrees of freedom and the constraints of the design space has its origin in one or more of the following: (*i*) there are many ways to select implementations of physical/chemical/biological/information processing tasks in unit operations/controllers; (*ii*) there are many topological options available to connect the unit operations (*i.e.* flowsheet structure), but every logically conceivable connection is physically feasible; (*iii*) there is the freedom to pick the operating conditions over a physical range, while still remaining within the domain in which the tasks can be effectively carried out; (*iv*) there is a range of conceivable operational policies; and (*v*) there is a range of geometric equipment design parameters. The number of possible combinations can easily run into many thousands.

The CPD task is carried out by specifying the state of the feeds and the targets on

the output streams of a system (Doherty and Buzad, 1992; Buzad and Doherty, 1995) and by making complex and emerging decisions. In spite of its inherent complexity, the development of novel CPD trends has lately gained increasing interest from within academia and industry. This phenomenon is reflected in the number of scientific publications focusing on CPD research issues and its applicability in industrial practice (Li and Kraslawski, 2004). For instance, the effective application of CPD practices in industry has lead to large cost savings, up to 60% as reported by Harmsen *et al.* (2000) and the development of intensified and multifunctional units (*e.g.* the well-documented methyl acetate reactive distillation unit as mentioned by Stankiewicz and Moulijn (2002); Harmsen and Chewter (1999); Stankiewicz (2003)).

CPD plays an important role under the umbrella of process development and engineering. As stated by Moulijn *et al.* (2001), process development features a continuous interaction between experimental and design programs, together with carefully monitored cost and planning studies. The conventional course of process development involves several sequential stages: an exploratory stage, a conceptual process design, a preliminary plant flowsheet, miniplant(s) trials, trials at a pilot plant level and design of the production plant on an industrial scale. CPD is used to provide the first and most influential decision-making scenario and it is at this stage that approximately 80% of the combined capital and operational costs of the final production plant are fixed (Meeuse, 2003). Performing individual economic evaluations for all design alternatives is commonly hindered by the large number of possible designs. Therefore, systematic methods, based on process knowledge, expertise and creativity, are required to determine which will be the best design given a pool of thousands of alternatives.

1.3.2 Developments in New Processes and Retrofits

From its introduction the development of CPD trends has been responding to the harmonic satisfaction of specific requirements. In the early stages of CPD development economic considerations were the most predominant issue to be taken into account. Seventy years on, the issues surrounding CPD methodologies have been extended to encompass a wide range of issues involving economics, sustainability and process responsiveness (Almeida-Rivera *et al.*, 2004*b*; Harmsen *et al.*, 2000). Spatial and temporal aspects must be taken into account when designing a process plant. Additionally, the time dimension and loss prevention are of paramount importance if the performance of a chemical plant is to be optimized over its manufacturing life-span. This broad perspective accounts for the use of multiple resources (*e.g.* capital, raw materials and labor) during the design phase and the manufacturing stages. In this context and in view of the need to support the sustainability of the biosphere and human society, the design of sustainable, environmentally benign and highly efficient processes becomes a

major challenge for the PSE community. Identifying and monitoring potential losses in a process, together with their causes are key tasks to be embraced by a CPD approach. Means need to be put in place to minimize losses of mass, energy, run time availability and, subsequently, profit. Poor process controllability and lack of plant responsiveness to market demands are just two issues that need to be considered by CPD engineers as causes of profit loss.

Li and Kraslawski (2004) have recently presented a detailed overview on the developments in CPD, in which they show that the levels of aggregation in CPD (*i.e.* micro-, meso- and macroscales) have gradually been added to the application domain of CPD methodologies. This refocus on the design problem has lead to a wide variety of success stories at all three scale levels and a coming to scientific maturity of the current methodologies.

At the **mesolevel** the research interests have tended towards the synthesis of heat exchange networks, reaction path kinetics and sequencing of multicomponent separation trains (Li and Kraslawski, 2004). A harmonic compromise between economics, environmental and societal issues is the driving force at the CPD **macrolevel**. Under the framework of multiobjective optimization (Clark and Westerberg, 1983), several approaches have been derived to balance better the trade-off between profitability and environmental concerns (Almeida-Rivera *et al.*, 2004*b*; Kim and Smith, 2004; Lim *et al.*, 1999). Complementary to this activity, an extensive list of environmental indicators (*e.g.* environmental performance indicators) has been produced in the last decades (Lim *et al.*, 1999; Kim and Smith, 2004; Li and Kraslawski, 2004). At the CPD **microlevel** the motivating force has been the demand for more efficient processes with respect to equipment volume, energy consumption and waste formation (Stankiewicz and Moulijn, 2002). In this context a breakthrough strategy has emerged: abstraction from the historically equipment-inspired design paradigm to a task-oriented process synthesis. This refocus allows for the possibility of task integration and the design of novel unit operations or microsystems, which integrate several functions/tasks and reduce the cost and complexity of process systems (Grossman and Westerberg, 2000). An intensified unit is normally characterized by drastic improvements, sometimes in an order of magnitude, in production cost, process safety, controllability, time to the market and societal acceptance (Stankiewicz, 2003; Stankiewicz and Moulijn, 2002). Among the proven intensified processes reactive distillation (RD) occupies a place of preference and it is this which is covered in the course of this thesis, coupled with an emphasis on RD conceptual design.

1.3.3 Key Challenges in the Design of Reactive Distillation

Due to its highly complex nature, the RD design task is still a challenge for the PSE community. The following intellectually challenging problems need to be considered by the PSE community (Grossman and Westerberg, 2000): (*i*) design methodologies for sustainable and environmentally benign processes; (*ii*) design methodologies for intensified processes; (*iii*) tighter integration between design and the control of processes; (*iv*) synthesizing plantwide control systems; (*v*) optimal planning and scheduling for new product discovery; (*vi*) planning of process networks; (*vii*) flexible modeling environments; (*viii*) life-cycle modeling; (*ix*) advanced large-scale solving methods; and (*x*) availability of industrial nonsensitive data. An additional PSE specific challenge is to define a widely accepted set of effectiveness criteria that can be used to assess process performance. These criteria should take into account the economic, sustainability and responsiveness/controllability performances of the design alternatives.

1.4 Scope of Research

During the course of this PhD thesis we deal with the design of grassroots reactive distillation processes. At this high level of aggregation, the process design is far more comprehensive than for most of the industrial activities (*e.g.* retrofit, debottlenecking and optimal operation of existing equipment) as it involves a wide range of domain knowledge and augmented (design) degrees of freedom.

Here it becomes necessary to introduce an explanatory caveat regarding the concept of *life span*. From a formal standpoint this term includes all stages through which a production system or activity passes during its lifetime (Schneider and Marquardt, 2002). From a product perspective, for instance, the life span describes one, the life of the product from *cradle to grave* (Meeuse, 2003; Korevaar, 2004). Two, each process step along the cradle-to-grave path is characterized by an inventory of the energy, materials used and wastes released to the environment and an assessment of the potential environmental impact of those emissions (Jimenez-Gonzalez *et al.*, 2000, 2004). If our viewpoint is the process rather than the product life span, we can foresee a sequence of stages including need identification, research and development, process design, plant operation and retrofit/demolition. As covering **all** these process stages in a unique methodology is a highly demanding task, we limited our research to the sustainability aspects that are exclusively under the control of the design and operational phases. Thus, in our scope of life span we do not consider any sustainability issue related to feed-stock selection, for example, (re-)use of catalyst, (re-)use of solvent, among others.

A life-span inspired design methodology (LiSp-IDM) is suggested as the first attempt towards a design program strategy. Although more refined and detailed approaches

are expected to be introduced in the future, their underlying framework will probably remain unchanged. In this framework, a life-span perspective is adopted, accounting for the responsible use of multiple resources in the design and manufacturing stages and a systems' ability to maintain product specifications (*e.g.* compositions and conversion) in a desired range when disturbances occur. In this thesis and for the first time, economic, sustainability and responsiveness/controllability aspects are embedded within a single design approach. The driving force behind this perspective is derived from regarding the design activity as a highly aggregated and large-scale task, in which process unit development and design are jointly contemplated.

All the aforementioned features of the LiSp-IDM are captured in the following definition,

> LiSp-IDM is taken to be a systematic approach that can be used to solve design problems from a life-span perspective. In this context, LiSp-IDM is supported by defining performance criteria that can be used to account for the economic performance, sustainability and responsiveness of the process. Moreover, LiSp-IDM framework allows a designer to combine, in a systematic way, the capabilities and complementary strengths of the available graphical and optimization-based design methodologies. Additionally, this design methodology addresses the steady-state behavior of the conceived unit and a strong emphasis is given to the unit dynamics.

The following set of goal-oriented engineering questions were formulated based in the above definition,

- Question 1. *What benefits can be gained from having a more integrated design methodology?*
- Question 2. *What are the practical constraints that need to be considered from a resources point of view (i.e. time, costs, tools and skill levels), when developing and applying a design methodology in a work process?*
- Question 3. *What are the essential ingredients for such a design methodology?*

Additionally, a set of specific scientific design questions were formulated based on the steps of a generic design cycle,

- Question 4. *What is the domain knowledge required and which new building blocks are needed for process synthesis?*
- Question 5. *What are the (performance) criteria that need to be considered from a life-span perspective when specifying a reactive distillation design problem?*

- Question 6. *What (new) methods and tools are needed for reactive distillation process synthesis, analysis and evaluation?*
- Question 7. *Are there structural differences and significant improvements in designs derived using conventional methodologies from those obtained using an integrated design methodology?*

These questions will be either qualitatively or quantitatively answered during the course of this thesis.

1.5 Outline and Scientific Novelty of the Thesis

This dissertation is divided into several chapters, covering the conceptual design of grass-roots RD processes. The fundamentals, weaknesses and opportunities of RD processing are addressed in chapter 2. A detailed description of the current design methodologies in RD forms the subject of chapter 3. Special attention is paid to the identification of the methodologies' strengths and missing opportunities and a combination of methodology capabilities is used to derive a new multiechelon[†] design approach, which is presented in detail in chapter 4. The essential elements of this design approach are then addressed using the synthesis of methyl-tert butyl ether as tutorial example. Chapter 5 deals with the feasibility analysis of RD processing based on an improved residue curve mapping technique and column sequencing. In chapter 6, the focus is on the synthesis of internal spatial structures, in particular. A multilevel modeling approach and the dynamic optimization of spatial and control structures in RD are introduced. The steady-state and dynamic performance in RD form the subjects of chapter 7. The performance criteria embedded in the proposed RD methodology are covered in chapter 8, in which a life-span perspective is adopted leading to the definition of performance criteria related to economics, thermodynamic efficiency and responsiveness. The interactions between those performance criteria in the design of RD are explored in particular. The information generated in the previous chapters is summarized in chapter 9, where a final evaluation of the integrated design is presented. The chapter is concluded with remarks and recommendations for further research in the RD field.

The scientific novelty of this work is embedded in several areas.

Formulation of an extended design problem. A renewed and more comprehensive design problem in RD is formulated in the wider context of process development and engineering. The nature of the extension is found in the identification of the design

[†]The term *echelon* refers to one stage, among several under common control, in the flow of materials and information, at which items are recorded and/or stored (source: `http://www.pnl.com.au/glossary/cid/32/t/glossary` visited in August 2005).

decision variables and their grouping into three categories: (*i*) those related to physical and operational considerations; (*ii*) those related to spatial issues; and (*iii*) those related to temporal considerations.

Integrated design methodology. An integrated design is presented (*i.e.* LiSp-IDM) based on a detailed analysis of the current design methodologies in RD. As industrial relevance requires that design issues are not separated from the context of process development and plant operations, a life-span perspective was adopted. The framework of this methodology was structured using the *multiechelon approach*, which combines in a systematic way the capabilities and complementary strengths of the available graphical and optimization-based design methodologies. This approach is supported by a decomposition in a hierarchy of imbedded design spaces of increasing refinement. As a design progresses the level of design resolution can be increased, while constraints on the physical feasibility of structures and operating conditions derived from first principles analysis can be propagated to limit the searches in the expanded design space.

Improvement in design tools. The proposed design methodology is supported by improved design tools. Firstly, the residue curve mapping technique is extended to the RD case and systematically applied to reactive mixtures outside conventional composition ranges. This technique is found to be particularly useful for the sequencing of (non-) reactive separation trains. Secondly, the models of the process synthesis building blocks are refined leading to the following sub-improvements: (*i*) a refined modular representation of the building blocks; (*ii*) changes/improvements in the models of the building blocks; and (*iii*) enhancements in synthesis/analysis tools. Regarding the last item, a multilevel modeling approach is introduced with the aim of facilitating the decision-making task in the design of RD spatial structures.

Performance criteria. To account for the process performance from a life-span perspective, criteria related to economic, sustainability and responsiveness aspects are defined and embraced in the proposed design methodology. For the first time the interactions between economic performance, thermodynamic efficiency and responsiveness in RD process design are explored and possible trade-offs are identified. This research suggests that incorporating a sustainability-related objective in the design problem formulation might lead to promising benefits from a life-span perspective. On one hand, exergy losses are accounted for, aiming at their minimization and on the other hand the process responsiveness is positively enhanced.

"The important thing is not to stop questioning. Curiosity has its own reason for existing."

Albert Einstein, scientist and Nobel prize laureate
(1879-1955)

2

Fundamentals of Reactive Distillation

The combination of reaction and separation processes in a single unit has been found to generate several advantages from an economic perspective. However, from a design and operational point of view this hybrid process is far more complex than the individual and conventional chemical reaction - distillation operation. In this chapter a general description of the fundamentals of reactive distillation is presented. A sound understanding and awareness of these issues will enable more intuitive explanations of some of the particular phenomena featured by a RD unit. The starting point of our approach is the systematic description of the physical and chemical phenomena that occur in a RD unit. Relevant combinations of those phenomena are grouped in levels of different aggregation scrutiny (*i.e.* one-stage, multistage, distributed and flowsheet levels). Each level deals with the particularities of the involved phenomena. Moreover, each level is wrapped-up with the identification of the design decision variables that are available to influence or control the phenomena under consideration.

Chapter 2

2.1 Introduction

It is a well-known and accepted fact that complicated interactions between chemical reaction and separation make difficult the design and control of RD columns. These interactions originate primarily from VLL equilibria, VL mass transfer, intra-catalyst diffusion and chemical kinetics. Moreover, they are considered to have a large influence on the design parameters of the unit (*e.g.* size and location of (non)-reactive sections, reflux ratio, feed location and throughput) and to lead to multiple steady states (Chen *et al.*, 2002; Jacobs and Krishna, 1993; Güttinger and Morari, 1999*b*,*a*), complex dynamics (Baur *et al.*, 2000; Taylor and Krishna, 2000) and reactive azeotropy (Doherty and Malone, 2001; Malone and Doherty, 2000).

To provide a clear insight on the physical and chemical phenomena that take place within a RD unit, a systems approach is proposed according to the following classification features,

- spatial scrutiny scale: where the system can be lumped with one-stage, lumped with multistages or distributed. Note that the spatial scales involved in this research are approached from bottom to top. A schematic representation of these scales is given in figure 2.1,
- contact with the surroundings: where the system can be either open or closed,
- equilibrium between the involved phases: where they can be either in equilibrium or non-equilibrium, and
- transient response: where the non-equilibrium system can be regarded as stationary or dynamic.

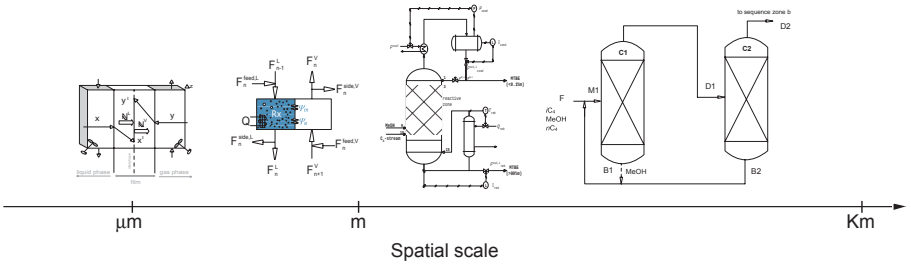

Figure 2.1. Schematic representation of the relevant spatial scales in reactive distillation

These four features can be smartly combined leading to 10 different system instances, as listed in table 2.1. Instances 2, 5 and 8 are not further considered in this explanatory chapter because of their reduced practical interest. As there is no interaction between

the system and surroundings, the closed system will gradually reach equilibrium state due to dynamic relaxation. Furthermore, instances 4, 7 and 10 are closely linked to their associated steady-state situation and are then embedded within instances 3, 6 and 9, respectively.

This analysis results in instances 1 (lumped one-stage, closed and equilibrium), 3 (lumped one-stage, open and non-equilibrium), 6 (lumped multistage, open and non-equilibrium) and 10 (distributed, open and non-equilibrium) for further consideration in the course of this chapter. A first classification of these instances is performed based on their spatial structure, aiming to cover the whole range of physical and chemical phenomena that occur in a RD unit. The following levels are then defined,

Level **A. One-stage level**: where the system is represented by a single lumped stage [embracing instances I_1 and I_3],

Level **B. Multi-stage level**: where the system is represented by a set of interconnected trays [embracing instance I_6], and

Level **C. Distributed level**: where the system is defined in terms of an spatial coordinate [embracing instance I_{10}].

Recalling the engineering and scientific design questions given in chapter 1, in this chapter we address question 4, namely,

- *What is the domain knowledge required and which new building blocks are needed for process synthesis?*

As the nature of this chapter is explanatory, the knowledge presented is borrowed from various scientific sources. Thus, the novelty of this chapter is exclusively given by the systems approach adopted to address the phenomena description. Note that the spatial scales involved in this research are approached from bottom to top.

Table 2.1. Systems instances to be considered for the analysis of physical and chemical processes in a RD unit

Instance	Spatial level	Contact	Phase behavior	Time response
I_1	lumped one-stage	closed	equilibrium	
I_2	lumped one-stage	closed	non-equilibrium	dynamic relaxation
I_3/I_4	lumped one-stage	open	non-equilibrium	steady state/dynamic
I_5	lumped multistage	closed	non-equilibrium	dynamic relaxation
I_6/I_7	lumped multistage	open	non-equilibrium	steady state/dynamic
I_8	distributed	closed	non-equilibrium	dynamic relaxation
I_9/I_{10}	distributed	open	non-equilibrium	steady state/dynamic

2.2 One-stage Level: Physical and Chemical (non-) Equilibrium

Phase equilibrium. For a n_c-component mixture phase equilibrium is determined when the Gibbs free energy G for the overall open system is at a minimum (Biegler *et al.*, 1997),

$$\begin{aligned} \text{Function} \quad &: \quad \min_{n_i^{(j)}, \mu_i^{(j)}} n \times G = \sum_{i=1}^{i=n_c} \sum_{j=1}^{j=n_p} n_i^{(j)} \times \mu_i^{(j)} \\ \text{s.t.} \quad &: \quad \sum_{j=1}^{j=n_p} n_i^{(j)} = n_{i,0} + \sum_{k=1}^{k=n_{rx}} \nu_{i,k} \times \varepsilon_k, \qquad i \in \mathbb{Z}^{n_c} \\ &\quad\;\; n_i^{(j)} \geq 0, \end{aligned} \tag{2.1}$$

where n_i is the total number of moles for component i, $n_i^{(\alpha)}$ is the number of moles of component i in phase (α), n is the total number of moles, n_p is the number of phases in the system, n_{rx} is the number of chemical reactions, ε_k is the extent of reaction k and $\mu_i^{(\alpha)}$ is the chemical potential of component i in phase (α) and given by,

$$\mu_i^{(\alpha)} = G_i^0 + \mathcal{R} \times T \times \ln f_i^{(\alpha)}, \qquad i \in \mathbb{Z}^{n_c}. \tag{2.2}$$

In the previous expression, the fugacity of component i in phase (α), $f_i^{(\alpha)}$, is estimated in terms of the fugacity coefficient and component's concentration in phase (α) (*i.e.* $a_i = \gamma_i \times x_i$).

The necessary condition for an extremum of the minimization problem is given by the equality of chemical potentials across phases and the thermal and mechanical equilibrium,

$$\mu_i^{(j)} = \mu_i^{(k)}, \qquad j,k \in \mathbb{Z}^{n_p}, \tag{2.3}$$

$$T^{(j)} = T^{(k)}, \qquad j,k \in \mathbb{Z}^{n_p}, \tag{2.4}$$

$$P^{(j)} = P^{(k)}, \qquad j,k \in \mathbb{Z}^{n_p}. \tag{2.5}$$

For the particular case of vapor-liquid equilibrium, the necessary conditions results in the well-known expression,

$$y_i \times \Phi_i \times P = x_i \times \gamma_i \times p_i^0, \qquad i \in \mathbb{Z}^{n_c}. \tag{2.6}$$

A detailed description of the thermodynamic model used to derive the VL equilibrium expression 2.6 is presented in appendix B.

Chemical Equilibrium. For a single-phase fluid and open system a fundamental thermodynamic property relation is given by Smith and van Ness (1987),

$$d(n \times G) = (n \times V)dP - (n \times S)dT + \sum_{j=n_c}^{i=1} \mu_i \times dn_i, \tag{2.7}$$

where $dn_i = \nu_i \times d\varepsilon$ denotes the change in mole numbers of component i, ν_i is the stoichiometric coefficient of component i, ε is the extent of reaction and S is the molar entropy of the system.

Knowing that $n \times G$ is a state function, an expression is obtained for the rate of change of the total Gibbs energy of the system with the extent of reaction at constant T and P,

$$\sum_{j=n_c}^{i=1} \nu_i \times \mu_i = \left[\frac{\partial(n \times G)}{\partial \varepsilon}\right]_{T,P}. \tag{2.8}$$

At equilibrium conditions the Gibbs energy expression 2.8 equals to zero and allows one to define the equilibrium state in terms of the measurable temperature-dependent equilibrium constant K_{eq},

$$-\mathcal{R} \times T \times \ln K_{\text{eq}} = \sum_{i=1}^{i=n_c} \nu_i \times G_i^0, \tag{2.9}$$

$$K_{\text{eq}} = \prod_{i=1}^{i=n_c} a_i^{\nu_i}, \tag{2.10}$$

where $\mathcal{R}$ is the universal gas constant, a_i denotes the activity of specie i and the exponent zero represents the standard state. Note that the liquid-phase activity a_i and fugacity are related according to the expression (Malanowski and Anderko, 1992),

$$f_i^L = f_i^0 \times a_i, \tag{2.11}$$

where f_i^0 is the reference state fugacity, which is estimated for pure liquid at equilibrium conditions.

2.3 Multi-stage Level: Combined Effect of Phase and Chemical Equilibrium

For the sake of clarifying the interaction between chemical and phase equilibrium in RD, several concepts need to be introduced. Note, firstly, that the spatial configuration at this level is assumed to allow efficient contact between the phases and in an staged-wise operation.

The concept of *stoichiometric lines* captures the concentration change of a given specie due to chemical reaction (Frey and Stichlmair, 1999*b*).

Let n_{i0} be the number of moles of specie i at time t_0 in a closed system. Chemical reactions proceed according to their extent of reaction ε_j ($j \in \mathbb{Z}^{n_{rx}}$). After chemical equilibrium is reached, the number of moles at anytime is is given by,

$$n_i = n_{i0} + \sum_j \nu_{i,j} \times \varepsilon_j, \qquad i \in \mathbb{Z}^{n_c}, j \in \mathbb{Z}^{n_{rx}}. \tag{2.12}$$

Knowing that the total number of moles in the closed system equals to,

$$n = n_0 + \sum_j \nu_{\text{total},j} \times \varepsilon_j, \qquad j \in \mathbb{Z}^{n_{rx}}, \tag{2.13}$$

it follows that the stoichiometric line is expresses as,

$$x_i = \frac{x_{i_0}(\nu_k - \nu_{\text{total}} \times x_k) + \nu_i(x_k - x_{k_0})}{\nu_k - \nu_{\text{total}} \times x_{k_0}}, \qquad i \in \mathbb{Z}^{n_c}, \tag{2.14}$$

where ν_{total} is the sum of the stoichiometric coefficients ($\nu_{\text{total}} = \sum \nu_i$) and k is a reference component ($k \in \mathbb{Z}^{n_c}$).

Any mixture apart from the chemical reaction equilibrium reacts along these lines to the corresponding equilibrium state (Frey and Stichlmair, 1999*a*). Thus, a family of stoichiometric lines results from the variation of initial components concentration, which intercept at the pole π (figure 2.2), whose concentration is defined as $x_{i\pi} = \nu_i \times \nu_{\text{total}}^{-1}$.

Another term to be introduced is the widespread *distillation line* concept, commonly used to depict phase equilibrium in conventional distillation. According to Frey and Stichlmair (1999*b*) and Westerberg *et al.* (2000), distillation lines correspond to the liquid concentration profile within a column operating at total reflux. It follows from this definition that a distillation line is characterized by sequential steps of phase equilibria and condensation. Thus, the following sequence is adopted for the case of an equilibrium stage model,

$$x_{i1} \xrightarrow{\text{phase equilibrium}} y^*_{i1} \xrightarrow{\text{condensation}} x^*_{i1} \cdot \cdot \tag{2.15}$$

The starting point of this sequence is the reactive mixture x_1 (depicted conventionally on the chemical equilibrium line in figure 2.2). This liquid mixture is in phase equilibrium with the vapor y^*_1, which is totally condensed to x^*_1.

It is relevant to mention that an alternative concept might be used to depict the phase equilibrium: *residue curve* (Fien and Liu, 1994; Westerberg and Wahnschafft, 1996). In contrast to distillation lines, residue curves track the liquid composition in a distillation unit operated at finite reflux. Although for finite columns distillation and residue lines differ slightly, this difference is normally not significant at the first stages of design. Graphically, the tangent of a residue curve at liquid composition $\mathbf{x}$ intercepts the distillation line at the vapor composition $\mathbf{y}$ in phase equilibrium with $\mathbf{x}$ (Fien and Liu, 1994). A more detailed application of residue curve is covered in chapter 5.

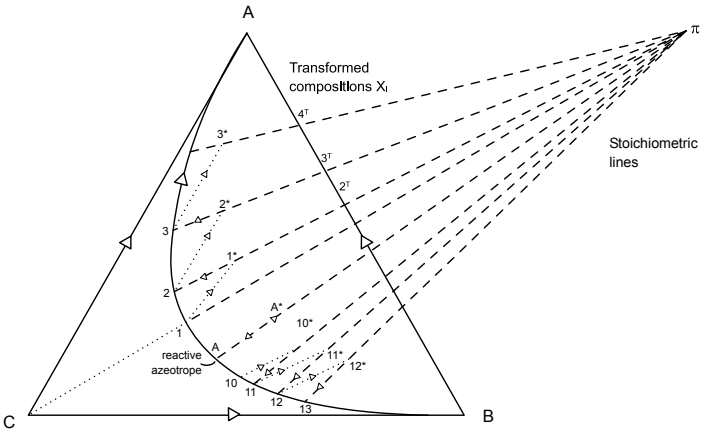

Figure 2.2. Representation of stoichiometric and reactive distillation lines for the reactive system A-B-C undergoing the reaction $A+B \rightleftharpoons C$. **Remark:** π denotes the pole at which stoichiometric lines coincide, $x_{i\pi} = \nu_i/\Sigma\nu_j$. **Legend:** dashed line: stoichiometric line; dotted line: phase-equilibrium line; continuous line: chemical equilibrium line. **System feature:** $T_C^{\text{boil}} > T_B^{\text{boil}} > T_A^{\text{boil}}$. (adapted from Frey and Stichlmair (1999*b*)).

A third concept is introduced when chemical reaction and phase equilibrium phenomena are superimposed in the unit: *reactive distillation lines*. The following sequence of phase equilibrium→chemical reaction steps is adopted for the evolution of reactive distillation lines,

$$x_{i1} \xrightarrow{\text{phase eq.}} y_{i1}^* \xrightarrow{\text{condensation}} x_{i1}^* \xrightarrow{\text{reaction}} x_{i2} \xrightarrow{\text{phase eq.}} y_{i2}^* \xrightarrow{\text{condensation}} x_{i2}^* \cdots \quad (2.16)$$

The starting point of this sequence is the reactive mixture x_1 on the chemical equilibrium line. This liquid mixture is in phase equilibrium with the vapor y_1^*, which is totally condensed to x_1^*. Since this mixture is apart from the chemical equilibrium line, it reacts along the stoichiometric line to the equilibrium composition x_2. As can be seen in figure 2.2, the difference of the slope between the stoichiometric and liquid-vapor equilibrium lines defines the orientation of the reactive distillation lines. This difference in behavior allows one to identify a point, at which both the phase equilibrium and stoichiometric lines are collinear and where liquid concentration remains unchanged. This special point (labelled 'A' in figure 2.2) is conventionally referred to as *reactive azeotrope* and is surveyed in section §2.4.

2.4 Multi-stage Level: Reactive Azeotropy

Unlike its nonreactive counterpart, reactive azeotropes occur in both ideal and nonideal mixtures, limiting the products of a reactive distillation process in the same way that ordinary azeotropy does in a nonreactive distillation operation (Doherty and Buzad, 1992; Harding and Floudas, 2001). In both cases, however, the prediction whether a given mixture will form (reactive) azeotropes and the calculation of their compositions are considered essential steps in the process design task (Harding *et al.*, 1997). Due to the high non-linearity of the thermodynamic models this prediction is not trivial at all and requires an accurate and detailed knowledge of the phase equilibria (expressed by residue or distillation lines), accurate reaction equilibria and the development of specialized computational methods. In addition to the difficulty of enclosing **all** azeotropes in a multicomponent mixture, azeotropy is closely linked to numerous phenomena occurring in the process (*e.g.* run-away of nonreactive azeotropes and the vanishing of distillation boundaries) as mentioned by Barbosa and Doherty (1988*a*); Song *et al.* (1997); Frey and Stichlmair (1999*b*); Harding and Floudas (2000); Maier *et al.* (2000); Harding and Floudas (2001). Accordingly, a solid understanding of the thermodynamic behavior of azeotropes becomes a relevant issue to address in process development. It allows one to determine whether a process is favorable and to account for the influence of operating conditions on process feasibility.

From a physical point of view, the necessary and sufficient condition for reactive azeotropy is that the change in concentration due to distillation is totally compensated for by the change in concentration due to reaction (Frey and Stichlmair, 1999*a*,*b*). As mentioned in the previous section, this condition is materialized when a stoichiometric line is colinear with the phase equilibrium line, as depicted in figure 2.2. If the residue curves are used to represent the phase equilibrium, the reactive azeotropic compositions are to be found according to the following graphical procedure (figure 2.3): (*i*) the points of tangential contact between the residue and stoichiometric lines (marker: •) define a curve of *potential reactive azeotropes* (thick line), which runs always between singular points; (*ii*) a reactive azeotrope (RAz, marker: ○) then occurs at the intersection point between the chemical equilibrium line and the curve of potential reactive azeotropes.

Based on the graphical estimation of reactive azeotropes, Frey and Stichlmair (1999*a*) establishes the following rules of thumb,

▷ Rule 1. A maximum reactive azeotrope occurs when the line of possible reactive azeotropes runs between a local temperature maximum and a saddle point and when there is only one point of intersection with the line of chemical equilibrium,

▷ Rule 2. A minimum reactive azeotrope occurs when the line of possible reactive azeotropes runs between a local temperature minimum and a saddle point and when there is only one point of intersection with the line of chemical equilibrium.

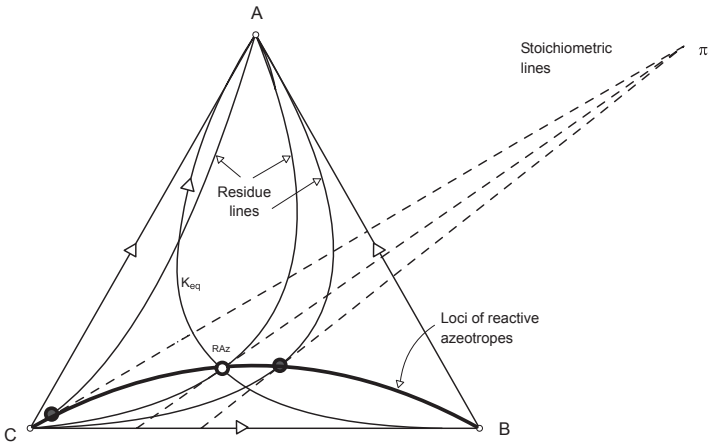

Figure 2.3. Graphical determination of reactive azeotropy. **Symbols:** (○): reactive azeotrope RAz at the given chemical equilibrium constant K_{eq}; π: pole at which stoichiometric lines coincide, $x_{i\pi} = \nu_i / \Sigma \nu_j$. **System features:** chemical reaction $A + B \rightleftharpoons C$. (adapted from Frey and Stichlmair (1999*b*)).

A practical limitation of this method is imposed by its graphical nature. Thus, this method has been only applied to systems of three components at the most undergoing a single reaction. Extending this method to systems with $n_c > 3$ might not be feasible due to the physical limitation of plotting the full-component composition space.

From a different and more rigorous perspective, a *reactive azeotrope* might be characterized by the satisfaction of the following necessary and sufficient conditions for a system undergoing a single equilibrium chemical reaction (Barbosa and Doherty, 1987*b*; Doherty and Buzad, 1992),

$$\frac{y_1 - x_1}{\nu_1 - \nu_{\text{total}} \times x_1} = \frac{y_i - x_i}{\nu_i - \nu_{\text{total}} \times x_i}, \qquad i \in [2, n_c - 1]. \tag{2.17}$$

It is relevant to point out that the azeotropy expression 2.17 also applies to the last component (n_c) as may be verified by knowing that $\sum_{i=1}^{i=n_c} x_i = \sum_{i=1}^{i=n_c} y_i = 1$ (Barbosa and Doherty, 1987*b*).

These necessary and sufficient conditions for reactive azeotropes have been generalized and theoretically established for the case of multicomponent mixtures undergoing multiple equilibrium chemical reactions by Ung and Doherty (1995*b*). The starting point for their analysis is the introduction of *transformed compositions*. It is widely recognized that mole fractions are not the most convenient measures of composition for equilibrium reactive mixtures, as they might lead to distortions in the equilibrium surfaces (Barbosa and Doherty, 1988*a*; Doherty and Buzad, 1992). In order to visualize in a much more

comprehensive manner the presence of reactive azeotropes, a transformed composition variable has been introduced by Doherty and co-workers (Barbosa and Doherty, 1987*a*; Doherty and Buzad, 1992; Ung and Doherty, 1995*a*,*c*; Okasinski and Doherty, 1997),

$$X_i \equiv \frac{\nu_k \times x_i - \nu_i \times x_k}{\nu_k - \nu_{\text{total}} \times x_k}, \qquad Y_i \equiv \frac{\nu_k \times y_i - \nu_i \times y_k}{\nu_k - \nu_{\text{total}} \times y_k}, \qquad i \in \mathbb{Z}^{n_c}, i \neq k, \tag{2.18}$$

where k denotes a reference component that satisfies the following conditions for ν_{total}: (i) k is a reactant if $\nu_{\text{total}} > 0$; (ii) k is a product if $\nu_{\text{total}} < 0$, and (iii) k is a product or reactant if $\nu_{\text{total}} = 0$.

The necessary and sufficient conditions for reactive azeotropy for the multicomponent, multireaction system can be then expressed in terms of the transformed variables (Ung and Doherty, 1995*b*),

$$X_i = Y_i, \qquad i \in \mathbb{Z}^{n_c-2}. \tag{2.19}$$

For this system, the transformed compositions are given by the following generalized expressions,

$$X_i = \frac{x_i - \nu_i^{\text{T}}(\mathcal{V}_{\text{ref}})^{-1}\mathbf{x}_{\text{ref}}}{1 - \nu_{\text{total}}^{\text{T}}(\mathcal{V}_{\text{ref}})^{-1}\mathbf{x}_{\text{ref}}}, \qquad i \in \mathbb{Z}^{n_c-n_{rx}}, \tag{2.20}$$

$$Y_i = \frac{y_i - \nu_i^{\text{T}}(\mathcal{V}_{\text{ref}})^{-1}\mathbf{y}_{\text{ref}}}{1 - \nu_{\text{total}}^{\text{T}}(\mathcal{V}_{\text{ref}})^{-1}\mathbf{y}_{\text{ref}}}, \qquad i \in \mathbb{Z}^{n_c-n_{rx}}, \tag{2.21}$$

where

$$\mathcal{V}_{\text{ref}} = \begin{pmatrix} \nu_{(n_c-n_{rx}+1),1} & \cdots & \nu_{(n_c-n_{rx}+1),n_{rx}} \\ \vdots & \nu_{i,r} & \vdots \\ \nu_{n_c,1} & \cdots & \nu_{n_c,n_{rx}} \end{pmatrix}, \tag{2.22}$$

$$d\tau_w = dt \times \left(\frac{1-\nu_{\text{total}}^{\text{T}}(\mathcal{V}_{\text{ref}})^{-1}\mathbf{y}_{\text{ref}}}{1-\nu_{\text{total}}^{\text{T}}(\mathcal{V}_{\text{ref}})^{-1}\mathbf{x}_{\text{ref}}}\right) \times V/L,$$

where ν_i^{T} is the row vector of stoichiometric coefficients for component $i \in \mathbb{Z}^{n_c-n_{rx}}$ in all the n_{rx} reactions $[\nu_{i,1} \;\; \nu_{i,2} \;\; \cdots \nu_{i,R}]$, $\nu_{\text{total}}^{\text{T}}$ is the row vector of the total mole number change in each reaction $\left[\sum_{i=1}^{i=n_c} \nu_{i,1} \;\; \cdots \sum_{i=1}^{i=n_c} \nu_{i,n_{rx}}\right]$, ref denotes the reference components for the n_{rx} reactions, numbered from $n_c - n_{rx} + 1$ to n_c and $\mathcal{V}_{\text{ref}}$ is the square matrix of stoichiometric coefficients for the n_{rx} reference components in the n_{rx} reactions.

These azeotropy expressions 2.19 state that in the space of transformed composition variables the bubble-point and dew-point surfaces are tangent at an azeotropic state (Barbosa and Doherty, 1988*a*), allowing the azeotropes to be found easily by visual inspection in the reactive phase diagram for the case of $n_c - n_{rx} \leq 3$ (figure 2.4). For systems beyond this space, a graphical determination of azeotropes might not be feasible.

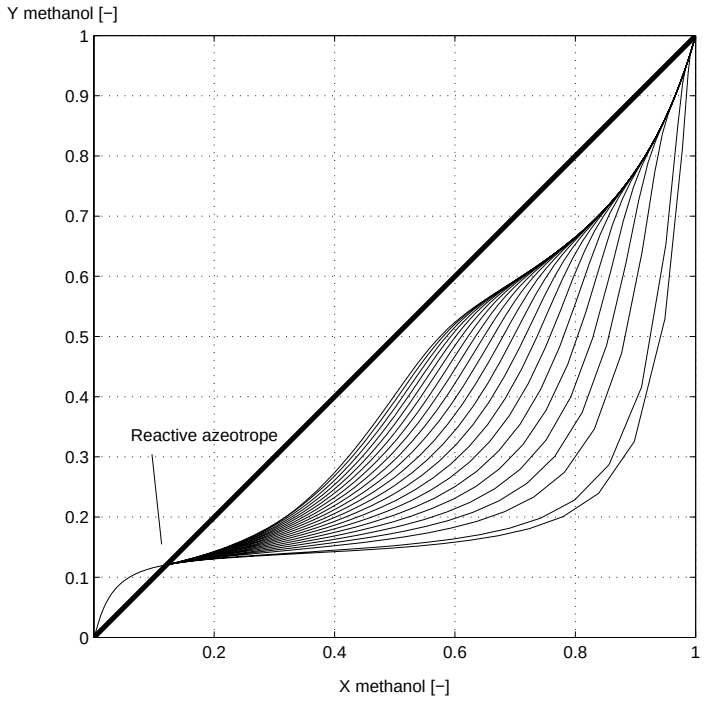

Figure 2.4. Phase diagram for methanol in the synthesis of MTBE expressed in terms of transformed compositions (equation 2.18). **Remarks:** the location of the reactive azeotrope is tracked down at the intersection of the residue curve and the line $X = Y$; reacting mixtures of various compositions are depicted. **System features**: operating pressure is $11{\cdot}10^5$ Pa; inert $n\mathrm{C}_4$ is present in the mixture.

Note that the azeotropy expression 2.19 holds also for pure components and nonreactive azeotropes surviving reaction. Moreover, the necessary and sufficient condition for reactive azeotropy resembles largely the conditions for nonreactive azeotropy in terms of molar fractions,

$$x_i = y_i, \qquad i \in \mathbb{Z}^{n_c}. \tag{2.23}$$

2.5 Non-equilibrium Conditions and Rate Processes

Phase non-equilibrium. If a chemical potential gradient exists between two adjacent and homogenous phases, the system is not in local phase equilibrium and a *rate-limited mass transfer phenomenon* occurs. A momentum balance of specie i results in the following expression for the driving force exerted on i as a function on the friction

forces due to diffusive motion of all other species,

$$\hat{f}_i = \sum_{j\neq i}^{i=n_c} \zeta_{i,j} \times x_j \times (u_i^{\text{diff}} - u_j^{\text{diff}}), \qquad i,j \in \mathbb{Z}^{n_c}, \tag{2.24}$$

where $\hat{f}$ is the frictional force, u_i^{diff} is the diffusive velocity of specie i and $\zeta_{i,j}$ is the friction coefficient between species i and j.

This expression is the well-known Maxwell-Stefan equation (MSE) and states that the driving force on a specie i in a mixture equals the sum of the friction forces between i and the other species j. MSE applied to multicomponent mixtures offers obviously a detailed description of the transfer phenomena, but on the other hand the model complexity and parametric uncertainty are considerably increased. The rate-based approach is of particular importance in (reactive) distillation, as the use of conventional stage efficiencies might be resulting in absurd variations ($-\infty$ to $+\infty$ as acknowledged by Kenig *et al.* (2000); Wesselingh (1997)). If MSE 2.24 is expressed in terms of Maxwell-Stefan diffusivities $\mathbb{D}$, species flux $\mathbb{N}$, average concentration C_{total} and chemical potential μ, the following MSE is obtained in a multidimensional space (Wesselingh and Krishna, 2000),

$$\begin{aligned} \frac{y_i}{\mathcal{R}\times T^V}\nabla_{T,P}\mu_i^V &= \sum_{j=1;j\neq i}^{j=n_c} \frac{y_i\times\mathbb{N}_j^V - y_j\times\mathbb{N}_i^V}{C_{\text{total}}^V\times\mathbb{D}_{ij}^V}, \quad i\in\mathbb{Z}^{n_c}, \\ \frac{x_i}{\mathcal{R}\times T^L}\nabla_{T,P}\mu_i^L &= \sum_{j=1;j\neq i}^{j=n_c} \frac{x_i\times\mathbb{N}_j^L - x_j\times\mathbb{N}_i^L}{C_{\text{total}}^L\times\mathbb{D}_{ij}^L}, \quad i\in\mathbb{Z}^{n_c}. \end{aligned} \tag{2.25}$$

A fully description of the non-equilibrium mass transfer phenomenon embraces simultaneously a Maxwell-Stefan diffusion model and a flow model. The most commonly used approach is the *film model*, which is addressed in more detail in the explanatory note 2.1.

Rate-limited chemical reaction. According to the universally applicable *law of mass action*, the rate of chemical reaction is directly proportional to the active masses of each of the reactants. For the particular case of a system not in chemical equilibrium, the term $\prod_{i=1}^{i=n_c} a_i^{\nu_i}$ is commonly called *reaction quotient*. At the limiting case, the non-equilibrium system tends to equilibrium state, which results in the reaction quotient tending to K_{eq}. The degree of separation between current system state and chemical equilibrium might be estimated by computing the Damköhler number,

$$Da = \frac{t_{\text{process}}}{t_{\text{reaction}}}. \tag{2.32}$$

According to this definition, Damköhler number gives the ratio of the characteristic process time to the characteristic reaction time (Doherty and Malone, 2001) and captures effectively the major dependence of conversion, production rate and product purities on the feed flowrate, catalyst level and holdup (Chen *et al.*, 2002). For an open

Film model is undoubtedly the most widespread approach for the rate-based mass and heat transfer through an interface (Wesselingh and Krishna, 2000). It effectively combines species diffusion and fluid flows and is based on the assumption that the resistance to mass and heat transfer is exclusively concentrated in a thin film where steady state diffusion and mass and heat convection take place (figure 2.5).

Thus, the interfacial mass and heat transfer fluxes are composed of a laminar, steady state diffusion term in the stagnant film and a convection term from the complete turbulent bulk phase (Taylor and Krishna, 1993),

$$\begin{array}{lll} \text{vapor} & \mathbb{N}_i^V = J_i^V + \mathbb{N}_{\text{total}}^V \times y_i, & i \in \mathbb{Z}^{n_c}, \\ & \mathbb{E}^V = h_{\text{HX}}^V \cdot (T^I - T^V) + \sum_{i=1}^{i=n_c} \mathbb{N}_i^V \times \overline{H}_i^V. & \\ \text{liquid} & \mathbb{N}_i^L = J_i^L + \mathbb{N}_{\text{total}}^L \times x_i, & i \in \mathbb{Z}^{n_c}, \\ & \mathbb{E}^L = h_{\text{HX}}^L \times (T^L - T^I) + \sum_{i=1}^{i=n_c} \mathbb{N}_i^L \times \overline{H}_i^L, & \end{array} \tag{2.26}$$

with

$$\mathbb{N}_{\text{total}}^{(\alpha)} = \sum_{i=1}^{i=n_c} \mathbb{N}_i^{(\alpha)}, \qquad (\alpha) \in \{\text{liquid, vapor}\}, \tag{2.27}$$

where $J_i^{(\alpha)}$ is the diffusion flux of component i in phase (α), $\overline{H}_i^{(\alpha)}$ is the partial molar enthalpy of component i in phase (α) and h_{HX} is the heat transfer coefficient.

With the assumption of perfectly mixed bulk phases and considering the flux direction (figure 2.5), the diffusion flux may be re-written in terms of the concentration gradient between the bulk and the interface,

$$\begin{array}{l} J_i^V = C_{\text{total}}^V \cdot k_{i,m}^V (y_i^I - y_i), \\ J_i^L = C_{\text{total}}^L \cdot k_{i,m}^L (x_i - x_i^I), \quad i \in \mathbb{Z}^{n_c}, \end{array} \tag{2.28}$$

with

$$C_{\text{total}}^{(\alpha)} = \sum C_i^{(\alpha)}, \tag{2.29}$$

where $k_{i,m}^{(\alpha)}$ is the mass transfer coefficient of component i in the mixture m in phase (α).

The *film model* assumes additionally, no accumulation in the interface and equilibrium state at the interface,

$$\begin{array}{l} \mathbb{N}_i^L = \mathbb{N}_i^V, \quad i \in \mathbb{Z}^{n_c}, \\ \mathbb{E}^L = \mathbb{E}^V, \end{array} \tag{2.30}$$

and

$$y_i^I = f_k(x_i^I, T), \quad i \in \mathbb{Z}^{n_c}, \tag{2.31}$$

where f_k is a nonlinear function of the distribution coefficients.

Note 2.1. Rate-based mass and heat transfer: the film model

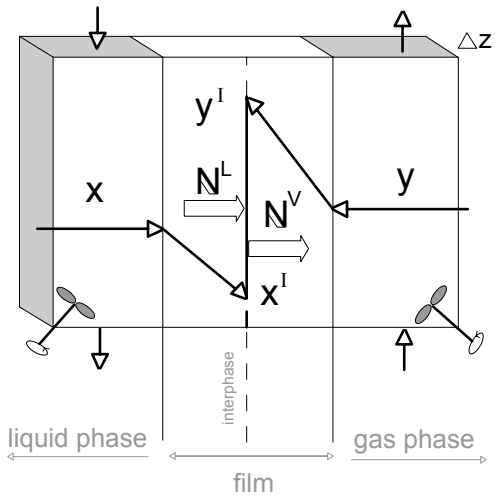

Figure 2.5. Schematic representation of the *Film Model*. The mass and heat transfer fluxes are assumed to be positive in the direction liquid → vapor.

system, for instance, with phase holdup M, feed flowrate F and undergoing a chemical reaction, the Damköhler number might be given as follows,

$$\begin{array}{lll} \text{homogenously catalyzed} & Da = & \frac{M \times k_{f,0}^{\text{hom}}}{F}, \\ \text{heterogeneously catalyzed} & Da = & \frac{W_{\text{cat}} \times k_{f,0}^{\text{het}}}{F}, \end{array} \tag{2.33}$$

where $k_{f,0}$ is the homogenously catalyzed forward rate constant evaluated at a reference temperature and W_{cat} is the amount of catalyst in the system.

The definition of Damköhler number implies that no reaction takes place if $Da << 1$ and chemical equilibrium limit is reached if $Da >> 1$.

2.6 Distributed Level: Column Structures

Hardware design in RD influences largely the performance of the unit, particularly in the formation of reactive azeotropes (Frey and Stichlmair, 1999*a*) and the prediction of multiple steady states (Baur *et al.*, 2000, 2001*d*; Baur and Krishna, 2002). Hardware configurations in RD (*e.g.* type of packing and tray geometry) are closely related to mass and heat transfer between phases and are ruled by considerations different to those for conventional distillation. Moreover, they are influenced by the state of aggregation of the involved catalyst (Bessling *et al.*, 1997).

Homogeneous reactive distillation takes place in bubble-cap or sieve trays columns, where the residence time and liquid holdup needed for the chemical reaction are de-

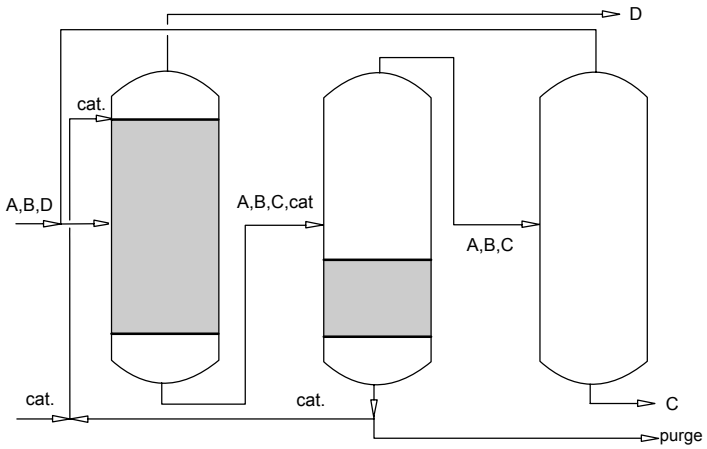

Figure 2.6. Separation train for an homogeneous catalyst. **Remark:** the dark sections of the columns represent reactive zones. **System features:** chemical reaction $A + B \rightleftharpoons C$; D is inert component. (adapted from Bessling *et al.* (1997))

pendent on the weir height and play a mayor role in the selectivity and conversion of the process (Baur *et al.*, 2000). In homogeneous RD, the catalyst is the highest-boiling component in the system and for fast reactions its recycling might involve more than a single piece of equipment (figure 2.6). Depending on the kinetic regime for mass transfer and chemical reaction, different situations might take place: (*i*) phase equilibrium exists and chemical reaction is rate-limited; (*ii*) phases are not in equilibrium and chemical reaction is equilibrium controlled; (*iii*) neither phase nor chemical reaction equilibria hold but phases are in thermal equilibrium; and (*iv*) no equilibrium occurs.

The solutions of each situation involve the simultaneous formulation of convenient chemical reaction and mass transfer models. For the case of phase equilibrium the widely spread equilibrium-based model (Seader, 1985) should be considered. In the case of rate limited mass transfer non-equilibrium models (Taylor and Krishna, 2000, 1993; Wesselingh, 1997) are to be used. The effect of Damköhler number on the unit performance should be taken into account if the chemical reaction is rate-limited. A detailed overview of the aforementioned situations is given in section §2.5.

Heterogeneous reactive distillation operation -sometimes referred to as *catalytic distillation*- is carried out in a catalyst-containing packed column. The chemical reaction takes place (mostly) within the catalyst particle, whereas the packing allows for simultaneous reaction and mass transfer between vapor and liquid phases (Yuxiang and Xien, 1992*b*,*a*; Subawalla and Fair, 1999). As stated by Yuxiang and Xien (1992*b*), five mass transfer/reaction processes may occur simultaneously in a reactive bed of catalytic

distillation: (*i*) mass transfer from vapor to liquid; (*ii*) mass transfer from liquid to catalyst granules; (*iii*) diffusion into the pores of the catalyst granules; (*iv*) adsorption of the reactive agents on the surface of the catalyst, and (*v*) chemical reaction.

Sundmacher and Hoffmann (1999) suggest that models can be distinguished with respect to mass transfer between the bulk phases, internal catalyst mass transport phenomena and chemical reaction. For the cases of chemical reaction and phase (non-)equilibrium, the models mentioned in homogeneous RD might be also used. As for the internal catalyst transport phenomena, two models are distinguished. Thus, heterogenous V/L/S models include mass and heat transfer limitations inside the solid catalyst, whereas quasi-homogeneous models assume that liquid bulk phase composition is present at each catalytically active site. This last simplification allows one to effectively regard heterogenous RD as a homogenous V/L case. Heterogeneous models are computationally more expensive than homogeneous models, requiring much more catalyst-related parameters. In some industrial applications, however, simplified approaches (*e.g.* quasi-homogenous, phase equilibrium models) are found to be well applicable, without compromising the output accuracy and reliability (Sundmacher and Hoffmann, 1999).

The design requirements of commercial RD packings differ to some extent from those in conventional distillation. For RD packing design two main features are to be taken into account (Subawalla and Fair, 1999): (*i*) the reaction efficiency should be maximized by providing intimate contact between vapor, liquid and solid catalyst, and (*ii*) the pressure drop through the catalyst bed should be minimized. These two desired characteristics should be reflected in the design variables in packings (*i.e.* hold-up, pressure drop, interfacial area and phase ratio). These key variables are detailed in section §2.7.

To improve the interphase mass transfer process a considerable variety of novel supports have been developed. In general terms, RD units for heterogeneous operation might be filled with traditional porous catalytic packing (*e.g.* Raschig rings, tea bag-, or sandwich-type) or with structured sheet metal packing with catalytic active surface. Industrially, the bale packing and the structured sheet-based packing are the most commonly used RD catalytic internals. In the first case, the particles of catalyst are enclosed in cloth wrapped in the form of bales, which are rolled with alternating layers of steel mesh to form a cylinder. In the second case, catalyst particles (size range: 1-3 mm (Tuchlenski *et al.*, 2001)) are enveloped in wire gauzes, which are then bound together in cubes. In both cases the spent catalyst is replaced with packing containing fresh catalyst. Due to the crossed flow path followed by the liquid in the sandwich-type, its radial distribution is about an order of magnitude higher than that reported for bale packing. This relevant advantage enhances the interest in designing novel variations of the sandwich-type structured packing.

In recent years considerable attention has been drawn to the use of multiphase mono-

lith structures in various applications (*e.g.* gas phase processing, VL reaction systems and biotechnology (Heiszwolf *et al.*, 2001)). Reactive distillation is not the exemption (Schildhauer *et al.*, 2005). Monolith structures offer attractive advantages over conventional packings regarding low-pressure drop, high-geometric surface, enhanced mass transfer rates and efficient catalyst utilization.

2.7 Distributed Level: Hydrodynamics

As mentioned by Malone and Doherty (2000), special attention should be paid to hydrodynamics and its interactions with the chemical reaction rate (*e.g.* good mixing and sufficient holdup for the intended extent of reaction). Unlike conventional columns, both the liquid and vapor flows have been found to determine the diameter of the RD column. Moreover, the liquid flow largely determines the residence time and flow patterns inside the unit (Tuchlenski *et al.*, 2001). For columns operating under diffusion limited conditions, a clear influence of catalyst thickness on steady state conversion is reported by Higler *et al.* (2000). All these facts lead to the necessity of deriving overall models, capable of predicting with acceptable reliability the performance of the column internals during RD operation.

2.7.1 Hydrodynamic Models

The development of an hydrodynamic model involves the prediction of pressure drop, hold-up, contact areas between phases, phases ratios and residence time distributions for a given column internal. Although various predictive models are available in the open domain (see *e.g.* Kooijman and Taylor (2000)), the model developed by The University of Texas Separations Research Program (SRP model) (Rocha *et al.*, 2004, 1996; Fair *et al.*, 2000) enjoys a widespread preference within packed columns internals. Lately, the *Delft* model has been introduced (Fair *et al.*, 2000) and validated for the case of zig-zag triangular flow channels. Note that the following descriptions are referred to a *VL* system.

Holdup models are extensively reported in the open literature and validated for specific types of packing and under specific operating conditions. Generally, a holdup expression is a function of the internals geometry, flow regime and physical properties of the involved phases,

$$M = f_M(\text{geometry}, \psi_{FR}(L,V), \psi_{PP}(L,V)), \tag{2.34}$$

where $\psi_{FR}(L,V)$ is a set of functions for the liquid and vapor flow regimes and $\psi_{PP}(L,V)$ is a set of physical properties functions for the liquid and vapor phases.

A reliable **pressure drop model** should contain all the hydrodynamic interactions that occur between the liquid-gas-internal (Fair *et al.*, 2000). Thus, the corresponding generic expression is given by,

$$\Delta P = f_P(\text{geometry}, \xi, \psi_{FR}(V), \psi_{PP}(V)), \tag{2.35}$$

where ξ is the total friction factor, which is composed of all independent contributions due to V/V, V/L and direction change friction.

The **interfacial area** is directly related to the liquid holdup in the internal (Rocha *et al.*, 2004). Thus, the generic correlation for the contact area between phases is,

$$a_\Psi = f_a(M). \tag{2.36}$$

For a three-phase system special attention should be paid to the areas between all phases (*i.e.* a_{LV}, a_{LS} and a_{VS}) in particular when incomplete wetting occurs.

The **phases ratio** in the internal is clearly dependent on the geometry and liquid holdup, namely,

$$\phi_p = f_\phi(\text{geometry}, M). \tag{2.37}$$

For the case of a monolith structure, the hydrodynamic models are slightly different (Heiszwolf *et al.*, 2001),

$$\text{holdup} \quad : \quad M = f_M(\text{geometry}, \psi_{FR}(L,V), \psi_{PP}(L,V)), \tag{2.38}$$

$$\text{pressure drop} \quad : \quad \Delta P = f_P(\text{geometry}, f_{fr}, \psi_{FR}(V), \psi_{PP}(V)), \tag{2.39}$$

$$\text{interfacial area} \quad : \quad a_\Psi = f_a(H, \text{geometry}, \psi_{FR}(L,V)), \tag{2.40}$$

$$\text{phases ratio} \quad : \quad \phi_p = f_\phi(\text{geometry}, M), \tag{2.41}$$

where f_{fr} is the two-phase friction factor.

Attaining control of the unit hydrodynamics involves the definition of a set of key decision variables: packing parameters (geometry and functionality) and flow regime of the involved phases.

2.8 Flowsheet Level: Units and Connectivities

Going one level up in aggregation we consider the structures of complete columns. Conventionally, RD columns are classified in hybrid and non-hybrid units, depending on the distribution of reactive trays inside the column. Thus, hybrid columns are distillation columns with a reactive core and nonreactive sections (rectifying and/or stripping sections). Non-hybrid RD columns denote columns where all trays including condenser and reboiler are reactive (Güttinger, 1998). Hybrid columns are commonly

designed for solid catalyst, whereas homogeneous catalyst would lead to non-hybrid column designs.

An additional classification of RD units is possible among the hybrid columns. If the reactive core is placed in the reactive section of the unit, the column is denoted as *reactive rectifying* unit. Accordingly, *reactive stripping* units are those with reactive core in the stripping section. The location of the reactive core involves a good compromise between the physical properties of the reactive species and the kinetic regime of the chemical reaction(s). In this respect, Schoenmakers and Bessling (2003*a*) present a comprehensive set of principles for equipment choice in homogeneous and heterogeneous RD. For fast chemical reactions, for instance, if the relative volatility of the component to be removed is low, a complete column with catalytic internals is required. On the other hand, for slow chemical reactions and high relative volatility, an evaporator and reactor are sufficient. In this case, all the energy required to evaporate the corresponding component is provided by a single stage evaporator followed by a reactor.

The recycle structures in RD may also vary depending on the physical properties of the reactive system and the kinetic regime of chemical reaction. For example, side stream reactors are in particular required for the case of rate-limited chemical reactions in heterogenous RD, whereas stirred vessels are needed in homogeneous RD.

The key design decision variables at this level of aggregation include: functionality of unit sections, number of trays or length of sections, section diameters, feeding and withdrawal points, energy exchange, column flowsheet configuration with recycle structures and heat integration.

2.9 Flowsheet Level: Steady-State Multiplicities

The phenomenon of multiple steady states (MSS) has been known and experimentally detected for already some decades, even for the simple case of binary distillation with ideal vapor-liquid equilibrium (Kienle *et al.*, 1995; Pellegrini and Possio, 1996; Bildea and Dimian, 1999; Grüner and Kienle, 2004). In the framework of RD, understanding the sources of multiplicity and their prediction within a RD unit have been topics of challenging interest for the CACE-community (see *e.g.* Jacobs and Krishna (1993); Ciric and Miao (1994); Hauan *et al.* (1995*a*,*b*); Gehrke and Marquardt (1997); Güttinger and Morari (1997); Güttinger (1998); Higler *et al.* (1999*b*); Güttinger and Morari (1999*b*,*a*); Chen *et al.* (2002); Baur *et al.* (2003); Rodriguez *et al.* (2001, 2004)). In this section, we address steady state multiplicity in an entire RD column structure.

2.9.1 Generalities of Multiple Steady States

Among many others, Güttinger (1998) and Sneesby *et al.* (1998*a*) study the occurrence of multiple steady states in columns with reactive core (*i.e.* hybrid RD column). Their research work suggests that two types of multiplicities may occur in RD,

- **Input multiplicities**: two or more sets of input variables give the same set of output variables. If a column of a given design and given feed (F, x_F, T_F) exhibits input multiplicities, the same product compositions x_D and x_B can be achieved for different values of operating parameters (*e.g.* Da and reboiler duty). This type of multiplicity is frequent in azeotropic and RD and has mainly economical importance.
- **Output multiplicities**: a column of a given design exhibits different column profiles and product compositions at steady state for the same set of inputs and the same values of operating parameters. This type of multiplicity will be addressed during the course of this section.

2.9.1.1 Sources of multiplicity

The actual causes of MSS in RD have been under discussion by the CACE-community for the last decades. Mathematically, MSS might be originated basically from the nonlinearity of the transformation between mass and molar flow rates and from the interaction between flows and composition due to energy balance (Bildea and Dimian, 1999). Jacobs and Krishna (1993) suggest that MSS occur in RD due the simultaneous physical and chemical equilibrium, which in turn is reflected in the topology of the residue maps. Thus, column profiles may develop along different paths, leading to distinctive stable nodes. Together with this hypothesis, Hauan *et al.* (1995*b*) provide a thermodynamic-based reasoning on the sources of MSS in the synthesis of MTBE. Based on a *lift-dilution* effect, high MTBE conversions are attained when the lower section of the column contains sufficient amount of MTBE to lift all the methanol and when the reactive mixture at the lower part of the reactive zone is highly diluted to avoid MTBE decomposition (Hauan *et al.*, 1995*b*; Stichlmair and Frey, 2001). Morari and co-workers (Güttinger, 1998; Güttinger and Morari, 1999*b*,*a*) study extensively the occurrence of multiplicities for the case of simultaneous reaction and phase equilibrium in RD systems. They present a combined approach of the $\infty/\infty/\infty$ analysis (*i.e.* infinite column length, infinite reflux flow rate and infinite fast reactions) with a singularity analysis of the product composition paths to predict the existence of MSS (Güttinger and Morari, 1997). Their study suggests that all non-hybrid RD columns (*i.e.* RD columns without nonreactive sections) operating with a feed mixture inside a certain region of the transformed composition space and using molar specifications will exhibit MSS caused by the

reactive VL equilibrium. Furthermore, for hybrid columns and for molar specifications of bottoms flow rate, the MSS are caused by the interactions between the reactive and the nonreactive column sections. Ciric and Miao (1994) attribute the origin of MSS to the combination of a bilinear reaction rate and a sharp volatility difference between the reactant feeds. The last source is also reported in the case of a two-phase reactor operating under boiling conditions (Waschler *et al.*, 2003). Gehrke and Marquardt (1997) apply a singularity approach to a one-stage RD column, with special emphasis to the effect of chemical reaction stoichiometry on MSS occurrence. For esterifications it has been reported that multiplicity occurs due to the same reason as multiplicity in conventional distillation; *i.e.* due to the different values of the heat of evaporation for pure components. Furthermore, the interaction between the temperature dependency of the reaction rates and the boiling temperature in the system has been suggested as one essential physical source for MSS. Mohl *et al.* (1997) identify two sources of MSS for esterification reactions: the interaction between separation and reaction (*i*) at simultaneous phase and reaction equilibria; and (*ii*) in the kinetic regime. According to Mohl *et al.* (2001) output multiplicity in RD appears to be caused essentially by the same phenomenon as in conventional distillation.

From a mathematical point of view, the sufficient and necessary conditions for output multiplicity are given by the following inequalities,

$$\frac{\partial D_v}{\partial L_v} > 0, \quad \frac{\partial B_v}{\partial Q_{\text{reb}}} > 0, \tag{2.42}$$

where D_v is the volumetric distillate flow rate, L_v is the volumetric reflux flow rate, B_v is the volumetric bottoms flow rate and Q_{reb} is the reboiler duty.

Mohl *et al.* (1999) mention that multiplicity in the synthesis of TAME is caused by kinetic instabilities, clearly contrasting with the statements given by Güttinger and Morari (1997); Mohl *et al.* (1997); Jacobs and Krishna (1993). According to Rehfinger and Hoffmann (1990), MSS in both a RD unit and a conventional CSTR might be originated by the same sources. In a later contribution, Mohl *et al.* (2001) suggest the kinetic instability as a source of MSS in the synthesis of MTBE. Special attention is paid to the influence of transport limitations on the kinetic instabilities in heterogeneously catalyzed RD processes. The influence of kinetics on multiplicity is investigated by Chen *et al.* (2002), resulting in finding non-reported isola multiplicity behavior. Recently, Rodriguez *et al.* (2001, 2004) study the sources of multiplicity in a reactive flash. It is derived from those contributions that the presence of VL equilibrium combined with a reaction can remove or create MSS, in both one-phase and two-phase regions. An extended classification of the steady state behavior in a reactive flash is presented in section §7.2.1, in the context of the design frame developed in this thesis. In this extended contribution a total of 25 qualitatively different bifurcation diagrams are identified. Moreover, the effect of system properties on multiplicity regions is covered.

2.9.1.2 Implications of Multiplicity

In the previous subsection multiplicity in RD has been described and possible causes have been discussed. This subsection addresses the consequences of multiplicity from an industrial point of view. Undesired situations can be encountered in RD processing due to multiplicity, namely,

- **Start-up operation**: if more than one stable steady state is possible for a certain set of operating conditions, an undesired steady state can be reached if the initial conditions are unsuitable. Furthermore, a given start-up policy can send the column to a completely inappropriate steady state (Scenna *et al.*, 1998; Mohl *et al.*, 1999; Bisowarno and Tade, 2000).
- **Perturbations leading to steady state transition**: perturbations in the feed stream, for instance, can potentially shift the operating point to an undesired steady state (Hauan *et al.*, 1995*a*; Schrans *et al.*, 1996; Sneesby *et al.*, 1998*b*; Mohl *et al.*, 1999; Baur *et al.*, 2001*a*, 2003).
- **Oscillatory behavior**: steady state multiplicity can trigger oscillatory behavior, as has been found by dynamic simulation (Hauan *et al.*, 1995*a*; Mohl *et al.*, 2001).
- **Difficult process control**: the strong nonlinear behavior of a RD column can seriously hinder the controllability of the process, as reported by Al-Arfaj and Luyben (2002*b*,*a*).

Implications for dynamic behavior. The strong nonlinearity and multiplicity of a RD column can cause undesirable behavior from a dynamic point of view, even leading to the occurrence of steady state transitions. According to Schrans *et al.* (1996), if a disturbance is large enough for a certain time, the system can jump to a different steady state. Sneesby *et al.* (1998*b*) perform rigorous dynamic simulations of a MTBE RD column that exhibits multiplicity. Certain perturbations in the feed composition cause transitions between parallel steady states. Steady state transitions are found only when no product flow rate is used as column input. Furthermore, the possibility of forcing a RD column from an undesired operating point to a desired operating point is studied, without coming up with a practical control mechanism. Mohl *et al.* (1999) determine experimentally that temporary disturbances in the operating conditions (*e.g.* feed flow rate) may cause a transition to an undesired steady state of the process. Using a non-equilibrium stage model, Baur *et al.* (2001*a*) show that when operating at a high-conversion steady state, small perturbations in the feed lead to a transition to a low-conversion branch. Additionally, it is suggested that the type and duration of a feed perturbation causing a transition from one to another steady state depends on the

Multiplicity region. The size and robustness of multiplicity regions play a key role in the design and operation of RD units. Mohl *et al.* (1997) show that the multiplicity region in the parameter space of the operating conditions occurs for high yields of desired MTBE in the bottoms but is fairly small with respect to the bottoms flow rate. Therefore, a design can easily be moved to the unique-steady state region by slightly adjusting the bottoms flow rate. Eldarsi and Douglas (1998) conclude that MSS can easily be eliminated by adjusting either the methanol-to-butylenes molar feed ratio, the reflux ratio, or installing a cooler on the last reactive stage. Higler *et al.* (1999*b*) find that for a decreasing iC$_4$ feed flow rate, the multiple steady states tend to disappear. On the other hand, Mohl *et al.* (1999) state that the multiplicity region for the column configuration used by Jacobs and Krishna (1993); Hauan *et al.* (1995*a*) and Hauan *et al.* (1995*b*) is relatively small to be verified experimentally. Furthermore, the multiplicity region is found to occur only at high reflux ratios. According to Mohl *et al.* (2001) operating in the kinetic regime can lead to a large number of different steady state solutions for a given set of operating conditions. However, kinetic multiplicities can be avoided by an increase of the Damköhler number, which is obtained by increasing the number of catalytically active sites, or by decreasing the feed rate. Moreover, MSS vanish if the column pressure is increased and the multiplicity regions for equilibrium controlled chemical reactions are much smaller than in the kinetic case. The effect of the kinetic regime on the multiplicity region is studied additionally by Chen *et al.* (2002). The solution multiplicities are predicted to disappear below a critical value of Damköhler, there being a *Da*-range at which high conversions are expected without solution multiplicities. These results imply that operation in the kinetic limited regime (low Damköhler) without MSS is possible. Qi *et al.* (2002) state that the values of reflux and reboil ratios where multiplicity regions occurs, are relatively near the values where the highest iC$_4$ conversion could be obtained.

Note 2.2. Multiplicity regions in the synthesis of MTBE

model description, on the column configuration and on the residence time distribution along the column height. In a later contribution, Baur *et al.* (2003) find that transitions from the low-conversion steady state to the high-conversion steady state are possible for sufficient large and long feed perturbations. During its start-up procedure, a RD column might move to an undesired steady state, specially if the operating conditions are within a multiplicity region (*cf.* explanatory note 2.2). Using dynamic simulations Scenna *et al.* (1998) and Bisowarno and Tade (2000) study the effect of start-up policies on the overall process performance. A start-up procedure is recommended (Bisowarno and Tade, 2000) to avoid low-conversion operation. The strategy is based on stabilization of the RD column at the optimum operating conditions before the reactants are fed. For the case of ETBE synthesis, an optimum operation is attained (*i.e.* high product purity, short start-up time and reduced energy requirement) by stabilizing exclusively the separation-controlled region.

Implications for process control. Avoiding multiplicity is certainly an important consideration for process control and its interactions with design (Chen *et al.*, 2002). An appropriate control configuration is an effective tool to avoid multiplicity. Güttinger and Morari (1997) show, for the MTBE column studied by Jacobs and Krishna (1993), that

multiplicities can easily be avoided by selecting the appropriate control configuration. Additionally, Sneesby *et al.* (1998*a*) show that an appropriate closed-loop control is able to prevent steady state transitions. In practice, reasonably tight control of almost any temperature within the column should be sufficient to prevent a steady state transition. Wang *et al.* (2003) study the control strategy of a RD column for MTBE synthesis. For output multiplicity, oscillation between steady states can occur even without observable disturbances. Input multiplicity results in the change in the sign of process gain around the nominal operating condition leading to control instability. The authors conclude that although these phenomena are present, a satisfactorily linear control is still possible to be designed. Monroy-Loperena *et al.* (2000) study the control problem of an ethylene glycol RD column. Despite the strong nonlinearity of the model equations and the uncertainties in the dynamics, the authors are able to design a robust PI controller. The impact of multiplicity and high nonlinearity on the control of RD synthesis of methyl acetate is discussed by Al-Arfaj and Luyben (2002*a*). It is suggested that for output multiplicity the control of open-loop unstable operating points is more difficult than the control of open-loop stable operating points.

2.9.2 Multiple Steady States in Industrial Applications

Multiplicity has been reported in various RD applications, with special emphasis in fuel ethers. In the case of MTBE synthesis, two conversion branches have been reported, corresponding to a low and high conversion of reactants (Jacobs and Krishna, 1993; Hauan *et al.*, 1995*a*,*b*; Schrans *et al.*, 1996; Güttinger and Morari, 1997, 1999*a*,*b*; Mohl *et al.*, 1997; Güttinger, 1998; Sundmacher and Hoffmann, 1999; Mohl *et al.*, 1999; Baur *et al.*, 2003). Studies on multiplicity in the production of ethylene glycol by RD have reported an impressive amount of nine different steady states (Ciric and Miao, 1994; Monroy-Loperena *et al.*, 2000). The production of methyl acetate by RD has been studied by Al-Arfaj and Luyben (2002*a*), identifying three steady states: a stable high-conversion, a stable low-conversion and an unstable intermediate-conversion steady state. MSS have been confirmed for TAME synthesis in pilot-scale columns operating in the kinetic regime (Mohl *et al.*, 1999; Sundmacher and Hoffmann, 1999; Baur *et al.*, 2003). Furthermore, multiplicity has been reported in the RD synthesis of ethyl *t*-butyl ether by Bisowarno and Tade (2000).

2.9.3 Additional Modeling Implications for Multiple Steady States

Equilibrium (EQ) and non-equilibrium (NEQ) models are generally used to represent the governing phenomena in RD. Lately, the effect of the modeling approach on the occurrence of MSS has become a hot topic within the CACE community. This trend is easily evident by listing the recent publications on EQ and NEQ models and their im-

plications to MSS (*e.g.* Krishnamurthy and Taylor (1985); Yuxiang and Xien (1992*a*); Ciric and Gu (1994); Ciric and Miao (1994); Yu *et al.* (1997); Wesselingh (1997); Podrebarac *et al.* (1998); Higler *et al.* (1998, 1999*a*,*b*, 2000); Higler (1999); Sundmacher and Hoffmann (1996); Taylor and Krishna (2000); Baur *et al.* (2000, 2001*a*,*b*,*c*, 2003); Wolf-Maciel *et al.* (2001); Peng *et al.* (2003); Taylor *et al.* (2003); Zheng *et al.* (2004)). The contributions of Baur *et al.* (2000, 2001*a*, 2003) and Higler *et al.* (2000, 1999*b*) are of particular relevancy as equilibrium and non-equilibrium stage modeling are compared in terms of the occurrence of MSS. The synthesis of fuel ethers and ethylene glycol are used as illustrative case studies. In the synthesis of MTBE, for instance, a higher conversion is attained by introducing mass transfer resistance. This counterintuitive situation is explained by the fact that in the low conversion branch the reaction proceeds in the reverse direction. Thus, any increment in mass transfer resistance promotes the desired direction (Baur *et al.*, 2000). Furthermore, the range in which MSS occur is highly influenced by the nature of the model. Thus, the region of multiplicity in MTBE synthesis is narrower for NEQ modeling than the exaggerated window encountered for EQ models (Higler *et al.*, 2000; Baur *et al.*, 2000). It should be mentioned that these modeling considerations are relevant for the representation of a part of the physical reality. In design, the implication of NEQ modeling on multiplicity could be that the phase contacting and hydrodynamics should be made such that NEQ conditions are realized.

Hardware configurations play a determinant role in the occurrence of MSS, as reported by Baur *et al.* (2000, 2001*d*); Baur and Krishna (2002) for NEQ models and by Pilavachi *et al.* (1997) for EQ models. Hardware configurations refer basically to the type of packing in packed columns (*e.g.* catalytic bales or active Raschig rings (Baur and Krishna, 2002)) and tray sizes and mixing pattern in trayed columns (Baur *et al.*, 2000). It is suggested that flooding and weeping conditions exclude unfeasible configurations when interface transfer is considered, whereas for EQ models hardware features may exclude some of the multiple solutions.

Presence of inerts is a key issue in the design and operation of RD processes (Espinosa *et al.*, 1996; Giessler *et al.*, 1998). Product composition regions can drastically change, influencing the efficiency and operability of the RD unit. Moreover, inerts in the system increase the occurrence of MSS since an additional azeotrope might be introduced, as is the case in the MTBE synthesis (Hauan *et al.*, 1995*b*). In that system and for highly diluted reacting mixtures (*e.g.* $x_{nC_4} > 72\%$), the methanol activity coefficient increases, leading to a decrease in the system's temperature; this results in an increment of the reaction equilibrium constant and the achievement of a high-purity MTBE product. On the other hand, high conversion profiles may be obtained for inert-free mixtures provided a sufficient number of reactive stages (Espinosa *et al.*, 1996). According to those authors, an optimal column design requires a bottom specification with a ratio

$\frac{x_{\text{inert}}}{x_{\text{limiting reagent}}} > 1.$

The physical and chemical behavior of the system requires the definition of key design decision variables. For one-stage and multistage levels those decision parameters and operational variables include operational pressure and temperature, chemical reaction kinetics (*i.e.* equilibrium or rate-limited chemical reaction), mass/heat transfer regime, phase velocity, residence time of the reactive phase and temporal operation (*i.e.* batch, fed batch and continuous).

2.10 Summary of Design Decision Variables

In the case of RD, design issues are far more complex than those involved in conventional distillation and may differ significantly from case to case. For instance, the design variables for conventional distillation include the number of trays, the feed tray location and the reflux ratio for a constant molar overflow system with single feed tray. In contrast, in a RD column the liquid hold-up is the major design parameter that determines the extent of reaction, the feed might be distributed within the unit and constant molar overflow (CMO) can not be assumed unless the reaction is thermally neutral and stoichiometrically balanced (Ciric and Gu, 1994). Additionally, RD design is far more complicated than conventional distillation because of: (*i*) the presence of additional variables (*e.g.* distribution of reactive core); (*ii*) the nonlinear interaction between phases and reactions; and (*iii*) stronger coupling between heat and mass flow throughout a RD unit.

All the key design decision variable mentioned previously in the levels of aggregation are summarized in this section and schematically presented in figure 2.7. In terms of priority of decision, a first class of key design decision variables involves temporal considerations. The variables of interest are related to the mode of operation of the system, namely batch, fed batch or continuous operation. The second class of design variables includes the physical and operational conditions of the system. Those aim to the favorable creation of enough reaction and separation driving forces and mutual synergy. In this class design variables such as as operation pressure, temperature, reflux ratio and phase velocity are of utmost importance. Moreover, chemical reaction regime and mass/heat transfer regime should be specified. The third and last class of design variables embraces all key spatial parameters, ranging from establishing section with different functionalities, packing parameters, number of trays or length of sections, feeding and withdrawal points, energy exchange, section diameters, column flowsheet configuration with recycle structures and heat integration.

Note that appropriate choices for those design decision variables are closely linked to the challenges of process design and operation of reactive distillation (*cf.* section §1.2.2). Thus, for instance, the development of novel catalyst should take into account both

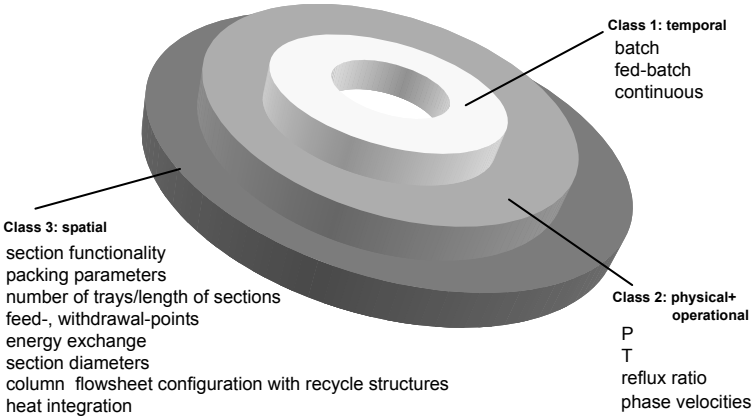

Figure 2.7. Key design decision variables in reactive distillation resulting from a systematic phenomenological analysis.

temporal considerations (*e.g.* operation mode and catalyst deactivation and spatial considerations (*e.g.* scale-up factors).

Mind journey to the scientific questions.

If we take a mind journey back to the engineering/scientific design question given at the beginning of this chapter, the following remark can be made. Regarding Question 4, the domain knowledge required for process synthesis in the case of RD is essentially composed of three classes of design decision variables (or building blocks): temporal, physical and operational and spatial. Each class embraces key design variables, which are identified by approaching the physical and chemical phenomena from a systems' perspective.

"The systems approach is a response to a pressing need for synthesizing and analyzing complexity."

Herb Simon, Nobel prize laureate (1916-2001)

3

Conceptual Design of Reactive Distillation Processes: A Review †

In this chapter the design methods for reactive distillation processing developed over the last decades are classified and described. A fingerprint of the most representative work in three categories (graphical, optimization-based and heuristic-based) is presented and missing opportunities are identified. Special attention is paid to the methods' description, outputs, assumptions, advantages and limitations. The result of this analysis, presented as a fingerprint chart, points forward to the development of an integrated conceptual design approach for reactive distillation processes. This *multiechelon approach* is covered in detail in the coming chapters and is a constitutive part of a highly-aggregated design methodology, which addresses the RD design problem from a life-span inspired perspective.

†Parts of this chapter have appeared in Almeida-Rivera *et al.* (2004*a*) and are based on publications until mid 2003

Chapter 3

3.1 Introduction

This chapter provides an exhaustive overview on current design methodologies with application to reactive distillation processing. By no means the presented material should be regarded as the ultimate overview, specially due to the dynamic developments lately experienced by RD research. The overview ends with a list of scientific literature published in 2003

The available approaches for the design of RD may be categorized into three main groups: those based on graphical/topologycal considerations, those based on optimization techniques and those derived from heuristic/evolutionary considerations. In the course of this chapter, representative methodologies of each category will be discussed focussing in particular on their description, outputs, assumptions, advantages and limitations.

A qualitative analysis of the features that play relevant roles in RD design result in the definition of an integrated strategy. This approach -termed *multiechelon approach* and extensively described in chapter 4- combines systematically the capabilities and complementary strengths of available graphical and optimization-based methods.

Recalling the engineering and scientific design questions given in chapter 1, in this chapter we address question 4, namely,

- *What is the domain knowledge required and which new building blocks are needed for process synthesis?*

3.2 Graphical Methods

The graphical methods are called so, because the decisions are made on the basis of graphical information. This information is often generated using models. These approaches rely on the behavior of residue curves or distillation lines and may be classified into two well-defined trends: (*i*) methods based on thermodynamic-topological analysis of distillation lines; and (*ii*), methods based on composition transformations.

3.2.1 Statics Analysis

The design method based on statics analysis in RD units involves finding the complete set of steady state modes and the set of corresponding operating parameters (Serafimov *et al.*, 1999). Since separation is the most costly task, the prime purpose of statics analysis method is the synthesis of RD processes with reduced separation costs and with improved reaction parameters (Serafimov *et al.*, 1999). For this purpose, several approaches are proposed, which are in general terms based on thermodynamic-topological analysis of distillation diagrams (Giessler *et al.*, 1999, 1998).

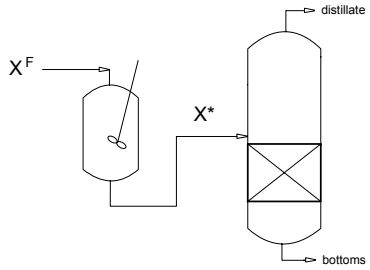

(a) Schematic representation of a RD sequence, where the feed stream is firstly converted to a pseudoinitial mixture X^*.

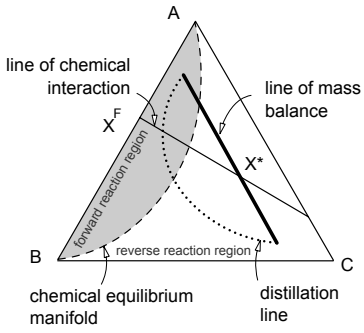

(b) Distillation lines for a system undergoing the reaction $A + B \rightleftharpoons C$.

Figure 3.1. Method of statics analysis (adapted from Giessler *et al.* (1999)).

Assumptions: (*i*) the vapor and liquid flow rates in the column are infinitely large; (*ii*) the capacity of the reaction part in the column is large enough to carry out a given conversion rate; (*iii*) the plant is operated at steady state and theoretical stages are chosen; and (*iv*) one reversible equilibrium reaction is considered.

These assumptions allow one to estimate the liquid composition on a tray as the composition of vapor one tray below (*i.e.* $x_i = y_{i+1}$) and the profiles may be estimated by using usual distillation lines.

Description: this method considers that composition change due to reaction is negligible on each stage and that RD is a succession of reaction and distillation operations (Giessler *et al.*, 1998), where the feed is firstly converted to a pseudoinitial mixture -with composition X^* assuming a certain extent of reaction ε- which is then separated in a distillation column (figure 3.1*a*). For that pseudo-initial mixture feasible steady states occur when: (*i*) the composition X^* and the product compositions satisfy the mass balance and (*ii*) a part of the distillation line lies inside the forward reaction rate region.

The number of theoretical and reactive stages is determined from the distillation line and from the intersection of the distillation line and chemical equilibrium manifold (CEM) and represents the boundary of the forward and backward reactions) (Giessler *et al.*, 1999). Since there are multiple pairs of X^* and product composition that satisfy the mass balance, the method sets one of the product composition as reference point and solves for the other two (for a 3-component system) by using material balance expressions. Thus, two of the components' compositions and X^* lie on the same *line of mass balance* (LMB) in the diagram and allow the estimation of the ratio D/B at a certain reboil ratio only by exploring the ratio of the line segments (figure 3.1*b*).

After fixing the reference point, all the compositions of LMB are explored to estimate the degree of conversion required in the reaction step. The highest conversion value is found by iteration among the feasible degrees of conversion and defines the *limiting steady state* (LSS) (*i.e.* condition of maximum conversion for a certain reactant (Giessler *et al.*, 1999)). At this condition, the location and the length of the reactive zone in the RD column are estimated by counting all reactive stages present in the forward reaction section. Attaining the LSS can proceed by several limiting paths, depending on the nature of the stability of the fixed point from which the distillation lines start or end. According to Giessler *et al.* (1998), if LSS is not convenient, the composition of the initial mixture, the structure of the phase equilibrium diagram and the reactions conditions (P, T) have to be changed and the iteration loop is performed again. The proposed method stresses the importance of identifying all feed composition regions, since they lead to the complete set of column configurations. Thus, the entire feed region is classified into several sub-regions, each of which has the same characteristics with respect to the product configurations (Giessler *et al.*, 2001).

Advantages: this method (*i*) gives a straight forward solution to the question whether or not a reaction should be performed in a RD column; (*ii*) allows one to synthesize flowsheets qualitatively (*e.g.* maximum degree of conversion, reactive zone location and length and column sequencing) (*iii*) for its application this method requires little data (*i.e.* feed composition, phase equilibrium model parameters, chemical equilibrium model parameters and reaction stoichiometry); this method (*iv*) provides an effective tool for the study of strongly nonideal mixtures with multiple chemical reactions and number of components; (*v*) allows the selection of the appropriate steady states from their complete set; (*vi*) simplifies troublesome calculations (including expensive full-scale experiments) reducing dramatically computational time (up to 5 times); (*vii*) represents a general method that does not depend on the concrete column structure; (*viii*) does not require that product compositions, extent of reaction and number of stages are fixed a priori; and (*ix*) allows one to determine the stability of various product regimes and derive the possible product compositions and the column structure for one fixed feed composition and the entire feed region.

Limitations: (*i*) this method assumes infinite separation efficiency; and (*ii*) matching the operating lines with the assumed product composition can be sometimes troublesome.

3.2.2 Residue Curve Mapping Technique

The *residue curve mapping* (RCM) technique has traditionally been considered a powerful tool for flowsheet development and preliminary design of conventional multicomponent separation processes. It represents a good approximation of actual equilibrium

behavior and allows one to perform feasibility analysis of separation processes where nonideal and azeotropic mixtures are involved (Siirola, 1996*b*,*a*; Malone and Doherty, 2000). Furthermore, residue curves have been used to predict the liquid-composition trajectories in continuous distillation units in the ∞/∞ case (Barbosa and Doherty, 1988*a*; Espinosa *et al.*, 1996). Although for finite columns those profiles differ slightly compared to the residue curves under same isobaric conditions (Fien and Liu, 1994), this difference is normally considered negligible at the first stages of design. A feasibility criterion may be derived from RCM considerations, where feasible composition profiles should be enclosed by the total reflux profiles (*i.e.* residue curves) and the reversible profiles (*i.e.* profiles at the minimum reflux ratio) (Espinosa *et al.*, 1999). Conceptually, residue curve mapping is a phase equilibrium representation for systems involving azeotropes (Siirola, 1996*a*,*b*) and qualitatively studies the behavior of a (non-) reactive mixture in a heated still. Analytically, RCM are constructed based on physical properties of the system (*i.e.* vapor-liquid equilibrium, liquid-liquid equilibrium and solubility data), wherein the composition of a non-reacting liquid remaining in the system may be determined by performing overall and component material balances (Westerberg *et al.*, 2000; Jimenez *et al.*, 2000).

For multicomponent systems undergoing n_{rx} equilibrium reactions, RCM are defined in terms of transformed molar compositions (Ung and Doherty, 1995*a*; Doherty and Buzad, 1992),

$$\frac{dX_i}{d\tau_w} = X_i - Y_i, \qquad \text{with } X_i(0) = X_{i,0}, \quad i \in \mathbb{Z}^{n_c - n_{rx} - 1}, \tag{3.1}$$

with

$$d\tau_w = dt \times \left(\frac{1 - \nu_{\text{total}}^T (\mathcal{V}_{\text{ref}})^{-1} \mathbf{y}_{\text{ref}}}{1 - \nu_{\text{total}}^T (\mathcal{V}_{\text{ref}})^{-1} \mathbf{x}_{\text{ref}}} \right) \times V/M^L, \tag{3.2}$$

$$X_i = \frac{x_i - \nu_i^T (\mathcal{V}_{\text{ref}})^{-1} \mathbf{x}_{\text{ref}}}{1 - \nu_{\text{total}}^T (\mathcal{V}_{\text{ref}})^{-1} \mathbf{x}_{\text{ref}}}, \quad Y_i = \frac{y_i - \nu_i^T (\mathcal{V}_{\text{ref}})^{-1} \mathbf{y}_{\text{ref}}}{1 - \nu_{\text{total}}^T (\mathcal{V}_{\text{ref}})^{-1} \mathbf{y}_{\text{ref}}}, \quad i \in \mathbb{Z}^{n_c - n_{rx}}, \tag{3.3}$$

$$\mathcal{V}_{\text{ref}} = \begin{pmatrix} \nu_{(n_c - n_{rx}+1),1} & \cdots & \nu_{(n_c - n_{rx}+1),n_{rx}} \\ \vdots & \nu_{i,r} & \vdots \\ \nu_{n_c,1} & \cdots & \nu_{n_c,n_{rx}} \end{pmatrix}, \tag{3.4}$$

where X_i and Y_i are the transformed composition variables for the component i in the liquid and vapor phases respectively ($i \in \mathbb{Z}^{n_c - n_{rx}}$), τ_w is a warped time, $\mathbf{x}_{\text{ref}}$ is the column vector composed of the liquid molar compositions of the n_{rx} reference components, $\mathcal{V}_{\text{ref}}$ is the square matrix of stoichiometric coefficients for the n_{rx} reference components in the n_{rx} chemical reactions. Note that non-reference components $\in [1, n_c - n_{rx}]$ and reference components $\in [n_c - n_{rx} + 1, n_c]$.

This new set of variables defines a sub-region of lower dimension in the composition space composed of the feasible product compositions for equilibrium controlled reactions. The RCM problem is solved by specifying the relation between the transformed

compositions of the vapor and liquid phases and by using relevant properties of the transformed compositions.

Description: (*i*) specify the compositions of the mixture charged to the pot (*i.e.* $X_{i,0} = X_i^e$); (*ii*) calculate composition of the equilibrium vapor; and (*iii*) calculate Y_i and integrate expression 3.1 until a singular point is reached (*i.e.* $X_i = Y_i$).

For *kinetically controlled reactions*, an *autonomous* residue curve expression can be derived in terms of the Damköhler number ($Da = \frac{k_{\mathrm{f,ref}} \times M^L}{V}$) and for the heating policy $V/V_0 = M^L/M_0^L$,

$$\frac{dx_i}{d\tau_w} = x_i - y_i + Da \times (\nu_i - \nu_{\mathrm{total}} \times x_i) \times \frac{k_f}{k_{f,\mathrm{ref}}} \times r, \qquad \text{with } x_i(0) = x_{i,0}, \quad i \in \mathbb{Z}^{n_c}, \tag{3.5}$$

where M_0^L is the initial mass of liquid in the pot, V_0 is the initial vapor flow, k_f is the rate constant for the forward reaction, r is the composition-dependent reaction rate, ref denotes the reference conditions of the system and $d\tau_w = dt \times V \times (M^L)^{-1}$.

The influence of Damköhler number on the trajectory of the residue curves is evident. For Da=0 the residue curve lines will end in the highest boiling stable node (*i.e.* pure component or nonreactive azeotrope), whereas for high Da the lines will also end in a stable node, corresponding to a pure component, chemical equilibrium point or a reactive azeotrope.

Advantages: (*i*) this method provides a reliable tool to perform feasibility analysis in RD; and (*ii*) for its application this method requires little data (*e.g.* feed compositions, phase equilibrium model parameters, chemical equilibrium model parameters and reaction stoichiometry).

Limitations: (*i*) although relevant improvements have been made towards multiple component ($n_c > 3$) mixtures (Malone and Doherty, 2000), the RCM technique is limited by its intrinsic graphical nature; and (*ii*) accurate thermodynamic data are required to correctly describe the RD process (Barbosa and Doherty, 1988*b*).

RCM techniques have been used as feasibility tools to develop a generalized and systematic design approach for reactive feeds outside conventional composition ranges (Almeida-Rivera and Grievink, 2002, 2004). For the synthesis of MTBE two separation sequences have been found that depend on the location of the reacting feed in the composition space.

3.2.3 Attainable Region Technique

The concept of *attainable region* (AR) has been extensively employed in the synthesis of reactor structures (Feinberg, 1999) and successfully extended to processes combining simultaneous reaction, mixing and separation (Nisoli *et al.*, 1997). In combination with

graphical methods, an activity based reaction-separation vector is defined, which satisfies the same geometric properties as the reaction vector does. Therefore, it allows one to construct the attainable region using the existing procedure for reaction-mixing systems. In general terms and for a given system of reactions with given reaction kinetics, the AR may be defined as the portion of concentration space that can be achieved from a given feed composition by any combination of reaction and mixing (Nisoli *et al.*, 1997; Gadewar *et al.*, 2003). Thus, this technique aims to identify feasible reactor networks -albeit not the optimum- based on graphical properties of simple models of CSTR and PFR.

Assumptions: [Given: c_1 and c_2 are two attainable product compositions]: (*i*) every composition that lies on the segment line $\overline{c_1 c_2}$ belongs to the AR; (*ii*) on the AR boundary the reaction vector points inward, is tangent or is zero; and (*iii*) in the complement of AR no reaction vector intersects the AR.

Description: for the case of CSTR a component mass balance has been expressed in terms of Damköhler number and the vapor fraction,

$$x_i - x_i^F = \underbrace{\phi_m \frac{MW(\mathbf{x}^F)}{MW(\mathbf{y})}(x_i - y_i) + Da\frac{MW(\mathbf{x}^F)}{MW(\mathbf{x})}\frac{r(\mathbf{x})}{k_{f,\min}}(\nu_i - \nu_{\text{total}} \times x_i)}_{\mathbf{RS}(x_i,y_i)\times Da}, \qquad i \in \mathbb{Z}^{n_c}, \tag{3.6}$$

where ϕ_m ($\equiv V_m/F_m$) is the mass-based vapor fraction, V_m is the mass-based vapor flow, F_m is the mass-based feed flow, MW is the average molecular weight, Da is defined as $Da = k_{f,\min} \times \rho_m \times \upsilon / F_m$, $k_{f,\min}$ is the forward rate constant evaluated at the lowest temperature on the boiling surface, ρ_m is the mass-based molar density, υ is the total liquid volume, $r(\mathbf{x})$ is the reaction vector, subscript m denotes mass-based values and $\mathbf{RS}(x_i, y_i)$ is the reaction-separation term.

For a PFR, the material balance is given by,

$$\frac{dx_i}{d\eta} = \underbrace{\frac{\phi_m}{Da}\frac{MW(\mathbf{x}^F)}{MW(\mathbf{y}^F)}(x_i - y_i) + \frac{MW(\mathbf{x}^F)}{MW(\mathbf{x}^F)}\frac{r(\mathbf{x})}{k_{f,\min}}(\nu_i - \nu_{\text{total}} \times x_i)}_{\mathbf{RS}(x_i,y_i)}, \qquad i \in \mathbb{Z}^{n_c}, \tag{3.7}$$

$$x_i(0) = x_{i,0}, \qquad i \in \mathbb{Z}^{n_c}, \tag{3.8}$$

$$d\eta = \frac{MW(x^F)}{MW(x^F)} \times \frac{k_{f,\min} \times \rho_m}{L_m(z)} A(z) \times dz, \tag{3.9}$$

where $A(z)$ is the cross sectional area of the PFR at the distance $z \in [0, l_{\text{PFR}}]$, l_{PFR} is the length of the PFR and η is a scaled time.

Expressions 3.6 and 3.7 are identical to those that describe the behavior of a CSTR and PFR and therefore, allow one to follow the same procedure for the construction of the AR (figure3.2).

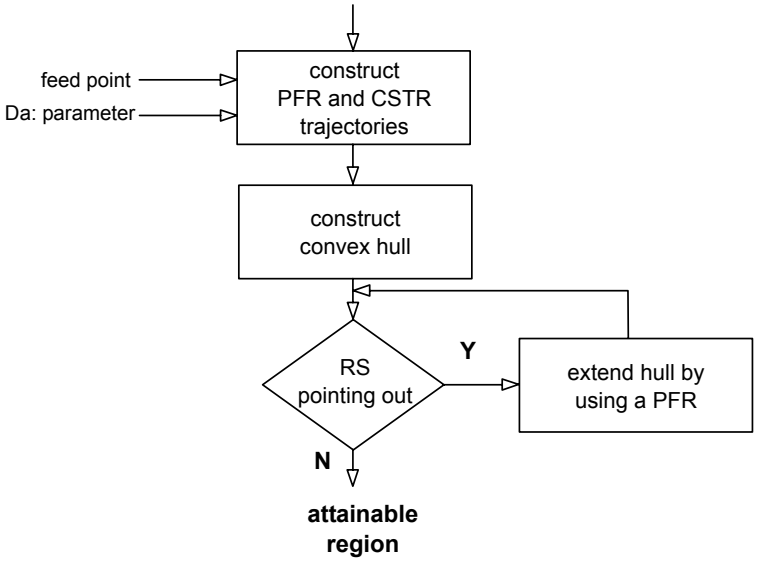

Figure 3.2. Procedure for the construction of attainable region. **Nomenclature:** RS: reaction-separation term.

Advantages: (*i*) this method allows one to point out promising flowsheets; (*ii*) the reaction-separation vector has the same geometric properties as simple reactor models, allowing the application of the theory derived for PFRs and CSTRs; and (*iii*) this method can be easily extended to multiphase systems.

Limitations: (*i*) economic considerations are not taken into account to rank the design alternatives.

3.2.4 Fixed-Point Algorithm

A sound understanding on fixed points (*cf.* explanatory note 3.1) and the prediction of their behavior as a function of design parameters have been lately used as a design tool for RD columns.

Assumptions: this technique is based on several assumptions, which depend on the nature of the contacting structure. Staged columns (Buzad and Doherty, 1994): (*i*) three component systems with a chemical reaction given by $\nu_A A + \nu_B B \rightleftharpoons \nu_C C$; (*ii*) ideal vapor-liquid equilibrium; (*iii*) iso-molar reaction; (*iv*) negligible heat of reaction; (*v*) negligible heat of mixing; (*vi*) equal latent heats; and (*vii*) constant liquid hold-up on the reactive stages. Okasinski and Doherty (1998) removed these assumptions in the development of their more generalized design method. Packed columns (Mahajani and Kolah, 1996): (*i*) applicability of the film theory of diffusion; (*ii*) uniform liquid composition in the bulk; (*iii*) negligible axial dispersion/diffusion; (*iv*) CMO; (*v*) saturated

Fixed points At total reflux conditions, certain points in the concentration space are reached where the composition on successive stages is constant (Buzad and Doherty, 1994, 1995) and in the vicinity of which the columns profiles behave in a peculiar manner (Mahajani and Kolah, 1996; Mahajani, 1999*a*). These *fixed points* occur at the pure component and azeotropic compositions (Buzad and Doherty, 1994; Okasinski and Doherty, 1998) and move to new positions as the reflux ratio (or external reboil ratio or Damköhler number) is changed. Fixed points can be nodes (stable or unstable) or saddles and have a significant influence on the column composition profiles, minimum reflux, etc. (Okasinski and Doherty, 1998). Unlike stable and unstable nodes, the location of fixed points is dependent on process parameters and represents chemical and physical equilibrium conditions. According to Espinosa *et al.* (1996), fixed points can be obtained by finding tangents to residue curves that pass through the distillate or bottom streams. In order to solve for the fixed-point compositions in terms of the Damköhler number -particularly in terms of the critical value Da^c- *continuation methods* are commonly used. These methods involve solving the design equations for a range of Damköhler numbers, where the lower bound corresponds to zero and the upper bound to the critical Damköhler number. The criterion for fixed-point location establishes that for low Da the end of the profile will be located in the negative reaction space (*i.e.* where the backward reaction is predominant), whereas for Da above the critical value the end of the profile will be located in the positive reaction space. If the balance expressions along the column are written as explicit finite difference equations (*i.e.* $x_{n+1} = f(x_n, p)$) the stability of the fixed points is determined by the eigenvalues λ_J of the Jacobian of f evaluated at the fixed points (Okasinski and Doherty, 1998).

Note 3.1. Fixed points in reactive distillation

liquid feed; (*vi*) negligible heat losses to the walls, heat of reaction and heat of mixing; (*vii*) total condenser; (*viii*) reboiler modelled as equilibrium stage with reaction; and (*ix*) constant mass transfer coefficients, interfacial area and liquid hold-up.

Description: most of the pioneering work in the field of RD design for *equilibrium controlled chemical reactions* is based on transformations of the molar compositions by Doherty and co-workers (Barbosa and Doherty, 1987*a*,*b*, 1988*a*,*b*; Doherty and Buzad, 1992; Ung and Doherty, 1995*a*,*c*). They devoted considerable effort in defining a design strategy for equilibrium chemical reactions in staged columns. The resulting approach is based on the boundary value design method for nonreactive columns. It introduces a novel composition coordinate system, expressions 3.3, to transform the RD problem into a form completely analogous to a non-RD problem, which may be solved using conventional algorithms.

Similarly to the molar fractions, molar flow rates are transformed as suggested by Güttinger (1998),

$$\underline{\vartheta} = \vartheta \times \left(1 - \nu^T_{\text{total}} \times \mathcal{V}^{-1}_{\text{ref}} \times x^{(\vartheta)}_{\text{ref}}\right), \tag{3.10}$$

where ϑ denotes any of the streams present in the RD column (*i.e.* distillate, bottoms, feed, liquid and vapor flows) and $\underline{\vartheta}$ represents the corresponding transformed value. As mentioned by Frey and Stichlmair (1999*b*), the transformed compositions can be interpreted as a projection of different chemical equilibrium states along their stoichiometric

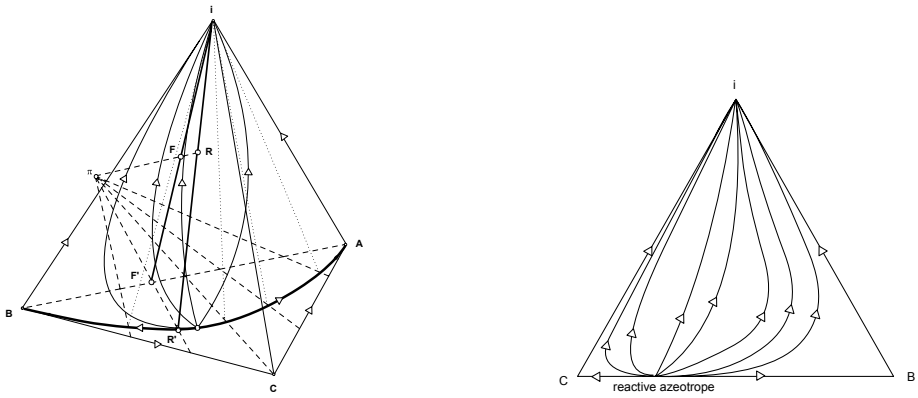

(*a*) Non-transformed composition space. (*b*) Transformed composition space.

Figure 3.3. Dimension reduction through transformed compositions. **Systems features:** chemical reaction $A+B+I \rightleftharpoons C+I$; where I is an inert component (adapted from Frey and Stichlmair (1999*b*)).

lines (figure 2.2).

These definitions present convenient and simplifying properties: (*i*) the dimensions of the system are reduced, simplifying the depiction of equilibrium (figure 3.3) (Frey and Stichlmair, 1999*b*; Barbosa and Doherty, 1987*a*); (*ii*) they have the same numerical values before and after reaction; (*iii*) they sum up to unity; (*iv*) they clearly indicate the presence of reactive azeotropes when $X_i = Y_i$; (*v*) the nonreactive limits are well defined; (*vi*) the number of linear independent transformed composition variables coincides with the number of independent variables that describe the chemical equilibrium problem; and (*vii*) the lever rule is valid as the chemical reaction no longer impacts the material balance.

However, the introduction of transformed variables reduces the understanding of the phase equilibrium as a whole, hiding eventually some nonreactive azeotropes (Frey and Stichlmair, 1999*b*).

For *kinetically controlled reactions*, the approach involves specifying all the degrees of freedom of the system and performing expanding envelope balances (material balances around the rectifying, stripping sections and the entire column) from the ends of the column towards the middle (Buzad and Doherty, 1994; Huss *et al.*, 1999). The methodology is supported by the RCM technique (*cf.* chapter 5) and allows both a fast screening for reactive azeotropes and feasible designs and the computation of the number of trays and the minimum reflux ratio (Ciric and Gu, 1994). If the target product compositions are feasible, the trajectories (for the rectifying and stripping sections) intersect. Then, for a given value of Damköhler there will be a single value of the reflux

ratio that satisfies the design equations (Doherty and Buzad, 1992). Intersection of profiles is a necessary but not sufficient condition. Thus, the accumulated extent of reaction in the rectifying section plus that in the stripping section must be equal to the initially assumed overall extent of reaction in the column (Okasinski and Doherty, 1998),

$$\frac{D \times x_i^D + B \times x_i^B - F \times x_i^{\text{feed}}}{\nu_i \times F} = (Da^{\text{rect}} \times \sum_{j=1}^{j=n_t^{\text{rect}}} \frac{M_j^L}{M_0^L} \frac{k_{f,r}}{k_0} \times r_j)_{\text{rect}} + (Da^{\text{strip}} \times \sum_{j=1}^{j=n_t^{\text{strip}}} \frac{M_j^L}{M_0^L} \frac{k_{f,r}}{k_0} \times r_j)_{\text{strip}}. \tag{3.11}$$

Fixed-point algorithm is not recommended by Ciric and Gu (1994) and Espinosa *et al.* (1996) for systems where the reaction kinetics, heat of reaction, liquid hold-up and residence times are the determining design variables. However, Okasinski and Doherty (1998) successfully use it to reproduce the ethylene glycol synthesis example of Ciric and Gu (1994).

Mahajani and Kolah (1996) successfully extend the approach of Doherty and co-workers to packed columns, where liquid phase backmixing is totally absent. This approach relies on the performance of mass balances over differential elements of length dz in both rectifying and stripping sections, which can be re-written as functions of dimensionless numbers (*e.g.* Da, HTU, dimensionless flux φ_i and ratio of characteristic times in the vapor and liquid sides $\beta(\equiv C^V_{\text{total}} \times k^V_m / C^L_{\text{total}} \times k^L_m)$).

Rectifying section ($i \subset \{1,3\}$):

$$\begin{array}{ll} \frac{dy_i}{d\zeta_z} = -\frac{\varphi_i}{HTU^V}, & \frac{dx_i}{d\zeta_z} = \left(\frac{RR+1}{RR}\right)\left[-\frac{\varphi_i}{HTU^V} + Da\frac{F}{V} \times g(x,T)\right], \\ y_i(0) = y_{i,0}, \quad i \in \mathbb{Z}^{n_c}, & x_i(0) = x_{i,0}, \quad i \in \mathbb{Z}^{n_c}. \end{array} \tag{3.12}$$

Stripping section ($i \subset \{1,3\}$):

$$\begin{array}{ll} \frac{dy_i}{d\zeta_z} = -\frac{\varphi_i}{HTU^V}, & \frac{dx_i}{d\zeta_z} = \left(\frac{RS+1}{RS}\right)\left[-\frac{\varphi_i}{HTU^V} + Da\frac{F}{L+F} \times g(x,T)\right], \\ y_i(0) = y_{i,0}, \quad i \in \mathbb{Z}^{n_c}, & x_i(0) = x_{i,0}, \quad i \in \mathbb{Z}^{n_c}. \end{array} \tag{3.13}$$

V-L equilibrium in the interface ($i \subset \{1,3\}$):

$$y_i - \varphi_i = f(\varphi_i \times \beta + x_i), \tag{3.14}$$

where ζ_z is the dimensionless height of the column and RR and RS are the reflux and reboil ratios, respectively.

The extent of reaction is given by,

$$\varepsilon_i = \int_0^{z^{\text{rect}}} r_i \times dz + \int_0^{z^{\text{strip}}} r_i \times dz, \qquad i \subset \{1,3\}, \tag{3.15}$$

where z^{rect} and z^{strip} are the lengths of the rectifying and stripping sections, respectively.

The solution procedure reported by Mahajani and Kolah (1996) for packed columns is quite similar to that described by Buzad and Doherty (1994) for staged columns: (*i*) expressions 3.12-3.14 are solved simultaneously for various values of Da, determining the range where the stripping and rectifying profiles intersect; (*ii*) the satisfaction of the second necessary condition is then evaluated; and (*iii*) the sizing of the RD column is performed.

Remarkable from Mahajani's contributions is the parametric analysis of the design, in terms of identifying the dependence of HTU^V with Da^c. It was concluded that for kinetically controlled reactions accompanied by slow mass transfer, the dimensionless number ($HTU^V \times Da^c$) plays a mayor role in the feasibility of the design. Thus, profiles intersect if and only if ($HTU^V \times Da^c$) falls in a specific range, whose width depends on the relative position of the fixed points (Mahajani, 1999*b*).

For RD columns where equilibrium controlled reactions are involved, the design methodology follows the same guidelines developed by Barbosa and Doherty (1988*a*,*b*) for staged columns. Thus, transformed variables can be introduced, reducing the dimensionality of the reactive system and simplifying the set of design equations.

It is revealed from this approach that the liquid hold-up has no direct influence on the performance of the column, highly resembling the nonreactive distillation case. Furthermore, the reflux ratio is found to determine exclusively the feasibility of the design. Thus, for low reflux ratio values stable nodes are reached before the concentration profiles intersect (*i.e.* non-feasible design) whereas at high reflux ratios the profiles intersect and the design turns to be feasible. The value at which the profiles just touch corresponds to the minimum reflux ratio. Although the parameters HTU^V and β do not play a role in the intersection of the profiles, they determine the column height and the extent of reaction.

Advantages: (*i*) this method is highly flexible in generating alternative designs at various design parameters (*e.g.* Damköhler number, reboil ratio or liquid hold-up in reactive zones) allowing one to put realistic bounds on those parameters (Okasinski and Doherty, 1998); and (*ii*) the mass and energy balances can be decoupled, allowing the determination of the column profile only using mass balance and equilibrium equations (Espinosa *et al.*, 1996).

Limitations: this algorithm is limited by its inherent graphical nature, that imposes practical limitations and complicates its extension to systems where the number of components minus the number of independent stoichiometric reactions exceeds a value of 3.

Fortunately, several modifications and extensions of the fixed-point method for staged and packed columns are available in the open literature, aiming to relax part of the

assumptions on which the original algorithm was based. These relaxations include: (*i*) double feed columns (Okasinski, 1998); (*ii*) kinetically controlled reactions, which account for the liquid hold-up in the column design and economics (Barbosa and Doherty, 1988*b*, 1987*a*,*b*; Buzad and Doherty, 1994, 1995; Doherty and Buzad, 1992; Mahajani, 1999*a*); (*iii*) multiple reactions (Ung and Doherty, 1995*c*); (*iv*) different hold-ups per section (Melles *et al.*, 2000; Okasinski and Doherty, 1998); (*v*) heat effects (Melles *et al.*, 2000; Okasinski and Doherty, 1998); and (*vi*) reactions where $\sum v_i \neq 0$ (Melles *et al.*, 2000; Okasinski, 1998).

3.2.5 Reactive Cascades

Chadda *et al.* (2003) and Gadewar *et al.* (2003) use the concept of reactive cascades to screen the feasibility of hybrid RD systems. This approach has been successfully applied to the preliminary design of single-feed and double-feed RD columns. The governing expressions for the stripping (n_t^{strip} stages) and rectifying (n_t^{rect} stages) cascades are,

$$\text{rectifying:} \quad \begin{aligned} & y_{i,j-1} = \phi_{R,j} \times y_{i,j} + (1-\phi_{R,j}) \times x_{i,j} - \nu_i \left(\tfrac{k_f}{k_{f,\text{ref}}}\right)\left(\tfrac{\mathcal{D}}{1-\mathcal{D}}\right) r(x_j) \\ & i \in \mathbb{Z}^{n_c-1}, j \in [2, n_t^{\text{rect}}]. \end{aligned} \tag{3.16}$$

$$\text{stripping:} \quad \begin{aligned} & x_{i,j-1} = \phi_{R,j} \times y_{i,j} + (1-\phi_{R,j}) \times x_{i,j} - \nu_i \left(\tfrac{k_f}{k_{f,\text{ref}}}\right)\left(\tfrac{\mathcal{D}}{1-\mathcal{D}}\right) r(x_j) \\ & i \in \mathbb{Z}^{n_c-1}, j \in [2, n_t^{\text{strip}}], \end{aligned} \tag{3.17}$$

where $\phi_{R,j} = \frac{V_j}{L_{j-1}}$ is the fraction of feed L vaporized in the j^{th} unit; and $\mathcal{D}$ is a normalized Damköhler number ($\mathcal{D} = \frac{Da}{1+Da}$).

Description: (*i*) for a given operating pressure, the feasibility diagram is drawn, which is obtained by solving the component balances for the liquid/vapor molar compositions in the stripping/rectifying sections. The independent variable $\phi_{R,j}$ is assigned a convenient value, whereas $\mathcal{D}$ is used as parameter to move from equilibrium to kinetically controlled regimes; (*ii*) for a given $\mathcal{D}$-value the column configuration (reactive or hybrid) is selected based on the satisfaction of the product specifications; (*iii*) the rectifying and stripping cascades expressions are solved at the given $\mathcal{D}$-value until the fixed points are reached; (*iv*) depending on the column configuration, the stripping and/or rectifying cascade expressions are solved for $\mathcal{D}$=0; (*v*) the transformed compositions in the liquid/vapor phases are estimated according to expressions 3.3 for the stripping/rectifying sections; and (*vi*) in the transformed composition space the lever rule is applied for a desired product composition. The design is deemed to be feasible if the lever rule intersects both the rectifying and stripping cascade profiles.

Advantages: (*i*) a global feasibility analysis can be performed as a function of the production rate, catalyst concentration and liquid hold-up; (*ii*) this method does not

have any restriction in the number of components or reactions; and (*iii*) this method is claimed to be easily implemented.

Limitations: (*i*) the Damköhler number is assumed to be invariant on all the reactive stages; (*ii*) the effect of structural aspects of the unit (*e.g.* feed ratio type, location of multiple feeds, reflux and reboil ratios) are not considered; and (*iii*) the energy balances are left out from the design methodology.

3.2.6 Thermodynamics-Based Approach

Stichlmair and co-workers (Frey and Stichlmair, 1999*b*; Stichlmair and Frey, 1999) study the RD design from a thermodynamic-driven point of view. Their approach is based on the existence of *reactive distillation lines* and *potential reactive azeotropes* (*cf.* §2.4).

Description: (*i*) the possible products (or feasible separation regions) are determined from the knowledge of the existing concentration profiles within the column, which in turn are represented by reactive distillation lines; (*ii*) the column mass balance is included; and (*iii*) possible separation borders are identified.

A thorough analysis of the behavior of reactive distillation lines with respect to the volatility values of the involved components and the feed staging suggests the following (Bessling *et al.*, 1997, 1998),

- RD is a feasible alternative for systems where the desired products are the nodes in a reactive distillation line diagram and their boiling points differ considerably,
- in the event that one of the desired products behaves as a saddle point, the conversion may be increased by adding a second feed stream in the column (*e.g.* synthesis of methyl acetate),
- the conversion of a two feed column reaches a maximum at finite reflux in the case of products that behave as saddle points,
- RD is a feasible and cost-effective alternative if one of the desired products behaves as a saddle point and,
  - high conversion is required at stoichiometric reactants ratio,
  - separation between desired and undesired products is difficult,
  - the boiling point difference between desired products is large,
  - there is no distillation boundary line, and
  - chemical equilibrium is on the side of the desired products (*e.g.* synthesis of methyl acetate).

Table 3.1. Combination of reactive and nonreactive sections (**nrs**) in a RD column. (source: Bessling *et al.* (1997))

Reaction	Inerts	Desired products	nrs
A $\rightleftharpoons$ B		A or B	yes
A $\rightleftharpoons$ B	C	B/C	yes
A $\rightleftharpoons$ B	C	A/C	yes
A $\rightleftharpoons$ B	C, D	BC/D;BD/C;B/CD	yes
A $\rightleftharpoons$ B	C, D	AC/D;AD/C;A/CD	yes
A+B $\rightleftharpoons$ C		C	yes
A+B $\rightleftharpoons$ C		A/B	no
A+B $\rightleftharpoons$ C	D	C/D	yes
A+B $\rightleftharpoons$ C	D	AD/B;A/BD	no
A+B $\rightleftharpoons$ C+D		A/B	no
A+B $\rightleftharpoons$ C+D		C/D	no

- all components that need a reactant for the forward or backward reaction(s) are located in the low-dimensional reaction space,
- all inert components are located in the reaction space, and,
- if it is aimed to separate a product that is not present in the reaction space, a nonreactive distillation section is required. Table 3.1 presents a general overview for the combination of reactive and nonreactive sections for several stoichiometries.

Advantages: (*i*) this approach can be applied to both fast and slow chemical equilibrium reactions; and (*ii*) feasible products can be determined within a RD column.

Limitations: (*i*) finding the reactive azeotropes might be sometimes troublesome; and (*ii*) detailed knowledge of phase equilibrium, reaction kinetics and residence time within the column is required.

3.2.7 Conventional Graphical Techniques

These techniques allow the distribution of reaction zones within a column using the *McCabe-Thiele* and *Ponchon-Savarit* methods for a given reaction conversion by adjusting the catalyst hold-up on each stage. Although the methods are currently limited to binary reactive mixtures, they provide fundamental insights towards multiple component systems. In general terms, it is suggested that if the reaction has a heavy reactant and a light product, the reaction zone should be placed in the rectifying section, whereas if the reaction has a light reactant and a heavy product, the reaction zone should be located in the stripping section (Lee *et al.*, 2000*b*,*c*,*d*).

Assumptions: (*i*) binary system with a single chemical reaction; (*ii*) CMO; and (*iii*) vapor-liquid equilibrium.

Ponchon-Savarit method. This method is traditionally considered a powerful visualization tool for the synthesis of distillation columns for binary mixtures. Thus, it allows the designer to account graphically for the enthalpy effects that cause a varying molar overflow when stepping off stages (Lee *et al.*, 2000*b*). The main issue of this approach is the definition of the *reactive cascade difference point*, which for an exothermic isomerization reaction occurring in the rectifying zone moves towards the reactant and downward as the calculation goes down the column. The following nomenclature is adopted for the diagram coordinates (Lee and Westerberg, 2000),

$$\delta_{R,n}^{\text{rect}} = \frac{D \times x^D - \mathbf{cP} \times \varepsilon_n + \mathbf{cR} \times \varepsilon_n}{D}, \tag{3.18}$$

$$h_{R,n}^{\text{rect}} = \frac{h^D + q_c + \Delta^r H \times \varepsilon_n}{D}, \tag{3.19}$$

$$q_c = \frac{Q_{\text{cond}}}{D}, \tag{3.20}$$

where $\delta_{R,n}^{\text{rect}}$ and $h_{R,n}^{\text{rect}}$ are the composition and enthalpy coordinates in the Ponchon-Savarit diagram, D is the distillate flow, $\mathbf{cP}$ is the product coefficient vector, $\mathbf{cR}$ is the reactant coefficient vector, ε_n is the sum of the extent of reactions occurring in stages n and above, h is the liquid enthalpy, Q_{cond} is the condenser duty and $\Delta^r H$ is the heat of reaction. It is concluded from this study that the number of reactive stages and the location of the feed stage are highly dependent on the extent of reaction ε in the RD column. Thus, the determination of the optimal feed stage is possible by connecting the bottom difference point and the final difference point of the rectifying section, which in turn depend on the assumed extent of reaction on each stage (Lee *et al.*, 2000*b*).

McCabe-Thiele method. This method is used to assess qualitatively the impact of changing a design variable (Lee *et al.*, 2000*c*). For the RD case, two main features are tracked to sketch the diagram for a binary mixture of reactants undergoing an isomerization reaction and under CMO assumption,

- the intersection point of the operating line with the $y = x$ line defines the *reactive cascade difference point*, which moves proportionally as the ratio molar extent of reaction to product flowrate (*i.e.* $x_n = x^D - \varepsilon_n/D$); where n denotes the stage number,
- the heat supplied by the reaction decreases the slope of the operating line provided that the location of the reactive cascade difference point is not changed.

A simplified procedure for sketching the McCabe-Thiele diagram is depicted in figure 3.4 for an isomerization reaction.

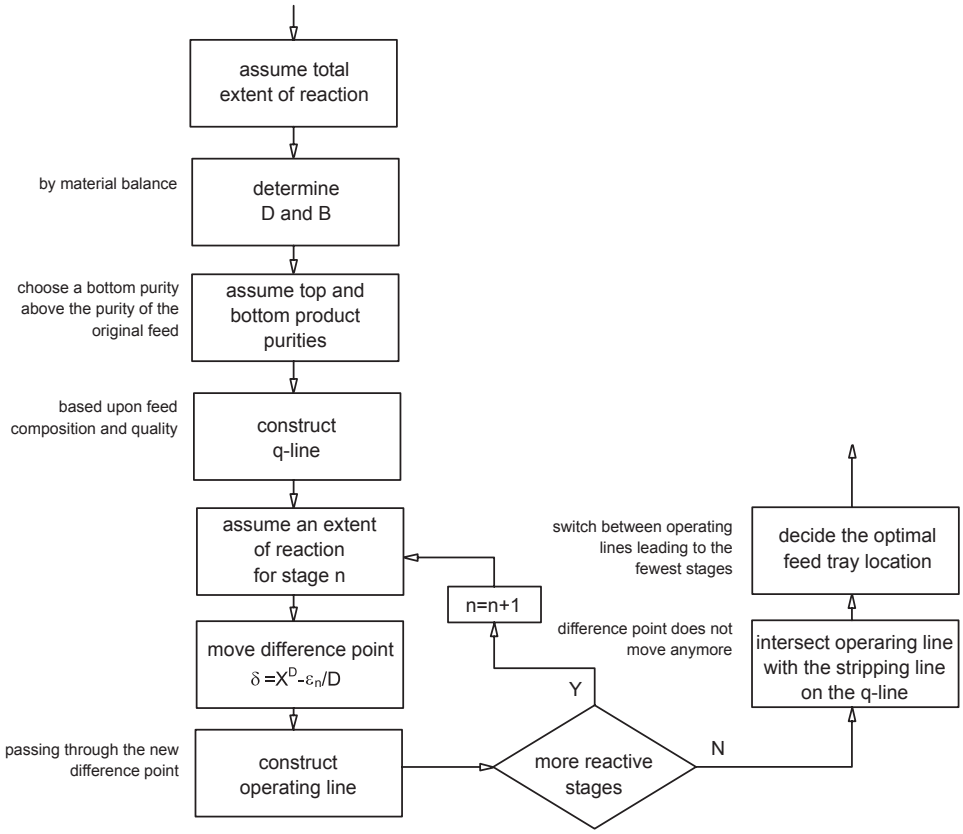

Figure 3.4. Procedure for sketching the McCabe-Thiele diagram. **Systems features:** isomerization reaction of the type $A \rightleftharpoons 2B$ (adapted from Lee *et al.* (2000*c*)).

Advantages: (*i*) these methods allow a transparent visualization of tray-by-tray calculations; (*ii*) they might be fundamental tools for the conceptual design of RD column; and (*iii*) they allow one to visualize the impact of the location of the reactive sections and the feed location within the column.

Limitations:(*i*) these methods are exclusively applied to isomerization reactions; and (*ii*) they are limited by their inherent graphical nature.

3.2.8 Phenomena-Based Approach

According to this method -proposed by Hauan (1998)- three independent phenomena take place simultaneously in a RD column: mixing, separation and reaction (Hauan and Lien, 1996; Westerberg *et al.*, 2000). These phenomena may be represented by vectors (figure 3.5) and allow the description of the total process profile of the system as a

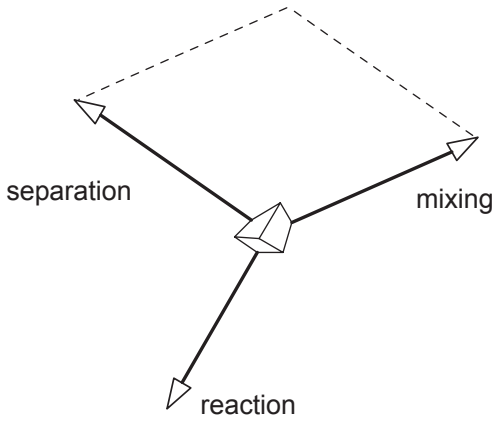

Figure 3.5. Schematic representation of the phenomena vectors in the composition space.

trajectory in the composition space for a control volume moving through a complete sequence of process units.

Thus, each step along the profile may be represented by the vectorial addition of the *phenomena vector* mixture ($\overrightarrow{M}$), separation ($\overrightarrow{S}$) and reaction ($\overrightarrow{R}$),

$$\frac{dx}{dt} = \overrightarrow{M} + \overrightarrow{S} + \overrightarrow{R}, \qquad \text{with } x(0) = x_0, \tag{3.21}$$

where x is the phase composition and the phenomena vectors are given by,

$$\begin{aligned}
\overrightarrow{M} &= \hat{\mathcal{M}} \times \begin{bmatrix} x_1^{\text{feed}} - x_1^0 \\ \vdots \\ x_{n_c}^{\text{feed}} - x_{n_c}^0 \end{bmatrix}, \\
\overrightarrow{S} &= \hat{\mathcal{S}} \times \begin{bmatrix} x_1 - y_1 \\ \vdots \\ x_{n_c} - y_{n_c} \end{bmatrix}, \\
\overrightarrow{R} &= \hat{\mathcal{R}} \times \begin{bmatrix} \nu_1 - x_1^0 \times \sum \nu_i \\ \vdots \\ \nu_{n_c} - x_{n_c}^0 \times \sum \nu_i \end{bmatrix},
\end{aligned} \tag{3.22}$$

where superscripts feed and 0 denote feed and initial values respectively, $\hat{\mathcal{M}}$ is the length of the mixing vector and is determined by the relative amount of material in the streams being mixed, $\hat{\mathcal{S}}$ is a matrix reflecting average mass transfer rates and $\hat{\mathcal{R}}$ is a scalar calculated from catalyst activity, hold-up, temperature and pressure. Each vector has a unique local direction (*i.e.* process feasibility) and vector length (*i.e.* process efficiency). Vector directions are calculated by physical and chemical data only, whereas vector lengths depend on the operating parameters and design variables.

Description: any composition change in the system due to chemical reaction may be represented by a straight line from the singular point, termed *difference point* (*i.e.* $x^s = \nu / \sum \nu$), through the local composition x^0 (Hauan *et al.*, 2000*b*),

$$x = x^0 + (x^s - x^0) \times \frac{\varepsilon \sum \nu}{n^0 + \varepsilon \times \sum \nu}, \tag{3.23}$$

where n is the total number of moles.

As the local compositions may be those of feeds and chemical reaction products, the composition in the desired point may be expressed as a normalized linear combination of the reaction difference points and distillate-, bottoms- or feed-composition vectors. From expression 3.21, a kinetic fixed point occurs when the vectorial contributions of the nonzero phenomena balance each other,

$$\frac{dx}{dt} = \overrightarrow{M} + \overrightarrow{S} + \overrightarrow{R} = 0, \qquad \text{with } x(0) = x_0. \tag{3.24}$$

Fixed points, which become evident by the presence of flat concentration profiles for large portions of the column, are by no means desired in RD and indicate a weak design or operation. Therefore, several ways to move away from a fixed point in the composition space are suggested,

- altering the mixing vector: by changing process variables (*e.g.* reflux and reboil policies, external feeds and hold-ups),
- altering the reaction vector length: by manipulating process variables (*e.g.* catalyst density, hold-up) or by introducing nonreactive stages in the reactive zone,
- incorporating pumparound reactors: in order to avoid a counter-productive separation vector.

Advantages: (*i*) only physical and chemical data are required to estimate the phenomena vectors, which are independent of the structural design of the unit; and (*ii*) this approach allows the designer to assess independently the effect of equipment structure and operating policies on the composition change in RD.

Limitations: (*i*) although this method is driven by fundamental considerations, its applicability requires further studies.

3.2.9 Scalar/Vectorial Difference Points Technique

The concepts of reactive cascade and scalar/vectorial difference points in reactive cascades (*cf.* explanatory note 3.2) have been successfully applied by Hauan *et al.* (2000*a*); Lee *et al.* (2000*a*) and Lee and Westerberg (2000) in the design of RD processes.

Reactive cascade difference points are defined as the combined points of stoichiometric coefficients vectors and product compositions. For the isomolar reaction $2R \rightleftharpoons P_1 + P_2$, the difference points in the rectifying and stripping sections are given by,

$$\begin{aligned} \delta_{R,n}^{\text{rect}} &= \frac{D \times x^{D} + 2\varepsilon_n(\mathbf{cR} - \mathbf{cP})}{D + 2\varepsilon_n - 2\varepsilon_n}, \\ \delta_{R,n}^{\text{strip}} &= \frac{B \times x^{B} + 2\varepsilon_n(\mathbf{cR} - \mathbf{cP})}{B + 2\varepsilon_n - 2\varepsilon_n}, \end{aligned} \tag{3.25}$$

where the material balances are estimated as follows,

$$\begin{aligned} &\text{rectifying:} \quad V_{n+1} \times y_{n+1} = x_n \times L_n + (D + 2\varepsilon_n - 2\varepsilon_n)\delta_{R,n}^{\text{rect}}, \\ &\text{stripping:} \quad V_s \times y_s = x_{s-1} \times L_{s-1} - (D + 2\varepsilon_s - 2\varepsilon_s)\delta_{R,s}^{\text{strip}} \end{aligned} \tag{3.26}$$

where subscripts s and n denote the number of stages in the stripping and rectifying sections, respectively. The difference points move parallel to the vector $(\mathbf{cR} - \mathbf{cP})$, in the direction defined by the dominant chemical reaction.

Note 3.2. Reactive cascade difference points

Assumptions: (*i*) known top and bottom compositions; (*ii*) known reflux ratio; (*iii*) CMO assumption; and (*iv*) chemical reaction of the type $2R \rightleftharpoons P_1 + P_2$.

Based on rigorous graphical considerations, the number and location of the reactive and nonreactive stages is obtained. For the system studied by Lee and Westerberg (2000), the reaction conversion of the feed stage is found to be always larger than that of any single stage in the rectifying and stripping sections. This situation allows one to guarantee the conversion on the feed stage at any reflux ratio. The location of the bubble point curve with respect to the chemical equilibrium curve plays a key role in the feasibility of the process within the stripping and rectifying sections. Thus, if the bubble point curve lies to the right of the reaction equilibrium curve, the rectifying section shows a better performance towards reactants' conversion than that of the stripping section. In this case, the forward reaction always takes place and enhances the separation task.

This approach is tested in the gas-phase disproportionation of toluene and in the dehydratation of methanol into water and dimethyl ether. In the first case study the most competitive configuration is reported to be the reaction zone in the stripping and feed sections. The effect of the reaction equilibrium constant is analyzed in the second example, resulting in feasible configurations with a single reactive stage.

Description [for a given phase and reaction equilibria in a stage RD column]: (*i*) for a liquid phase chemical reaction at the operating pressure P draw the reaction equilibrium and the bubble point curves (for gas phase chemical reactions, the dew point curve should be drawn and an equivalent procedure should be followed (Lee and Westerberg, 2000)); (*ii*) specify the top and bottom compositions, reboil and reflux ratios; (*iii*) step up/down from the feed stage to the top/bottom stage; (*iv*) from graphical considerations (according to expressions 3.25, 3.26 and phase equilibrium relationship), the accumulated extents of reactions for stripping/rectifying sections are determined; (*iv*) the liquid composition on the tray is calculated; and (*v*) tray-by-tray

calculations are performed upwards/downwards until the calculated liquid composition equalizes the top/bottom product composition.

3.3 Optimization-Based Methods

This second group of design methods is composed of those methodologies, which are supported by the power of computational subroutines and take into account important elements of an overall design strategy (*e.g.* types of phase equilibrium, number of components, occurrence or not of chemical reaction on a given stage) (Giessler *et al.*, 1998). In this category, the work of Ciric and Miao (1994); Ciric and Gu (1994); Pekkanen (1995); Cardoso *et al.* (2000); Bessling *et al.* (1997); Seferlis and Grievink (2001); Bansal *et al.* (2000); Bansal (2000); Bedenik *et al.* (2001); Poth *et al.* (2001); Frey and Stichlmair (2001); Stichlmair and Frey (2001); Gumus and Ciric (1997) and Georgiadis *et al.* (2002) compile the fundamentals of this design approach. This section gives an individual description of the methods and concludes with the advantages and limitations of this design method category.

3.3.1 Mixed-Integer Nonlinear Programming (MINLP)

This method is particularly helpful to find fully or partially optimized solutions for RD design variables (Malone and Doherty, 2000). The *objective function* for the RD problem is commonly composed of two basic terms: annual operating cost (*e.g.* consumption of raw materials, steam and cooling water) and the annualized investment (*i.e.* column, internals, reboiler and condenser). The *constraints* are formed from the MESH equations on each tray, material balances at the top and bottom of the column, kinetic and thermodynamic relationships and logical relationships between process variables and the number of trays.

Assumptions: (*i*) the vapor and liquid phases are in equilibrium on each tray; (*ii*) no reaction takes place in the vapor phase; (*iii*) the liquid phase is always homogeneous; (*iv*) the enthalpy of liquid streams is negligible; (*v*) the heat of evaporation is constant; (*vi*) temperature dependence of the reaction rates can be expressed in Arrhenius form; and (*vii*) the cost of separating products downstream is given by an analytical function.

The solution to the RD problems results in the optimum number of trays, the optimal feed tray location, reflux ratio, condenser and reboiler duties and liquid hold-ups on each tray. Since the model contains both continuous (*e.g.* temperature and composition) and discrete (*i.e.* number of trays) design variables, it should be solved by MINLP optimization technique.

Description: (*i*) a master sub-problem decomposition approach selects integer variables (*i.e.* number of trays) in a master program; and (*ii*) an optimal column design is

obtained with a fixed number of trays in the primal problem.

Due to their combinatorial nature, MINLP problems have been lately tackled using evolutionary algorithms (*e.g.* genetic algorithm, simulated annealing and evolution strategies), which require only information regarding the objective function (Costa and Oliveira, 2001). However, these novel approaches demand huge computational time and lack robustness when solving highly constrained problems.

Ciric and Gu (1994) present a MINLP-based approach for the design of RD columns for systems where multiple reactions take place and/or where reactive equilibrium or thermal neutrality cannot be assured. This method is based on the combination of a rigorous tray-by-tray model and kinetic-rate-based expressions to give basic constraints of an optimization model that minimizes the total annual cost. The major variables are the number of trays in the column, the feed tray location, the temperature and composition profiles within the column, the reflux ratio, the internal flows within the column and the column diameter.

Lately Poth *et al.* (2001) apply MINLP technique to the synthesis of MTBE and compare the optimal processes for the assumption of chemical equilibrium and kinetically limitations. Their results show that the total cost of the kinetic column is higher than that of the equilibrium case. Cardoso *et al.* (2000) apply a simulated annealing-based algorithm to solve a non-equilibrium RD column in the synthesis of ethylene glycol. The results obtained from this approach coincide satisfactorily with those reported by Ciric and Gu (1994) using commercial optimization packages. Pekkanen (1995) applies a local optimization algorithm to take advantage of the large number of degrees of freedom ($\geqslant 3 + n_c$) in the design of RD columns. In that study, the stage hold-ups and tray efficiencies are taken as optimization variables and the local optimum is found by tracking the directions of the concentration vectors in successive stages. Frey and Stichlmair (2001) optimize the RD column for the synthesis of methyl acetate in the kinetically controlled regime with respect to total annualized cost. Multiple feeding of reactants is allowed in the optimization routine leading to a decrease in the energy demand. Stichlmair and Frey (2001) design RD columns for the synthesis of MTBE and methyl acetate. Their starting point is the definition of the process superstructure, which in turn is derived from thermodynamic fundamentals (*e.g.* stoichiometric lines and lines of possible reactive azeotropes). A generalized modular representation for process synthesis is presented and extended by Papalexandri and Pistikopoulos (1996) and Ismail *et al.* (2001), respectively. That approach is supported by fundamental mass and heat transfer principles, which allow the definition of a *multipurpose mass/heat transfer module*. The optimized combination of building blocks defines the process superstructure. The effectiveness of this steady state approach is tested in homogeneous and two phase-reactions, absorption/extraction and RD processes. Ismail *et al.* (2001) include Gibbs free energy-based driving forces as constraints to guarantee the feasibility

of the reaction/separation/RD processes. The design of RD units with VLL equilibrium is studied by Gumus and Ciric (1997). Their optimization problem is formulated as a MINL-bilevel exercise, whose underlying feature involves the development of a single-level optimization problem. The solution of the single-level problem is a lower bound for the solution of the bilevel problem. The objective function is the Gibbs free energy on each tray subjected to the mass, energy balances, constitutive expressions and integer variables defining the number of trays at the minimum total annualized cost.

3.3.2 Orthogonal Collocation on Finite Elements (OCFE)

MINLP has been found to be troublesome for units with large number of trays and for the simultaneous design of more than one distillation unit due to the considerable computational time required for attaining the solution (Seferlis and Grievink, 2001). Furthermore, special attention must be paid in the MINLP model formulation and initial guesses outside the feasibility domain may lead into convergence difficulties. OCFE techniques is suggested by Seferlis and Grievink (2001) for the design and optimization of staged RD columns. This approach transforms the discrete number of stages in the column into a continuous variable and treats the composition and temperature as functions of the position.

Assumptions: (*i*) complete mixing of each phase at each stage; (*ii*) constant liquid hold-up and no vapor hold-up at each stage; (*iii*) no liquid entrainment from stage to stage; (*iv*) adiabatic stages; and (*v*) thermal equilibrium between the liquid and vapor streams leaving each stage.

Description: (*i*) the column is separated into sections; (*ii*) each column section is divided into smaller sub-domains (*i.e.* fine elements); (*iii*) for each fine element a number of collocation points is specified, where the mass and energy balances are exclusively satisfied; (*iv*) the collocation points are chosen as the roots of the discrete Hahn family of orthogonal polynomials; and (*v*) Lagrange interpolation polynomials are used within each finite element to approximate the liquid- and vapor- component flow rates, the total stream flow rates and the liquid and vapor stream enthalpies.

In the study by Seferlis and Grievink (2001), the oscillatory behavior in the composition space of highly-diluted components is circumvented by transforming the molar fractions of those components. Additionally, a second alternative is proposed, where inert components with low concentrations are removed from the energy and mass balances. Both approaches are found to increase the stability and robustness of the solution at the same level of accuracy. This technique is successfully applied to the design of a RD column for the synthesis of ethyl acetate (Seferlis and Grievink, 2001), using a single element with four collocation points in the rectifying section, three elements with three collocation points per element in the reactive section and two elements with two

collocation points per element in the stripping section. The study concludes that the production of ethyl acetate is strongly favored by large liquid-stage hold-ups in the reactive and stripping sections because of the relatively low rate of reactions. Furthermore, a double-column production flowsheet is selected, which allows the production of high purity ethyl acetate.

3.3.3 Mixed Integer Dynamic Optimization (MIDO)

In general a chemical process that shows poor ability of meeting control objectives gives rise to missing opportunities with respect to economic performance and satisfaction of product specifications. This fact may imply the existence of a trade-off between those processes designed with respect to control performance considerations and those driven by economic issues. In order to circumvent this duality, relevant improvements are recently done towards the integration (Russel *et al.*, 2000) and simultaneous optimization (Georgiadis *et al.*, 2002; Bansal, 2000; Bansal *et al.*, 2000) of the design and control tasks. The general design and control problem (*cf.* explanatory note 3.3) involves finding parameters (continuous and/or integers) that define the RD column and control tuning parameters at the minimum economic cost and with an acceptable dynamic performance in the presence of disturbances. The continuous parameters include column diameter, reboiler and condenser areas and tuning parameters (gain K, set-point SP and reset time τ_c), while integer variables -$\tilde{y}$- involve the existence or not of catalyst on a given stage ($f_{rx}^k \in \{0,1\}$). According to Georgiadis *et al.* (2002), the simultaneous approach takes advantage of the interactions between design and control and provides a fully operational process design that is cheaper and more controllable than that generated by the sequential approach.

Description: (Bansal *et al.*, 2000; Bansal, 2000; Georgiadis *et al.*, 2002) (*i*) set the termination tolerance, ϵ; initialize the iteration counter, $k = 1$; lower bound, $LB = -\infty$; and upper bound, $UB = \infty$; (*ii*) for fixed values of the integer variables, $\tilde{y} = \tilde{y}^k$, solve the k^{th} primal problem to obtain a solution, J^k. Omit the search variables and constraints that are superfluous due to the current choice of integer variables. Set $UB = \min(UB, J^k)$ and store the continuous and integer variables corresponding to the best primal solution; (*iii*) solve the primal problem at the solution found in step (*ii*) with the full set of search variables and constraints included. Convergence will be achieved in one iteration. Obtain the Lagrange multipliers needed to construct the k^{th} master problem; (*iv*) solve the k^{th} master problem to obtain a solution η^k. Update the lower bound, $LB = \eta^k$; and (*v*) if $UB - LB \leq \epsilon$, or the master problem is infeasible, then stop. The optimal solution corresponds to the values stored in step (*ii*). Otherwise set $k = k + 1$, $\tilde{y}^{k+1}$ equal to the integer solution of the k^{th} master problem and return to step (*ii*).

Mixed-Integer Dynamic Optimization Problem

$$
\begin{aligned}
\text{Obj.:}\quad & \min_{z^p, z^c, \tilde{y}} J(x(t_f), u(t_f), d(t_f), y(t_f), p^p(t_f), p^c(t_f), z^p, z^c, \tilde{y}, t_f), \\
\text{s.t.}\quad & 0 = f(\dot{x}(t), x(t), u(t), d(t), y(t), p^p(t), p^c(t), z^p, z^c, \tilde{y}), && t \in [t_0, t_f] \\
& 0 = g(x_d(t), x_a(t), u(t), d(t), y(t), p^p(t), p^c(t), z^p, z^c, \tilde{y}), && t \in [t_0, t_f] \\
& 0 \geq h(x(t), u(t), d(t), y(t), p^p(t), p^c(t), z^p, z^c, \tilde{y}), && t \in [t_0, t_f] \\
& 0 \geq i(x(0), u(0), d(0), y(0), p^p(0), p^c(0), z^p, z^c, \tilde{y}), && t \in [t_0, t_f], \\
& z^p \in Z^p, \quad z^c \in Z^c, \quad \tilde{y} \in [0,1] \\
& p^p(t) \in P^p \subseteq \mathbb{R}^{p^p}, \quad p^c(t) \in P^c \subseteq \mathbb{R}^{p^c} && t \in [t_0, t_f] \\
& x(t) \in X \subseteq \mathbb{R}^x, \quad x(0) \in X \subseteq \mathbb{R}^x,
\end{aligned}
\tag{3.27}
$$

where the objective function $J(\cdot)$ represents the overall cost of the RD processes (*i.e.* capital and operational costs), the equalities $f(\cdot)$ and $g(\cdot)$ comprise the differential and algebraic expressions, respectively; $h(\cdot)$ represents the path constraints that must be satisfied at all times during the system operation, $i(\cdot)$ is the set of initial conditions, x denotes the set of state variables, u is the set of input variables, y is the set of output variables, d is the set of disturbance variables, p^p and p^c are the sets of time-varying variables for the process and control scheme, respectively; z^p and z^c are the sets of time-invariant parameters for the process and control scheme, respectively; and $\tilde{y}$ is the set of integer variables.

Note 3.3. Mixed-integer dynamic optimization problem formulation (Bansal *et al.*, 2000; Bansal, 2000).

Advantages: (*i*) optimization-based approaches are applicable for multiple reactions and where reactive equilibrium or thermal neutrality cannot be assured; and (*ii*) it allows the generation of optimum designs with respect to economics and controllability.

Limitations: (*i*) special care should be paid to the model formulation and the physical significance of the solution; scaling of optimization variables might be required to reduce computational effort; (*ii*) the optimization problem might be difficult to solve; (*iii*) huge computational time can be required for multiple alternative optimizations; (*iv*) it is difficult to perform sensitivity analysis of the optimum solution; and (*v*) local limitations can be found when the initial guess lies outside the feasibility region.

3.4 Evolutionary/Heuristic Methods

A third trend of conceptual design approaches may be identified from the evolution of RD as a derivation from conventional distillation processes. As stated by Subawalla and Fair (1999), residue curve map techniques and fixed-point algorithms have been traditionally very useful tools for preliminary screening and design of RD systems. However, they cannot be used for detailed design, since they rely on several limiting assumptions and do not account for the special nature of reactive column internals. Those authors propose a *post*-design algorithm to estimate parameters such as column pressure, reactive zone location, catalytic mass, reactant feed location, reflux ratio, column diameter, number of equilibrium stages and packed height. Moreover, the feasibility of up-stream

pre-reactor is taken into account. For equilibrium-limited reactions, the following issues are addressed (Subawalla and Fair, 1999),

- **use of a pre-reactor**: incorporating a pre-reactor could profitably enhance the conversion of equilibrium-limited reactions, especially when it handles a substantial part of the reaction duty.

  ▷ Rule of thumb 1: use a pre-reactor when reaction rate at 80% conversion is more than half the initial rate.

- **operating pressure**: the column pressure ranges from the condenser pressure (determined by the condenser coolant temperature) to the reboiler pressure (fixed by the heating medium temperature and the column pressure drop). In general terms and within this range, the operating pressure depends on the reaction temperatures, relative volatility and the effect of pressure on azeotropes. An upper pressure limit exists beyond which rates decrease because of reaction depletion due to relative volatility and/or azeotropic effects and due to departure from chemical equilibrium.

- **reactive zone location**: this parameter represents the best trade-off between conversion and product purity. For instance, when the limiting reactant is the most volatile component and the product is the heaviest component, the reactive zone is located towards the top of the column. For high purity requirements, stripping or rectifying sections must be incorporated either below or above the reaction zone.

  ▷ Rule of thumb 2: a reactive zone section should be located where the concentration of at least one reactant (preferably the limiting reactant) is the maximum.

- **feed location**: a right choice of feed location guarantees high concentrations of reactants in the reactive zone, as shown in figure 3.6 for the synthesis of methyl acetate. The following rules of thumb might be suggested:

  ▷ Rule of thumb 3: if the reactants are the most volatile components, then the feed should be introduced at the bottom of the reactive zone,

  ▷ Rule of thumb 4: if the volatilities of the reactants are very different, an additional feed location may be required to ensure stoichiometric reactant quantities

  ▷ Rule of thumb 5: a pre-reacted product-containing feed enters the column at some distance from the reactive zone, ensuring thereby that separation between reactants and products takes place on stages between the feed point and the reactive zone.

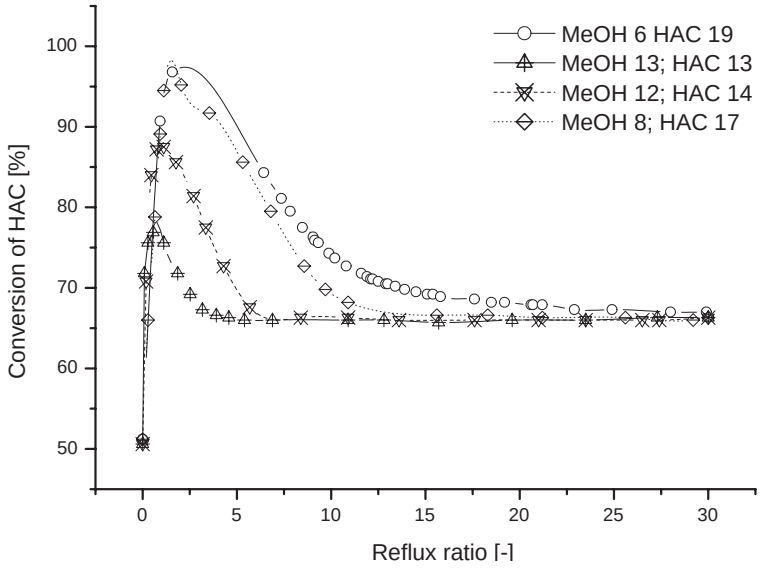

Figure 3.6. Influence of feed location on reactant conversion. **Systems features:** synthesis of methyl acetate from methanol and acetic acid. **Legend:** the numbers in the data series denote the feed tray location from the top of the column. Conversion reaches a maximum when the feed flows are located directly below and above the reactive section of the column. (adapted from Bessling *et al.* (1998)).

- **reactant ratio**: reactants' requirements can be calculated from product specifications, desired conversion and azeotropic compositions at different operating pressures.

- **catalyst mass**: the minimum catalyst requirements are determined by simulating a series of isothermal PFRs and ideal separators in series. As depicted in figure 3.7, the feed to the first PFR contains the necessary quantity of unconverted reactants; the partially reacted effluent is fed to an ideal separator that completely separates reactants from products. This procedure is repeated for different temperatures until the desired conversion is reached, where the operating temperature defines the minimum amount of catalyst. Since there is a relevant influence of operating temperature on catalyst life, chemical equilibrium and column pressure, the adopted operation temperature value differs from the highest possible value. In order to account for the non-isothermal operation and for the imperfect separation on each stage, the mass of catalyst should be 20-30% greater than the estimated value. Additionally, inadequate catalyst volume reduces residence time and gives poor conversion.

- **number of theoretical stages**: the number of stages may be estimated to

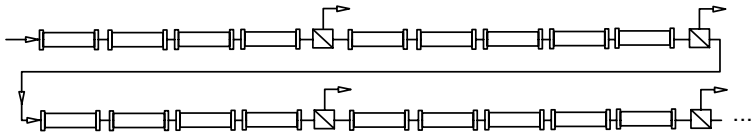

Figure 3.7. Column internals' driven design: ideal reactor-separator train for the estimation of minimum catalyst requirements. The partially reacted effluent is fed to an ideal separator that completely separates reactants from products.

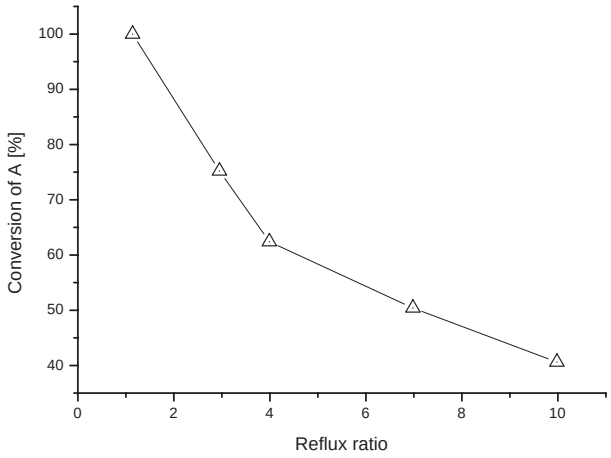

Figure 3.8. Relation between conversion and reflux ratio for a RD column. **Systems features:** chemical reaction $A + B \rightleftharpoons C + D$; components volatilities: A/B/C/D = 4/1/8/2. (adapted from Bessling *et al.* (1997)).

a certain extend by short-cut methods (*e.g.* Fenske Underwood), especially for the nonreactive zones (stripping and rectifying). Note that there is an optimum number of reactive stages, which allows one to obtain the highest reaction extent for given vapor flow and column height (Solokhin and Blagov, 1996).

- **reactive zone height and column diameter:** the diameter of the column is determined by the flooding velocity, vapor-liquid traffic, pressure-drop and packing catalyst density; the reactive zone height, on the other hand, depends on the catalyst mass, packing catalyst density and column diameter.

- **reflux ratio**: in RD columns, the rate and ratio of reflux play an important role in reaction and separation phenomena. For equilibrium-controlled systems, a high reflux rate increases the separation of products from reactants, thereby increasing the reaction driving force. As noted in figure 3.8, excessive reflux leads

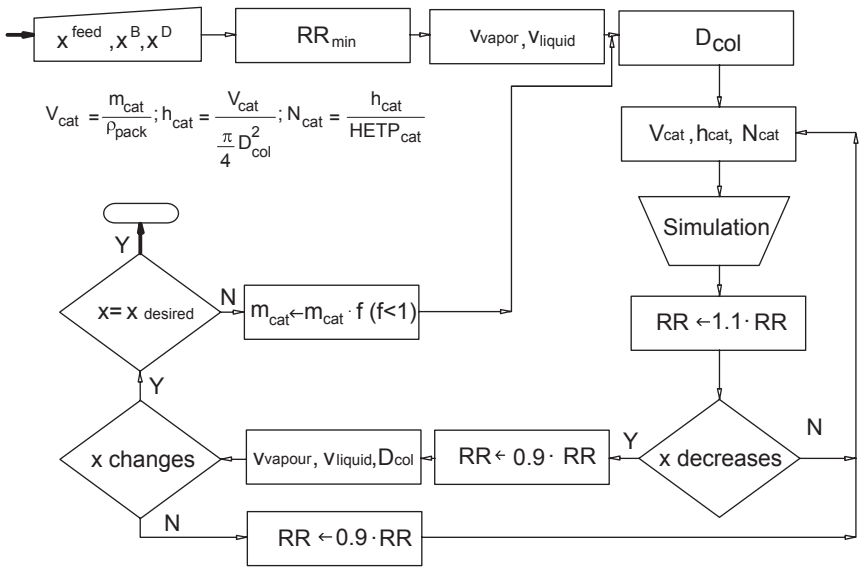

Figure 3.9. Procedure to estimate reactive zone height, reflux ratio and column diameter for a catalytic distillation column (adapted from Subawalla and Fair (1999)).

to operating problems and insufficient reaction hold-up, leading to incomplete conversion.

▷ Rule of thumb 6: use a factor of 1.2-1.4 × the minimum ratio.

Short-cut methods derived from conventional distillation have been found to be inappropriate for the estimation of reflux ratio for reactive case and new approaches have been adopted. Methods derived from the boundary-value approach (*cf.* §3.2.4) allow the determination of the minimum and real reflux ratio, which are key factors in the determination of vapor and liquid velocities. The reflux ratio can be calculated using an iterative procedure, described in Subawalla and Fair (1999) and summarized in figure 3.9.

- **reboil ratio**: the feasibility of RD processes has been closely related to the minimum reboil ratio ($RS_{\min}$), at which the composition of the rectifying fixed point equals the composition of the stripping fixed point (Okasinski and Doherty, 1998). The reboil ratio normally ranges from 3 to 8 and reaches a minimum when plotted versus the total number of stages.

- **actual trays/packed height**: For the stripping and rectifying sections experimental tray efficiency or packing HETP should be used, whereas for the reactive section mass-transfer coefficients should be calculated from experimental data at the operating conditions of the system. In the event that thermo-physical data,

transport phenomena data and hydraulic models are available, non-equilibrium design approaches are found to provide a better agreement between experimentation and simulation.

The proposed approach may be extended by incorporating hydraulic models which account for the column capacity in terms of pressure drop and for mass-transfer efficiency estimations in terms of liquid hold-up, mass-transfer coefficients and interfacial area.

Advantages: this method estimates easily several equipment and/or operational variables.

Limitations: this method is basically a post-design algorithm and as such it requires an already defined process structure.

3.5 Concluding Remarks

Both the graphical and optimization-based design methods have already proven their potential in RD process design but have also shown some significant limitations. Graphical methods are fairly flexible in generating alternative designs at various design parameters, allowing the designer to define realistic bounds on them. Furthermore, the graphical nature of the methods clarifies the understanding of those fundamental issues in RD, which might be disguised by other approaches (*e.g.* reactive azeotropes). On the other hand, graphical methods are strongly limited by their graphical nature (*i.e.* $(n_c - n_{rx}) \leq 3$). Optimization-based methods overcome the last limitation and have successfully solved design problems, where multicomponent mixtures, multiple chemical reactions and multiple units are involved. However, additional caution is required in the problem formulation and inappropriate initial guesses of the optimization variables may lead into convergence difficulties. The evolutionary method proposed by Subawalla and Fair (1999) covers in more detail some physical aspects of the design of RD columns. However, this approach requires a pre-defined structure and accordingly the optimum design is not guaranteed.

Based on their assumptions, limitations and outputs a fingerprint chart was produced for the methods described in this chapter. From this qualitative plot (table 3.2) the following conclusions can be drawn: (*i*) most of the graphical methods provided fundamental insights on the feasibility of the RD process and define the initial process structure; (*ii*) economic considerations are taken into account exclusively by optimization-based methods; (*iii*) the availability of the process has not been included as design output by any method, since this temporal feature is normally dealt at the next level of engineering design; (*iv*) the heuristic-based methodology is based on an already designed process and is therefore a post-design tool; (*v*) most of the design methods have been developed for steady state operation; (*vi*) the initial effort required for optimization-based meth-

ods is far more significant than that for graphical approaches, but the output generated by the programming-based design is more comprehensive.

Due to the size and conceptual/computational complexity of the RD design problem, a single comprehensive design strategy might not be available for years to come. Almeida-Rivera and Grievink (2001); Almeida-Rivera *et al.* (2004*a*), however, propose an integrated design approach -termed *multiechelon design approach*. This strategy allows the designer to combine in a systematic way the capabilities and complementary strengths of the available graphical and optimization-based methods. As discussed in detail in the course of the coming chapters, this approach is supported by a decomposition in a hierarchy of imbedded design spaces of increasing refinement. Moreover, it constitutes the framework of a highly aggregated design methodology, which focuses on the RD design problem from a life-span perspective.

Mind journey to the scientific questions.

If we take a mind journey back to the engineering/scientific design question given at the beginning of this chapter, the following remark can be made. An overview and analysis of representative design methodologies are provided in this chapter. Based on identified opportunities, an integrated design approach is briefly mentioned, which offers the benefit of combining the capabilities and complementary strengths of available methodologies. The domain knowledge in RD design is addressed. Therefore, the material presented in this chapter contributes to the answering of Question 4.

Table 3.2. Qualitative fingerprint of the design methods used in reactive distillation. **Nomenclature.** G_1: Statics analysis; G_2: RCM; G_3: Attainable region G_4: Fixed-points; G_5: Reactive cascade; G_6: Thermodynamic-based; G_7: Conventional graphic techniques; G_8: Phenomena-based; G_9: Difference points; M_1: MINLP; M_2: OCFE; M_3: MIDO; H_1: Heuristics. **Key**. ■: applicable; □: nonapplicable/nonmentioned; ▲: original assumption relaxed by later contributions

	G_1	G_2	G_3	G_4	G_5	G_6	G_7	G_8	G_9	M_1	M_2	M_3	H_1
Input													
phase equilibrium model	■	■	■	■	■	■	■	■	■	■	■	■	■
chemical reaction equilibrium	■	■	■	■	■	■	■	■	■	■	■	■	■
chemical reaction kinetics	■	■	■	■	■	■	■	■	■	■	■	■	■
feed compositions	■	■	■	■	■	■	■	■	■	■	■	■	■
compositions of product streams	□	■	■	■	■	■	■	■	■	■	■	■	■
reboil/reflux ratios	□	□	□	□	□	□	□	□	■	□	□	□	■
initial spatial superstructure	□	□	□	□	□	□	□	□	□	■	■	■	■
type packing/hydrodynamic features	□	□	□	□	□	□	□	□	□	■	■	■	■
temporal disturbance scenario	□	□	□	□	□	□	□	□	□	□	□	■	□
Knowledge required													
Model assumptions													
phase equilibrium	■	■	■	▲	■	■	■	■	■	▲	■	■	□
negligible heat effects	■	■	□	▲	■	■	■	■	□	■	■	□	□
equilibrium controlled regime	■	■	□	■	■	■	□	■	■	□	□	■	□
kinetically controlled regime	□	■	■	■	■	■	□	■	■	□	□	□	□
steady state operation	■	□	□	□	■	■	■	■	□	■	■	□	□
multicomponent systems (≤ 3)	■	■	□	▲	□	□	■	□	■	□	□	□	□
single reaction	□	□	□	▲	□	■	■	□	■	□	■	□	□
constant molar overflow	■	□	□	▲	□	□	■	□	■	□	□	□	□
constant liquid holdup	□	□	□	▲	■	□	■	□	□	□	■	□	□
isomolar stoichiometry	□	□	□	▲	□	□	■	□	■	□	□	□	□
negligible axial dispersion	□	□	□	▲	□	□	□	□	□	□	■	□	□
constant volatilities	□	□	□	□	□	■	□	□	□	□	□	□	□
infinite vapor/liquid flows	■	□	□	□	□	□	□	□	□	□	□	□	□
film theory validity	□	□	□	■	□	□	□	□	□	□	□	□	□
constant mass transfer coefficients	□	□	□	■	□	□	□	□	□	□	□	□	□
Rules													
connectivity, units' selection	□	□	□	□	□	□	□	□	□	□	□	□	■
operating conditions	□	□	□	□	□	□	□	□	□	□	□	□	■
Output													
feasibility of the RD process	■	■	■	■	■	■	■	■	□	□	□	□	□
definition process superstructure	■	■	■	■	■	□	□	□	□	□	□	■	□

Continue in next page

Table 3.2. Qualitative fingerprint of the design methods used in reactive distillation (continuation). **Nomenclature.** G_1: Statics analysis; G_2: RCM; G_3: Attainable region G_4: Fixed-points; G_5: Reactive cascade; G_6: Thermodynamic-based; G_7: Conventional graphic techniques; G_8: Phenomena-based; G_9: Difference points; M_1: MINLP; M_2: OCFE; M_3: MIDO; H_1: Heuristics. **Key**. ■: applicable; □: nonapplicable/nonmentioned; ▲: original assumption relaxed by later contributions

	G_1	G_2	G_3	G_4	G_5	G_6	G_7	G_8	G_9	M_1	M_2	M_3	H_1
operating conditions (reflux, reboil)	□	□	□	■	□	□	■	■	□	■	■	■	■
number of (non-) reactive stages	□	□	□	■	□	□	■	□	■	■	■	■	■
location feed stages	□	■	□	■	□	□	■	□	■	■	■	■	■
location (non-) reactive azeotropes	□	■	□	■	□	□	■	□	□	□	□	■	□
determination MSS	■	□	■	□	□	□	□	□	□	□	□	□	□
Life-span perspective													
economic considerations	□	□	□	□	□	□	□	□	□	■	■	■	□
exergy efficiency considerations	□	□	□	□	□	□	□	□	□	□	□	□	□
controllability considerations	□	□	□	□	□	□	□	□	□	□	■	■	□
Nature of output													
structure	■	■	■	■	■	■	■	■	■	■	■	■	■
performance (economics)	□	□	□	□	□	□	□	□	□	■	■	■	□
physical behavior (operability)	■	■	■	■	□	□	□	□	□	□	□	■	□
physical behavior (availability)	□	□	□	□	□	□	□	□	□	□	□	□	□
Effort													
model complexity	□	□	□	□	□	□	□	□	□	□	■	■	□
implementation time	□	□	□	□	□	□	□	□	□	■	■	■	□
tools' complexity	□	□	□	□	□	□	□	□	□	■	■	■	□

Coming from previous page

"A problem clearly stated is a problem half solved."

Dorothea Brande, '*Becoming A Writer*' (1934)

4

A New Approach in the Conceptual Design of Reactive Distillation Processes[†]

The potential benefits of applying RD processes are taxed by significant complexities in process development and design. Several topics regarding these two activities are addressed in this chapter. The interactions between process development and design activities are considered first. The RD design problem is then formulated in the wider context of process development and engineering. The identification of requested output information from current methodologies results in the introduction of a set of performance criteria SHEET (safety, health, environment, economics, technology). The focus is on the design problem from a life-span perspective. A *multiechelon approach* is subsequently introduced, in which a hierarchy of embedded design spaces of increasing refinement is used and the strengths of current design methods are conjugated.

[†]Parts of this chapter have appeared in Almeida-Rivera *et al.* (2004*a*) and Almeida-Rivera and Grievink (2001)

Chapter 4

4.1 Introduction

When chemical reactions and physical separations have some overlapping operating conditions the combining of these tasks into a single process unit can offer significant benefits. These benefits may involve: avoidance of reaction equilibrium restrictions, higher conversion, selectivity and yield, removal of side reactions and recycling streams, circumvention of nonreactive azeotropes and a reduction in number of units (*i.e.* investment cost) and energy demands (*i.e.* heat integration) (Schembecker and Tlatlik, 2003; Subawalla and Fair, 1999; Stichlmair and Frey, 1999; Jimenez *et al.*, 2001; Malone and Doherty, 2000). However, there is a price to pay in terms of increased complexity in design and operations. The nonlinear coupling of reactions, transport phenomena and phase equilibria can give rise to highly system-dependent features, possibly leading to the presence of reactive azeotropes and/or the occurrence of steady-state multiplicities. The number of design decision variables for such an integrated unit will be high. Industrial relevance requires that design issues are not separated from the context of process development and plant operations. Hence, the design problem is addressed in this chapter from a process life-span perspective.

The starting point of this approach is the qualitative analysis of current design methodologies in RD presented in chapter 3. Table 3.2 clearly shows the complementary aspects of the graphical, programming-based and heuristic-based methods. The graphical methods are capable of generating feasible process structure options under somewhat idealized chemical and physical conditions. Optimization-based methods, once given a superstructure, can generate more detailed and complete designs from an engineering perspective and can even be used to strive to account for controllability aspects. Heuristic-based methodologies provide only rough estimates of the design variables and require a pre-defined process structure.

The complexity and full range of design variables in process integrated RD units are, as yet, not considered in the scope of the current RD design methods. Process integrated designs should take into account the economic and exergy-related interactions of the RD units with the process surroundings and comply with the desired dynamics and control of the overall process supply chain.

In view of the size and of the conceptual and computational complexity of a RD design problem, a single comprehensive design technique is unlikely to become available for some years to come. An integrated design strategy (Almeida-Rivera and Grievink, 2001; Almeida-Rivera *et al.*, 2004*a*) is introduced in the forthcoming sections. This design strategy allows the designer to combine, in a systematic way, the capabilities and complementary strengths of the available graphical and optimization-based methods. This integrated approach is embedded within a highly-aggregated design methodology, which is characterized by a set of performance criteria. In clear agreement with a life-

span perspective (*cf.* explanatory caveat in section §1.4) these criteria account for the economic, exergy-related and temporal performance of a design focussed on prevention of loss of resources.

It is worth mentioning here that the present contribution focuses on the definition of the RD process structure, paying less explicit attention to a detailed analysis of the actual dynamics of the unit, which might be described using non-equilibrium models. An extended review on this last topic can be found in the publications of Taylor and Krishna (2000); Krishnamurthy and Taylor (1985); Taylor and Krishna (1993, 2003). Furthermore, the temporal features of the process unit(s) (*e.g.* operability and availability) are not fully considered in the proposed methodology, as availability is foreseen to be taken into account at the next level of engineering detail.

Recalling the engineering and scientific design questions given in chapter 1, in this chapter we address question 5, namely,

- *What are the (performance) criteria that need to be considered from a life-span perspective when specifying a reactive distillation design problem?*

4.2 Interactions between Process Development and Process Design

The aim of *chemical process design* has, conventionally, been considered as the finding of equipment sizes, configurations and operating conditions that will allow for the economical, safe and environmental responsible conversion of specific feed stream(s) into specific product(s). This task is in principle carried out only by specifying the state of the feeds and the targets on the output streams of a system (Doherty and Buzad, 1992; Buzad and Doherty, 1995). Frequently, however, the design activity is found to be severely complicated by the difficulty of identifying feasible equipment configurations and ranges of suitable operating conditions. This situation can be explained by the fact that the design of chemical process units is only a constitutive part of a larger scale and, therefore, more complex problem: the joint consideration of process unit development and design. At this higher level of aggregation, the objective of the design problem includes sizing the unit and establishing the requirements of the design, screening the process feasibility and, at the top, identifying the process opportunities (figure 4.1).

From this point of view, two parallel and inter-related activities can be identified: the design program and the development program. For a given level of design detail all the design tasks should be considered from top (*i.e.* higher aggregation/process level) to bottom (*i.e.* low aggregation/unit level). The information leaving the design program is compared with the desired outputs. If an acceptable agreement exists the level of detail is increased and the same strategy is adopted. For non-acceptable outputs the

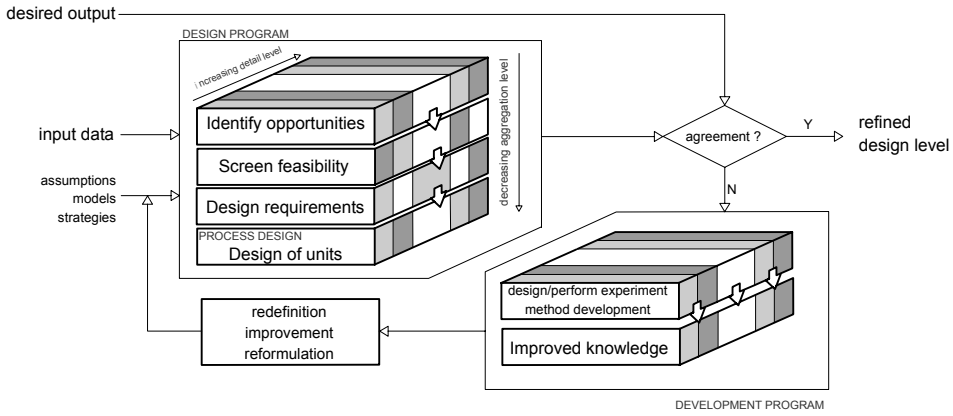

Figure 4.1. The design problem regarded as the combination of a design program and a development program.

loop is performed at the same level of detail after redefining/reformulating appropriate assumptions/models/generalities in the design program. This is attained by designing and performing an appropriate development program, which allows the designer to extend/improve/correct the existing knowledge and methodology (*e.g.* removing the uncertainties introduced by estimation of parameters).

Within the design program, the following design tasks are defined.

Identification of opportunities. This task permits one to select qualitatively the set of competing process technologies/equipment configurations, which might be used to convert the given feeds to the desired products. Schoenmakers and Bessling (2003*b*), for instance, use the physical/chemical characteristics of the system (*e.g.* reaction velocity and relative volatility) to choose the equipment configuration. Proven technologies together with novel configurations might arise at this stage (*e.g.* dividing wall columns, pump-around reactors, side-reactors, etc.) (Baur and Krishna, 2003; Krishna, 2003; Mutalib and Smith, 1998*a*,*b*).

Screening of feasibility. The feasibility of the selected opportunities is then screened with respect to the attainable products of a given set of feed streams. In this stage the concepts of attainable region (Feinberg, 1999; Nisoli *et al.*, 1997) and ∞ / ∞ approach (Westerberg and Wahnschafft, 1996; Fien and Liu, 1994; Güttinger and Morari, 1997; Güttinger, 1998; Güttinger and Morari, 1999*a*,*b*) might be used.

Design requirements. The set of functional requirements for the design can be deemed the basis of the design. This information involves the boundary conditions, the process structure, its physical behavior (*i.e.* operability and availability) and minimum performance (*e.g.* safety and economics).

Design of units. The final stage in the overall design problem involves defining the spatial and temporal variables of the unit(s), together with its (their) operation window(s) and mode(s) of operation.

4.3 Structure of the Design Process

Following the definitions given above it is noticeable that the first three tasks in the design program are related to the scope of design, whereas the last task involves essentially the design of the units. If the general design paradigm (Siirola, 1996*a*,*b*; Biegler *et al.*, 1997) is used as the framework for the design task, the overall design problem can be represented as a multistage goal-directed process, with dynamic flow of information between the design tasks, method development and knowledge development (figure 4.2).

In the case of RD, the design issues are far more complex than those involved in conventional distillation and may differ significantly from case to case. For instance, the design variables for conventional distillation include the number of trays, feed tray location and reflux ratio for a constant molar overflow system with single feed tray. In contrast, in a RD column the liquid hold-up is the major design parameter that determines the extent of reaction, the feed might be distributed within the unit and constant molar overflow can not be assumed unless the reaction is thermally neutral and stoichiometrically balanced (Ciric and Gu, 1994). All these facts have led to a smaller number of RD applications in the chemical industry (Gorissen, 2003), than might be expected given the economic benefits that this combined process offers (Doherty and Buzad, 1992; Taylor and Krishna, 2000; Georgiadis *et al.*, 2002). The endeavors of the RD scientific community have resulted in the development of design algorithms mostly based on equilibrium models applied to systems with simplified thermodynamics and reactions kinetics (Malone and Doherty, 2000; Okasinski and Doherty, 1998, 1997; Ung and Doherty, 1995*a*,*c*; Smejkal and Soos, 2002; Venkataraman *et al.*, 1990). Lately, however, non-equilibrium (NEQ) models have been developed to use for the accurate modeling of RD units, accounting for mass transfer limitations and the interaction between mass transfer and chemical reaction (Baur *et al.*, 2000, 2001*b*,*a*,*c*; Baur and Krishna, 2002, 2003; Higler *et al.*, 1998, 1999*a*,*b*; Higler, 1999; Higler *et al.*, 2000; Taylor and Krishna, 1993, 2000; Krishna, 2003; Krishnamurthy and Taylor, 1985; Taylor and Krishna, 2003; Wesselingh, 1997). Although NEQ-based models are highly recommended for a more realistic description of the process, especially in advanced stages of the design cycle, their implementation still relies on the designer's expertise. Furthermore, inappropriate parameters' estimators may introduce an increased number of uncertainties in the design problem.

Three core questions arise when reviewing the currently available design methods for RD processes,

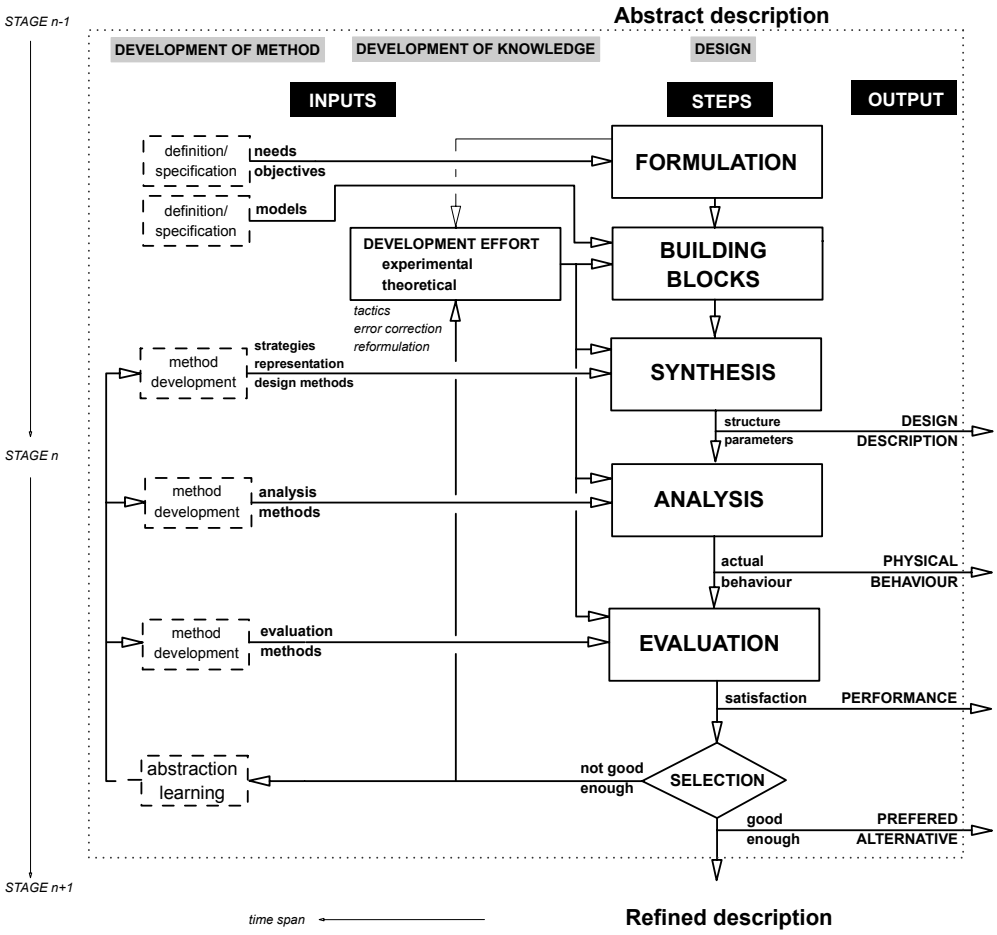

Figure 4.2. Overall design problem. Some ideas have been borrowed from Siirola (1996*b*), Biegler *et al.* (1997) and Bermingham (2003).

- *What is the output information requested from the design program?*
- *To what extent are the current methods able to provide this output?*
- *What resources (i.e. time wise, tools, costs) are required for the design program?*

In order to answer the first question, an extended list of output design variables (figure 2.7) is defined. The output variables together with the design problem statement in RD are summarized in table 4.1. It can be noticed that the desired outputs from the design program might be grouped into two main categories: those related to the process structure and performance (*i.e.* minimum economic performance) and those related to temporal features of the unit(s) (*i.e.* operability and availability). For the sake of clarity, the definitions adopted for each category are included in table 4.2.

Table 4.1. Design problem statement in reactive distillation

Designing a reactive distillation processes can be seen as the creative task of structuring and sizing the RD process providing a set of constraints, **windows** of feed specifications and **ranges** of product targets. The design problem might be formulated as follows,

- Given,
  - a set of components and chemical reactions
  - the characteristics of the feed streams (P, T, $\mathbf{x}$)
  - a set of different modes of operation for the process
  - a set of product specifications and safety and operational constraints for each mode of operation
  - data regarding the process economic targets based on prices of the products and the reactants as well as correlations for the investment and utility costs
  - ranges of possible values for the major model parameters and ranges of variation for key process variables
  - disturbances' scenarios
  - targets of availability of the unit(s)
- Determine,
  - the number/type of units and their tasks (*i.e.* reaction, distillation, reactive-distillation)
  - the connectivity of the units (*i.e.* flowsheet)
  - the type of internal contacting structure (*i.e.* continuous or structured packing, discontinuous or stages and dividing wall) and hydrodynamic features (*i.e.* ΔP, RTD, contacting area and volumetric hold-up)
  - the total number of stages in the column (*i.e.* reactive/nonreactive)
  - the location of the feed, withdraw and turn-around stages
  - the hold-up of the liquid phase for homogeneous reactions or the catalyst load for heterogeneous reactions
  - flow regimes, column diameter
  - control structure, controllers type and tuning parameters, placing of actuators and sensors
  - operating conditions (*e.g.* operating pressure)
  - reboil and reflux ratios
  - reactant ratio
  - economic, safety and environmental performance

Regarding the second question, the output space of the design methodologies under consideration is mapped in table 3.2. It should be noticed that most of the methodologies focus on the estimation of spatial variables, paying less explicit attention to the temporal response of the design. Moreover, no method up to now has addressed exergy considerations for the case of RD.

Table 4.2. Categories of information resulting from the design process in reactive distillation.

Structure	includes the complete spatial structure of the process, together with the control loops and operating conditions (*i.e.* ranges of temperature, pressure and reboil/reflux ratios).
Performance	involves the estimation of criteria related to: safety, health, environment and economics. Technological aspects are addressed in the next category. This group of criteria are referred to as **SHEET**.
Operability	involves the ability to operate the unit(s) at preferred conditions in spite of disturbances and changes in operational policies.
Availability	is rarely considered and is a measure of the degree to which the unit(s) is in an operable state at any time.

The amount of resources required for each methodology is directly dependent on their complexity (*cf.* table 3.2). Thus, as optimization-based methods are more sophisticated than graphical methods, they require far more significant effort, especially in modeling.

Based on the above a set of performance criteria is defined in the next section. These criteria allow one to focus on the design problem from a life-span perspective, embracing all the output categories of interest. An extended analysis of sustainability issues in conceptual design is given in Korevaar (2004).

4.4 Life-Span Performance Criteria

Aiming at a design methodology that addresses the problem from a life-span perspective, Grievink (2005) suggests a set of performance criteria. The motivation behind this perspective relies on the relevance of bearing in mind economic performance and potential losses over the process life span. Specifically, exergy-efficiency and responsiveness aspects in the operational phase need to be considered. As stated in section §1.4 we **only** consider sustainability aspects that are exclusively under the control of the process design and aim at the effective utilization of resources in the operational phase.

The SHEET set of criteria embraces issues related to safety, health, environment, economics and Technology. Although safety and health aspects are of utmost relevance for the chemical industry, we consider them to be implicitly outside the scope of our proposed methodology. We acknowledge that safety issues are key drivers for the innovation and technological breakthroughs that characterize intensified processes. Aiming at cheaper, cleaner, safer and simpler manufacturing of products, process intensification faces various challenges, such as the minimization of chemicals inventory and

the simplification of equipment complexity. Disasters such as, for example, the forty metric tons of methyl isocyanate released in Bhopal, 1984 should never have happened if a conscious safety-oriented process design had been carried out.

The starting point of our approach is the assumption that we (society) have learnt from past mistakes. Therefore, provided that safety and health issues are inherent in any responsible design approach, the remaining issues define a novel performance space. Thus, in the course of this dissertation we pay explicit attention to the EET performance space. Environmental considerations are directly linked to the minimization of mass, energy and exergy losses. Economic performance is translated quantitatively to the capital and operational costs of the design. The total annualized cost (TAC) is a convenient index for this. Technical considerations are grouped into two sub-categories: availability and operability. Availability embraces both reliability and maintainability, whereas operability includes process design attributes such as flexibility (steady-state), stability (multiplicity), controllability (dynamic) and switchability (start-up/shut-down). Controllability and switchability are lumped conveniently into a *responsiveness* criteria, which accounts for the dynamic response of the design in the presence of disturbances. A schematic representation of the performance criteria set is given in figure 4.3.

It is worth mentioning the link between our environment-related index and commonly used approaches such as life cycle assessment. According to our scope of research (see explanatory caveat in section §1.4) we limit our contribution to the design and operational space in the process life span. Thus, our focus is exclusively on the sustainability aspects that are under the control of the design and operational phases. In this regard, we aim at an operational efficiency, which means basically an effective utilization of resources in the process operation. Similar to life cycle assessment, we quantify the

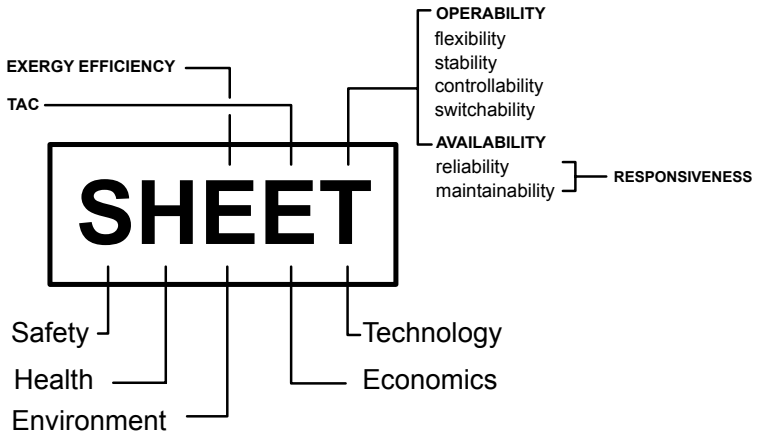

Figure 4.3. SHEET approach for the definition of life-span performance criteria.

materials, energy and exergy used and assess the environmental impact of those flows, via loss minimization. However, we explicitly do not address any sustainability issue related to feedstock selection, (re-)use of catalyst, (re-)use of solvents, among others. The thrust in our rather liberal approach is that these steps (*i.e.* design and operation) in the overall process life span (*i.e.* upper aggregation level '*from cradle-to-grave*') contribute largely to the overall life-span goals.

As these EET proposed performance criteria are of different natures, their formulation into an objective function involves the assignment of appropriate weighing factors. Assigning these values, however, is not a trivial task as it is an ultimate decision of the designer and made according to the requirements of the design problem (Clark and Westerberg, 1983). Pareto curve mapping (*cf.* explanatory note 8.1) is a convenient way to depict the effects of the weighing factors in a multi-objective optimization problem.

The design approach is introduced in the next section and represents the framework of the integrated design methodology.

4.5 Multiechelon Approach: The Framework of the Integrated Design Methodology

Due to the size and conceptual/computational complexity of the RD design problem, a single comprehensive design strategy may not be available for years to come. As a first step towards such an integrated design approach, Almeida-Rivera and Grievink (2001); Almeida-Rivera *et al.* (2004*a*) propose a *multiechelon design approach*, which allows the designer to combine, in a systematic way, the capabilities and complementary strengths of the available graphical and optimization-based methods. In general terms, the methodology is supported by a decomposition in a hierarchy of imbedded design spaces of increasing refinement. As a design progresses the level of design resolution can be increased, while constraints on the physical feasibility of structures and operating conditions derived from first principles analysis can be propagated to limit the searches in the expanded design space.

The general design paradigm of Siirola (Siirola, 1996*a*,*b*) is taken as the framework for the approach. As depicted in figures 4.4 and 4.5 different decisions are made at the different levels, supported by specific design tools. Furthermore, all the levels are inter-related by the flow of information coming from the lower levels. As one steps up the design pyramid, the scope of design decreases whereas the information flow is incremented.

The following design spaces are derived for this approach.

Space 1. Formulation: sustainability issues are considered, the basis of design (*e.g.* product and feedstock purities ranges, production modes, operating window

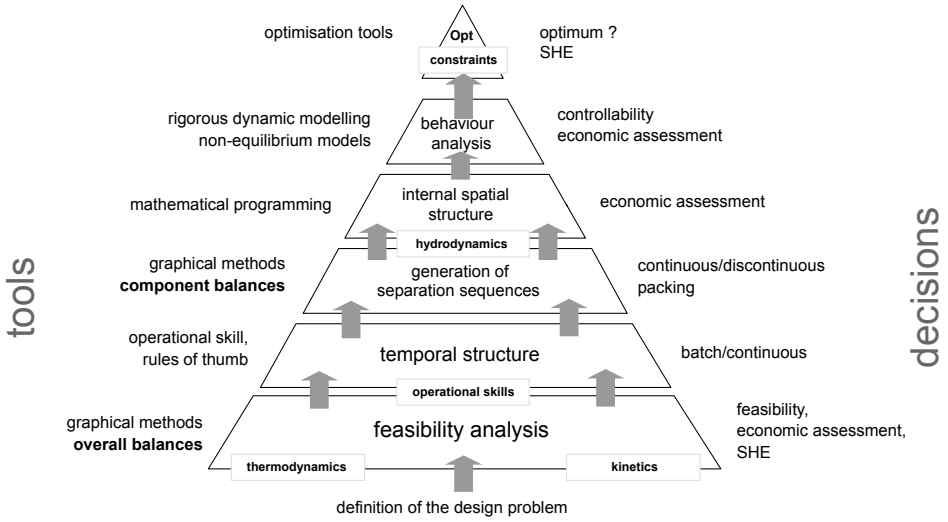

Figure 4.4. Multiechelon design approach in the conceptual design of RD processes: tools and decisions

and economics) are defined and the building model blocks are developed (*e.g.* thermodynamic, kinetic, hydrodynamic).
▷ this corresponds to levels Formulation and Building Blocks in figure 4.2.

Space 2. Feasibility analysis: using graphical methods the feasible product compositions are determined for a given set of input variables (*e.g.* feed composition and Damköhler number), incorporating all occurring phenomena (*e.g.* distillation boundaries and (non)-reactive azeotropy). If the process occurs to be feasible, economically attractive and satisfies SHE issues, proceed to level 3. Otherwise, stop the design and explore other processes alternatives.
▷ this corresponds to level Synthesis in figure 4.2.

Space 3. Temporal structure: the mode of operation (*e.g.* batch, continuous or semibatch) is selected based on operational skills, production requirements and supply chain dynamics.
▷ this corresponds to level Synthesis in figure 4.2.

Space 4. Generation of separation sequences: rigorous graphical methods allow the identification and organization of feasible column sequences. Their type of task is estimated (*e.g.* fully reactive, hybrid and nonreactive columns), together with the number of units and their connectivity. In this regard, each column might be considered as a compartment performing a given task. A decision has to be made related to the type of internal (*i.e.* continuous or

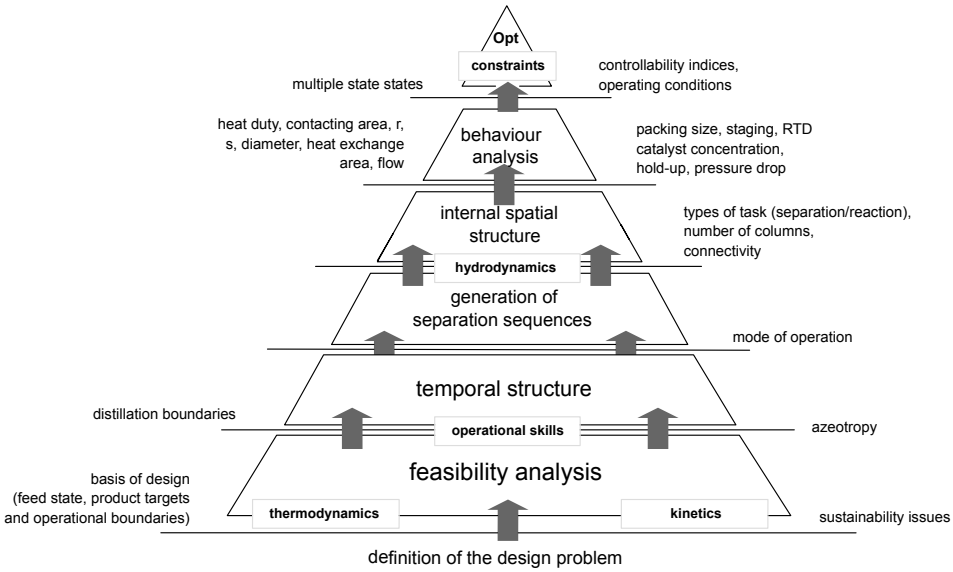

Figure 4.5. Multiechelon design approach in the conceptual design of RD processes: interstage flow of information.

structured packing and discontinuous or stages).
▷ this corresponds to level Synthesis in figure 4.2.

Space 5. Internal spatial structure: the process structure obtained from the previous level is used as the starting point for this stage. Using optimization-based methods continuous variables (*e.g.* column diameter, heat exchange areas, contacting area, catalyst concentration, reboil and reflux ratios, RTD, pressure drop, hold-up, flooding and wetting conditions) and discrete variables (*e.g.* feed staging, reactive and nonreactive stages, withdrawal staging) are obtained. It is relevant to mention that at more detailed design level, rigorous simulation methods are foreseen as key tools (*e.g.* FEM and CFD). If the process structure options are economically attractive, proceed to the next level. Otherwise, relax, if applicable, some of the constraining assumptions made for level 1 and resume level 2.
▷ this corresponds to level Synthesis in figure 4.2.

Space 6. Behavior analysis: steady state simulations are carried out to explore the kinetics, gas/liquid mass transfer, hydrodynamics and multiplicities inside the units. Dynamic simulations are performed to check the robustness of the design, in terms of the ability to maintain product purities and conversion in a desired range when disturbances occur. If the process is controllable and economically attractive at the estimated operating conditions, go to the next

level. Otherwise, relax, if applicable, some of the constraining assumptions made for level 1 and resume level 2.
▷ this corresponds to level Analysis in figure 4.2.

Space 7. Evaluation: the design options are checked with respect to their performance. Within the wide range of SHEET criteria specific choices are made for economic performance, sustainability and technology. For economics, the capital and operational costs of the process during the time horizon (*i.e.* TAC) are calculated. Exergy efficiency is used as a sustainability metric, while a systems response time is used to define the responsiveness of the processes. Thus, sustainability aspects like proper choice of feedstocks and products' supply chain are not considered. From a scientific perspective, we choose exergy efficiency and responsiveness to exploit their underlying link: the rate of entropy production. If the designed process satisfies all three constraining criteria the design task is finished. Otherwise, a trade-off is sought.
▷ this corresponds to level Evaluation in figure 4.2.

The successful application of the integrated design approach relies on considering the output of the graphical methods as initial structure for the optimization-driven design approaches. In this way, the optimized design is likely to be embedded within the feasible space and the computational effort becomes less demanding due to the reduced number of design variables. This approach is intended to reduce the complexity of the design problem and it should **not** be considered as a mechanistic recipe.

4.6 Concluding Remarks

A *multiechelon approach* was introduced aimed at an integrated and generalized design methodology for RD. An attempt is made with this design strategy to conjugate the strengths of graphical and optimization-based methods. Economic performance, sustainability considerations and process responsiveness are included as evaluation criteria under the umbrella of the SHEET set. A decomposition of the design problem is proposed in this approach to give a hierarchy of design spaces of increasing refinement.

The challenges in the design of RD are numerous and exciting. The drive for process intensification and more sustainable plant operations can lead to more intricate geometric structures (*e.g.* packings, dividing walls, distributed heat exchange) and to more refined models, which couple mass and energy transfer in a more realistic way. Finally, incorporating supply chain motivated temporal features within the design task (*e.g.* operation and switching modes) may increase tremendously the degrees of freedom and the problem complexity.

Chapter 4

Mind journey to the scientific questions.

If we take a mind journey back to the engineering/scientific design question presented at the beginning of this chapter, the following remark can be made. The analysis of strengths and weaknesses of current design methodologies is addressed in this chapter. Practical constraints regarding their development and application are mentioned. The multiechelon approach is introduced and its building blocks are described. With respect to Question 5, a set of performance criteria are suggested for a life-span inspired design approach.

"What saves a man is to take a step; then another step."
Antoine De Saint-Exupery, writer and pilot (1900-1944)

5

Feasibility Analysis and Sequencing: A Residue Curve Mapping Approach[†]

The second (feasibility analysis) and fourth (column sequencing) spaces of the multiechelon approach (*cf.* chapter 4) in RD design are studied. Applications of residue curve mapping to RD processes have recently been reported, but a generalized and systematic approach is still missing for the case of reactive feeds outside the conventional composition ranges (*i.e.* stoichiometric ratio of reactants for the case of MTBE synthesis). This chapter is addressing these design aspects. The reaction invariant space, defined in terms of transformed composition variables, is divided into sub-regions characterized by separation boundaries. A feasibility analysis of the RD process is performed based on the location of the reacting mixture and initial separation sequences are generated according to the feed transformed-composition. The practical conclusion of this chapter is that by using RCM technique one can virtually generate RD trains over the entire possible feed composition space. The synthesis of MTBE is used as case study.

[†]Parts of this chapter have appeared in Almeida-Rivera and Grievink (2002) and Almeida-Rivera and Grievink (2004)

5.1 Introduction

The art of process design involves finding process configurations, operating conditions and size of equipment that will allow an economical, safe and environmental responsible operation, only by specifying the state of the feeds and the targets on the output streams of a system (Almeida-Rivera *et al.*, 2004*a*; Doherty and Buzad, 1992; Buzad and Doherty, 1995). This task is not trivial and requires the development of specialized design tools (*e.g.* computational methods, algorithms and procedures). At early stages of the design activity (*e.g.* conceptual phase) the chemical process designer faces a largely influencing question: *is the processing route feasible*? The impact of preliminary design and feasibility analysis on the fate of the final plant is enormous. Surprisingly, it is a common practice to allocate a relative small fraction ($<$ 2-3%) of total budget for the conceptual phase. Due to the coarse level of detail, the design tools in the conceptual phase should be powerful enough to screen feasible design alternatives within a huge design space.

Recalling the engineering and scientific design questions given in chapter 1, in this chapter we address question 6, namely,

- *What (new) methods and tools are needed for reactive distillation process synthesis, analysis and evaluation?*

5.2 Input-Output Information Flow

Each level of the proposed multiechelon approach (*cf.* §4.5) is characterized by flows of information needed as input and obtained as result from that design stage. Moreover, set of tools are required to assist the design task and design decisions are to be made.

In the case of the feasibility analysis stage (Space 2 in section §4.5) the required input information involves the process basis of design. In other words, feedstock and product purities and operational boundaries should be defined. Additionally, sustainability and

Table 5.1. Input-output information for the feasibility analysis phase. The multiechelon approach is explained in section §4.5.

Design specifications	**Design/operational variables**	**Domain knowledge**
Process:	Discrete:	- thermodynamics
- set of components	- distillation boundaries	- kinetics
- set of chemical reactions	- (non-) reactive azeotropes	- overall balances
- feed composition	Continuous:	
- operational pressure	- product feasible compositions	
Product:		
- composition target(s)		
- SHE constraints		

Table 5.2. Input-output information for the column sequencing phase. The multiechelon approach is explained in section §4.5.

Design specifications	**Design/operational variables**	**Domain knowledge**
Process: - mode of operation	Discrete: - type of task (separation and/or reactive) - number of columns - columns connectivity Continuous: - feed ratio of reactant streams	- operational skill - component balances

safety constraints should be included as inputs. The output information comprises the determination of distillation boundaries, (non-) reactive azeotropic mixtures and feasible product compositions. The domain knowledge at this design space belongs to the field of thermodynamics, kinetics and overall mass balances. An extended overview of input and output information at this design level is given in table 5.1.

The generation of separation sequences (Space 4 in section §4.5) is composed of process requirements related to the mode of operation, which is in turn determined using operational skills. The temporal mode of operation mode is chosen based on operational expertise in RD processing. For the sake of analysis simplification and without restricting the validity of the approach to other temporal modes, a continuous operation is chosen. The output information at this design space includes the type of task required for the design specifications (*i.e.* separation and/or reaction), the type of column internal (*i.e.* tray or packing), the number of units and their connectivity. The relevant domain knowledge at this design space corresponds to operational thumb-ruled skills and basic component balances. An extended overview of input and output information at this design level is given in table 5.2.

Making each stage of the design approach operational requires the use of (novel) design tools. The Residue Curve Mapping technique (RCM) is found to be of particular effectiveness in the case of RD feasibility analysis and generation of column sequencing. The next sections apply this concept in the corresponding design spaces 2 and 4.

5.3 Residue Curve Mapping Technique

The RCM technique has been considered a powerful tool for the flowsheet development and preliminary design of conventional multicomponent, nonideal separation processes (Fien and Liu, 1994). It represents a good approximation to actual equilibrium behavior and allows the designer to perform feasibility analysis of separation processes where nonideal and azeotropic mixtures are involved. Traditionally, nonreactive residue curves have been used to predict the liquid-composition trajectories in continuous distillation

units in the ∞/∞ case (*i.e.* infinite number of stages and infinite reflux). Although for finite columns -either batch or continuous- those profiles differ slightly compared to the residue curves under same isobaric conditions (Fien and Liu, 1994), the difference might be considered negligible at the first stages of design. It is relevant to mention that the applicability of RCM technique is fundamentally valid for both continuous and batch separation units.

Analytically, RCMs are constructed based on physical properties of the system (*i.e.* VL equilibrium, LL equilibrium and solubility data), wherein the composition of a non-reacting liquid remaining in the system (figure 5.1) may be determined by performing an overall and component material balances in the system (Westerberg *et al.*, 2000),

$$\frac{dM^L}{dt} = -V, \quad \text{with } M^L(0) = M_0^L, \tag{5.1}$$

$$\frac{d(x_i M^L)}{dt} = M^L \frac{dx_i}{dt} + x_i \frac{dM^L}{dt} = -y_i V, \quad \text{with } x_i(0) = x_{i,0}, \quad i \in \mathbb{Z}^{n_c}, \tag{5.2}$$

where M^L is the mass of liquid in the system, V is the vapor flow, x_i is the molar composition of component i in the liquid phase, y_i is the molar composition of component i in the vapor phase and n_c is the number of components present in the system. Apart from liquid hold-up no equipment related data are required.

Replacing expression 5.1 in 5.2 and introducing a warped time ($d\tau_w = dt \times V/M^L$)

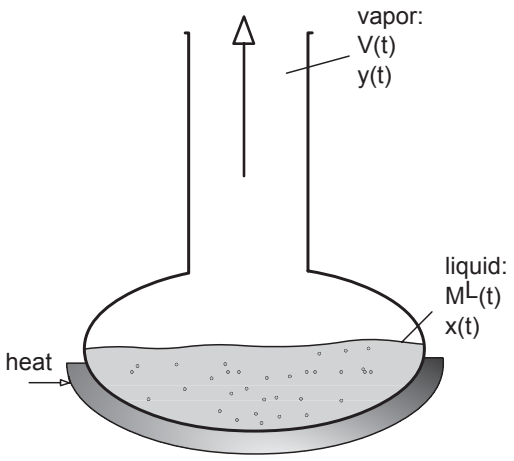

Figure 5.1. Schematic representation of a simple batch still for the experimental determination of (non-) reactive residue curves

allow one to rewrite the RCM expression in vectorial notation,

$$\frac{d\mathbf{x}}{d\tau_w} = \mathbf{x} - \mathbf{y}, \qquad \text{with } \mathbf{x}(0) = \mathbf{x}_0, \tag{5.3}$$

where $\mathbf{x}$ is the composition vector in the liquid phase $[x_1 \;\; x_2 \;\; x_3 \cdots x_{n_c}]^{\mathrm{T}}$ and $\mathbf{y}$ is the composition vector in the vapor phase $[y_1 \;\; y_2 \;\; y_3 \cdots y_{n_c}]^{\mathrm{T}}$.

Combining the previous [*n-1*] independent expressions 5.3 with and appropriate vapor-liquid equilibrium model enables to define the set of simultaneous equations that describe the residue curves,

$$\frac{dx_i}{d\tau_w} = x_i - y_i, \qquad \text{with } x_i(0) = x_{i,0}, \quad i \in \mathbb{Z}^{n_c-1}, \tag{5.4}$$

$$y_i = f(T, P, x_i), \qquad i \in \mathbb{Z}^{n_c}, \tag{5.5}$$

$$1 = \sum_{i=1}^{i=n_c} x_i = \sum_{i=1}^{i=n_c} y_i. \tag{5.6}$$

When a mixture of n_c-components undergoes n_{rx} simultaneous *equilibrium* chemical reactions, the RCM expression may be described in terms of transformed molar compositions and a reaction-warped time (Ung and Doherty, 1995*a*),

$$\frac{dX_i}{d\tau_w} = X_i - Y_i, \qquad \text{with } X_i(0) = X_{i,0}, \quad i \in \mathbb{Z}^{n_c-n_{rx}-1}, \tag{5.7}$$

with,

$$X_i = \frac{x_i - \nu_i^{\mathrm{T}}(\mathcal{V}_{\mathrm{ref}})^{-1}\mathbf{x}_{\mathrm{ref}}}{1 - \nu_{\mathrm{total}}^{\mathrm{T}}(\mathcal{V}_{\mathrm{ref}})^{-1}\mathbf{x}_{\mathrm{ref}}}, \qquad i \in \mathbb{Z}^{n_c-n_{rx}}, \tag{5.8}$$

$$Y_i = \frac{y_i - \nu_i^{\mathrm{T}}(\mathcal{V}_{\mathrm{ref}})^{-1}\mathbf{y}_{\mathrm{ref}}}{1 - \nu_{\mathrm{total}}^{\mathrm{T}}(\mathcal{V}_{\mathrm{ref}})^{-1}\mathbf{y}_{\mathrm{ref}}}, \qquad i \in \mathbb{Z}^{n_c-n_{rx}}, \tag{5.9}$$

where

$$\mathcal{V}_{\mathrm{ref}} = \begin{pmatrix} \nu_{(n_c-n_{rx}+1),1} & \cdots & \nu_{(n_c-n_{rx}+1),n_{rx}} \\ \vdots & \nu_{i,r} & \vdots \\ \nu_{n_c,1} & \cdots & \nu_{n_c,n_{rx}} \end{pmatrix}, \tag{5.10}$$

$$d\tau_w = dt \times \left(\frac{1-\nu_{\mathrm{total}}^{\mathrm{T}}(\mathcal{V}_{\mathrm{ref}})^{-1}\mathbf{y}_{\mathrm{ref}}}{1-\nu_{\mathrm{total}}^{\mathrm{T}}(\mathcal{V}_{\mathrm{ref}})^{-1}\mathbf{x}_{\mathrm{ref}}}\right) \times V/L,$$

where X_i and Y_i are the transformed composition variables for the component $i \in \mathbb{Z}^{n_c-n_{rx}}$ in the liquid and vapor phases respectively, ν_i^{T} is the row vector of stoichiometric coefficients for component $i \in \mathbb{Z}^{n_c-n_{rx}}$ in all the n_{rx} reactions $[\nu_{i,1} \;\; \nu_{i,2} \;\; \cdots \nu_{i,R}]$, $\nu_{\mathrm{total}}^{\mathrm{T}}$ is the row vector of the total mole number change in each reaction $\left[\sum_{i=1}^{i=n_c} \nu_{i,k}\right]_k$, $k \in \mathbb{Z}^{n_{rx}}$, ref denotes the reference components for the n_{rx} reactions, numbered from $n_c - n_{rx} + 1$ to n_c and $\mathcal{V}_{\mathrm{ref}}$ is the square matrix of stoichiometric coefficients for the n_{rx} reference components in the n_{rx} reactions.

From the above-mentioned expressions it can be inferred that,

- the new set of variables defines a sub-region of lower dimension in the composition space, *reaction invariant space*, composed of the feasible product compositions for equilibrium controlled reactions,
- the transformed compositions keep the same value for a liquid mixture before and after reaction equilibrium is attained (*i.e.* $X_i^0 = X_i^e$) and are normalized (*i.e.* $\sum_{i=1}^{n_c-n_{rx}} X_i = \sum_{i=1}^{n_c-n_{rx}} Y_i = 1$),
- in the new composition space the reactive curves may be described by a simplified expression, which has exactly the same functional form as the distillation equation for non-reacting mixtures in terms of mole fractions,
- ref can be a product or a reactant, depending on the value of $\nu_{\text{total}} < 0$, and
- the reaction warped time increases monotonically with time

$$\tau_w|_{t_0} = 0; \tau_w|_{t_{L=0}} = \infty. \tag{5.11}$$

The reactive problem is completed by calculating the chemical equilibrium constants for the multicomponent vapor-liquid mixture,

$$K_{\text{eq}} = \prod_{i=1}^{i=n_c} (\gamma_i \times x_i)^{\nu_i} = f(x_i, \gamma_i(x_i, T)), \tag{5.12}$$

where K_{eq} is the chemical equilibrium constant for reaction $r \in \mathbb{Z}^{n_{rx}}$.

The equations involved in the reactive problem include $[n_c - n_{rx} - 1]$ RCM expressions, $[2n_c - 2n_{rx}]$ transformed composition definitions, $[n_c]$ phase equilibrium conditions, $[n_{rx}]$ chemical equilibrium constant and [2] normalization expressions, resulting in $[4n_c - 2n_{rx} + 1]$ equations. On the other hand, the involved variables are $x_{i\in\mathbb{Z}^{n_c}}$, $y_{i\in\mathbb{Z}^{n_c}}$, $X_{i\in\mathbb{Z}^{n_c-n_{rx}}}$, $Y_{i\in\mathbb{Z}^{n_c-n_{rx}}}$, P and T, resulting in $[4n_c - 2n_{rx} + 2]$ variables. Since the problem has only one degree of freedom, all the unknown variables may be found by specifying a single variable (*e.g.* P) and solving simultaneously the following set of differential and algebraic expressions,

$$\frac{dX_i}{d\tau_w} = X_i - Y_i, \qquad i \in \mathbb{Z}^{n_c-n_{rx}-1}, \tag{5.13}$$

$$X_i(0) = X_{i,0}, \qquad i \in \mathbb{Z}^{n_c-n_{rx}-1}, \tag{5.14}$$

$$X_i = \frac{x_i - \nu_i^{\text{T}}(\mathcal{V}_{\text{ref}})^{-1}\mathbf{x}_{\text{ref}}}{1 - \nu_{\text{total}}^{\text{T}}(\mathcal{V}_{\text{ref}})^{-1}\mathbf{x}_{\text{ref}}}, \qquad i \in \mathbb{Z}^{n_c-n_{rx}}, \tag{5.15}$$

$$Y_i = \frac{y_i - \nu_i^{\text{T}}(\mathcal{V}_{\text{ref}})^{-1}\mathbf{y}_{\text{ref}}}{1 - \nu_{\text{total}}^{\text{T}}(\mathcal{V}_{\text{ref}})^{-1}\mathbf{y}_{\text{ref}}}, \qquad i \in \mathbb{Z}^{n_c-n_{rx}}, \tag{5.16}$$

$$y_i = f(T, P, x_i), \qquad i \in \mathbb{Z}^{n_c}, \tag{5.17}$$

$$K_{\text{eq}} = \prod_{i=1}^{i=n_c} (\gamma_i \times x_i)^{\nu_i}, \qquad r \in \mathbb{Z}^{n_{rx}}. \tag{5.18}$$

The integration of differential expression 5.13 stops when either pure components or reactive azeotropes are met. These singular points are given by the following conditions:

$$\text{Pure component:} \quad X_i = Y_i = 1, \{X_j, Y_j\} = 0, \qquad i \neq j, i, j \in \mathbb{Z}^{n_c} \tag{5.19}$$

$$\text{Reactive azeotrope:} \quad 0 < X_i = Y_i < 1, \qquad i \in \mathbb{Z}^{n_c}. \tag{5.20}$$

Note, however, that the reference composition vectors $\mathbf{x}_{\text{ref}}$ and $\mathbf{y}_{\text{ref}}$ are back calculated after each time integration of X using the corresponding definition expression. Assigning the operation pressure is a task that should be carefully analyzed since *bifurcation pressures* have been reported (Fien and Liu, 1994; Okasinski and Doherty, 1997). At those system-dependent P values the thermodynamic and topological behavior of the reacting mixture changes considerably.

5.4 Feasibility Analysis: An RCM-Based Approach

Residue curve maps provide a powerful tool to represent relevant properties of the system, particularly those aiming to predict feasible design sequences. In addition, analytical material balances may be represented in a RCM, resulting in constraints to feasible product compositions and convenient operating strategies (*e.g.* direct or indirect distillation).

The presence of (non-)reactive singular points (*i.e.* pure components and (non-)reactive azeotropes) in RCMs allows the division of the (transformed) composition diagram into separate *(reactive) distillation regions* by introducing *(reactive) distillation separatrices*, which connect two singular points in the composition space. The explanatory note 5.1 gives a brief overview of the concepts of nodes and saddle points, as features of singular points.

If a separatrice ends at a saddle point, it is commonly referred to as *boundary curve*. Crossing distillation boundaries has been extensively reported for industrial cases and especially for those with curved distillation boundaries. For those systems, the boundaries can be crossed by simple recycle methods provided an appropriate entrainer. However, conventional design strategies require that the feed and products remain in the same distillation region (Fien and Liu, 1994).

Since sharp separations are not possible in the industrial practice, short-cut methods have been developed to assist in the design of distillation sequences. A transparent example of those procedures is the so-called *bow-tie region* method (figure 5.2), which intends to find for a specific feed a set of feasible top and product compositions for columns at finite reflux or when distillation-boundaries are crossed. The following procedure for the construction of bow-tie regions (*cf.* figure 5.2) is suggested by Fien and Liu (1994): (*i*) the distillation boundaries are identified and drawn in a composition

Saddle point is defined in the stability theory of ODE as the point of a function or surface, which is a stationary point but not an extremum. Let

$$f = f(x_1, x_2, x_3, ...x_n) \tag{5.21}$$

be a scalar function of n variables. Then a saddle point is any point $(x_1^s, x_2^s, x_3^s....x_n^s)$ where the gradient of f evaluated at $\mathbf{x}^s$ is zero, but which is not a local maximum or minimum because the Hessian matrix is indefinite, namely,

$$f'(\mathbf{x}^s) = 0 \tag{5.22}$$

$$\exists \mathbf{a}, \mathbf{b} \in \mathbf{x}, \mathbf{a} \neq \mathbf{b} \quad : \quad \mathbf{a}^{\mathrm{T}}\mathbf{H}(\mathbf{x}^s)\mathbf{a} < 0 \wedge \mathbf{b}^{\mathrm{T}}\mathbf{H}(\mathbf{x}^s)\mathbf{b} > 0 \tag{5.23}$$

In RCM technique saddle points are considered to be those intermediate-boiling vertices (pure components or (reactive) azeotropes), at which no residue curve has neither its initial nor final point (Fien and Liu, 1994).

Stable node is a fixed point for which the gradient of f evaluated at $\mathbf{x}^n$ is zero and the Hessian matrix at $\mathbf{x}^n$ is negative definite (Fien and Liu, 1994), namely,

$$f'(\mathbf{x}^n) = 0 \tag{5.24}$$

$$\mathbf{x}^{\mathrm{T}}\mathbf{H}(\mathbf{x}^n)\mathbf{x} < 0, \quad \text{for all nonzero } \mathbf{x} \in \mathbb{R}^{\dim(\mathbf{H})} \tag{5.25}$$

Unstable node is a fixed point for which the gradient of f evaluated at $\mathbf{x}^n$ is zero and the Hessian matrix at $\mathbf{x}^n$ is positive definite (Leon, 1998), namely,

$$f'(\mathbf{x}^n) = 0 \tag{5.26}$$

$$\mathbf{x}^{\mathrm{T}}\mathbf{H}(\mathbf{x}^n)\mathbf{x} > 0, \quad \text{for all nonzero } \mathbf{x} \in \mathbb{R}^{\dim(\mathbf{H})} \tag{5.27}$$

In RCM technique stable nodes are considered to be those high-boiling vertices (pure components or (reactive) azeotropes), to which a residue curve is converging. Alternatively, unstable nodes are those low-boiling vertices, from which a residue curve is diverging.

Note 5.1. Definition of stable nodes, unstable nodes and saddles points

space diagram; (*ii*) mass-balance lines are drawn for both direct and indirect splits considering the constraints imposed by the distillation boundaries; (*iii*) a mass-balance line is drawn for an infeasible intermediate split; (*iv*) the regions that are not crossed by this split are shaded; and (*v*) the final bow-tie area is defined by considering that each feasible residue curve must go through both shaded areas. Further information on the construction of bow-tie areas is given by Fien and Liu (1994).

For separations that involve entrainers, the selection of them is without question the most determining task. For reactive distillation, the entrainment agent should react selectively with one of the azeotropic components allowing to cross distillation boundaries.

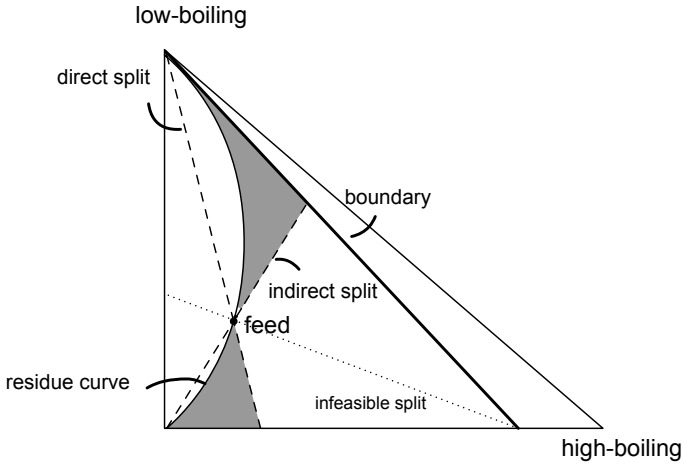

Figure 5.2. Construction of bow-tie regions in RCM. **Remark:** feasible residue curves must go through both shaded areas, so that top and bottom compositions line on a material balance line passing through the feed.

5.5 Case Study: Synthesis of MTBE

The esterification of $i\mathrm{C}_4$ with methanol in the presence of inert $n\mathrm{C}_4$ and an acidic ion-exchange resin is used as case study. A detailed description of the system's features, together with relevant physical-chemical data are available in appendix B. For the feasibility analysis the following parameters and design specifications are of interest,

- number of components, $n_c = 4$,
- number of independent reactions, $n_{rx} = 1$,
- desired product and purity: MTBE (>97%),
- feed composition: outside conventional MeOH/$i\mathrm{C}_4$ stoichiometric ratios,
- continuous mode of operation.

The novelty of the approach relies on the fact that it addresses feed mixtures outside conventional composition ranges. With this, an extended picture of the feasibility analysis and column sequencing in RD processing is attained. To the best of our knowledge, such exceptional feeds have not been reported yet in the open knowledge domain.

5.5.1 Simulation Problem

The simulation problem encompasses the solution of the RCM expressions for two cases: nonreactive and reactive mixture of $i\mathrm{C}_4$-MeOH-MTBE-$n\mathrm{C}_4$ system. According to the

degree of freedom analysis of the previous sections, only the total pressure is specified ($P = 11{\cdot}10^5$ Pa). The criterion for choosing this value is determined by the solubility of iC$_4$ in the liquid phase and enables to carry out the reaction to a desirable extent (Zhang and Datta, 1995).

In this study gPROMS©/gOPT© programming software (Process Systems Enterprise Ltd.) is used to solve the set of simultaneous differential and nonlinear algebraic expressions. The solving algorithm is composed of an DAE integrator based on variable step-size/variable order backward differentiation formulae. Initial molar compositions in the nonreactive case and transformed variables in the reactive case are specified to generate the residue lines, aiming -by visual inspection- to completely cover the composition space. In this contribution, the initial points are uniformly distributed in the corresponding composition space. It is possible, however, to efficiently localize them by considering that finer grids (*i.e.* more initial points) are required around singular points.

The simulations are performed until singular solutions are found, which correspond to pure component or (non-) reactive azeotropes (*i.e.* $\mathbf{x}$=$\mathbf{y}$ and $\mathbf{X}$=$\mathbf{Y}$).

5.5.2 Nonreactive System: Feasibility Results

Three minimum boiling point azeotropes are found for the nonreactive system at the operating pressure of $11{\cdot}10^5$ Pa,

- binary azeotrope iC$_4$-MeOH occurring at $x_{i\mathrm{C}_4}$=0.917; [label (a) in figure 5.3]
- binary azeotrope MeOH-nC$_4$ ocurring at $x_{n\mathrm{C}_4}$=0.8794; [label (b) in figure 5.3]
- binary azeotrope MeOH-MTBE occurring at x_{MTBE}=0.577; [label (c) in figure 5.3].

These three azeotropic mixtures represent the corners of a nonreactive distillation boundary plane and divides the composition simplex into a MTBE-rich and a MeOH-rich regions (Güttinger, 1998). As depicted in figure 5.3, all the residue curves originate at the iC$_4$-MeOH azeotrope and end either at the MeOH or MTBE pure component.

5.5.3 Reactive System: Feasibility Analysis and Generation of Reactive Distillation Sequences

When chemical reaction takes place all the reactive residue curves start at either pure iC$_4$ corner or at the MeOH-nC$_4$ azeotrope (MNAz) and end predominantly at the pure MeOH corner (figure 5.4). The remaining low-boiling azeotropes did not survive the

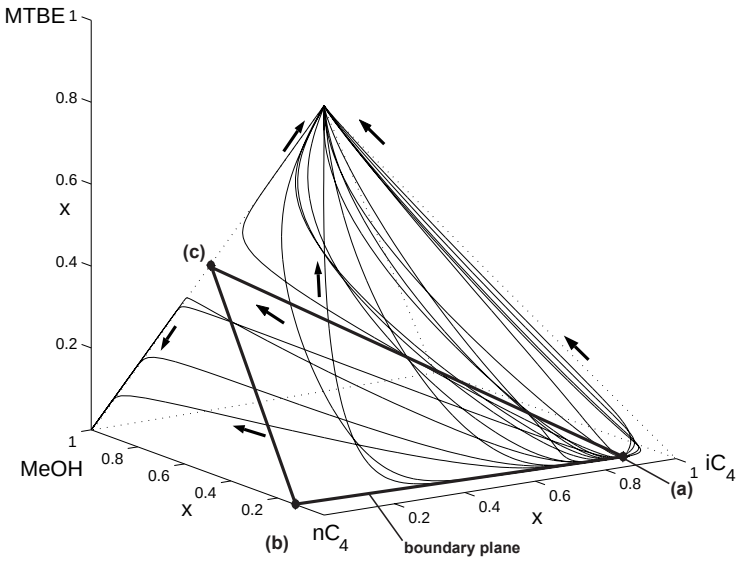

Figure 5.3. Residue curve map for the nonreactive system iC$_4$-MeOH-MTBE-nC$_4$ at an operating pressure of $11{\cdot}10^5$ Pa.

reaction, whereas an additional saddle point (quaternary azeotrope QAz) has appeared close to the pure nC$_4$ corner. For highly inert-containing mixtures, the residue curves are found to end at the nC$_4$ pure corner.

A clearer representation of the reactive system is possible when the conventional composition axis are substituted by the Doherty's composition transformations (figure 5.5). This composition space allows to easily visualize the saddle behavior of the quaternary azeotrope (figure 5.6*a*) and, furthermore, to identify a *pseudo*[‡]-reactive azeotrope, PRAz, (figure 5.6*b*) located in the hypotenuse of the transformed composition simplex and corresponding to an iC$_4$-MeOH-MTBE mixture at high conversion.

The PRAz is characterized by the fact that the residue lines curve toward it but never converge to it (Ung and Doherty, 1995*c*) and for practical purposes it imposes the limit beyond which distillation can not proceed (Ung and Doherty, 1995*c*). This reactive mixture is located halfway up the hypothenuse and behaves as a severe pinch point. As depicted in figure 5.7, the singular points of the reacting system define five reactive distillation boundaries: (QAz:MNAz), (QAz:iC$_4$), (QAz:MeOH), (QAz:nC$_4$) and (QAz:PRAz).

The composition space is divided into the following five sub-regions,

[‡]The *pseudo* terminology has been introduced by Ung and Doherty (1995*c*,*a*) due to the dual topological behavior of this point, as it acts as a saddle on one side and as a stable node on the other side of the map.

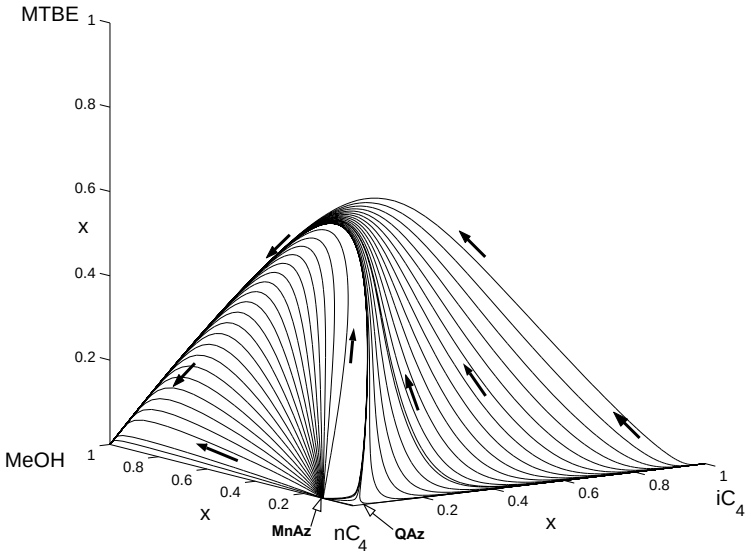

Figure 5.4. Residue curve map for the synthesis of MTBE at an operating pressure of $11{\cdot}10^5$ Pa. **Remark:** reference component is MTBE

- region I:(QAz:MNAz:nC$_4$),
- region II: (QAz:iC$_4$:nC$_4$),
- region III: (QAz:MeOH:MNAz),
- region IV: (QAz:PRAz:iC$_4$),
- region V: (QAz:PRAz:MeOH).

Due to their relative small size, the regions I ($\sim 0.1\%$), II ($\sim 0.25\%$) and III ($\sim 0.8\%$) might be neglected at the first stage of design without incurring in measurable errors. This assumption simplifies considerably the feasibility of the process, since all but one of the boundaries have been removed. The composition simplex is then divided into two well defined zones,

- *zone a*: where residue curves start at MNAz azeotrope and end at pure MeOH corner with a saddle point at the PRAz (*i.e.* region IV),
- *zone b*: where residue curves start at pure iC$_4$ and MNAz and end at the PRAz (*i.e.* region V).

Thus, the separation sequences may differ depending on the location of the feed in the composition simplex. Zone b embraces mainly feed streams at reactants' ratios close

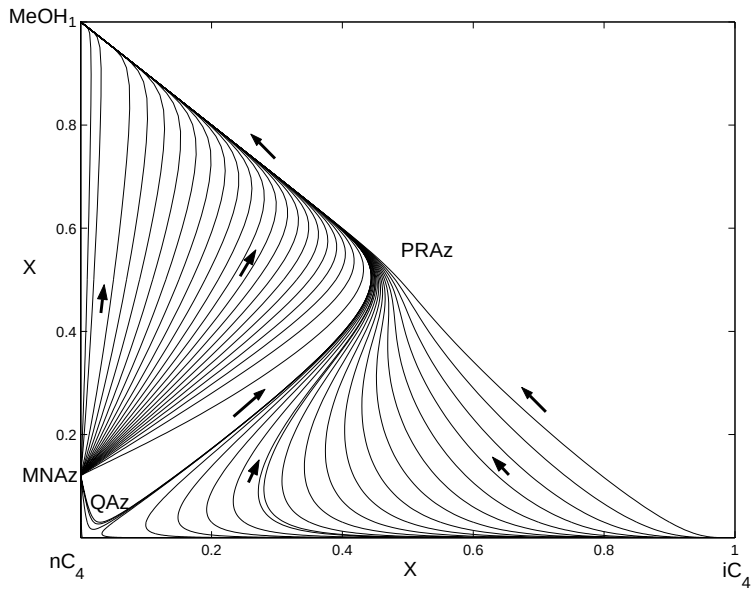

Figure 5.5. Residue curve for the MTBE synthesis at an operating pressure of $11{\cdot}10^5$ Pa in terms of the transformed compositions as defined in equation 5.8.

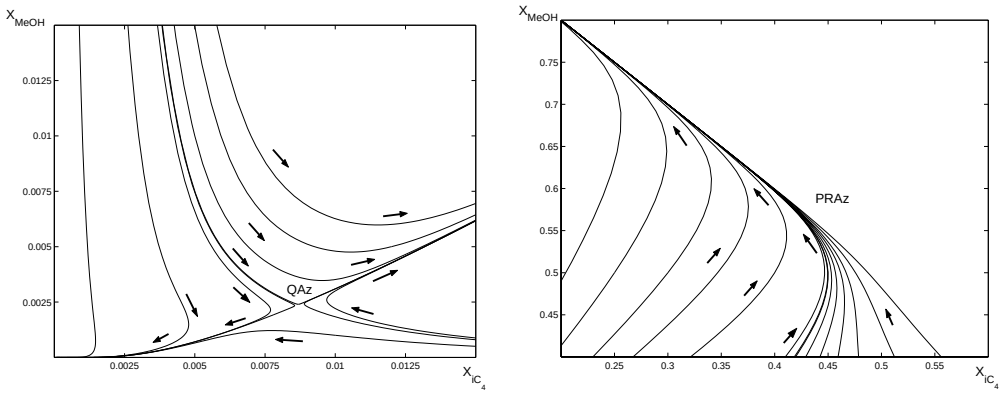

(a) Quaternary azeotrope

(b) Pseudo azeotrope

Figure 5.6. Quaternary and pseudo-azeotropes in synthesis of MTBE at an operating pressure of $11{\cdot}10^5$ Pa. **Remark:** transformed compositions (equation 5.8) are used.

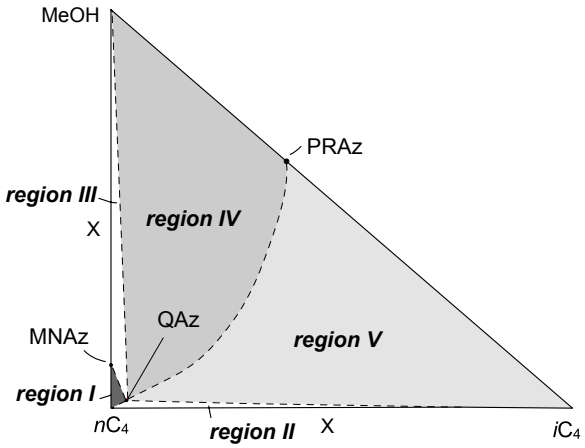

Figure 5.7. Schematic representation of distillation boundaries and zones for MTBE synthesis. **Remarks:** transformed compositions are used; operating pressure is set at $11{\cdot}10^5$ Pa.

to unity and, therefore, are conventionally treated as normal feed compositions (*i.e.* $x_{iC_4}/x_{\mathrm{MeOH}} \simeq 1.0$). Zone *a*, on the other hand, is composed of those feed compositions outside conventional reactant ratios (*i.e.* $0 \leq x_{iC_4}/x_{\mathrm{MeOH}} \leq 0.5$).

According to the sequencing analysis zone *b* sequence is composed of a single column[†] as depicted in figure 5.8. In this case the fresh feed stream ($i\mathrm{C}_4$, MeOH and $n\mathrm{C}_4$) is mixed with a recycle stream (enriched in $i\mathrm{C}_4$ after purging most of the existing inert $n\mathrm{C}_4$) before entering the column, while the product stream (*i.e.* PRAz) is continuously removed at the bottom in an indirect separation strategy.

When the feed to the column is embedded within zone *a* the sequence synthesis is not straightforward and requires some additional insight originated from the residue curve map (figure 5.9*a*). Thus, a distillation sequence is generated for the MTBE synthesis using MeOH as an entrainer, according to the approach presented by Fien and Liu (1994) for nonreactive mixtures. The sequence involves the following operations (figure 5.9*b*),

- feed *F* (MeOH:$i\mathrm{C}_4$:$n\mathrm{C}_4$) may be mixed with stream *B2* to obtain feed mixture *M1*,
- *M1* is fed to column *C1* and separated into distillate *D1* (reactive mixture close to separation boundary) and bottoms *B1* (pure MeOH),

[†]In this case, the term sequence might be loosing its meaning, as only one compact device is considered.

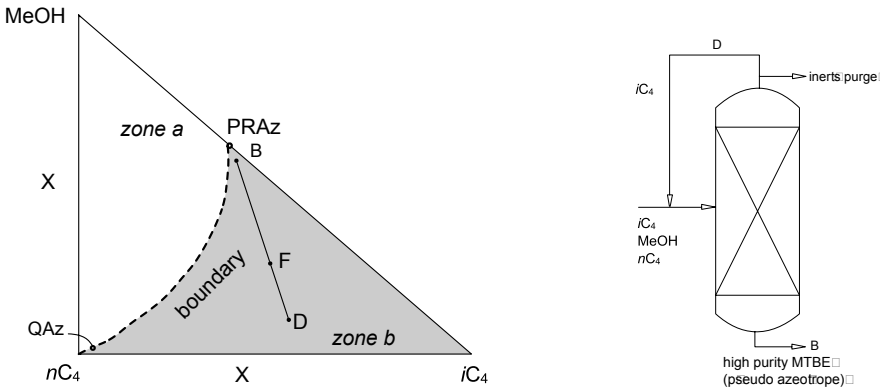

(*a*) Residue curve map (*b*) Separation train.

Figure 5.8. Residue curve map and separation sequence for zone *b* in the synthesis of MTBE by reactive distillation. **Remark:** high purity MTBE (pseudo azeotrope) is recovered at the bottom of the column in an indirect separation; operating pressure is set at $11{\cdot}10^5$ Pa.

- *D1* enters column *C2* and is divided into stream *D2* (high purity nC$_4$ containing stream) and stream *B2* (high purity MTBE containing stream). It is of utmost importance acknowledging that the distillation balance line is able to cross the boundary because of the concavity of the distillation boundary,
- stream *D2* may be then eventually separated following the sequence designed for zone *b* depending on its composition. Moreover, stream *B1* may be recycled back to the first column,
- stream *B2* may be recycled back to the first column, allowing to shift the feed mixture towards the distillation boundary. Alternatively, stream B2 may be withdrawn from the system when its composition is similar to that of the PRAz.

It can be noticed that the PRAz is an intermediate boiling reacting mixture and behaves like a tangent pinch that prohibits designing the separation sequence towards pure MTBE.

5.6 Concluding Remarks

Residue curve maps have shown to provide valuable insights and design assistance for nonideal systems, particularly for reactive distillation. Transforming the composition variables according to Doherty's approach allows to define a *reaction invariant space* of

lower dimension, formed by attainable product compositions and where the conventional concepts for residue curves can be applied.

For the MTBE synthesis two main subregions were defined in the modified composition simplex, each of both characterized by singular points (nodes and saddles) and delimited by separation boundaries. Two different separation sequences were generated, covering **all** the possible reacting mixture compositions. In the generated sequences, high-purity MTBE was obtained as a product, due to the appearance of a pseudo reactive azeotrope, which imposes limitation to the separation task. As all geometrical methods, the RCM technique is limited by its intrinsic graphical nature and requires accurate thermodynamic data to correctly describe reactive distillation processes. Furthermore, RCM technique is suitable only for equilibrium-based processes, which are relatively common in industrial practice (Fien and Liu, 1994).

The combinatorial number of possible separation sequences for multicomponent mixtures is considerably large and calls for the definition of heuristics and thermodynamic guidelines based on RCMs to find convenient initial designs. Furthermore, operational issues should be addressed in terms of, for instance, predicting the controllability of the sequence and defining feasible operational parameters (*e.g.* reflux ratios).

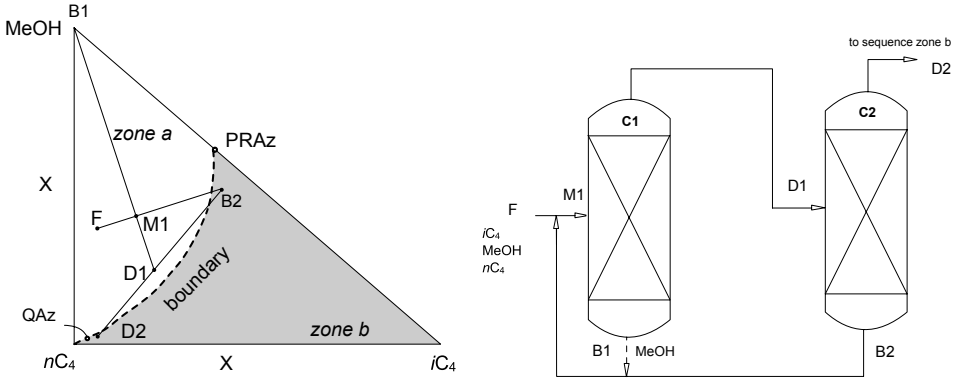

(*a*) Residue curve map (*b*) Separation train.

Figure 5.9. Residue curve map and separation sequence for zone *a* in the synthesis of MTBE by reactive distillation. **Remark:** operating pressure is set at $11{\cdot}10^5$ Pa; stream *D1* may contain all species and be close to the distillation boundary; stream *D2* may be an inert nC$_4$- stream; stream *B2* may have a composition similar to the PRAz.

Feasibility Analysis and Sequencing: A Residue Curve Mapping Approach

Mind journey to the scientific questions.

If we take a mind journey back to the engineering/scientific design question given at the beginning of this chapter, the following remark can be made. Two design aspects of the multiechelon design approach are considered in this chapter: feasibility analysis and column sequencing. The RCM technique is identified as an effective easy-to-use tool to assist the designer in those tasks, particularly for the case of reactive feeds outside conventional composition ranges. Regarding Question 6, a new (at least more refined) tool is developed to assist the design of RD processes.

"If people never did silly things, nothing intelligent would ever get done."

Ludwig Wittgenstein, philosopher (1889-1951)

6

Spatial and Control Structure Design in Reactive Distillation †

In this chapter the fifth space (internal spatial structure) of the multiechelon approach (*cf.* chapter 4) in RD design is studied. This design space is addressed from two perspectives. In the first section, a multilevel modeling approach is proposed as a tool for the decision-making task in the design of spatial structures of RD processes. The proposed strategy involves formulating the simulation problem at different levels of increasing degree of complexity, in which mass, energy and momentum balances are conveniently applied to represent the behavior of the process. In the second section of this chapter, the interactions between spatial and control design are discussed. Both spatial-related and control-related design variables are optimized with respect to economic and dynamic performance in the presence of time-varying disturbances. The synthesis of MTBE is used as tutorial example in the course of this chapter.

†Parts of this chapter have appeared in Almeida-Rivera *et al.* (2003)

Chapter 6

6.1 Multilevel Modeling

6.1.1 Introduction

As already discussed in previous chapters, model development and design methodologies of RD processes are far more complex than those involved in conventional reactors and separation technologies. Therefore, novel and systematic approaches are required to support the decision-making tasks for planning, design and operation of this integrated process. In this section an approach is suggested as a decision-making tool in the conceptual design of RD processes. This approach allows the designer to obtain first estimates of the spatial design variables at an external level or envelop and subsequently determine their real values at an internal level using more sophisticated and detailed models.

6.1.1.1 Input-Output Information Flow

This space of the multiechelon approach (*cf.* section §4.5) involves the flow of information listed in table 6.1. This information is related basically to the unit and internals sizing. Moreover, operational parameters such as reflux ratio and heat duty are considered. It is worth mentioning that although a staged-column configuration is considered in this subsection, the approach is not restricted to stages geometries. Figure 6.1 depicts a generic design structure for a RD column configuration. It is composed of several building blocks: condenser, reflux drum, reboiler and (non-) reactive compartments. The compartments allow mass and heat flows to enter and leave the unit at any location. A detailed description of the compartments' characteristics is covered in chapter 8. All building blocks are connected according to generic rules detailed in chapter 8.

Table 6.1. Input-output information for the internal spatial structure space. The multiechelon approach is explained in section §4.5.

Design specifications	**Design/operational variables**	**Domain knowledge**
Process:	Continuous:	- overall balances
- type of task	- column diameter	- component balances
- number of columns	- heat exchange/contacting areas	- dynamic behavior
- columns connectivity	- catalyst concentration	
- feed ratio of reactants	- reboil and reflux ratios	
	- controllers' parameters	
	Discrete:	
	- feed staging	
	- reactive and nonreactive stages	
	- withdrawal staging	
	- control configuration	

For this spatial configuration the multilevel approach involves the derivation of two levels of different complexity and degree of aggregation. These levels are characterized by inherent assumptions, particular constraints and modeling objectives. All these features are derived from mass, energy and momentum balances and thermodynamic constitutive expressions.

The outer input-output level (steady-state) and inner task level (dynamic) are conveniently linked by the extent of reaction (ε), which allows one to establish whether or not the business-related decision variables cope with the constraints imposed by the problem formulation. Moreover, from this approach it can be elucidated whether or not the corresponding models are well specified and mutually consistent. A successful realization at the outer level (column-level) would suggest relaxing constraining assumptions and stepping up to the more rigorous modeling framework (task-level). Furthermore, this approach allows the designer to determine whether or not the business-related decision variables cope with the operational constraints imposed by the problem formulation.

Recalling the engineering and scientific design questions given in chapter 1, in this chapter we address question 6, namely,

- *What (new) methods and tools are needed for reactive distillation process synthesis, analysis and evaluation?*

6.1.2 Level 1: Input-Output Level

The envelop defined at this level of aggregation is delimited by the overall superstructure (see figure 6.1). The streams of mass and heat are given by: (*i*) the feed streams entering the structure; (*ii*) the product and side streams leaving the structure; and (*iii*) all heat transferred to the structure.

At this input-output level the following assumptions are considered: (*i*) steady-state modeling; (*ii*) multiple feeds ($n_{\text{feed}} \in \mathbb{Z}^+$), side draw-off streams ($n_{\text{off}} \in \mathbb{Z}^+$), heat streams ($n_q \in \mathbb{Z}^+$), reactions ($n_{rx} \in \mathbb{Z}^+$) and components ($n_c \in \mathbb{Z}^+$); and (*iii*) single bottom and distillate streams. Component and energy balances are performed over the structure. The component molar balances ($\mathcal{MC}$) include the distillate, bottom, feed and draw-off streams and the production (or consumption) of species due to chemical reaction,

$$\begin{aligned} \mathcal{MC}_i \quad = \quad & \sum_{j=1}^{j=n_{\text{feed}}} F_j^{\text{feed}} \times \mathbf{z}_j^{\text{feed}} + \mathcal{V}_i^{\text{T}} \times \varepsilon + \cdots \\ & \cdots - D \times \mathbf{x}_i^D - B \times \mathbf{x}_i^B - \sum_{k=1}^{k=n_{\text{off}}} F_k^{\text{side}} \times \mathbf{p}_k = 0, \qquad i \in \mathbb{Z}^{n_c}, \end{aligned} \tag{6.1}$$

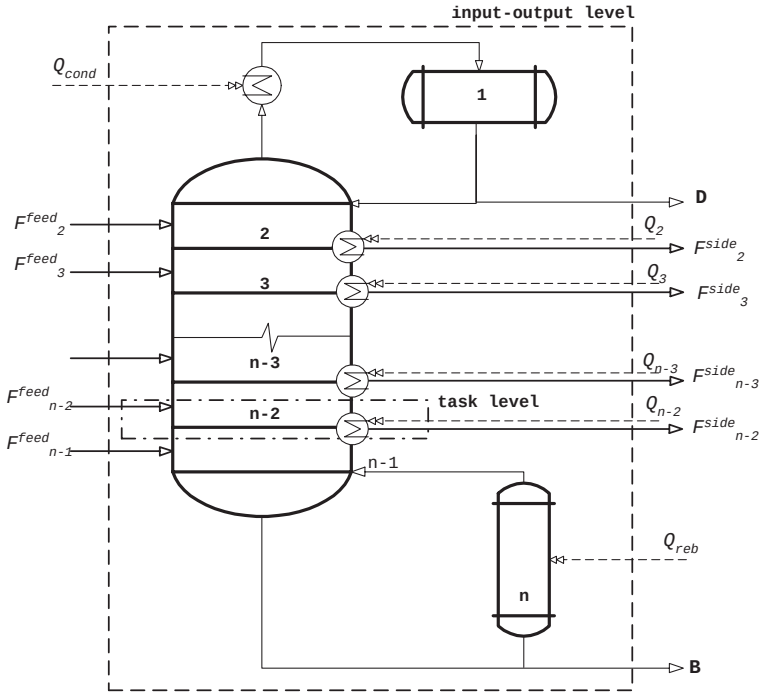

Figure 6.1. Schematic representation of the overall design structure for a RD structure. **Nomenclature:** F^{feed}: feed flowrate; B: bottom flowrate; D: distillate flowrate; F^{side}: side stream; Q: heat duty. **Remarks:** mass and heat flows are allowed to enter and/or leave the unit at any point; compartments are numbered from top to bottom; dashed lines define the envelopes for input-output and task levels.

where F^{feed}, B, D, F^{side} are the molar rates of feed, bottom, distillate and side draw-off streams, respectively; $\mathbf{z}^{\text{feed}}$, $\mathbf{x}^D$, $\mathbf{x}^B$, $\mathbf{p}$ are the molar fractions vector for the feed, distillate, bottom and side draw-off streams, respectively; $\mathcal{V}_i$ is the vector $(n_{rx} \times 1)$ of stoichiometric factors of component i in the n_{rx} reactions and ε is the vector $(n_{rx} \times 1)$ of the overall extents of reaction.

The overall energy balance ($\mathcal{E}$) is given by the heat requirements of the reboiler and condenser, heat of reaction, draw-off heat duties and the enthalpy of all involved streams. Thus,

$$\begin{aligned} \mathcal{E} \quad = \quad & \sum_{i=1}^{i=n_{\text{feed}}} F_i^{\text{feed}} \times (h_i^{\text{feed}}) + (-\Delta^r H)^{\text{T}} \times \varepsilon - B \times h^B + \cdots \\ & \cdots - D \times h^D - \sum_{j=1}^{j=n_{\text{off}}} F_j^{\text{side}} \times h_j^P + \sum_{k=1}^{i=n_q} Q_k - Q_{\text{cond}} + Q_{\text{reb}} = 0, \end{aligned} \tag{6.2}$$

where h is the molar enthalpy without heat of formation, Q_{cond} is the condenser duty, Q_{reb} is the reboiler duty, Q_k is the draw-off heat rate at stage k and $\Delta^r H$ is the row vector of heats of chemical reaction.

Normalization expressions for molar fractions are additionally included in the problem formulation. The set of balance expressions 6.1 and 6.2 turns to be well-posed by specifying appropriate decision variables according to a degree of freedom analysis. Thus, for a given set $[n_c, n_{\text{feed}}, n_q, n_{\text{off}}, \Delta H_{rx}, \mathcal{V}]$ and an extent of reaction ε, the modeling problem is consolidated by removing the degrees of freedom, grouped in vector $\mathbb{A}$,

$$\mathbb{A} = \begin{bmatrix} (n_c-1)(n_{\text{feed}})\mathbf{z}^{\text{feed}} & (n_c-1)(n_{\text{off}})\mathbf{p} & (n_c-1)\mathbf{x}^D & (n_{\text{feed}})T^F \\ (n_{\text{off}})T^P & T^D & (n_q)Q & Q_{\text{reb}} \\ Q_{\text{cond}} & (n_{\text{feed}})\mathbf{F}^{\text{feed}} & (n_{\text{off}})\mathbf{F}^{\text{side}} & B \end{bmatrix}. \tag{6.3}$$

Special attention should be paid in the definition of $\mathbb{A}$. The specification of its variables should take into account the physical feasibility of the problem solution. Thus, vector $\mathbb{A}$ includes variables such as compositions of all incoming streams, compositions of all outgoing streams (side, distillate and bottom streams), temperatures of all incoming and outgoing streams, heat duties of reboiler and condenser, heat flows transferred to each compartment and the molar flows of all feed streams, side streams and bottom stream.

The column-level simulation problem is then stated as follows,

$$\begin{array}{lcl} \text{Given} & : & \varepsilon \text{ and } \mathbb{A}, \\ \text{Solve for} & : & \mathbb{X}_{\text{variables}}, \\ \text{s.t.} & : & |\mathbb{Y}^{\text{total}}_{\mathbb{X}}| = 0, \\ & & \mathbf{F}^{\text{feed}}, D, B, \mathbf{F}^{\text{side}} \in \mathbb{R}^+, \\ & & Q_{\text{reb}}, Q_{\text{cond}}, \mathbf{Q} \in \mathbb{R}, \\ & & \mathbf{z}^{\text{feed}}, \mathbf{x}^D, \mathbf{x}^B, \mathbf{p}, \in [0,1], \end{array} \tag{6.4}$$

where $\mathbb{X}_{\text{variables}}$ is the set of all involved variables $(2(n_{\text{feed}}+n_{\text{off}})+n_c(n_{\text{feed}}+n_{\text{off}}+2)+6+n_q)$, $\mathbb{Y}^{\text{total}}$ is the set of algebraic equations obtained from mass (expression 6.1) and energy balances (expression 6.2) and normalization expressions $(n_c+n_{\text{feed}}+n_{\text{off}}+3)$.

Relevant information is extracted from this level with respect to process flow/block diagram possibilities and estimation of boundary conditions. The practical gain of this approach is the assessment of the effect of the extent of reaction vector on the product stream(s). More specifically, at a given set of input design variables, flow and composition might be computed having the extent of reaction vector as an input parameter. Moreover, the output of this aggregation level defines good design targets for the task-oriented level.

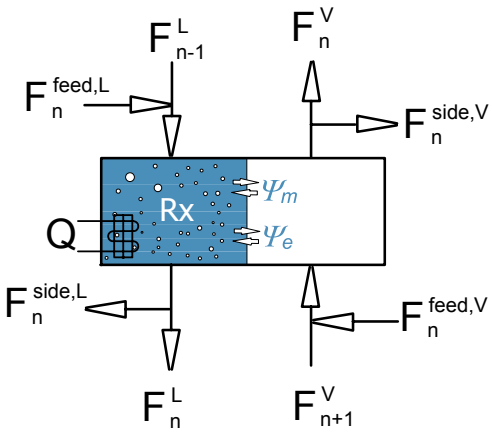

Figure 6.2. Schematic representation of the generic lumped reactive distillation volume element (GLRDVE). **Nomenclature:** $F_i^{\text{feed},(\alpha)}$: feed flowrate of phase (α) at position i; $F_i^{\text{side},(\alpha)}$: flowrate of side stream corresponding to phase (α) at position i; Ψ_m: interfacial mass transfer flux; Ψ_e: interfacial energy transfer flux; Q: heat duty.

6.1.3 Level 2: Task-Level

At this modeling level the internal working of the column is taken into account (*i.e.* reaction rates, mass and heat transfer). A generic lumped RD volume element (GLRDVE) is conceived to represent any element within the RD column along with its occurring tasks and around the steady-state defined in level 1. As depicted in figure 6.2 the GLRDVE allows one to account for the presence of incoming and outgoing streams (feeds/draw-offs), the change of chemical identity and the removal/addition of heat. The novelty of this approach stems from the derivation of four independent sub-modules within the GLRDVE. Those sub-modules are characterized by the *dynamic* behavior of unique tasks: reaction/separation, separation without reaction, mixing and heat exchange module. A detailed derivation of the first principles occurring within the GLRDVE is addressed in section §8.2.

Along the same line of reasoning Papalexandri and Pistikopoulos (1996) present a generalized modular approach for process synthesis, which includes among other reactive-separation building blocks. Relevant is the definition of thermodynamic-based connectivity rules among the different blocks and the optimization-driven approach used. Recent contributions by Proios and Pistikopoulos (2005) extend the work of Papalexandri with a particular focus on separation trains. All dynamic sub-models imply characteristic assumptions and the presence of species mass and energy balances in the volume element and the inclusion of hydraulic, constitutive and normalization expressions. In

general terms, the key sets of equations include: (*i*) conservation equation of species mass, energy and electrical charge; (*ii*) phase and reaction equilibrium equations; (*iii*) thermodynamic constitutive equation per phase, involving density, specific heat and fugacity coefficients; (*iv*) approximations to the momentum balance involving pressure drop, phase ratio and phase contact area; and (*v*) kinetic equation for chemical reactions, mass and heat transfer between lumped phases.

Thus, for any GLRDVE the set of involved expressions is given with respect to mathematical structure by,

$$\begin{array}{lll} \text{Given} & : & f(\dot{x}(t), x(t), u(t), y(t), z) = 0, \quad t \in [t_0, t_f], \\ & & g(x(t), u(t), y(t), z) = 0, \quad t \in [t_0, t_f], \\ & & h(x(t), u(t), y(t), z) \leq 0, \quad t \in [t_0, t_f], \\ & & i(x(0), u(0), y(0), z) = 0, \\ \text{Solve for} & : & x(t) \in X \subseteq \mathbb{R}^x, u(t) \in U \subseteq \mathbb{R}^u, y(t) \in Y \subseteq \mathbb{R}^y, \quad t \in [t_0, t_f], \\ & & z \in Z \subseteq \mathbb{R}^z, \end{array} \tag{6.5}$$

where $f(\cdot)$, $g(\cdot)$ and $h(\cdot)$ are sets of differential, algebraic equality and inequality equations, respectively, $i(\cdot)$ is the set of initial conditions, x is the set of state variables, u is the set of input variables, y is the set of output variables and z denotes time-invariant parameters.

During the model development for the GLRDVE the following assumptions are made: (*i*) the liquid and vapor streams leaving a compartment are in thermodynamic equilibrium; (*ii*) the liquid and vapor in each compartment are perfectly-well mixed (*i.e.* no radial gradient in temperature and composition); (*iii*) the reactions are taking place in the liquid phase and enhanced by a solid catalyst; (*iv*) the reactions occur only in the compartments containing catalyst; and (*v*) vapor and liquid entrainment is neglected.

The assumed extents of reaction at level 1 (input-output) define the targeted conversion for the various species. At the inner level (task level) the cumulative effect of all local conversions should match the targets at the outer level, whenever physically feasible. This constraining information might be expressed as follows (Melles *et al.*, 2000),

$$\text{s.t.} \quad : \quad |\varepsilon^{\text{input-output level}} - \varepsilon^{\text{task level}}| - \epsilon_\varepsilon \leq 0. \tag{6.6}$$

Figure 6.3 visualizes the link between both levels and the streams shared by them. Note that the actual input variables to both levels are given by formulation 6.4.

6.1.4 Case Study: Synthesis of MTBE

The multilevel modeling approach is applied to the synthesis of MTBE at $11{\cdot}10^5$ Pa in a staged RD column loaded with solid catalyst. A detailed description of the system can

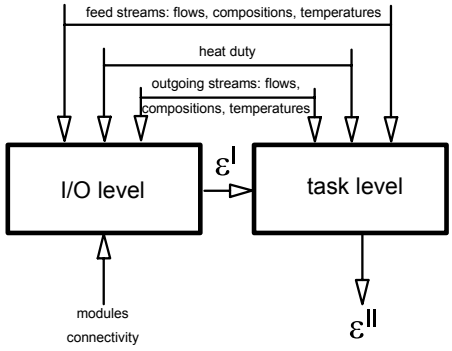

Figure 6.3. Schematic representation of the link between the input-output level and the task level. **Remark:** the actual input variables to the levels are given by the formulation 6.4.

be found in appendix B. The reaction kinetics is estimated according to the pseudo-homogenous expression reported by Mohl *et al.* (1999); Sundmacher and Hoffmann (1999) and Schrans *et al.* (1996),

$$g_j(\mathbf{x}, T) = \left(\frac{a_{i\mathrm{C}_4}}{a_{\mathrm{MeOH}}} - \frac{a_{\mathrm{MTBE}}}{K_{\mathrm{eq}} \times a_{\mathrm{MeOH}}^2} \right), \tag{6.7}$$

where $g(\cdot)$ is the chemical reaction driving force based on activities and K_{eq} is the temperature-dependent chemical equilibrium constant.

The spatial structure of the reactive distillation column is similar to that reported by Hauan *et al.* (1995*a*) and Jacobs and Krishna (1993) and detailed in the upper section of table 6.2.

At the input-output level an initial decision is made according to formulation 6.4. Bottom compositions are specified, from which the extent of reaction is computed using input-output model. A desired value of 150 mol$\times$s^{-1} is imposed to the overall extent of reaction and the set $\mathbb{Y}_{\mathbb{X}}^{\mathrm{total}}$ is successfully solved for a wide range of $\mathbb{A}$ values. As feasible solutions are shown to exist, the decision of solving the simulation problem according to the task model formulation 6.5 is made. The task-level model is developed in gPROMS©/gOPT©(PSEnterprise, Ltd.) equation-oriented environment. The set of expressions $f(\cdot)$, $g(\cdot)$ and $h(\cdot)$ are simultaneously solved provided an appropriate set of initial conditions $i(\cdot)$. Moreover, the sizing design variables (column diameter and reboiler and condenser areas, listed at the lower section of table 6.2) are conveniently chosen by the algorithm to avoid any violation of the extent of reaction constraint 6.6 and hydraulic considerations. As depicted in figure 6.4, the components' compositions show an expected behavior at a simulation time that guarantees steady-state condition. A highly pure MTBE stream is drawn at the bottom of the unit; whereas the top stream

Table 6.2. Nominal values in the MTBE synthesis. **Remark:** operational conditions are those reported in Hauan *et al.* (1995*a*); Jacobs and Krishna (1993); Seader and Henley (1998).

	Value
Number of trays	15 [2:rectifying;8:reactive; 5:stripping]
Feed 1: location	iC$_4$+ nC$_4$: 10$^{\underline{\text{th}}}$ tray (g)
Feed 1: flowrate	455 mol$\times$s^{-1}
Feed 1: composition	iC$_4$: 0.37; nC$_4$: 0.63
Feed 1: temperature	350K
Feed 2: location	MeOH: 9$^{\underline{\text{th}}}$ tray (l)
Feed 2: flowrate	168 mol$\times$s^{-1}
Feed 2: composition	MeOH: 1.00
Feed 2: temperature	320K
Operating pressure	11$\cdot$10^5 Pa (top)
Reflux ratio	7
Mass of catalyst/tray	204.1 kg=1000 eq$_{[H^+]}$
Extent of reaction	150 mol$\times$s^{-1}
Column diameter	3.573 m
Condenser area	4.460$\cdot$10^1 m^2
Reboiler area	2.456$\cdot$10^2 m^2

is predominantly composed of inert nC$_4$. Furthermore, the problem formulations 6.5, 6.4 and 6.6 are solved without violating any constraint at both levels of detail.

6.2 Simultaneous Optimization of Spatial and Control Structures in Reactive Distillation

The interactions between spatial and control design have been classical subjects of academic research during the last decade. It is widely accepted -in both academia and industry- that controllability and operability issues play an essential role in the design of chemical processes. The traditionally-used sequential approach (*i.e.* spatial design followed by control structure design) leads frequently to units/process with poor controllability and responsiveness properties and inoperative in the presence of disturbances and/or uncertainties in design parameters. Relevant developments in this field have been reported (*e.g.* Skogestad and Postlethwaite (1999) and recently by Meeuse and Tousain (2002)) with the aim to consider operability and controllability aspects in the early stage of the design cycle. However, most of such contributions rely on linearization techniques around operational points, steady state models or nonapplicable/complicate controllability indices.

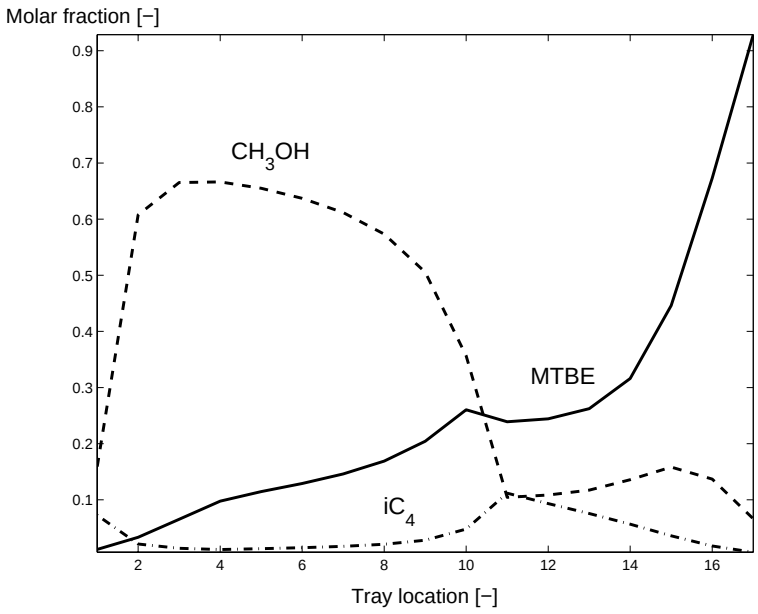

Figure 6.4. Composition profiles in the synthesis of MTBE obtained by a multilevel modeling approach. **Remarks:** the molar fraction of $n\mathrm{C}_4$ is not plotted; a target value of 150 mol×s^{-1} is imposed to the overall extent of reaction; the spatial configuration of the unit is given in table 6.2; time horizon is 14400 s.

This section addresses the application of a dynamic optimization-based design approach to RD. The liquid-phase esterification reaction of $i\mathrm{C}_4$ and methanol in the presence of inert $n\mathrm{C}_4$ in a staged RD column is used as tutorial example. Similar to the study on binary distillation (Bansal *et al.*, 2000; Bansal, 2000) and on the synthesis of ethyl acetate by RD (Georgiadis *et al.*, 2002), both spatial-related (*e.g.* column diameter and heat exchanger areas) and control-related (*e.g.* gain, set-point and reset time) design variables are optimized with respect to economic and dynamic performance in the presence of time-varying disturbances.

6.2.1 Description of the Design and Control Problem in Reactive Distillation

Generally speaking, a chemical process that shows poor ability of meeting control objectives gives rise to missing opportunities with respect to economic performance and satisfaction of product specifications. This fact may imply the existence of a trade-off between those processes designed with respect to control performance considerations

and those driven by economic issues. In order to circumvent this inconvenient duality, a novel design approach has been proposed (Bansal *et al.*, 2000; Bansal, 2000; Georgiadis *et al.*, 2002) where both economic and control oriented issues are conveniently incorporated in the formulation of the optimization problem and simultaneously solved.

In the case of RD design, the general design and control problem involves finding parameters (continuous and/or integers), which define the RD column and control tuning parameters at the minimum economic cost and with an acceptable dynamic performance in the presence of disturbances. The continuous parameters include column diameter, reboiler and condenser areas and tuning parameters (gain K_c, set-point SP and reset time τ_c), while integer variables involve the existence or not of catalyst on a given stage ($\tilde{y} = 1$ for reactive stage and $\tilde{y} = 0$ for nonreactive stage). Alternatively, the presence of catalyst on a tray can be expressed using the Kronecker delta function. For the sake of comparison with literature data, the amount of catalyst is assumed to be identical on all reactive trays.

6.2.2 Description of the Dynamic Optimization Problem in Reactive Distillation

All involved expressions are combined in the formulation of an optimization problem. The set of expressions includes: (*i*) conservation equation of species mass, energy and electrical charge; (*ii*) phase and reaction equilibrium equations; (*iii*) thermodynamic constitutive equation per phase, involving density, specific heat and fugacity coefficients; (*iv*) approximations to the momentum balance involving pressure drop, phase ratio and phase contact area; and (*v*) kinetic equation for chemical reactions, mass and heat transfer between lumped phases. Additionally, algebraic expressions are included to account for constitutive relations and to estimate physical properties of the components, plate hydraulics, column sizing and economic performance indices. A detailed description of the model can be found in appendix A. Thus, the general optimization problem is formulated as follows (Bansal *et al.*, 2000; Bansal, 2000),

$$
\begin{aligned}
\text{Obj.} \quad &: \min_{z^p, z^c, \tilde{y}} \int_0^{t_f} J(x_d(t_f), x_a(t_f), u(t_f), d(t_f), y(t_f), p^p(t_f), p^c(t_f), z^p, z^c, \tilde{y}, t_f) dt, \\
\text{s.t.} \quad &: f(\dot{x}(t), x(t), u(t), d(t), y(t), p^p(t), p^c(t), z^p, z^c, \tilde{y}) = 0, && t \in [t_0, t_f], \\
&\quad g(x(t), u(t), d(t), y(t), p^p(t), p^c(t), z^p, z^c, \tilde{y}) = 0, && t \in [t_0, t_f], \\
&\quad h(x(t), u(t), d(t), y(t), p^p(t), p^c(t), z^p, z^c, \tilde{y}) \leq 0, && t \in [t_0, t_f], \\
&\quad i(x(0), u(0), d(0), y(0), p^p(0), p^c(0), z^p, z^c, \tilde{y}) \leq 0, && t \in [t_0, t_f], \\
&\quad x(t) \in X \subseteq \mathbb{R}^x, u(t) \in U \subseteq \mathbb{R}^u, d(t) \in D \subseteq \mathbb{R}^d, y(t) \in Y \subseteq \mathbb{R}^y, && t \in [t_0, t_f], \\
&\quad z^p \in Z^p \subseteq \mathbb{R}^{z^p}, z^c \in Z^c \subseteq \mathbb{R}^{z^c}, \\
&\quad p^p(t) \in P^p \subseteq \mathbb{R}^{p^p}, p^c(t) \in P^c \subseteq \mathbb{R}^{p^c}, && t \in [t_0, t_f], \\
&\quad \tilde{y} \in [0, 1],
\end{aligned}
\tag{6.8}
$$

where the objective function is the cumulative value of $J(\cdot)$ over the time horizon under consideration, the equalities $f(\cdot)$ and $g(\cdot)$ comprise the differential and algebraic expressions respectively, $h(\cdot)$ represents the path constraints that must be satisfied at all times during the system operation (Bansal *et al.*, 2000; PSE, 1999), $i(\cdot)$ represents the set of initial conditions, x denotes the set of state variables, u is the set of input variables, y is the set of output variables, d is the set of disturbance variables, p^p and p^c are the sets of time-varying variables for the process and control scheme respectively, z^p and z^c are the sets of time-invariant parameters for the process and control scheme respectively and $\tilde{y}$ is the set of integer variables. Additionally, bounds are specified for the time-invariant and time-varying variables for both process and control scheme.

6.2.3 Spatial and Control Design Variables

Due to the high non-linearity of the physical phenomena, even small variations in the input variables might lead to highly sensitive conditions. This fact implies that a feasible operation of a RD column requires several control loops to mitigate the effects of disturbances. To identify the variables to be controlled and manipulated and then fully formulate the design problem a rigorous degree of freedom analysis is performed (tables A.1-A.3 in appendix A). This analysis suggests that for a given set $\{RR, n_t \times D_{\text{col}}, A_{\text{cond}}, A_{\text{reb}}\}$ a 4×4 SISO control structure could be implemented to cope with the disturbances' effects. The pairing of controlled-manipulated variables aims to the satisfaction of product specifications and to the protection of the unit. The proposed control structure is depicted in figure 6.5 and detailed in table 6.3. Note that PI controllers are *a-priori* chosen.

Table 6.3. Control loops in a RD stage column. **Remark:** the schematic representation of the unit is given in figure 6.5.

Unit	Controlled variable	Manipulated variable
P_1	Liquid level in condenser, $\text{level}_{\text{cond}}$	Outgoing flowrate in condenser, $F_{\text{cond}}^{\text{out},L}$
P_2	Pressure in condenser, P_{cond}	Flowrate of cold utility in condenser, F^{cool}
P_3	Liquid level in reboiler, $\text{level}_{\text{reb}}$	Outgoing flowrate in reboiler, $F_{\text{reb}}^{\text{out},L}$
P_4	Temperature in reboiler, T_{reb}	Heat duty of hot utility in reboiler, Q_{reb}

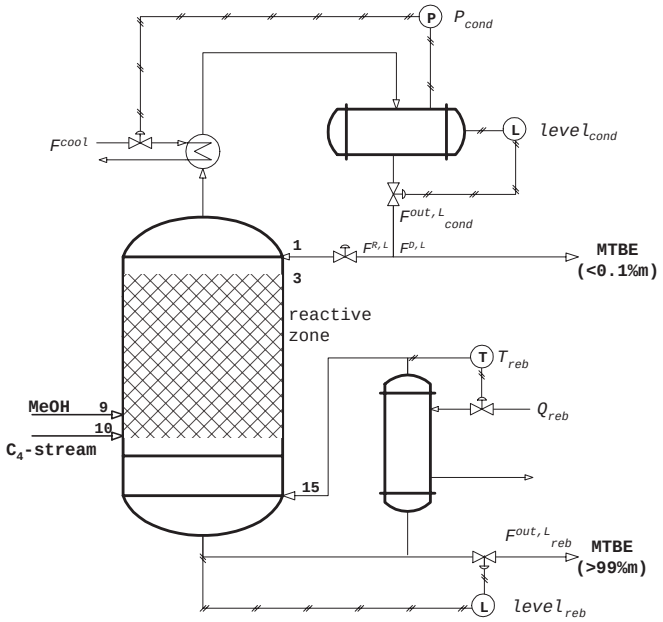

Figure 6.5. Control structure in the synthesis of MTBE by RD. **Remark:** the manipulated and controlled variables for each control loop are listed in table 6.3.

6.2.3.1 Case Study: Synthesis of MTBE

A detailed description of this system is available in appendix B. The spatial structure of the RDC is similar to that reported by Hauan *et al.* (1995*a*) and Jacobs and Krishna (1993) and detailed in the upper section of table 6.2. Two sinusoidal disturbances (figure 6.6) are included in the problem description. They account for both the variation in the feed composition of the C_4-stream and the change in the inlet temperature of the cold utility $T^{\text{in,cool}}$ during the process operation. As suggested by Georgiadis *et al.* (2002); Bansal *et al.* (2000), the feed composition disturbance is modelled as a fast moving function and represented by the following general expression,

$$\mathbf{z}^{\text{feed}} = \begin{bmatrix} z^{\text{feed}}_{iC_4,0} + \sigma_f(t) \\ z^{\text{feed}}_{MeOH,0} \\ z^{\text{feed}}_{nC_4,0} - \sigma_f(t) \\ z^{\text{feed}}_{MTBE,0} \end{bmatrix}, \quad \text{with} \quad \sigma_f(t) := 0.05 \times \sin(\frac{2 \times \pi}{3600} \times t). \tag{6.9}$$

The composition disturbance frequency mimic an upstream time response of 1 hour, which is commonly occurring in industrial practice.

The temperature disturbance tries to represent the variation of inlet temperature of the

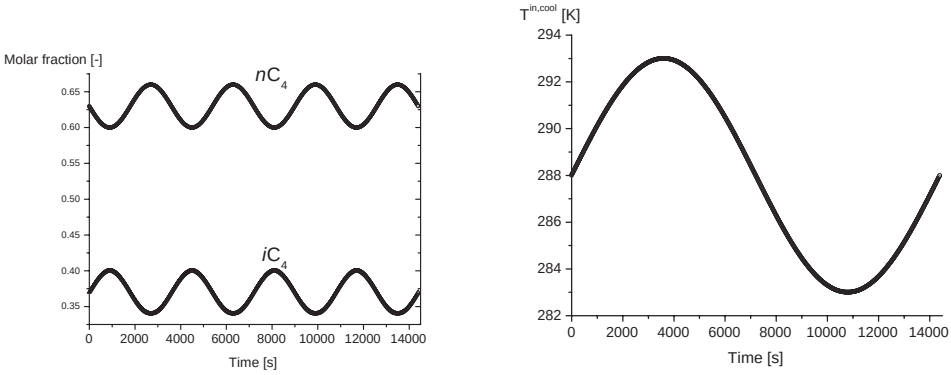

(a) Fast moving disturbance in the feed compositions of iC_4 and nC_4, $\mathbf{z}^{\text{feed}}$.

(b) Slow disturbance in the inlet temperature of the cold utility, $T^{\text{in,cool}}$.

Figure 6.6. Time dependence of the disturbances scenario in the dynamic optimization of MTBE synthesis by reactive distillation. Time horizon=14400 s.

cooling medium during the time horizon. Thus,

$$T^{\text{in,cool}} = 298 + \sigma_s(t), \quad \text{with} \quad \sigma_s(t) := 5 \times \sin(\frac{2 \times \pi}{14400} \times t). \tag{6.10}$$

In this case, the temperature disturbance has a time response of 4 hours.

6.2.3.2 Nominal Spatial/Control Design

Nominal design values of the spatial structure of the column for the synthesis of MTBE (*i.e.* column diameter and reboiler and condenser heat exchange areas) are firstly estimated. They are obtained by solving a steady-state optimization problem, which minimizes the total annualized cost of the RD unit in the absence of disturbances. The following constraints are included to the problem formulation: (*i*) the column diameter is bounded by flooding conditions; (*ii*) the heat exchange areas of the condenser and reboiler are estimated by bounded values of outlet temperatures of the hot and cold utilities, and (*iii*) the molar fraction of MTBE at the top and bottom stream is constrained to values lower than 0.1% and 99% respectively. Thus, the statics optimization problem results in,

$$\begin{aligned} \text{Function:} \quad & \min_{D_{\text{col}}, A_{\text{reb}}, A_{\text{cond}}} J = \text{TAC}, \\ \text{s.t. :} \quad & g(\cdot) = 0, \\ & h(\cdot) \leq 0, \\ & D_{\text{col}}^{\min} \leq D_{\text{col}} \leq D_{\text{col}}^{\max}, \\ & A_{\text{reb}}^{\min} \leq A_{\text{reb}} \leq A_{\text{reb}}^{\max}, \\ & A_{\text{cond}}^{\min} \leq A_{\text{cond}} \leq A_{\text{cond}}^{\max}, \\ & x_{\text{MTBE}}^{D} \leq 0.1\% \text{ and } x_{\text{MTBE}}^{B} \geq 99\%, \end{aligned} \tag{6.11}$$

where TAC is the total annualized cost of the RD unit and includes operational and investment costs. A detailed specification of the terms involved in the definition of TAC is presented in the appendix A.1.

The relevant results of the optimized steady-state nominal design together with the nominal design inputs are presented in table 6.4. According to the sequential approach, the control structure is chosen and controllers' parameters are estimated only after the spatial structure is known and a disturbance scenario is defined. For the sake of simplicity and according to the degree of freedom analysis in appendix A, the control structure depicted in figure 6.5 is implemented in the RD unit.

Table 6.4. Optimized steady-state design of a RD column for MTBE synthesis. The parameter Δx_{MTBE} accounts for the error between computed and set-point values for the molar fractions of MTBE in the top and bottom streams.

	Value
Number of trays	15 [2:rectifying;8:reactive; 5:stripping]
Feed 1: location	iC$_4$+ nC$_4$: 10$^{\underline{\text{th}}}$ tray (g)
Feed 1: flowrate	455 mol$\times$s^{-1}
Feed 1: composition	iC$_4$: 0.37; nC$_4$: 0.63
Feed 1: temperature	350K
Feed 2: location	MeOH: 9$^{\underline{\text{th}}}$ tray (l)
Feed 2: flowrate	168 mol$\times$s^{-1}
Feed 2: composition	MeOH: 1.00
Feed 2: temperature	320K
Operating pressure	11$\cdot$10^5 Pa (top)
Reflux ratio	7
Mass of catalyst/tray	204.1 kg=1000 eq$_{[H^+]}$
Bottom flowrate	197 mol$\times$s^{-1}
Δx_{MTBE}	2.2 $\cdot$10^{-5}
Column diameter	7.132 m
Condenser area	1.059$\cdot$10^3 m^2
Reboiler area	6.93$\cdot$10^2 m^2

Tuning the controllers is initially carried out based on engineering judgement in combination with the rules of thumb given by Luyben (2002). Hence biases are set to the corresponding steady state values, gains are such that a variation of approximately 50% of the controlled-variable value is achieved by a change of 1% in the value of the manipulated variable and reset times are set around 1-2 minutes. To better estimate the values of the controllers gains a sensitivity analysis is performed considering a simplified disturbance scenario given by the variation (+10%) of the flowrate of methanol. For the sake of exemplification, figures 6.7*a-d* depict the dynamic behavior of the controllers' input variables in this simplified disturbance scenario. It can be noticed that an acceptable dynamic behavior of the different condenser and reboiler blocks is obtained (see bold curves in figures 6.7*a-d*). For practical purposes these controllers parameters are considered only as initial guesses for the optimization formulation addressed later on. The problem of estimating the controllers' parameters is now formulated as an optimization problem in the time domain, aiming at a minimization of the integral absolute error of the control loops. This criteria is in particular chosen for the sake of comparison with the work of Georgiadis *et al.* (2002).

The two sinusoidal disturbances introduced previously (expressions 6.9 and 6.10) are included in the optimization problem, resulting in the generic formulation,

$$
\begin{array}{lll}
\text{Function:} & \min\limits_{K_i, Bias_i, \tau_{c,i}, SP_i} J = \int\limits_0^{t_f} \left[(x_b - \bar{x_b})^2 + (x_d - \bar{x_d})^2 \right] dt, & \\
\text{s.t.:} & f(\cdot) = 0 & t \in [t_0, t_f], \\
 & g(\cdot) = 0 & t \in [t_0, t_f], \\
 & h(\cdot) \leq 0 & t \in [t_0, t_f], \\
 & d(\cdot) = 0 & t \in [t_0, t_f], \\
 & T_{\text{reb}}^{\min} \leq T_{\text{reb}} \leq T_{\text{reb}}^{\max} & t \in [t_0, t_f], \\
 & T_{\text{water}}^{\text{out,min}} \leq T_{\text{water}}^{\text{out}} \leq T_{\text{water}}^{\text{out,max}} & t \in [t_0, t_f], \\
 & T_{\text{steam}}^{\text{out,min}} \leq T_{\text{steam}}^{\text{out}} \leq T_{\text{steam}}^{\text{out,max}} & t \in [t_0, t_f],
\end{array}
\tag{6.12}
$$

where the objective function J accounts for deviations from product and top specifications ($\bar{x}$), the constraint paths set bounds for the temperature in the reboiler and the outlet temperatures of the cold and hot utilities and the set of disturbances (Equations 6.9 and 6.10) are grouped in the vector $d(\cdot)$.

Solving problem 6.12 leads to the set of controllers' parameters listed in the second column of table 6.5.

6.2.3.3 Simultaneous Optimization of Spatial and Control Structures

In this subsection the sequential approach adopted previously is effectively replaced by a formulation in which both spatial and control-related constraints are included in the optimization problem and solved for the most economic operation. Besides the

already mentioned constraint paths, the following spatial-related constraints have been included,

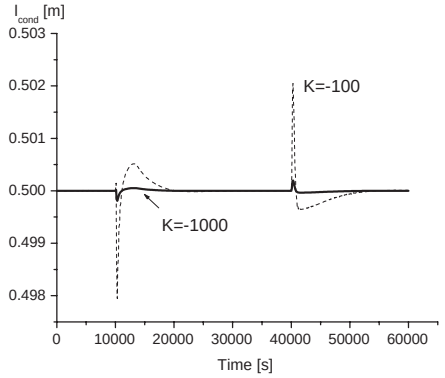

(a) Level in the condenser

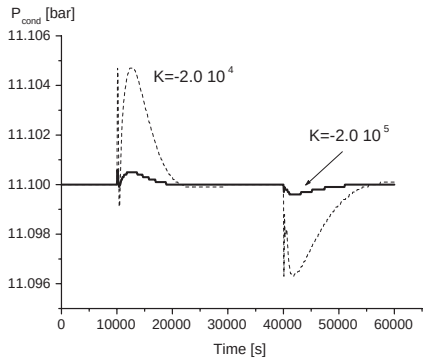

(b) Pressure in the condenser

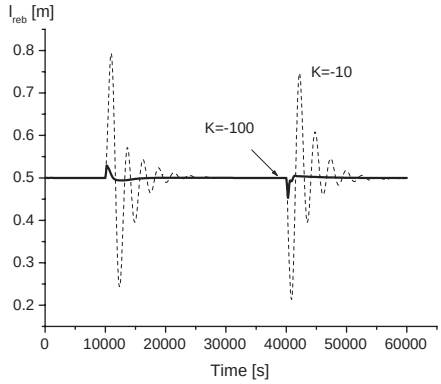

(c) Level in the reboiler

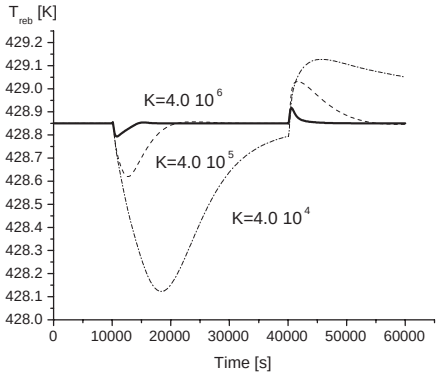

(d) Temperature in the reboiler

Figure 6.7. Dynamic behavior of the controllers' input (controlled) variables in the synthesis of MTBE. **Remarks:** the disturbance scenario involves the time dependent variation of the flowrate of methanol: $F_{\mathrm{MeOH}} = F^{SS}_{\mathrm{MeOH}} + \delta(t)_{F_{\mathrm{MeOH}}}$, with $\delta(t)_{F_{\mathrm{MeOH}}} = 0.1 \times F^{SS}_{\mathrm{MeOH}}$ if $10000s < t < 40000s$ and $\delta(t)_{F_{\mathrm{MeOH}}} = 0$ if $10000s > t$ or $t > 40000s$; controllers parameters are only considered as initial estimates.

$$
\begin{array}{lll}
\text{Function:} & \min\limits_{K_i, Bias_i, \tau_{c,i}, SP_i, D_{\text{col}}, A_{\text{reb}}, A_{\text{cond}}} J = \int\limits_0^{t_f} [\text{TAC}] dt & \\
\text{s.t.:} & f(\cdot) = 0 & t \in [t_0, t_f] \\
 & g(\cdot) = 0 & t \in [t_0, t_f] \\
 & h(\cdot) \leq 0 & t \in [t_0, t_f] \\
 & d(\cdot) = 0 & t \in [t_0, t_f] \\
 & T_{\text{reb}}^{\min} \leq T_{\text{reb}} \leq T_{\text{reb}}^{\max} & t \in [t_0, t_f] \\
 & T_{\text{cool}}^{\text{out,min}} \leq T_{\text{cool}}^{\text{out}} \leq T_{\text{cool}}^{\text{out,max}} & t \in [t_0, t_f] \\
 & T_{\text{heat}}^{\text{out,min}} \leq T_{\text{heat}}^{\text{out}} \leq T_{\text{heat}}^{\text{out,max}} & t \in [t_0, t_f] \\
 & D_{\text{col}}^{\min} \leq D_{\text{col}} \leq D_{\text{col}}^{\max} & \\
 & A_{\text{reb}}^{\min} \leq A_{\text{reb}} \leq A_{\text{reb}}^{\max} & \\
 & A_{\text{cond}}^{\min} \leq A_{\text{cond}} \leq A_{\text{cond}}^{\max} &
\end{array}
\tag{6.13}
$$

The optimized parameters of problem 6.13 are listed in the third column of table 6.5. By comparing the TAC of both approaches, it can easily been inferred that the simultaneous optimization of both spatial and control structures leads to a cheaper and more controllable process than that obtained via the conventional sequential strategy. Although the relative difference between both economic indexes is fairly small, the accumulative cost saving sums up to 0.2 million euros per year. This cost reduction is predominantly originated from the reduced column diameter and smaller reboiler.

The time evolution of the product compositions and temperature profile at the endpoint are depicted in figure 6.8 for the simultaneous approach. It should be noticed that the variations of MTBE composition are negligible from a practical stand-point. Moreover, the temperature along the unit presents a steep increase only at the stripping section. Heat effects due to exothermicity are relatively mild.

6.3 Concluding Remarks

The conclusions derived from this chapter are grouped in accordance to the abovementioned sections. Firstly, it is worth mentioning that the approach presented in this chapter has been applied to staged units, without it being restricted to that geometry. Moreover, variables pairing for the control configuration has not been considered. A MINLP approach could be used to address this last issue, as applied by Bansal *et al.* (2000, 2003) for binary ideal distillation.

Multilevel modeling. The proposed multilevel modeling approach is able to provide an easy-to-handle tool in the early stages of design. Two model levels of different degree of complexity were derived to model the processes taking place in a RD column. Rigorous and reliable degree of freedom analysis were performed at each level, where appropriate business-related decision variables were included. The outer (input-output) and

Table 6.5. Simulation results for the conventionally-used sequential and simultaneous approaches. **Remarks:** inputs of the design problem are given in table 6.4; the notation used in the control loops corresponds to the description of table 6.3 and figure 6.5; the convergence tolerance of the design variables is $1 \cdot 10^{-8}$; catalyst hold-up is considered constant (relaxation of this assumption is addressed in chapter 8).

Variable		Unit	Sequential	Simultaneous
P_1	K_1	-	-1.000×10^{3}	-4.999×10^{2}
	$Bias$	mol×s^{-1}	2.556×10^{3}	2.556×10^{3}
	τ_c	s	1.000×10^{0}	5.047×10^{-1}
	SP	m	5.000×10^{-1}	5.000×10^{-1}
P_2	K_2	-	-2.000×10^{4}	-9.999×10^{4}
	$Bias$	mol×s^{-1}	4.973×10^{4}	4.973×10^{4}
	τ_c	s	1.200×10^{2}	5.000×10^{-1}
	SP	bar	1.100×10^{1}	1.100×10^{1}
P_3	K_3	-	-5.000×10^{0}	-2.500×10^{1}
	$Bias$	mol×s	1.517×10^{2}	1.517×10^{2}
	τ_c	s	1.200×10^{2}	1.500×10^{1}
	SP	m	5.000×10^{-1}	5.000×10^{-1}
P_4	K_4	-	4.000×10^{5}	2.000×10^{6}
	$Bias$	J×s	4.350×10^{7}	4.350×10^{7}
	τ_c	s	1.000×10^{2}	4.761×10^{0}
	SP	K	4.289×10^{2}	4.289×10^{2}
D_{col}		m	7.132×10^{0}	6.924×10^{0}
A_{cond}		m^2	1.059×10^{3}	1.250×10^{3}
A_{reb}		m^2	6.933×10^{2}	4.500×10^{2}
C_{total}		euro/y	2.112×10^{8}	2.108×10^{8}

inner (task) levels were linked by the extent of reaction vector, which allows establishing whether or not the models are well specified and mutually consistent. Additionally, the approach allows one to determine whether or not the business-related decision variables cope with the operational constraints imposed by the problem formulation (*e.g.* SHE issues, reactants availability and market demand).

Simultaneous dynamic optimization. In order to validate this approach, the synthesis of MTBE is used as case study. Three spatial variables and sixteen control-related parameters were optimized during a time horizon of 14400 s. A tradeoff between control and economic performances exists in the design of RD processes, as shown in table 6.5. The design optimized sequentially with respect to dynamic behavior led to a RD process

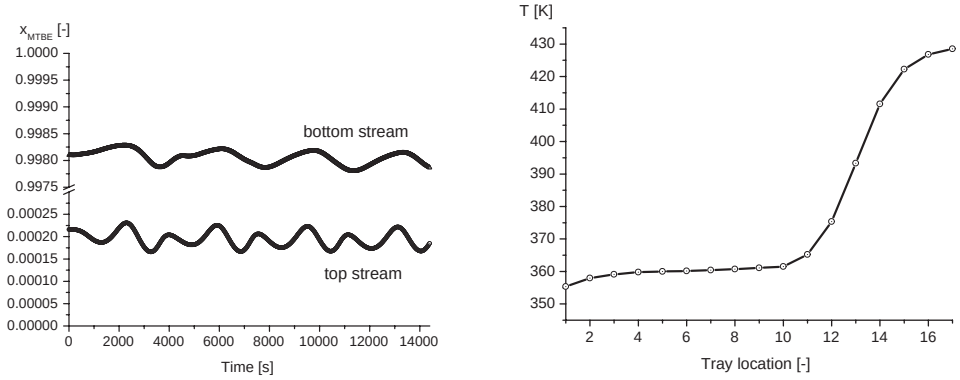

(a) Molar fraction of MTBE. Time horizon: 14400 s.

(b) Temperature profile along the RD column.

Figure 6.8. Time evolution of MTBE molar fraction in the top and bottom streams (left) and temperature profiles at the end-point (right) for the simultaneous optimization of spatial and control structures. **Remarks:** the trays are numbered from top to bottom ($1^{\underline{st}}$: condenser; $17^{\underline{th}}$: reboiler); the sizing and control parameters are listed in table 6.5.

with a total annualized cost higher than that obtained using simultaneous optimization of spatial and control structures. This multiobjective optimization problem was solved by incorporating appropriate time-invariant parameters (*e.g.* column diameter, heat transfer areas and controllers' parameters), in the frame of a dynamic optimization in the presence of deterministic disturbances. A rigorous degree of freedom analysis was performed to the involved building blocks and an adequate control structure was implemented.

Mind journey to the scientific questions.

If we take a mind journey back to the engineering/scientific design question given at the beginning of this chapter, the following remark can be made. The complexities of RD process design are handled in this chapter by the definition of an easy-to-handle *tool* to assist the modeling task. Furthermore, a more *design* advanced approach is addressed, which involves the simultaneous dynamic optimization of spatial and control structures in the presence of a disturbance scenario. Therefore, the material presented in this chapter contributes to the answering of Question 6.

"Engineering is the art or science of making practical."

Samuel C. Florman, writer and engineer

7

Steady and Dynamic Behavior Analysis[†]

The steady-state and dynamic behavior in RD are studied in line with the proposed design procedure. Two levels of aggregation are considered: a single stage reactive flash and a full column. The first configuration is used to address the steady-state behavior, whereas the full column is used as case study for the process dynamics. By selecting a reactive flash we focus exclusively on the phenomena interaction rather than on equipment effects. In this regard, twenty-five bifurcation diagrams are presented, exhibiting a maximum of three steady states and five feasibility boundaries. Singularity theory is used to divide the parametric space into regions with qualitatively different behavior. Furthermore, parametric dependence of MSS regions is studied. Additionally, the dynamic behavior of a complete MTBE RD column is covered. Two deterministic disturbances are included to analyze the unit dynamics. The control structure is a conventional SISO and PID based one, aiming at disturbance rejection. This structure is defined based on a combination of rigorous degree of freedom analysis and engineering judgement. The variations encountered in product compositions reveal that the unit operates effectively in the presence of disturbances. The output of this analysis defines the reference case for the new developments to be introduced in chapter 8.

[†]Section §7.2.1 on multiplicities in a reactive flash has appeared as Lakerveld *et al.* (2005).

Chapter 7

7.1 Introduction

The sixth design space of the multiechelon approach (*cf.* chapter 4) in reactive distillation is the focus of this chapter. After having defined the spatial and control structures the process behavior in steady-state and dynamic domains are now addressed. The input and output information flow at this design space is detailed on table 7.1.

Table 7.1. Input-output information for the behavior analysis space. The multiechelon approach is explained in section §4.5.

Design specifications	**Design/operational variables**	**Domain knowledge**
Process:	Continuous:	- steady-state behavior
- unit structure	- controllability index	- dynamic behavior
- control structure	- operating conditions	

The analysis of steady-state behavior allows the designer to explore the effect of kinetics, gas/liquid mass transfer and hydrodynamics and the steady-states of the unit. On the other hand, dynamic simulations are carried out to check the robustness of the design, in terms of the ability of maintain product purities and conversion in desired range when disturbances are occurring.

This chapter addresses those two aspects of process behavior: steady-state and dynamic operation. In the first case, a reactive flash with a rather ideal exothermic isomerization reaction is considered. This simplified system is selected to account exclusively on the effect of phenomena interaction on the occurrence of input and output multiplicity. Therefore, any effect related to unit configuration is considered outside the scope of the analysis.

The second part of this chapter deals with the dynamic behavior of a full RD column, with special focus on the synthesis of MTBE. Although the design of the control structure is rather conventional (SISO and PI controllers), it is regarded as reference case for the new developments to be introduced in chapter 8.

Recalling the engineering and scientific design questions given in chapter 1, in this chapter we address question 6, namely,

- *What (new) methods and tools are needed for reactive distillation process synthesis, analysis and evaluation?*

7.2 Steady-State Behavior

7.2.1 Introduction

Section 2.9 has addressed the generalities and sources of steady-state multiplicity in RD processing. Furthermore, special attention has been paid to the implications of MSS for the design and operation of RD. In this section the steady-state behavior of a simplified RD unit (*i.e.* reactive flash) is covered for the case of an exothermic isomerization reaction with first-order kinetics and light-boiling reactant. Several approaches are employed to analyze the steady-state behavior of a process model. For instance, regions of MSS can be identified by tracing the dependence of the steady state on one varying parameter (Mohl *et al.*, 1999; Hauan *et al.*, 1995*a*; Ciric and Miao, 1994; Baur *et al.*, 2001*b*; Sneesby *et al.*, 1998*b*,*a*; Chen *et al.*, 2002). The starting point of our approach is provided by the study on MSS in a reactive flash by Rodriguez *et al.* (2001, 2004). They show that multiplicity is caused by the interaction between separation and reaction in systems in which the activation energy and the gradient of boiling temperature with composition are sufficiently large. Because VL equilibrium can create multiple steady states, state multiplicity becomes possible in endothermic or slightly exothermic systems, which typically do not display multiplicity in a one-phase CSTR. Several examples were considered and parametric studies were performed. In addition, for an isomerization reaction, necessary conditions for multiplicity were derived. These conditions are somehow difficult to apply, because they are expressed in terms of system properties (*e.g.* heat of vaporization or heat of reaction), but also include, however, the unknown liquid and vapor phase compositions.

Although Rodriguez's work is restricted to a single stage flash, it clearly shows that the combination of reaction and separation is a key cause for multiplicity in RD.

In this section, we approach the reactive flash from a different perspective. We employ a dimensionless model and distinguish the state variables (*e.g.* liquid and vapor compositions), from system physical parameters (*e.g.* heat of reaction or activation energy) and control parameters (*e.g.* feed rate or heat duty). Aiming to uncover the possible behavior patterns, we present a considerable number of bifurcation diagrams that are qualitatively different. We demonstrate the importance of the feasibility boundaries corresponding to no-liquid or no-vapor products, illustrated in bifurcation diagrams exhibiting three and even five such points. Finally, we show that high heat of reaction, activation energy and reactant volatility enlarge the range of operating parameters for which multiple states exist. To the best of our knowledge, such a detailed analysis has not been provided yet for the case of RD. Section §7.2.1 is based on the contribution entitled *Exothermic isomerization reaction in reactive flash: steady state behavior* by Lakerveld *et al.* (2005).

7.2.2 System's Features and Model Development

The system under consideration intends to be as simplified and ideal as possible, so that we focus exclusively on the interaction between occurring phenomena. Thus, the properties of the system include: (*i*) binary system undergoing a kinetically controlled isomerization reaction $A \rightarrow B$, (*ii*) the RD flash is operated at isobaric conditions, (*iii*) the chemical reaction takes place exclusively in the liquid phase and is exothermic, (*iv*) the reactant A is the lighter component in the system, (*v*) both phases are assumed to be well mixed, (*vi*) gas and liquid phases behave ideally, (*vii*) vapor holdup is negligible compared to the liquid holdup, (*viii*) vapor pressures are described by Antoine's correlation and (*ix*) both components have equal physical properties (*i.e.* heat of vaporization, heat capacity and density).

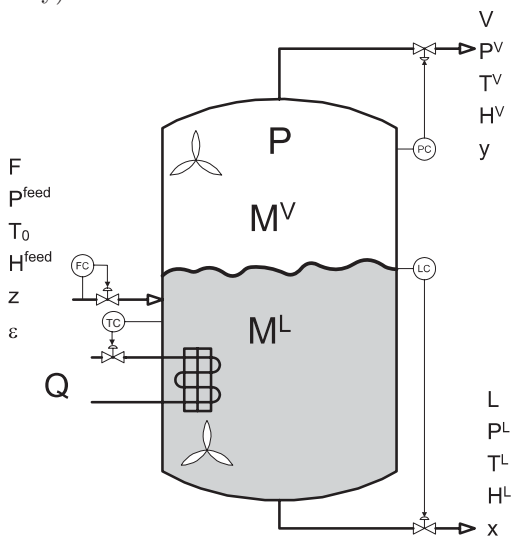

Figure 7.1. Schematic representation of a reactive flash for an isomerization reaction in the liquid phase.

According to the scheme of figure 7.1, pure reactant A is fed to the unit with a flow rate F, pre-heated to temperature T_0 and with a vapor fraction ε. The flash is equipped with a level controller and a pressure controller to maintain the liquid holdup M^L and operating pressure P at desired values. The liquid flow rate L and vapor flow rate V are used as manipulated variables, respectively. Heat is allowed to be added or removed at a rate Q in the liquid phase. For the sake of model solvability, a dimensionless model has been derived for the configuration depicted in figure 7.1. The set of governing equations and physical properties of the system are given in tables 7.2 and 7.3, respectively. The reference values for temperature, flow rate and pressure are: the boiling point of component A (*i.e.* $T_{b,A}$) and the nominal values of feed flow rate (*i.e.* F_{ref}) and pressure (*i.e.* P_{ref}) for an existing design, respectively.

Table 7.2. Set of governing dimensionless expressions for the reactive flash as depicted in figure 7.1.

Balance	**Dimensionless expression**
Overall mass	$0 = l + v - f$
Component	$\frac{dx}{dt} = \frac{1}{Da}(f \times z - l \times x - v \times y) - x \times e^{\frac{\dot{\gamma} \times \theta}{1+\theta}}$
BP condition	$0 = x \times p_1^0 + (1-x) \times p_2^0 - p$
L-V equilibrium	$0 = y \times p - x \times p_1^0$
Energy	$0 = f \times (\theta_0^* - \theta) + Da \times B \times x \times e^{\frac{\dot{\gamma} \times \theta}{1+\theta}} - v \times \lambda + q$
Feed temperature	$\theta_0^* = \begin{cases} \theta_0 & : \text{ liquid feed}, \theta_0 < 0 \\ \varepsilon \times \lambda & : \text{ liquid-vapor feed}, \theta_0 = 0 \\ \lambda + \frac{Cp^V}{Cp} \times \theta_0 & : \text{ vapor feed}, \theta_0 > 0 \end{cases}$

$$\mathbb{X} \equiv \begin{bmatrix} x \\ l \\ y \\ v \\ \theta \end{bmatrix}, \quad \mathbb{O} \equiv \begin{bmatrix} Da \\ f \\ z \\ \theta_0^* \\ p \\ q \end{bmatrix} = \begin{bmatrix} k(T_{\text{ref}}) \times \frac{M}{F_{\text{ref}}} \\ \frac{F}{F_{\text{ref}}} \\ z \\ \frac{T_0^* - T_{\text{ref}}}{T_{\text{ref}}} \\ \frac{P}{P_{\text{ref}}} \\ \frac{Q}{F_{\text{ref}} \times Cp \times T_{\text{ref}}} \end{bmatrix}, \quad \mathbb{S} \equiv \begin{bmatrix} \dot{\gamma} \\ B \\ \lambda \\ a_1 \\ b_1 \\ a_2 \\ b_2 \end{bmatrix} = \begin{bmatrix} \frac{E_a}{\mathcal{R} \times T_{\text{ref}}} \\ \frac{-\Delta^r H}{Cp \times T_{\text{ref}}} \\ \frac{\Delta^v H}{Cp \times T_{\text{ref}}} \\ A_1 \\ 1 \\ A_2 \\ \frac{A_1 \times B_2}{A_2 \times B_1} \end{bmatrix}$$

Remark: the validity of the model is limited by the boundaries $v = 0$ and $l = 0$.
Nomenclature: $\mathbb{X}$ are unknown variables, $\mathbb{O}$ are operation parameters, $\mathbb{S}$ are system parameters; z, x and y are the molar fractions in the feed, liquid and vapor phases, respectively; f, l and v are the dimensionless feed, liquid and vapor flow rates, respectively ($f = F/F_{\text{ref}}$, $l = L/F_{\text{ref}}$, $v \equiv V/F_{\text{ref}}$), θ is the dimensionless temperature ($\theta = \frac{T - T_{\text{ref}}}{T_{\text{ref}}}$), ε is the vapor fraction in the feed ($\varepsilon \in [0, 1]$), the component saturation pressure is given by: $p_j^0 = \exp(a_j \frac{1 - b_j + \theta}{1+\theta})$, $i \in \mathbb{Z}^{n_c}$, Cp is the heat capacity and the feed temperature is estimated as,

$$T_0^* = \begin{cases} T_0 & : \quad T_0 < T_{b,A} \\ T_{b,A} + \varepsilon \times \frac{\Delta^v H}{Cp} & : \quad T_0 = T_{b,A} \\ T_{b,A} + \frac{\Delta^v H}{Cp} + \frac{Cp^V}{Cp} \times (T_0 - T_{b,A}) & : \quad T_0 > T_{b,A} \end{cases}$$

7.2.3 Classification of Steady States

From the model parameters the dimensionless feed, f, is chosen as distinguished continuation parameter and used to depict the dependence of liquid composition, x, for a VL feed (ε=0.13, T_0^*=280K) at different values of dimensionless heat duty, q (figure 7.2). The relevance of the parameter choice is grounded by the fact that feed flow rate determines the process throughput and is frequently an operational parameter subjected to input disturbances (*e.g.* market demands and supply fluctuations). The parametric space considered in this study is given by Damköhler number and dimensionless heat duty.

Table 7.3. Properties of the reactive flash system as depicted in figure 7.1. **Remarks:** data are taken from Rodriguez *et al.* (2001, 2004); accordingly, the reactant is the light-boiling component.

Property	Dimensional variable	Dimensionless variable
Pre-exponential factor	k_0=5.88 $\cdot 10^{10}$ s^{-1}	
Antoine coefficients	$A_1 = 9.784$	$a_1 = 9.784$
	$A_2 = 7.704$	$a_2 = 7.704$
	$B_1 = 2428$	$b_1 = 1$
	$B_2 = 2428$	$b_2 = 1.27$
Heat of vaporization	$\Delta^v H = 4807$ kcal$\times$kmol^{-1}	
Heat capacity	$Cp = 20.0$ kcal$\times$(kmol$\times$K)$^{-1}$	$\lambda = 1$
Heat of reaction	$\Delta^r H$= 500 kcal$\times$kmol^{-1}	$B = 0.1$
Activation energy	E_a= 14454 kcal$\times$kmol^{-1}	$\dot{\gamma} = 30$

Three qualitatively different *bifurcation* diagrams* can be observed if the heat input to the system is varied. For adiabatic operation (q=0) no feasible solution exists for small f. As f increases, the number of steady states changes from 0-2-3-1. The lower branch of the curve starts at a *feasibility boundary* (v=0, marker: $\square$) and exhibits two *turning points* (marker: $\diamond$), also known as *limit* or *fold*. If the heat duty is further increased (q=1), the bifurcation diagram presents the pattern 0-1-3-1. For even larger values of q, the bifurcation curves start at the l-boundary (*i.e.* $l = 0$ feasibility boundary, marker: $\bullet$) and a single steady state occurs. It can be noted that the type of diagram depends on the number and relative location of turning points and feasibility boundaries. These points are normally termed *codimension-1 bifurcation* or *singular points*, as they correspond to certain values of one single parameter (*e.g.* f).

Based on the multiplicity behavior of the RD model, a singularity theory approach (Bildea and Dimian, 1999; Gehrke and Marquardt, 1997; Balakotaiah and Luss, 1984) is used to divide the space of model parameters, excluding the distinguished one, into regions of qualitatively different bifurcation pattern. All nonlinear equations are solved with a Newton-Raphson solver routine combined with a local parametrization algorithm (Seydel and Hlavacek, 1987; Razon and Schmitz, 1987; Wayburn and Seader, 1987; Vadapalli and Seader, 2001; Dhooge *et al.*, 2003) to track possible turning points. To deal with the large number of parameters involved, we adopt the following strategy. First, we achieve the classification in the *Da-q* space, for a system characterized by small heat of reaction, moderate activation energy and high relative volatility. For a VL feed, we identify the main types of behavior occurring in large regions and the

*The following notation is used for the bifurcation diagrams: $BD(p, x; p_1, p_2)$, where p denotes the distinguished parameter, x is the state variable and p_1 and p_2 are system's parameters. A BD can be effectively defined by specifying parameter p_1 or p_2 in addition to the distinguished parameter p.

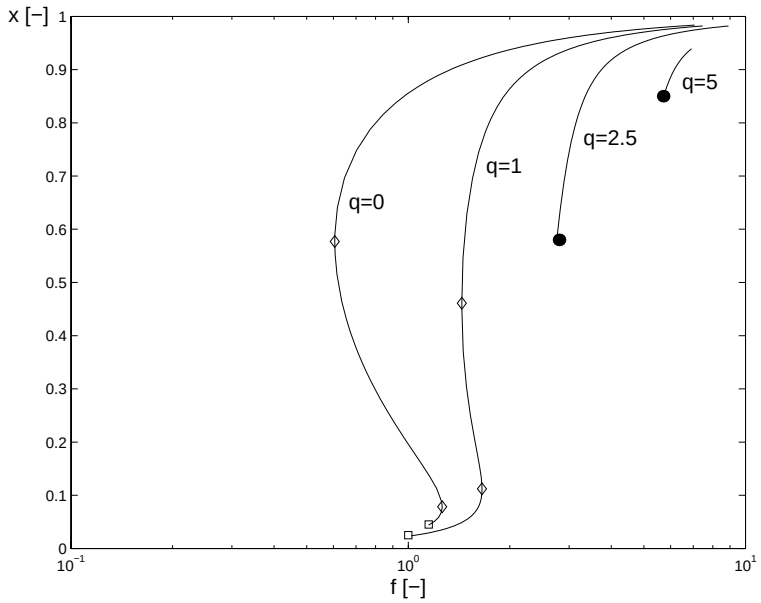

Figure 7.2. Bifurcation diagram f-x at different values of dimensionless heat duty for a reactive flash undergoing an exothermic isomerization. **Symbols:** (□): $v = 0$ feasibility boundary; (•): $l = 0$ feasibility boundary; (◇): limit point. **Systems features:** Da=0.10; z=1; p=1; θ_0^*=0.13; physical properties of the system are listed in table 7.3; governing expressions are given in table 7.2.

important varieties bounding these regions. Afterwards, the effect of the feed condition θ_0^*, the remaining control parameter, is investigated. Finally, we look at the effect of larger heat of reaction, larger activation energy and lower relative volatility.

Singularity theory states that the qualitative features of the bifurcation diagram may change only when the parameter set crosses the hysteresis, isola, or double-limit varieties (Golubitsky and Schaeffer, 1985). Only the hysteresis variety is found to exist for the reactive flash model. When the hysteresis variety is crossed, the number of possible steady states changes by two, as two limit points appear or disappear. When feasibility boundaries exist, the bifurcation diagram may also change at special sets of parameters (Balakotaiah and Luss, 1984). The following varieties are considered in this study,

Variety 1. boundary-limit set (BL): a limit point occurs at a feasibility boundary,

Variety 2. boundary - tangent set (BT): the bifurcation diagram is tangent to the feasibility boundary. After crossing this set (*e.g.* moving from high to low dimensionless heat duty q in figure 7.5) the bifurcation diagram changes by appearance / disappearance of two feasibility boundaries,

Variety 3. cross-and-limit set (CL): the position of one limit point changes relative to one solution located at the feasibility boundary,

Variety 4. corner set (C): the bifurcation parameter and the state variable are, simultaneously, at their boundaries.

Because the defining conditions can be solved for the state variables and two parameters (*e.g.* f and q), the above mentioned varieties are said to be of *codimension-2*. The dynamic model of the reactive flash contains several algebraic, but only one differential equation, when the holdup and pressure are fixed and the phase equilibrium is instantaneous. Such one-dimensional systems cannot exhibit Hopf bifurcations leading to oscillatory behavior. Therefore, dynamic classification is not necessary.

A better understanding of the steady state classification is carried out by depicting the loci of codimension-1 singular points in a f-q plot (figure 7.3). As the $BD(f, x, q)$ bifurcation diagrams are obtained for a given value of q, the number and relative location of singular points can be obtained by the intersection of q=constant (dotted horizontal lines in figure 7.3) with the loci of codimension-1 singular points. It can be extracted from the figure that at large q, there is only one intersection with the l-boundary, corresponding to the bifurcation diagram I+III in figure 7.4. As q decreases, a narrow region with three l-boundaries is encountered. This region is bounded by the boundary-tangent points BT_1 and BT_2 in the q-f plot (zoomed view in figure 7.5a). Diagram II in figure 7.4 represents the behavior in this region. As q is further decreased, two turning points are met below the cusp H. State multiplicity becomes possible, as shown in diagram IV of figure 7.4. Note that the loci of cusp points is called *hysteresis*.

Many qualitative changes occur within a small *elbow* region around q=0, which is zoomed in Figs. 7.5b-d. If we decrease the value of q, the boundary-tangent BT_3 is firstly crossed to region V (figure 7.5c) leading to two v- boundaries. Immediately, the relative locations of a turning point and a v-boundary change at a cross-and-limit point CL, leading to diagram VI (figure 7.4). By further decreasing q to region VII (figure 7.5b), the v- and l-boundaries move towards f=0 (left section in figure 7.3) and disappear at a corner point (not shown). One turning point leaves the feasible domain at the boundary limit BL_1 and the maximum number of steady states becomes two, as in diagram $VIII$ (figure 7.4). Finally, the turning point left becomes unfeasible and the state multiplicity disappears as depicted in figure 7.4-diagram XI. Furthermore, a very narrow range of q values exists (figure 7.5d) where three v-boundaries occur (diagrams IX, X in figure 7.4).

7.2.4 Effect of Damköhler Number, Da

The steady state classification is achieved by tracing the codimension-2 singular points when an additional parameter (*e.g.* Da) is changed. In this way, the Da-q space is divided into regions where qualitatively different f-x bifurcation diagrams exist (figure 7.6). For each region, the corresponding diagram is presented in figure 7.4. It should be noticed that regions *II*, *V*, *IX* and *X*, exhibit three feasibility boundaries and are very small.

7.2.5 Effect of Feed Condition

In the previous section a VL feed ($0 < \theta_0^* < 1$) has been considered. Among the bifurcation diagrams of figure 7.4, those presenting two disconnected branches and three feasibility boundaries should be remarked. Such diagrams are obtained when BT sets are crossed (see figures 7.5*a*-*d*), but are occurring exclusively in narrow regions of the $Da - q$ space (figure 7.6). This subsection discusses the effect of the feed condition (*i.e.* sub-cooled liquid: $\theta_0^* < 0$ and over-heated vapor: $\theta_0^* > 1$) on the regions with qualitatively different bifurcation pattern.

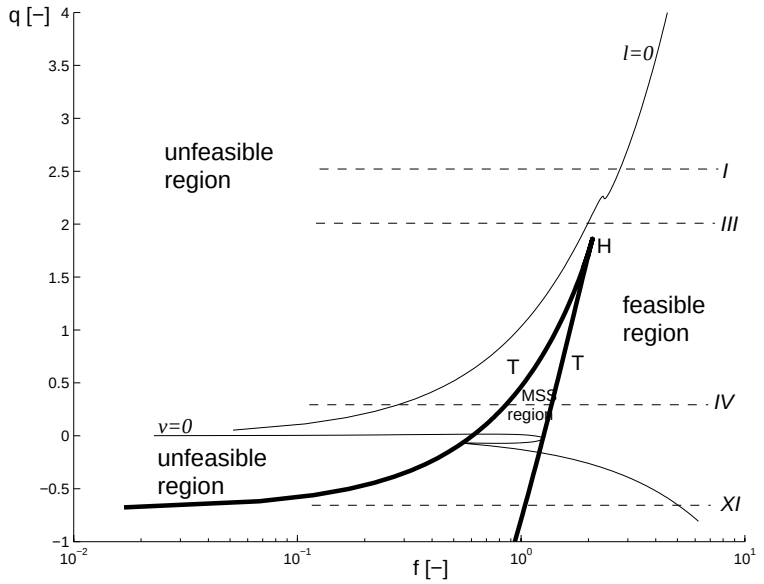

Figure 7.3. Codimension-1 singular points for a reactive flash undergoing an exothermic isomerization. **Nomenclature:** H: hysteresis variety; T: turning point loci. **Systems features:** Da=0.10; z=1; p=1; θ_0^*=0.13; physical properties of the system are listed in table 7.3; governing expressions are given in table 7.2.

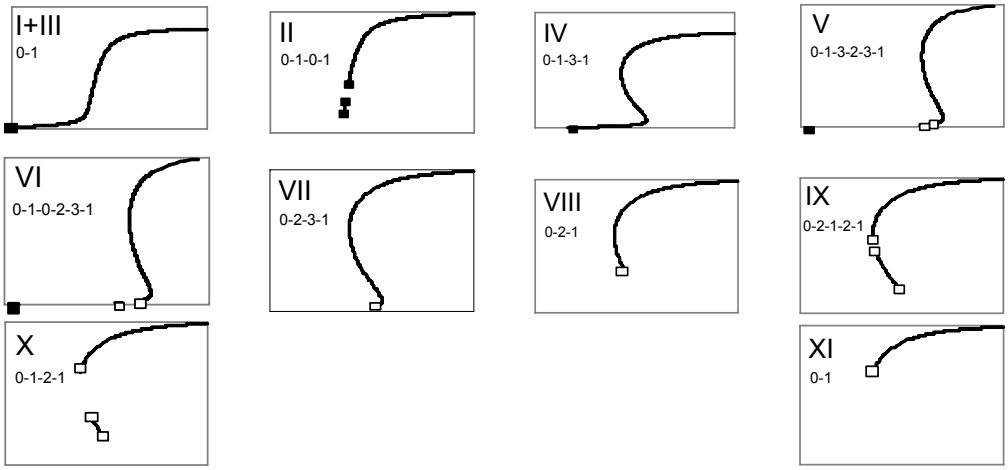

Figure 7.4. Qualitatively different bifurcation diagrams for a reactive flash undergoing an isomerization reaction. **Symbols:** (□): if $v = 0$; (■): if $l = 0$; **Systems features:** Da=0.10; z=1; p=1; θ_0^*=0.13; physical properties of the system are listed in table 7.3; governing expressions are given in table 7.2.

In the $f - q$ space (figure 7.7), the qualitative bifurcation pattern of the v- and l-boundaries change at values of $\theta_0^* = 0$ and $\theta_0^* = \lambda = 1$, respectively. By comparing figure 7.5*b-d* with figure 7.7a, it can be noticed that the boundary tangent sets BT_3 and BT_5 disappear when the vapor fraction increases (*e.g.* $\varepsilon \to 1$) and when the feed is a sub-cooled liquid (*i.e.* $\theta_0^* < 0$), respectively. However, the distance between two boundary-tangent sets becomes larger, which is reflected by larger regions where the bifurcation diagram consists of two disconnected branches separated by $v = 0$ points. Moreover, for the l-boundary (figure 7.7b), the set BT_2 disappears at $\theta_0^* = \lambda = 1$.

It is noted, additionally, that for vapor-only ($\theta_0^* > 1$) or liquid-only ($\theta_0^* < 0$) feeds the $f - x$ bifurcation diagram exhibits at least one v-boundary and one l-boundary. Finally, for nominal feed conditions (*i.e.* $0 < \theta_0^* < 1$) at least one feasibility boundary exists, depending on the value of q.

As a vapor product from a liquid feed ($\theta_0^* < 0$) is possible only if heat is supplied ($q > 0$), the feasible region in figure 7.7*a* is located at the upper plane. Similarly, as a liquid product from a vapor feed ($\theta_0^* > 1$) is attained exclusively by heat removal ($q < 0$), the feasible region in figure 7.7*b* occupies the lower plane. Thus, when the feed is sub-cooled liquid or over-heated vapor, the reactive flash model has feasible steady states only over a finite range of heat duty.

Phase diagrams for these three θ_0^*-regimes (*i.e.* $\theta_0^* < 0$; $0 < \theta_0^* < 1$ and $\theta_0^* > 1$) exhibit different qualitative topology (see figure 7 in Lakerveld *et al.* (2005)). That figure

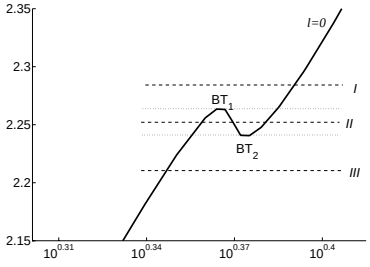

(a) Zoomed view at inflection point

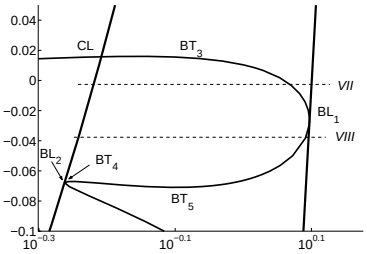

(b) Zoomed view at elbow location

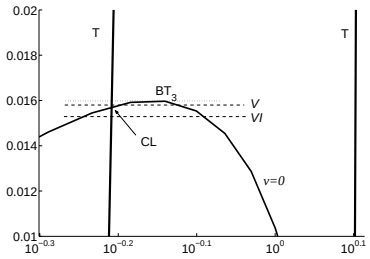

(c) Zoomed view at upper elbow branch

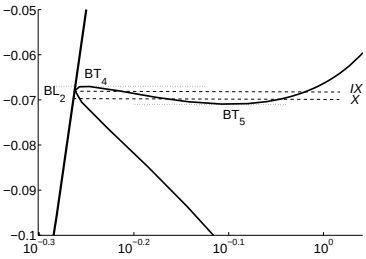

(d) Zoomed view at lower elbow branch

Figure 7.5. Zoomed view of figure 7.3. Codimension-1 bifurcation points in the $f - q$ plane. **Remark:** the parametric space is f (x-axis)-q (y-axis). **Nomenclature:** BT: boundary tangent; CL: cross-and-limit; BL: boundary limit. **Systems features:** Da=0.10; z=1; p=1; θ_0^*=0.13; physical properties are listed in table 7.3; governing expressions are given in table 7.2.

suggests that increasing Damköhler number might move an operating point into a region with multiplicity if $\theta_0^* < 1$. Furthermore, regardless the θ_0^*-value, lower heat input q might move an operating point into a multiplicity region. Additionally, increasing θ_0^* (with $\theta_0^* < 1$) reduces the multiplicity region as the hysteresis variety is shifted to the right of the plane. At $\theta_0^* \to 1$ the hysteresis variety moves to negative values of q and a qualitatively different topology is obtained[‡].

The effect of the system's properties on the steady state behavior is conveyed in the next subsection. As the level of detail might be considerably increased, three physical properties are considered: heat of reaction, activation energy and relative volatility. The ultimate goal of this analysis involves the definition of trends in the steady state behavior, rather than a rigorous quantitative classification. For the sake of comparison, the system introduced in table 7.3 is labelled as reference case.

[‡]The work of Lakerveld *et al.* (2005) presents 14 additional bifurcation diagrams, obtained by detailed analysis of the influence of feed condition and system's physical properties on the codimension-1 singular points.

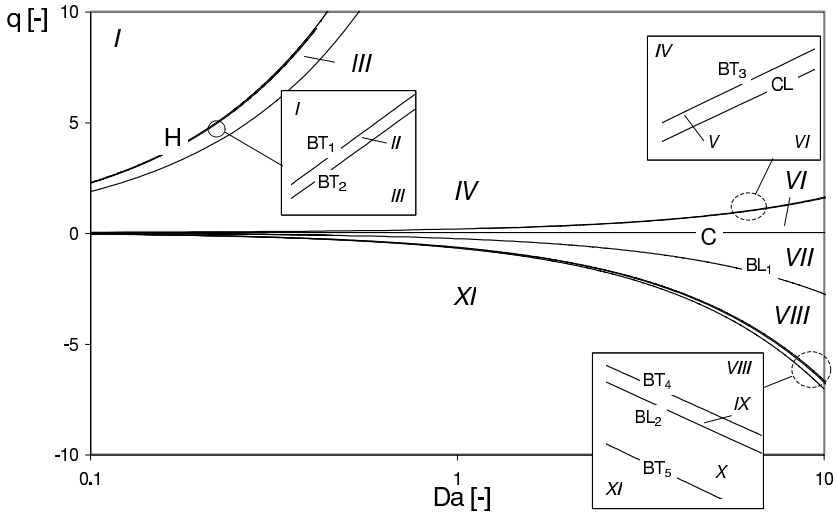

Figure 7.6. Phase diagram for the reactive flash model. **Remark:** numbers correspond to $f - x$ bifurcation diagrams in figure 7.4. **Nomenclature:** *H*: hysteresis variety; *C:* corner set; *BT:* boundary tangent set; *CL:* cross-and-limit set; *BL:* boundary limit set. **Systems features:** z=1; p=1; θ_0^*=0.13; physical properties of the system are listed in table 7.3; governing expressions are given in table 7.2.

7.2.6 Effect of Heat of Reaction

Increasing the adiabatic temperature rise B (from $B = 0.1$ (reference case) to $B = 1.0$) leads to the relocation of the hysteresis variety to lower values of Da and higher values of q. This situation results in a larger area of state multiplicity. However, the MSS region does not vanish when the heat of reaction is reduced to zero. Figure 7.8 depicts the feasibility boundaries at large heat of reaction and different feed condition θ_0^*.

Compared to the reference case (*cf.* figure 7.7), the feasibility boundaries exhibit different shapes and are located at lower values of the heat input q. This last situation is justified by the fact that as more heat is generated by the reaction, less heat has to be added to the system to vaporize the entire feed (l=0), or to generate vapors from a given feed (v=0). Furthermore, the above-mentioned limiting cases (*i.e.* $\theta_0^* = 0$ and $\theta_0^* = \lambda$) are recognized.

In figure 7.9 the loci of codimension-1 points are depicted in the $f - q$ space. As the heat of reaction is increased, the cusp point H crosses the l-boundary at a codimension-3 point and moves into the unfeasible region. Although the area between the loci of

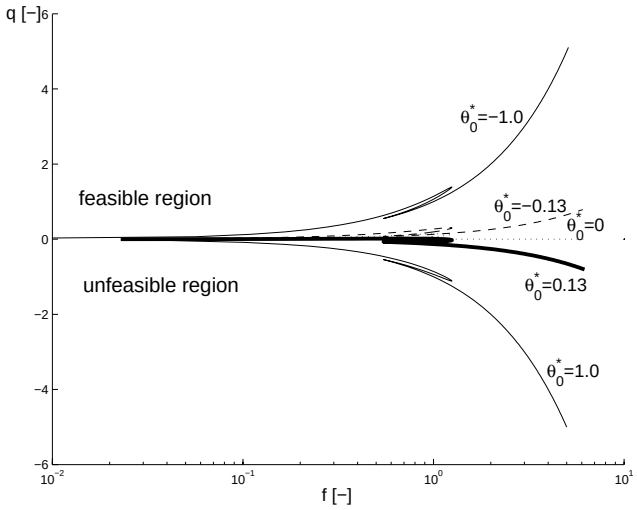

(a) $v = 0$ feasibility boundaries

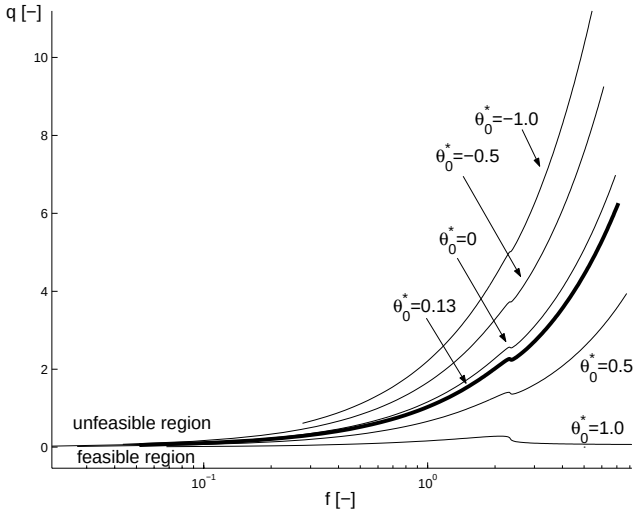

(b) $l = 0$ feasibility boundaries

Figure 7.7. Effects of feed condition on feasibility boundaries. **Systems features:** Da=0.10; z=1; p=1; physical properties are listed in table 7.3; governing expressions are given in table 7.2.

the turning points is partly in the unfeasible region, not all branches of the bifurcation diagram are unfeasible. These changes result in new types of bifurcation diagrams, as has been reported by Lakerveld *et al.* (2005) (*cf.* figure 13 in Lakerveld *et al.* (2005)).

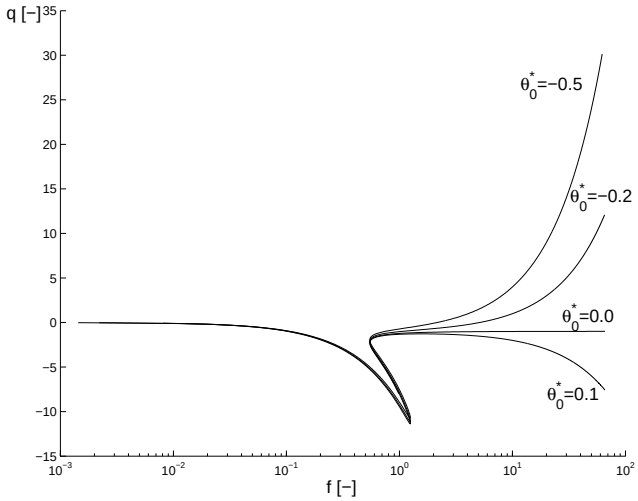

(a) $v = 0$ feasibility boundaries

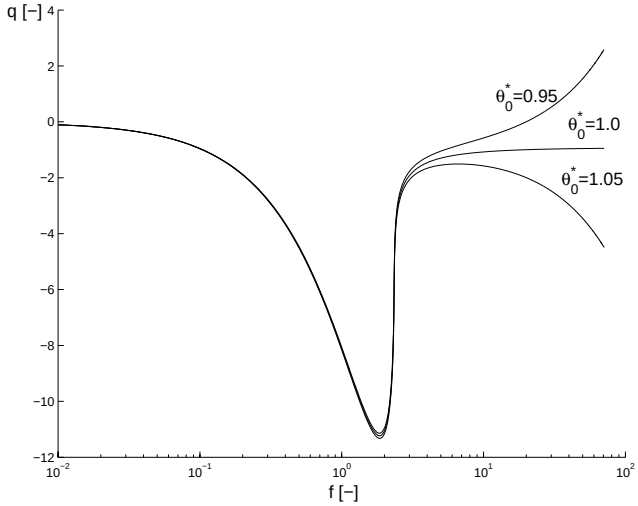

(b) $l = 0$ feasibility boundaries

Figure 7.8. Effects of feed condition on feasibility boundaries at large heat of reaction. **Systems features:** B=1.0; Da=0.10; z=1; p=1; physical properties are listed in table 7.3; governing expressions are given in table 7.2.

7.2.7 Effect of Activation Energy

As shown in figure 7.10*a*, increasing the activation energy (from $\dot{\gamma} = 30$ (reference) to $\dot{\gamma} = 45$) leads to a larger multiplicity area. The cusp point becomes physically unfeasible, as it occurs at $l < 0$. The elbow region in the l-boundary becomes more pronounced, resulting in larger regions with bifurcation diagrams exhibiting three fea-

sibility boundaries.

7.2.8 Effect of Relative Volatility

In the reference case, the relative volatility $\dot{\alpha}$ $(=p_1^0/p_2^0)$ has a large value (≈ 8). As reported in the case of synthesis of ethylene glycol by RD (Ciric and Miao, 1994), high volatility contributes to state multiplicity. The effect of reducing the relative volatility is addressed in this subsection. A value of $\dot{\alpha}$=4.4 is considered, keeping all other parameters at their reference value. As depicted in figure 7.10*b*, the extent of the multiplicity region becomes smaller than that in the reference case (*cf.* figure 7.3). Moreover, the feasibility boundaries are less relevant, as the elbow region on the l-boundary disappears and the region between the turning points on the v=0 curve is quite small.

The effect of increasing reaction heat and activation energy and decreasing relative volatility is illustrated in figure 7.11. The multiplicity area remains small with respect to the reference case, but the feasibility boundaries become more significant. Lakerveld *et al.* (2005) report bifurcation diagrams that exhibit up to five feasibility boundaries.

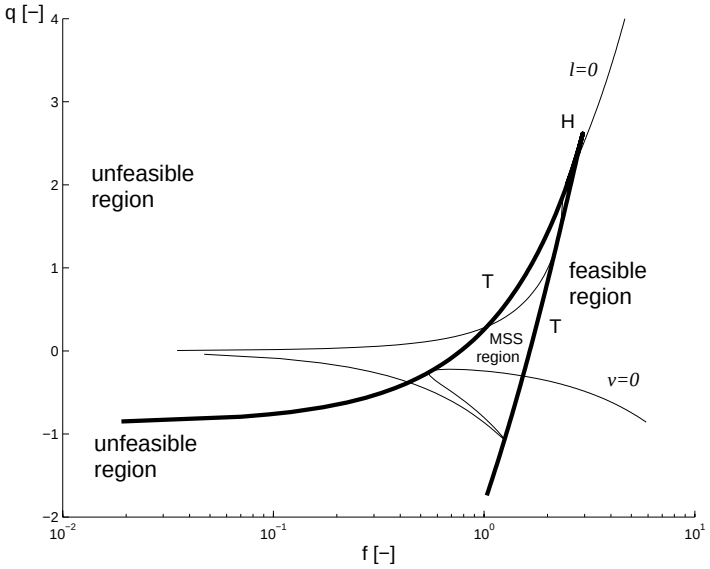

Figure 7.9. Effects of heat of reaction on codimension-1 singular points. **Nomenclature:** H: hysteresis variety (cusp loci); T: turning point loci. **Systems features:** B=1.0; Da=0.10; z=1; p=1; θ_0^*=0.13; physical properties are listed in table 7.3; governing expressions are given in table 7.2.

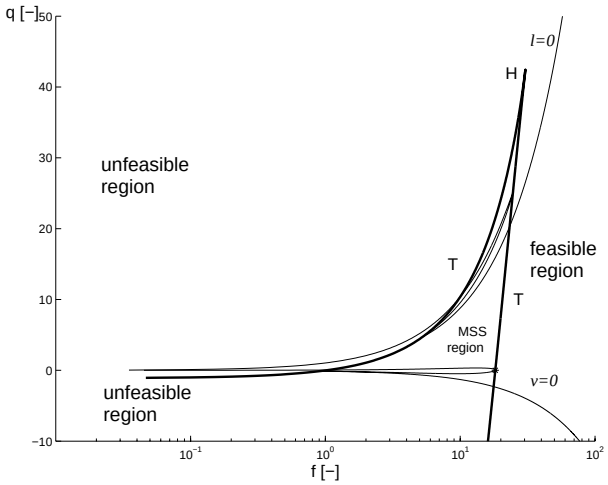

(a) Large activation energy, $\dot{\gamma}$=45

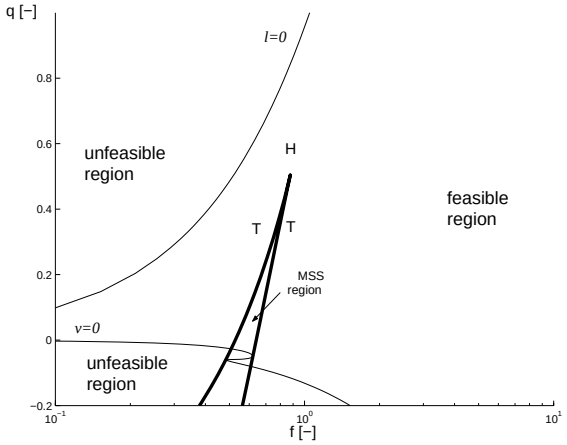

(b) Smaller relative volatility, $\dot{\alpha}$=4.4

Figure 7.10. Effects of activation energy and relative volatility on codimension-1 singular points. **Nomenclature:** H: hysteresis variety (cusp loci); T: turning point loci. **Systems features:** Da=0.10; z=1; p=1; θ_0^*=0.13; physical properties are listed in table 7.3; governing expressions are given in table 7.2.

7.2.9 Significance of Results and Extension Possibilities

The results of this section show that a considerable number of bifurcation diagrams can be identified even for a simplified RD application. By addressing a single reactive tray we aim to explore exclusively the interaction between phase equilibrium and chemical reaction. The possibilities to extend this approach to a more realistic and full-scale RD

system are numerous.

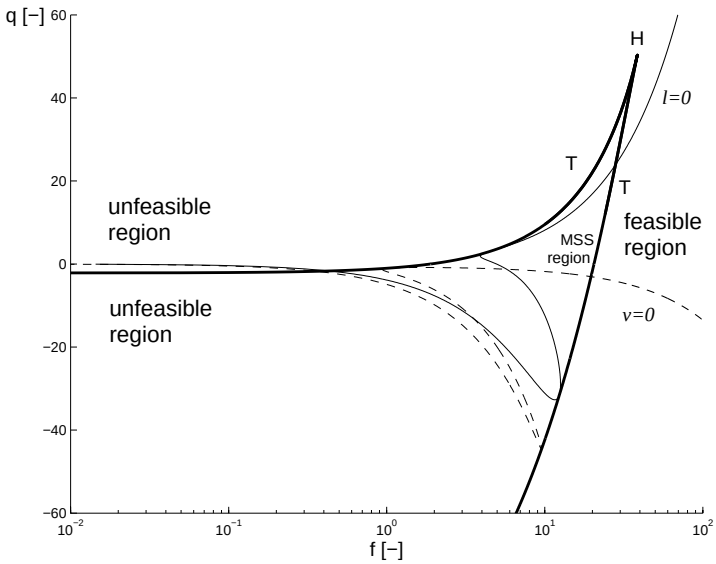

Figure 7.11. Combined effects of heat of reaction, activation energy and relative volatility on codimension-1 singular points. **Nomenclature:** H: hysteresis variety; T: turning point loci. **Systems features:** B=5; $\dot{\gamma}$=50; $\dot{\alpha}$=4.4; Da=0.10; z=1; p=1; θ_0^*=0.13; physical properties are listed in table 7.3; governing expressions are given in table 7.2.

For instance, the idealized physical properties of the system could be replaced by rate-limited mass/heat transfer models, as suggested by Baur *et al.* (2001*c*); Higler *et al.* (1999*b*). Multiplicity behavior is reported in both models for the case of MTBE synthesis and only differing in the relative size of region of occurrence. Additionally, if we extend our reactive tray to a RD column with reactive and nonreactive sections, the effect of both regions on MSS occurrence should be borne in mind. As mentioned by (Güttinger and Morari, 1997), these interactions could be largely responsible for multiplicity. In both cases, singularity theory approach could be useful to investigate the main behavior patterns. The approach presented in this section is not restricted to our case study but could be equally applicable to more complex reactive distillation systems, including multicomponent, multireaction and nonideal systems.

7.3 Dynamic Behavior

7.3.1 Introduction

The nonlinear coupling of reactions, transport phenomena, phase equilibria and hardware hydraulics can give rise to highly complicated dynamic behavior of the system. In the previous section, we showed that even for a simplified reactive flash and an idealized system a large number of bifurcation diagrams could be identified. The main source of multiplicity is then suggested to be the strong nonlinear coupling of reactions, transport phenomena and phase equilibria.

The strong parametric sensitivity resulting from this coupling largely determines the start-up procedure, steady-state and transient operations (Ruiz *et al.*, 1995). Moreover, even small variations in the input variables might lead to unstable conditions (Alejski and Duprat, 1996). This fact implies that a feasible operation of a RD column requires several control loops to mitigate the effects of disturbances.

In this section, we explore the process dynamics of a full RD unit. The scope of this analysis is restricted to a limited version of control system design, as a SISO structure and PID controllers are a priori selected. The starting point of the analysis involves the development of a reliable mathematical model, capable of predicting with acceptable accuracy the unit behavior. Moreover, the model should not be computational expensive at this conceptual design level. To identify the variables to be controlled and manipulated and then fully analyze the dynamic behavior of the system a rigorous degree of freedom analysis is performed. Moreover, the controllers have to be effectively tuned and a realistic disturbance scenario has to be defined. The analysis of the unit involves assessing its capability of coping with the disturbance scenario without violating the specification constraints. It is worth mentioning that this approach does not address any interaction between column design and control design.

The content of this rather classical control approach sets the stage for a next novel contribution to be introduced in chapter 8, involving the trade-off between design, responsiveness and sustainability aspects. Thus, the outcome of this section serves as a reference case to be compared with that of the life-span inspired design methodology (*cf.* section §1.4).

As in previous chapters, the synthesis of MTBE is used as case study. As the focus of this section is the dynamic behavior of the unit around a desired steady state, we choose appropriate processing conditions and design parameters to avoid multiplicity as much as possible. The steady state of interest is the high-purity one as given elsewhere Hauan *et al.* (1995*a*,*b*); Jacobs and Krishna (1993); Schrans *et al.* (1996).

7.3.2 Model Description, Control Structure and Disturbance Scenarios

7.3.2.1 Model Description

A RD column is considered for modeling and analysis purposes. During the model development of this unit the following set of assumptions are made: (*i*) the liquid and vapor streams leaving a trays are in thermodynamic equilibrium; (*ii*) both liquid and vapor hold-ups are fully considered; (*iii*) the liquid and vapor on each tray are perfectly-well mixed (*i.e.* no radial gradient in temperature and composition and the liquid on the tray has a concentration equal to that of the liquid leaving the tray); (*iv*) the reactions are taking place in the liquid phase and enhanced by a solid catalyst; (*v*) the reactions occur only on the trays containing catalyst; (*vi*) vapor and liquid entrainment is neglected; (*vii*) the column is equipped with a condenser, reflux drum and reboiler; (*viii*) the location(s) of the feed stream(s) and product stream(s) are known a priori; (*ix*) the sizing parameters of the unit and operational variables are obtained from previous design stages (*cf.* section §6.2); (*x*) the liquid hold-up on a tray is related to the liquid outflow according to Francis weir formula; (*xi*) the flow of vapor leaving a tray is determined by the pressure drop between two consecutive trays; (*xii*) the tray pressure drop includes contributions of dry pressure drop, liquid height (weir height plus height over the weir) and residual head; (*xiii*) the physical properties of the involved streams are computed as a function of temperature and/or phase composition; (*xiv*) the heat of reaction is omitted in the energy balance, because the heat of formation at standard conditions ($1.033 \cdot 10^5$ Pa/298 K) is used as reference in the enthalpy computations; (*xv*) the reboiler, condenser and reflux drum are nonreactive units; (*xvi*) the tray sizing is estimated by rules-of-thumb criteria (Coulson and Richardson, 1991); (*xvii*) the column diameter is larger than the minimum flooding value.

The RD model consists of sets of algebraic and differential equations, which are obtained from the mass, energy and momentum balances performed on each tray, reboiler, condenser, reflux drum and PI controller instances. Additionally, algebraic expressions are included to account for constitutive relations and to estimate physical properties of the components, plate hydraulics and column sizing. Moreover, initial values are included for each state variable. A detailed description of the mathematical model can be found in appendix A. The model is implemented in gPROMS©/gOPT©and solved using for the DAE a variable time step/variable order Backward Differentiation Formulae (BDF).

A rigorous degree of freedom analysis is performed to asses the consistency of the model and identify the set of controlled and manipulated variables. According to this analysis (tables A.1-A.3 in appendix A), the following set of input variables should be fixed,

- the reflux ratio, RR
- the RD column diameter at each location, $n_t \times D_{\text{col}}$,

Table 7.4. Optimized design of a RD column for MTBE synthesis as obtained in chapter 6.

	Value
Number of trays	15 [2:rectifying;8:reactive; 5:stripping]
Feed 1: location	iC$_4$+ nC$_4$: $10^{\underline{\text{th}}}$ tray (g)
Feed 1: flowrate	455 mol×s^{-1}
Feed 1: composition	iC$_4$: 0.37; nC$_4$: 0.63
Feed 1: temperature	350K
Feed 2: location	MeOH: $9^{\underline{\text{th}}}$ tray (l)
Feed 2: flowrate	168 mol×s^{-1}
Feed 2: composition	MeOH: 1.00
Feed 2: temperature	320K
Operating pressure	$11{\cdot}10^5$ Pa (top)
Reflux ratio	7
Mass of catalyst/tray	204.1 kg=1000 eq$_{[H^+]}$
Bottom flowrate	197 mol×s^{-1}
Column diameter	7.132 m
Condenser area	$1.059{\cdot}10^3$ m^2
Reboiler area	$6.93{\cdot}10^2$ m^2
MTBE bottom fraction	0.990-0.998

- the condenser area, A_{cond}, and
- the reboiler area A_{reb}.

The synthesis of MTBE from a C$_4$-stream and methanol in the presence of an acidic catalyst is used as tutorial application. A detailed description of this system is available in appendix B. The spatial structure of the RDC is that obtained by optimization in chapter 6 and summarized again in table 7.4. Discrete variables are arbitrarily fixed for the sake of simplicity. Thus, the structural configuration (*i.e.* number of trays and streams' staging) used in this example corresponds to the one used by Jacobs and Krishna (1993); Hauan *et al.* (1995*a*); Seader and Henley (1998). The values of these variables are also included in table 7.4.

7.3.2.2 Control Structure

To mitigate any effect caused by a disturbance scenario a control structure is proposed for the RD unit depicted in figure 7.12. The following assumptions are considered: (*i*) four control valves are associated with the RD unit; (*ii*) the unit is operated at constant reflux ratio RR ($=F^{R,L}/F^{D,L}=7$); and (*iii*) the throughput of the unit is set.

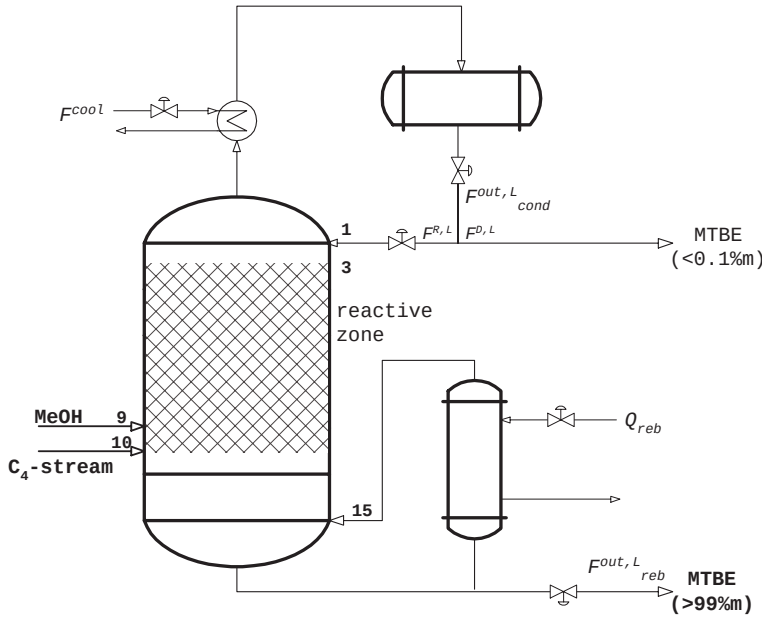

Figure 7.12. Schematic representation of a RD column in the synthesis of MTBE. **Remark:** numbers represent tray location.

In agreement with the degree of freedom analysis in table A.3 (appendix A) a 4×4 SISO control structure is suggested. The controlled variables are chosen aiming at the satisfaction of product specifications and protection of the unit. The pairing of controlled-manipulated variables, on the other hand, tries to minimize cross interactions between manipulations of input variables on the controlled output variables and looks for a dominant 1-1 correspondence between input and output variables. Thus, two control valves are used to control the liquid levels in the reflux drum and column bottom. As the reflux ratio is larger than a value of 4 ($RR > 4$), the reflux drum level is controlled with the liquid reflux or drum liquid outflow (Richardson's rule (Luyben *et al.*, 1999)). The level at the column bottom might be by convention controlled with the reboiler liquid outflow. The third control valve is used to manipulate the flowrate of cooling utility to control the column pressure. The remaining control degree of freedom is used to control the purity of the MTBE product by manipulating the reboiler heat duty. The composition of MTBE at the bottom stream is conveniently inferred from temperature measurements at a given tray. Steady-state open loop simulations are carried out to assess the effect of varying manipulated variable (*i.e.* reboiler duty Q_{reb}). Figure 7.13 shows that the largest temperature changes are occurring either at the rectifying section, the top section of the reactive section or at the reboiler. By selecting the reboiler temperature to infer the MTBE composition in the bottom stream, any hydraulic lag is effectively avoided.

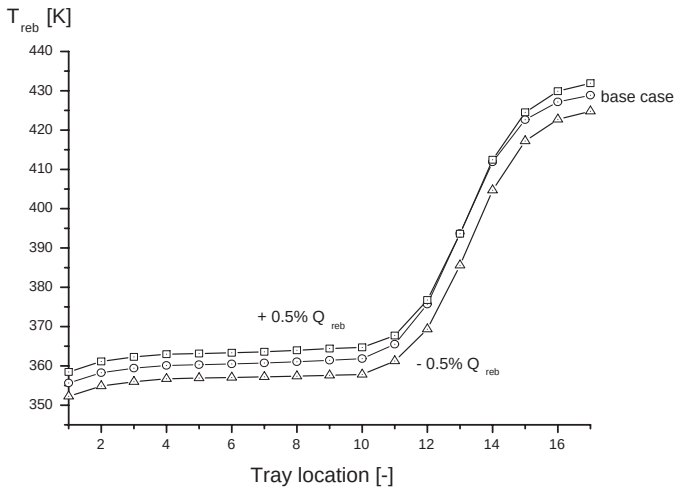

Figure 7.13. Effect of reboiler heat duty on the temperature profile in an MTBE RD column. **Remarks:** trays are numbered from top (condenser: $1^{\underline{st}}$) to bottom (reboiler: $1^{\underline{st}}$); MTBE product stream is withdrawn from the bottom location; column specifications are listed in table 7.4 .

This single-end point composition control structure is originated from the assumption of invariant reflux ratio. As mentioned by Luyben *et al.* (1999), this control structure is advantageous from both operational (*i.e.* easy tuning) and economical (*i.e.* comparable energy consumption) point of view compared to a dual composition control. The overall control structure is labelled $[RR] - Q_{\text{reb}}$, meaning that the reflux ratio is fix and the reboiler heat duty is used to control the bottom stream purity. Figure 7.14 depicts the proposed control structure and table 7.5 details each control loop. The controllers are tuned according to the guidelines presented in section §6.2.3.2. Table 6.5 lists all controllers parameters obtained using optimization and adopting a sequential approach (*i.e.* optimization of sizing parameters followed by optimization of control parameters). The controllers are assumed to be correctly tuned. Alternative control configurations are proposed for the MTBE synthesis by Wang *et al.* (2003); Sneesby *et al.* (1998*b*) addressing switch-over to different steady states. As the focus of this section is the dynamic behavior around a known steady state, no steady-state transition is considered by constraining the disturbances' variability.

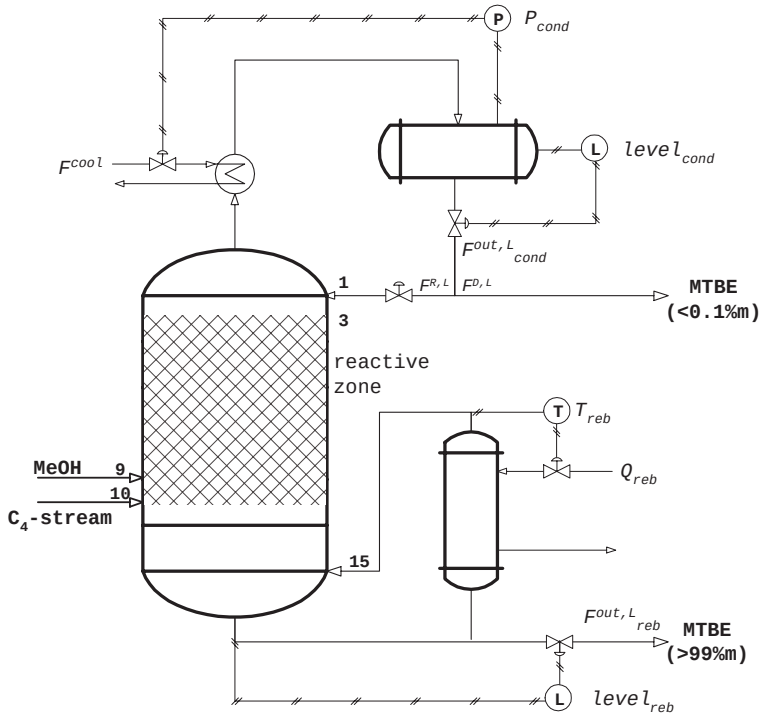

Figure 7.14. Schematic representation of a MTBE RD column with a 4×4 SISO control structure. **Remarks:** the coupling between controlled and manipulated variables for each control loop are listed in table 7.5; numbers represent tray location.

Table 7.5. Control loops in a reactive distillation stage column. The schematic representation of the unit is given in figure 7.14.

Unit	Controlled variable	Manipulated variable
P_1	Liquid level in condenser, $\text{level}_{\text{cond}}$	Outgoing flowrate in condenser, $F_{\text{cond}}^{\text{out},L}$
P_2	Pressure in condenser, P_{cond}	Flowrate of cold utility in condenser, F^{cool}
P_3	Liquid level in reboiler, $\text{level}_{\text{reb}}$	Outgoing flowrate in reboiler, $F_{\text{reb}}^{\text{out},L}$
P_4	Temperature in reboiler, T_{reb}	Heat duty of hot utility in reboiler, Q_{reb}

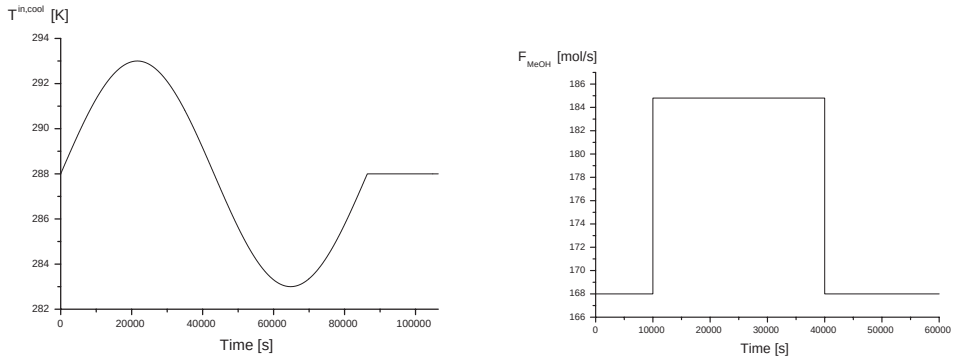

(a) Disturbance in the inlet temperature of the cold utility, $T^{\text{in,cool}}$, as defined in equation 7.1. Time horizon=86400 s.

(b) Disturbance in the feed flowrate of methanol, F_{MeOH}, as defined in equation 7.2. Time horizon=60000 s.

Figure 7.15. Disturbance scenarios considered for the analysis of the dynamic behavior of a MTBE RD column. **Remark:** column specifications are listed in table 7.4.

7.3.2.3 Disturbance Scenarios

In addition to the disturbance scenarios already defined in section §6.2, two disturbances are considered for this behavioral analysis (figure 7.15),

- a sinusoidal variation of coolant inlet temperature during 24 h (=86400 s) and defined as,

$$T^{\text{in,cool}} = 298 + \sigma_s(t), \quad \text{with} \quad \sigma_s(t) := 5 \times \sin(\frac{2 \times \pi}{8.64 \cdot 10^4} \times t). \tag{7.1}$$

- a step variation in the flowrate of methanol during the time horizon of $6{\cdot}10^4$ s and defined as,

$$F_{\text{MeOH}} = \begin{cases} F^{SS}_{\text{MeOH}} & \text{if } t < 1 \cdot 10^4 \text{ s or } t > 4 \cdot 10^4 \text{ s}, \\ 1.1 \times F^{SS}_{\text{MeOH}} & \text{if } 4 \cdot 10^4 \text{ s} > t > 1 \cdot 10^4 \text{ s}. \end{cases} \tag{7.2}$$

It is relevant to mention that the disturbance scenarios are defined in such a way that multiplicities are avoided. Since a detailed MSS analysis in RD has been already addressed in section 7.2.1, this section focuses exclusively on the dynamic behavior of the RD unit around an already known steady state. Thus, the control structure is defined so that no steady-state transitions are occurring. The effect of large methanol feed disturbances ($\Delta F_{\text{MeOH}} > 0.1$) on the operational steady state has been covered by Schrans *et al.* (1996); Sneesby *et al.* (1998*a*,*b*).

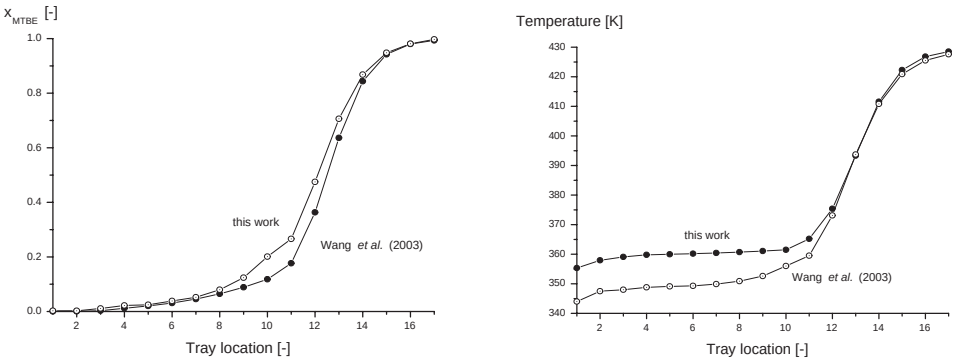

(a) MTBE composition profile.

(b) Temperature profile.

Figure 7.16. Comparison between steady-state profiles obtained in this work and by Wang *et al.* (2003). **Remarks:** trays are numbered from top (condenser: $1^{\underline{st}}$) to bottom (reboiler: $17^{\underline{th}}$); MTBE product stream is withdrawn from the bottom location; column specifications are listed in table 7.4.

7.3.3 Dynamic Response in the Presence of Disturbances

A preliminary analysis of the RD model is performed in the absence of any disturbance scenario. For the sake of model validation, the profiles of MTBE molar fraction and stage temperature are compared with those reported by Wang *et al.* (2003).

As noticed from figure 7.16 a relatively good agreement exists between both simulations. In the temperature profile, however, a slight difference is reported in the rectifying and reactive sections of the unit. The origin of this mismatch could be attributed to the different inert component considered in both cases. Wang *et al.* (2003) assume that the C_4-stream contains n-butene as inert component, whereas in the course of this thesis work inert n-butane is used. The different physical properties of these components might be leading to slightly altered energy balances and subsequently to different tray temperature. As the temperature mismatch starts to play a role on the reactive trays, it could be suggested that differences exist between the estimations of reaction heat. Moreover, the kinetic and thermodynamic models used in both cases do not fully coincide. On the other hand, the degree of agreement between MTBE molar fractions obtained by Wang *et al.* (2003) and this work is quite satisfactory.

At this point the dynamic behavior of the RD unit is analyzed with respect to disturbance rejection. Figure 7.17 depicts the evolution of MTBE bottoms composition in presence of the deterministic disturbances. Oscillations around the set-point value are noticed, but of extremely small magnitude σ, specially for the disturbance in the

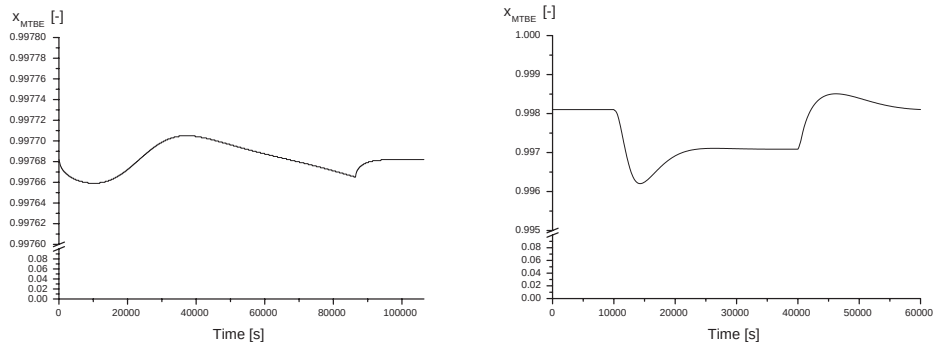

(a) $T^{\text{in,cool}}$ disturbance scenario. Time horizon: $8.64{\cdot}10^4$ s.

(b) F_{MeOH} disturbance scenario. Time horizon: $6{\cdot}10^4$ s.

Figure 7.17. Time variation of MTBE product stream in the presence of deterministic disturbance scenarios. **Remarks:** MTBE product stream is withdrawn from the bottom location; the column specifications are listed in table 7.4.

coolant inlet temperature,

- $|\sigma| < 0.002\%$ for the $T^{\text{in,cool}}$ disturbance
- $|\sigma| < 0.2\%$ for the F_{MeOH} disturbance

After the disturbances the RD column returns to its initial state, without any steady-state transition. From these results it can be suggested that the unit operates coping with product specification in spite of the presence of the defined disturbances. Obviously, more aggressive disturbance scenarios might lead to unit instability or even steady-state transitions. Schrans *et al.* (1996); Sneesby *et al.* (1998*a*,*b*) show that instabilities are expected to occur at slightly higher methanol flow disturbances.

7.4 Concluding Remarks

The conclusions derived from this chapter are grouped in accordance to the presented sections.

Steady-state behavior. In this first section, a reactive flash with a rather ideal system (mildly exothermic isomerization reaction and light-boiling reactant) was considered. This simplified system was selected to account exclusively for the effect of phenomena interaction on the occurrence of input and output multiplicity. Therefore, any effect related to unit configuration is considered outside the scope of the analysis.

For this particular case, the number and relative location of the turning points and feasibility boundaries corresponding to no-liquid or no-vapor products determined the qualitative nature of the bifurcation diagram. State multiplicity was present in a large area of the parameter space, for the case under consideration. A large number (25) of qualitatively different bifurcation diagrams could be identified for the system. The feasibility boundaries played an important role in the classification of the reactive flash. Up to five feasibility boundaries and a maximum of 3 steady states were found in a single bifurcation diagram. Bifurcation diagrams exhibiting more then two feasibility boundaries are common for liquid or vapor feed. Increasing the heat of reaction, activation energy or relative volatility enlarges the area of multiplicity. Furthermore, a large heat of reaction can create regions in parameter space with 5 feasibility boundaries in a single bifurcation diagram. The singularity theory approach could be useful to investigate the main behavior patterns in more complex reactive distillation systems, including multicomponent, multireaction and nonideal systems. Moreover, the effect of mass transfer would be worthwhile to examine, having as initial step the contributions of Baur *et al.* (2001*c*); Higler *et al.* (1999*b*).

Dynamic behavior. The second part of this chapter deals with the dynamic behavior of a full RD column, with special focus on the synthesis of MTBE. The content of this rather classical control approach (SISO and PI controller) sets the stage for a next novel contribution to be introduced in chapter 8, involving the trade-off between design, responsiveness and sustainability aspects. A generic dynamic model was developed for a complete RD column. The model was composed of instances of (non-) reactive trays, condenser, reflux drum, reboiler and PI controllers. Based on a rigorous degree of freedom analysis and engineering judgement a control structure was defined. The synthesis of MTBE was used as tutorial example for this section. The sizing of the unit corresponded to the optimized values obtained in previous chapters (*cf.* chapter 6). A set of deterministic disturbances were included, accounting for a sinusoidal variation of coolant inlet temperature and a methanol feed flowrate pulse. Moreover, the disturbances were defined in such a way that steady-state transitions were avoided. The controllers were tuned based on the optimization of the integral absolute error (*cf.* section §6.2.3.2). To first validate the model, a comparison was made between the profiles obtained in this work and those reported in literature. A satisfactory degree of agreement was noticed. When the unit was dynamically simulated in the presence of the disturbances scenarios, minor variations in the MTBE bottom fraction were found. As the magnitude of these set-point deviations was very small, it is suggested that the unit operates under product specifications in the presence of the defined disturbance scenarios. Thus, the outcome of this section serves as a reference case to be compared with that of the life-span inspired design methodology (*cf.* section §1.4).

Chapter 7

Mind journey to the scientific questions.

The steady-state and dynamic behavior in RD are addressed in this chapter. Fundamental understanding of multiplicity in a reactive flash is provided. Moreover, the domain knowledge is extended by dynamic analysis, whose tasks include model development, control structure selection, controller tuning and simulation of closed loop dynamics. The output of this section serves as reference case to be compared with that of the life-span inspired design methodology (*cf.* section §1.4). The material presented in this chapter answers partially Question 6.

"It is not the strongest of the species that survive, nor the most intelligent, but the one most responsive to change."

Charles Darwin, naturist (1809-1882)

8

A Design Approach Based on Irreversibility[†]

The interactions between economic performance, thermodynamic efficiency and responsiveness in RD process design are explored in this chapter. This motivation is derived from taking a sustainable life-span perspective, where economics and avoidance of potential losses of resources (*i.e.* mass, energy and exergy) in process operation over the process life span are taken into consideration. The approach to the column design involves defining a building block, generic lumped RD volume element and the development of rigorous dynamic models for the behavior of the element. As an extension of conventional existing models, this model, which is used as a standard building block, includes entropy and exergy computations. Three objective functions are formulated which account for the process performance regarding economy, exergy loss and responsiveness. A fundamental understanding of the strengths and shortcomings of this approach is developed by addressing a case study: (*i*) steady- state simulation of a classical MTBE design based on economics only, useful as a reference case; the multiobjective optimization of a MTBE RD column with respect to (*ii*) economics and thermodynamic efficiency; and (*iii*) economics, thermodynamic efficiency and responsiveness. Finally, structural differences and dynamic response are identified between the optimized and classical designs, to stress the importance of considering exergy and responsiveness criteria.

[†]Parts of this chapter have appeared in Almeida-Rivera *et al.* (2004*b*)

Chapter 8

8.1 Introduction

Advances in computing and information technology allow chemical engineers to solve complex design problems arising from a need to improve sustainability of the biosphere and human society. In such a context the performance of a chemical plant needs to be optimized over its manufacturing life span, while accounting for the use of multiple resources in the design and manufacturing stages. Since such resources are of a different nature (*e.g.* capital, raw materials and labor) with different degrees of depletion and rates of replenishment the performance of a chemical plant is characterized by multiple objectives with trade-offs. An integrated unit operation like RD can offer significant benefits for resource utilization, when it is accompanied with the avoidance of chemical equilibrium limitations, enhancement of conversion, selectivity and yield and the reduction of both operational and capital costs. The nonlinear coupling of chemical reaction, phase equilibria and transport phenomena can however, leads to undesired, system-dependent features, such as multiple steady states and reactive azeotropes (Malone and Doherty, 2000). The results of a case study on the interactions between economics, exergy efficiency and process responsiveness in the conceptual design of RD processes are discussed in this chapter.

In the wider context of conceptual process design, sustainability issues like feedstock selection, (re-)use of catalyst and (re-)use of solvents are of key importance. In our perspective of life span (*cf.* explanatory caveat in section §1.4), we do not cover those aspects as we focus exclusively on the minimization of loss of resources in the operational phase.

Currently, conceptual design in chemical engineering is predominantly driven by (steady state) economic considerations, postponing to latter engineering stages any issue related to exergy analysis, responsiveness and control performance. The importance of incorporating exergy efficiency in the early stages of the design cycle is stressed by the increasing depletion of nonrenewable energy resources and the relatively low second law efficiencies (5-20%) for the majority of chemical processes. In spite of these facts, exergy analysis is exclusively performed as a follow-up task to the process synthesis (Koeijer *et al.*, 2002). Controllability and process responsiveness are important to maintain product quality and to avoid excessive use of utilities for control actions and reprocessing of off-spec material.

Regarding the multiechelon approach in RD design (*cf.* chapter 4) in this chapter the last design space is addressed. The evaluation of the design obtained so far is checked with respect to economic performance, exergy efficiency and responsiveness. The focus of this chapter is the importance of including interactions between economics, exergy efficiency and process responsiveness in RD conceptual design. Aiming at these goals, a generic compartment model is defined, which accounts for mass, energy and momen-

Table 8.1. Input-output information for the thermodynamic-based evaluation space. The multiechelon approach is explained in section §4.5.

Design specifications	**Design/operational variables**	**Domain knowledge**
Process: - spatial configuration - control structure and settings - operational parameters - disturbance scenario	Continuous: - optimal design variables - performance criteria	- non-equilibrium thermodynamics - steady-state simulation - dynamic simulation - multiobjective optimization

tum balances and includes entropy and exergy computations. This behavioral model is integrated to give a column structure. The design is cast into a nonlinear optimization problem, where degrees of freedom in the design model are fixed by optimization of multiple objectives and applying constraints, reflecting heuristics and engineering knowledge. At this column level three performance criteria are defined for the optimization of the unit design. These embrace the unit performance regarding economics, thermodynamic efficiency and process responsiveness. The economic performance index is given by the total annualized cost (TAC), whereas the thermodynamic efficiency index accounts for the process irreversibilities and is expressed in terms of the entropy production rate by chemical reaction, heat and mass transfer. The responsiveness index, in turn, is similar to the response time defined by Luyben *et al.* (1999). The three objective functions are solved simultaneously within a single multiobjective optimization problem. At this level of understanding, it is believed that a multiobjective optimization gives more insight into trade-offs between objectives than combining the three objectives into a single monetary objective function using ad-hoc weighting factors. Comparing the design based on the three-fold performance criteria with a reference economic-driven design allows us to identify structural differences. The response of the optimized design in the presence of a deterministic disturbance scenario is validated using dynamic simulation.

The input-output flow of information is given in table 8.1. It is worth mentioning that the thrust of this chapter is the optimization-based design approach. Multiple objective functions are considered and embedded in a large scale optimization problem.

Recalling the engineering and scientific design questions given in chapter 1, in this chapter we address question 7, namely,

- *Are there structural differences and significant improvements in designs derived using conventional methodologies from those obtained using an integrated design methodology?*

8.2 Generic Lumped Reactive Distillation Volume Element

The starting point for a fundamental understanding of the strengths and shortcomings of the proposed multiobjective design approach is to define a generic lumped RD volume element (GLRDVE) . This element, or compartment, was chosen as building block in the design approach (*cf.* section §6.1.3) and selected to represent the governing phenomena occurring in RD processing. Thus, this behavioral model accounts for: (*i*) mass, energy and momentum balances, together with entropy and exergy computations; (*ii*) thermodynamic equations of state for the specific heat and specific density and for the chemical potential per species; (*iii*) thermodynamic phase equilibrium conditions at the contact surface between phases; (*iv*) the constitutive rate equations for chemical reactions; (*v*) the rate equations for interphase transport of species mass and energy; (*vi*) the rate equation for heat transfer with an external solid surface; (*vii*) the hydrodynamics-based rate equations for convective mass and energy flows with the external world and the pressure drop; and (*viii*) the equations for the interphase contact surfaces and for the void fraction of the vapor phase in the liquid phase.

The following attributes are introduced: (*i*) two internally (well mixed) homogeneous fluid phases; and (*ii*) chemical reactions in the liquid phase only. Thus, mass transfer between phases and heat exchange are allowed in the compartment and chemical reaction is triggered by the presence of an appropriate catalyst (figure 8.1). Each GLRDVE has its own complexities due to the many interacting phenomena. However, this does not account for the interactions between the stages in a real multistage column. The latter class of interactions could give rise to nonlinear dynamic behavior and poor controllability if an unfortunate combination of reflux ratio and number of (non) reactive trays is chosen. Issues related to connecting compartments and superstructure description are addressed in section §8.3.

8.2.1 Mass/Energy/Entropy/Momentum balances

Component, energy and entropy balances are developed in the GLRDVE. The entropy and, in particular, the entropy production rate are of paramount importance to determine exergy losses and the responsiveness of the process. The balances lead to the following set of DAEs,

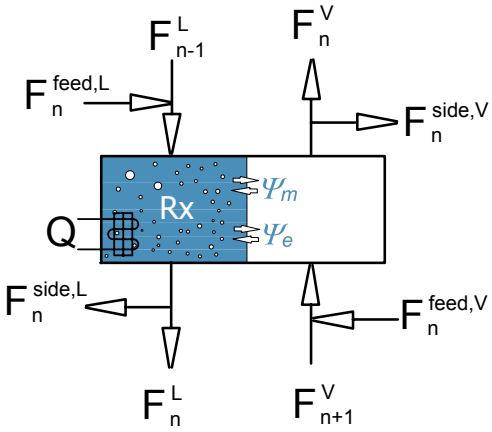

Figure 8.1. Schematic representation of the generic lumped reactive distillation volume element (GLRDVE). **Remark:** feed and side draw-off streams and heat exchange are allowed. **Nomenclature:** $F_i^{\text{feed},(\alpha)}$: feed flowrate of phase (α); $F^{\text{side},(\alpha)}$: flowrate of side stream corresponding to phase (α); Ψ_m: interfacial mass transfer flux; Ψ_e: interfacial energy transfer flux; Q: heat duty.

$$\frac{\partial\left(\rho_i^{(\alpha)} \times V^{(\alpha)}\right)}{\partial t} = \sum_{j=1}^{j=n_{st}} F_i^{j,(\alpha)} - \Psi_i \times a_\Psi + \delta_{(\alpha)} \times r_i \times V_{RX}^L, \quad i \in \mathbb{Z}^{n_c}, \tag{8.1}$$

$$\begin{aligned}\frac{\partial \mathrm{U}^{(\alpha)}}{\partial t} &= \sum_{j=1}^{j=n_{st}} \sum_{i=1}^{i=n_c} F_i^{j,(\alpha)} \times h_i^{j,(\alpha)} + \Psi_e \times a_\Psi + \cdots \\ &\quad \cdots + \sum_{j=1}^{j=n_{st}} \sum_{i=1}^{i=n_c} F_i^{j,(\alpha)} \times g_i^{j,(\alpha)} + \delta_{(\alpha)} \times Q^{(\alpha)},\end{aligned} \tag{8.2}$$

where $c_i^{(\alpha)}$ is the molar density of component i ($i \in \mathbb{Z}^{n_c}$) in phase $(\alpha) \in \mathbb{Z}^{n_p}$, $F_i^{j,(\alpha)}$ is the convective flow of component i in phase (α) in the incoming or outgoing stream j ($j \in \mathbb{Z}^{n_{st}}$) for the exchange with the external world, Ψ_i is the interfacial molar flux of component i, a_Ψ is the mass and heat transfer area, V_{RX}^L is the reaction volume in the liquid phase, r_j is the net cumulative rate of reaction of specie j per unit, U is the internal energy of the compartment, $h_i^{j,(\alpha)}$ is the molar enthalpy of component i in stream j and phase (α), $g_i^{j,(\alpha)}$ is the external force exerted on component i per molar unit (including the contribution from electrical field) in stream j and phase (α), Ψ_e is the energy flux associated with the interface mass and heat transfer, $Q^{(\alpha)}$ is the external heat exchange rate in phase (α), which is assumed to only occur in the liquid phase (*i.e.* $Q^{(\alpha)} = Q^L$), n_c is the number of components, n_{st} is the number of incoming and

outgoing streams, n_p is the number of phases and $\delta_{(\alpha)}$ is the Kronecker delta function defined as,

$$\delta_{(\alpha)} := \begin{cases} 0, \text{ if } (\alpha) \neq L \\ 1, \text{ if } (\alpha) = L. \end{cases} \tag{8.3}$$

The energy flux associated with the interface mass and heat transfer Ψ_e is composed of a measurable heat flux and the partial molar enthalpies brought by the component fluxes. namely,

$$\Psi_e = -\sum_{i=1}^{i=n_c} \Psi_i \times h_i^{(\alpha)} + q^{(\alpha'-\alpha)}, \tag{8.4}$$

where $q^{(\alpha'-\alpha)}$ is the heat flux from phase (α') to phase (α).

The entropy balance in the transient state at a macroscopic level is given by the net amount of entropy transferred into the volume element per unit time and the amount of entropy used/produced in the control volume per unit time. Thus, the entropy balance for a given phase (α) can be stated as,

$$\frac{\partial \mathrm{S}^{(\alpha)}}{\partial t} = \sum_{i=1}^{i=n_{st}} \sum_{j=1}^{j=n_c} F_j^{i,(\alpha)} \times s_j^{i,(\alpha)} + \Sigma_V^{(\alpha)}, \tag{8.5}$$

where $\mathrm{S}^{(\alpha)}$ is the entropy of the compartment in phase (α), $S_j^{i,(\alpha)}$ is the molar entropy of component j in stream i and phase (α) and $\Sigma_V^{(\alpha)}$ is the entropy production rate in phase (α), which includes exclusively interfacial diffusional and chemical reaction contributions.

Alternatively, the entropy balance can be expressed in terms of the entropy density and the fluxes of entropy density (Kjelstrup and Bedeaux, 2001; Marquardt, 2004),

$$\frac{\partial s^{(\alpha)}}{\partial t} = -\nabla J_s^{(\alpha)} + \sigma_V^{(\alpha)}, \tag{8.6}$$

where $\sigma_V^{(\alpha)}$ is the entropy production rate per unit of volume in phase (α) and $J_s^{(\alpha)}$ is the entropy flux in phase (α).

The flux of entropy of stream i in phase (α) is related to the total flux of energy $J_e^{i,(\alpha)}$ and mass fluxes $J_m^{i,(\alpha)}$ according to the expression (Kjelstrup and Bedeaux, 2001),

$$J_s^{i,(\alpha)} = \frac{1}{T} \times J_e^{i,(\alpha)} - \sum_{j=1}^{j=n_c} \frac{\mu_j^{i,(\alpha)}}{T} \times J_{m,j}^{i,(\alpha)}, \quad i \in \mathbb{Z}^{n_{st}}, \tag{8.7}$$

where $\mu_j^{i,(\alpha)}$ denotes chemical potential of component j $(j \in \mathbb{Z}^{n_c})$ in stream i and phase (α).

The fluxes of mass and energy required in expression 8.7 can be obtained from the equation of continuity per volume unit and energy balance, respectively, for an open unsteady state multicomponent system. Let (α) be a given phase, then the fundamental equation of continuity is given by convective, diffusive and chemical reaction contributions,

$$\frac{\partial}{\partial t}\rho_i^{(\alpha)} = \underbrace{-(\nabla\rho_i^{(\alpha)}\cdot\mathbf{v}^{(\alpha)}) - (\nabla\mathbf{j}_i^{(\alpha)})}_{-(\nabla\cdot\{\rho_i^{(\alpha)}\mathbf{v}^{(\alpha)}+\mathbf{j}_i^{(\alpha)}\})\equiv-\nabla\mathbf{J}_{m,i}^{(\alpha)}} + r_i^{(\alpha)}, \qquad i\in\mathbb{Z}^{n_c}, \tag{8.8}$$

and

$$\mathbf{J}_{m,i}^{(\alpha)} = \rho_i^{(\alpha)}\mathbf{v}^{(\alpha)} + \mathbf{j}_i^{(\alpha)}, \qquad i\in\mathbb{Z}^{n_c}, \tag{8.9}$$

where $\mathbf{v}^{(\alpha)}$ is the fluid velocity in phase (α) and the molar diffusion flux vector $\mathbf{j}_i^{(\alpha)}$ involves terms originated by mechanical and thermal driving forces (Bird *et al.*, 2003). It is worth mentioning that the $\mathbf{j}_i^{(\alpha)}$ vector is composed of the elements $j_i^{k,(\alpha)}$ with $k\in\mathbb{Z}^{n_{st}}$.

Similarly, the energy flux $J_e^{i,(\alpha)}$ ($\mathbf{J}_e^{(\alpha)}$ in vectorial notation) can be obtained by the energy equation derived for the volume element in an open multicomponent dynamic system,

$$\frac{\partial}{\partial t}u^{(\alpha)} = \underbrace{-(\nabla\cdot u^{(\alpha)}\mathbf{v}^{(\alpha)}) - (\nabla\mathbf{q}^{(\alpha)}) - (\pi^{(\alpha)}:\nabla\mathbf{v}^{(\alpha)})}_{-(\nabla\cdot\{u^{(\alpha)}\mathbf{v}^{(\alpha)}+\mathbf{q}+[\pi^{(\alpha)}\cdot\mathbf{v}^{(\alpha)}]\})\equiv-\nabla\mathbf{J}_e^{(\alpha)}} + \sum_{i=1}^{i=n_c}\mathbf{J}_{m,i}^{(\alpha)}\cdot\mathbf{g}_i^{(\alpha)} + E\times j, \tag{8.10}$$

where u is the internal energy density of the volume element, $\pi^{(\alpha)}$ is the pressure tensor in phase (α), which accounts for the increase of the rate of internal energy by reversible pressure forces and by irreversible viscous forces (Bird *et al.*, 2003), $\mathbf{q}^{(\alpha)}$ is the multicomponent energy flux through the element interphase relative to the mass average velocity in phase (α), E is the electric field and j the electric current density.

If it is assumed that the energy flux $\mathbf{q}^{(\alpha)}$ includes mainly conductive and interdiffusive energy fluxes (*i.e.* $\mathbf{q}^{(\alpha)} = \mathbf{q}^{\text{conductive}} + \mathbf{q}^{\text{diffusive}}$) and that the medium is isotropic, the total energy flux $\mathbf{J}_e^{(\alpha)}$ with respect to stationary coordinates is given, after eliminating negligible terms, by,

$$\mathbf{J}_e^{(\alpha)} = \mathbf{J}_{\mathbf{q}}^{(\alpha)} + \sum_{i=1}^{i=n_c}\mathbf{J}_i^{(\alpha)}\cdot\mathbf{h}_i^{(\alpha)}, \tag{8.11}$$

where $\mathbf{J}_{\mathbf{q}}{}^{(\alpha)}$ is the measurable heat flux of phase (α).

The entropy production rate at macroscopic level, $\Sigma_V^{(\alpha)}$ (equation 8.5) can be obtained after integration of the local entropy production rate density $\sigma^{(\alpha)}$ over the volume element in phase (α). For the sake of simplification the following assumptions are adopted: (i) entropy contributions of all involving phases in the GLRDVE are combined in a single variable ($\Sigma_V^{(*)} = f(\Sigma_V^{(\alpha)})$); (ii) entropy is produced due to mass and heat diffusion in

the liquid-vapor interphase, chemical reaction in the bulk of the liquid and heat transfer from external heat sources/sinks and the surrounding environment to the liquid phase only; and (*iii*) the effects of electric field, external forces ($\mathbf{g} = 0$) and diffusive momentum fluxes are neglected. The following expression for the integral entropy production term can be then derived (Seider *et al.*, 1999; Bedeaux and Kjelstrup, 2004; Kjelstrup and Bedeaux, 2001),

$$\begin{aligned}\iiint_V \sigma^{(*)} dV = \Sigma_V^{(*)} &= \frac{1}{T^L} \sum_{i=1}^{i=n_{rx}} \mathcal{A}_i^L \times \varepsilon_i^L \times V_{RX}^L + J_q^L \times a_\Psi \times X_q + \cdots \\ &\cdots + \sum_{i=1}^{i=n_c} J_i \times a_\Psi \times h_i \times X_e + \left(- \sum_{i=1}^{i=n_c} J_i \times a_\Psi \times X_{m,i} \right) + \cdots \\ &\cdots + Q \times X^{HX},\end{aligned} \tag{8.12}$$

where $\mathcal{A}_i^L$ is the affinity of chemical reaction i ($i \in \mathbb{Z}^{n_{rx}}$) in the liquid phase, ε_i^L is the degree of advancement of chemical reaction i in the liquid phase, J_q^L is the measurable heat flux into the liquid phase, a_Ψ is the mass/heat transfer area, h_i is the molar enthalpy of component i, X_q, X_e, $X_{m,j}$ and X^{HX} are the conjugated driving forces for heat exchange between phases, interfacial heat diffusion, interfacial mass diffusion of component j and heat exchange with the external world, respectively (Koeijer *et al.*, 2002), Q is the heat flow to the liquid phase, T is the absolute temperature of the volume element and n_{rx} is the number of chemical reactions.

The entropy contribution due to chemical reaction contains the affinity of chemical reaction and its degree of advancement, which are defined respectively as,

$$\mathcal{A}_j^L = - \sum_{i=1}^{i=n_c} \nu_{i,j}^L \cdot \mu_i^L, \qquad j \in \mathbb{Z}^{n_{rx}}, \tag{8.13}$$

$$r_i^L = \sum_{j=1}^{j=n_{rx}} \nu_{ij}^L \times \varepsilon_j^L, \qquad i \in \mathbb{Z}^{n_c}, \tag{8.14}$$

where r_i^L is the net change of the amount of component i in the liquid phase due to all reactions.

In order to estimate the driving forces and fluxes occurring in the volume element additional assumptions are introduced: (*i*) the GLRDVE is composed of incoming and outgoing streams of liquid and vapor phases; (*ii*) the vapor phase behaves ideally; (*iii*) the flux of mass and heat through the interface is positive from the liquid side to the gas side; (*iv*) dynamic changes in gas phase hold-ups of species mass and energy are ignored; (*v*) Gibbs free energies at liquid and vapor sides are equal; and (*vi*) there is a negligible effect of pressure on Gibbs free energies, so that $G_i^L(P,T) = G_i^L(p_i^0, T)$.

The underlying reasoning behind the inclusion of these assumptions is a more transparent derivation of the forces and fluxes expressions, but without compromising the

validity of the approach.

The driving force for chemical reaction j, $X_{rx,j}$, is a function of the chemical affinity and temperature, according to the expression,

$$X_{rx,j} = \frac{\mathcal{A}_j^L}{T} \tag{8.15}$$

The flow associated to this driving force is given by the degree of advancement ε_i. The driving force for mass transfer $X_{m,i}$ is related to the chemical potential gradient between the incoming and outgoing vapor streams (Koeijer, 2002; Kjelstrup, 2005). Thus, according to figure 8.1 the conjugated driving force $X_{m,i}$ is,

$$X_{m,i} = -\frac{1}{T}\Delta\mu_{i,T}, \qquad i \in \mathbb{Z}^{n_c}, \tag{8.16}$$

$$= \mathcal{R} \times \ln \frac{y_i^{\text{in}} \times P^{\text{in}}}{y_i \times P}, \qquad i \in \mathbb{Z}^{n_c}. \tag{8.17}$$

The flux of component i ($i \in \mathbb{Z}^{n_c}$) associated to $X_{m,i}$ through the interface can be calculated by mass balance over the vapor phase (Koeijer, 2002),

$$J_i \times a_\Psi = \sum_{j=1}^{j=n_{st}} \underline{F}^{j,V} \times y_i^j, \quad i \in \mathbb{Z}^{n_c}, \tag{8.18}$$

where y_i^j denotes the vapor molar fraction of component i ($i \in \mathbb{Z}^{n_c}$) in stream j ($j \in \mathbb{Z}^{n_{st}}$) and $\underline{F}^{j,V}$ is the total flow of stream j in the vapor phase and equals to $\underline{F}^{j,V} = \sum_{i=1}^{i=n_c} F_i^{j,V}$.

Note that the previous flux expression is consistent with the component balance given by expression 8.1 if Ψ_i equals J_i. Moreover, the total stream flow is related to the component flow according to,

$$\underline{F}^{j,V} \times y_i^j = F_i^{j,V}, \quad i \in \mathbb{Z}^{n_c}. \tag{8.19}$$

The driving force for heat transfer, X_e, can be estimated as suggested by Koeijer and Rivero (2003),

$$X_e = \Delta\left(\frac{1}{T^V}\right) = \frac{1}{2}\left(\frac{1}{T^{\text{out},V}} - \frac{1}{T^{\text{in},V}}\right). \tag{8.20}$$

The measurable heat flux through the interphase can be derived from the energy balance in the vapor side (Koeijer, 2002),

$$J_e \times a_\Psi = \sum_{j=1}^{j=n_{st}} \underline{F}^{j,V} \times h^{j,V}. \tag{8.21}$$

In this case also the energy expression 8.21 is consistent with the general energy balance given in expression 8.2 if Ψ_e equals J_e.

According to Koeijer *et al.* (2002); Koeijer (2002) the average thermal driving force for external heat transfer X^{HX} (*e.g.* when a heat exchanger is present) is given by the expression,

$$X^{HX} = \frac{1}{T} - \frac{2}{T^{u,\text{in}} + T^{u,\text{out}}}, \tag{8.22}$$

where T^u denotes temperature of the utility present in the GLRDVE.

The momentum balance in the GLRDVE involves, in its general form, contributions due to convection of the fluid bulk, pressure, viscous transfer and gravitational force in each phase (Bird *et al.*, 2003),

$$\frac{\partial \rho^{(\alpha)} \cdot \mathbf{v}^{(\alpha)}}{\partial t} = -[\nabla \cdot \rho^{(\alpha)} \cdot \mathbf{v}^{(\alpha)}\mathbf{v}^{(\alpha)}] - \nabla P^{(\alpha)} - [\nabla \cdot \varsigma] + c^{(\alpha)} \cdot \mathbf{g}^{(\alpha)}, \tag{8.23}$$

where $\rho = \sum_{i=1}^{i=n_c} \rho_i$, $[\nabla \cdot \rho \cdot \mathbf{v}^{(\alpha)}\mathbf{v}^{(\alpha)}]$ is the rate of momentum gain by convection of the fluid per unit volume and $\nabla \cdot \varsigma$ is the rate of momentum gain by viscous transfer per unit volume.

If viscous effects are considered unimportant the following simplified expression might be obtained,

$$\frac{\partial \rho^{(\alpha)} \cdot \mathbf{v}^{(\alpha)}}{\partial t} = -[\nabla \cdot \rho^{(\alpha)} \cdot \mathbf{v}^{(\alpha)}\mathbf{v}^{(\alpha)}] - \nabla P^{(\alpha)} + \rho^{(\alpha)} \cdot \mathbf{g}^{(\alpha)}. \tag{8.24}$$

In the development of the GLRDVE a reduced form of the momentum balance is considered. We assume a pseudo steady state and negligible viscous contribution. Moreover, the gradient of pressure is assumed to be much larger than the rate of momentum gain by convention of the fluid. Thus, the resulting momentum balance is of the form,

$$\nabla P^{(\alpha)} = \rho^{(\alpha)} \cdot \mathbf{g}^{(\alpha)}. \tag{8.25}$$

8.2.2 Availability and Availability Function

Two additional variable of key importance for this thermodynamic-based approach are the availability A and the availability function B. The availability is regarded as a measure of the maximum amount of useful energy that can be extracted when the system is brought to equilibrium with the dead state surroundings (Seider *et al.*, 1999). Thus, the availability of the system in phase (α) and state (T_1, P_1) is given by the expression,

$$\mathrm{A}^{(\alpha)} = (h^{(\alpha)} - T_0 \times S^{(\alpha)})_{T_1,P_1} - (h^{(\alpha)} - T_0 \times S^{(\alpha)})_{T_0,P_0}, \tag{8.26}$$

where the dead state conditions are those at which $T_0 = 298.15K$ and $P_0 = 1$ atm.

The availability function at state given by (T, P) is computed according to the following equality,

$$\mathrm{B}^{(\alpha)}_{T,P} = (h^{(\alpha)} - T_0 \times S^{(\alpha)})_{T,P}. \tag{8.27}$$

Contrary to the availability the availability function of the system at a given state (T_1, P_1) can be referenced to any other state (T_2, P_2),

$$\Delta \mathrm{B}^{(\alpha)} = (h^{(\alpha)} - T_0 \times S^{(\alpha)})_{T_1,P_1} - (h^{(\alpha)} - T_0 \times S^{(\alpha)})_{T_2,P_2} \tag{8.28}$$

From the definitions of availability and availability function it should be noticed that both variables increase with increasing enthalpy and decrease with increasing entropy and the numerical values of their variation coincide (*i.e.*$\Delta \mathrm{B}^{(\alpha)} = \Delta \mathrm{A}^{(\alpha)}$).

Based on the combination of energy and entropy balances and according to the definition of availability an exergy balance can be obtained for a given phase (α) (appendix A in Luyben *et al.* (1999)),

$$\frac{\partial \mathrm{B}^{(\alpha)} \times M^{(\alpha)}}{\partial t} = \sum_{j=1}^{j=n_{st}} \underline{F}^{j,(\alpha)} \times \mathrm{B}^{j,(\alpha)} + \left(1 - \frac{T_0}{T_Q}\right) Q^{(\alpha)} - T_0 \times \Sigma_V, \tag{8.29}$$

where $M^{(\alpha)}$ is the molar hold-up of material in phase (α) and T_Q is the temperature of the heat source/sink. Note that in the previous expression the external force term has been omitted.

To solve the set of balances mentioned in this section it is necessary to specify the initial conditions for all DAEs. Thus, the following variables per phase should be known,

$$[\rho_i^{(\alpha)}(0), \quad U^{(\alpha)}(0), \quad S^{(\alpha)}(0), \quad \rho^{(\alpha)}(0) \cdot \mathbf{v}^{(\alpha)}(0), \quad \mathrm{B}^{(\alpha)}(0) \cdot M^{(\alpha)}(0)]. \tag{8.30}$$

A degree of freedom analysis should be then performed to indicate how many design decision variables need to be picked per volume element. Appendix A gives a detailed overview of a degree of freedom analysis for the case of a complete RD column.

8.2.3 Design Decision Variables

According to a degree of freedom analysis performed in the GLRDVE the following design variables are to be specified for a given operating conditions and feed specifications,

- reaction volume $V_{RX}^{(\alpha)}$,

$$V_{RX}^{(\alpha)} = \begin{cases} V^{(\alpha)} & \text{for liquid phase homogeneously catalyzed reaction(s)} \\ m_{\mathrm{cat}} \times \rho_{m,\mathrm{cat}}^{-1} & \text{for heterogeneously catalyzed reactions(s)} \end{cases}$$

- external and heating/cooling flowrate Q,
- the interfacial area for heat and mass transfer a_Ψ.

Note that operational variables such as reflux ratio and pressure are fixed at appropriate reference value and the connecting streams and associated flowrates $F_i^{j,(\alpha)}$ are assumed to be given.

The perspective adopted for selecting the design decision variables is task-oriented rather than the conventionally used equipment-oriented design approach. Firstly, the task-based concept would allow us to derive the phase volume $V^{(\alpha)}$ from the reaction time (*i.e.* residence time in element) to meet a specified degree of advancement of reaction[‡]; secondly, the amount of heat to be added or removed allows one to compute the heat exchange surface and coolant flows; and thirdly, the interfacial areas for species mass and heat transfer may be translated into the mechanical design of a tray and its prevailing hydrodynamic regime such that the required areas can be met within constraints.

The main benefit of this functional, task-oriented perspective involves the process design unconstrained by equipment geometry. Thus, task-oriented design prevails against equipment-oriented design.

8.2.4 Economics/Exergy Efficiency and Responsiveness Objective Functions

A set of three performance criteria indices are defined for the GLRDVE: the economic performance index f_{econ}, the sustainability performance index f_{exergy} and the responsiveness performance index f_{response}.

The economic performance indicator f_{econ} represents the total annualized cost TAC of the GLRDVE, including capital investment and operational costs of the process,

$$f_{\text{econ}} \equiv \text{TAC} = \sum_{j=1}^{j=n_{st}} \sum_{i=1}^{i=n_c} F_i^{j,(\alpha)} c_i + F_{cu} c_{cu} + F_{hu} c_{hu} + c_{\text{unit + catalyst}}, \quad \alpha \in \mathbb{Z}^{n_p}, \tag{8.31}$$

where c_j is the cost of component j or utility per molar unit, $c_{\text{unit+catalyst}}$ is the investment cost of the unit and catalyst and cu and hu denote cool and hot utilities respectively.

The exergy efficiency, f_{exergy}, is accounting for the process irreversibilities and is expressed in terms of the 2$^{\text{nd}}$ law thermodynamic efficiency, η^{II},

$$f_{\text{exergy}} \equiv \eta^{II} = \frac{W_{\text{ideal}}}{W_{\text{ideal}} - T_0 \Sigma_V}, \tag{8.32}$$

where W_{ideal} is the minimum work required by the process ($W_{\text{ideal}} < 0$), as given in Seider *et al.* (1999). Note that from a sustainable perspective the desired goal is the

[‡]From a more practical perspective it is easier to vary residence time than work with several extents of reactions in parallel.

minimization of f_{exergy}, which might be explicitly translated into the minimization of Σ_V. In this contribution we adopt this approach and compute $T_0 \times \Sigma_V$.

The responsiveness index f_{response} is approximated to the settling time defined by Luyben *et al.* (1999),

$$f_{\text{response}} \equiv \tau = \max_{\mathbf{x}} \frac{\Delta \mathrm{B}(\mathbf{x})}{T_0 \Delta \Sigma_V(\mathbf{x})}, \tag{8.33}$$

where T_0 represents the temperature of a infinitely large sink, which approximates to the surrounding conditions.

At steady state conditions $\mathrm{B}(\mathbf{x})$ is at its minimum value and increases when the system is perturbed by a disturbance. Since a similar situation holds for $\Sigma_V(\mathbf{x})$, the response time τ measures how fast a small variation $\Delta \mathrm{B}(\mathbf{x})$ would dissipate due to an increased $\Delta \Sigma_V(\mathbf{x})$ (Luyben *et al.*, 1999).

In the previous definition of f_{response} Luyben *et al.* (1999) assume that both the availability and entropy production rate are exclusively functions of the vector of state variables $\mathbf{x}$. Although this assumption is fundamentally correct, it somehow disguises the way of estimating the effect of a small disturbance or a change in an input on the system. Therefore, we propose a subtle modification of the arguments of B and Σ_V, by which a second argument is included, representing the systemic view on a dynamic system. Thus, the availability and entropy production rate are regarded as functions of an internal state vector $\mathbf{x}$ and a vector of disturbances and/or manipulated external excitations $\mathbf{u}$,

$$\text{exergy} \quad : \quad \mathrm{B}(\mathbf{x}, \mathbf{u}), \tag{8.34}$$

$$\text{entropy production rate} \quad : \quad \Sigma_V(\mathbf{x}, \mathbf{u}). \tag{8.35}$$

Combining definitions 8.33 and 8.34 leads to a more generalized expression for f_{response},

$$f_{\text{response}} \equiv \tau = \frac{\Delta \mathrm{B}(\mathbf{x}, \mathbf{u})}{T_0 \Delta \Sigma_V(\mathbf{x}, \mathbf{u})}. \tag{8.36}$$

The previous expression could be further elaborated by defining the values of state variables $\mathbf{x}$ and disturbances $\mathbf{u}$ at each state. Hence,

$$\Delta \mathrm{B}(\mathbf{x}, \mathbf{u}) = \mathrm{B}(\mathbf{x}, \mathbf{u}) - \mathrm{B}(\mathbf{x}_0, \mathbf{u}_0), \tag{8.37}$$

$$\Delta \Sigma_V(\mathbf{x}, \mathbf{u}) = \Sigma_V(\mathbf{x}, \mathbf{u}) - \Sigma_V(\mathbf{x}_0, \mathbf{u}_0), \tag{8.38}$$

with

$$\mathbf{u} = \mathbf{u}_0 + \Delta \mathbf{u}, \tag{8.39}$$

$$\mathbf{x} = \mathbf{x}(\mathbf{u}), \tag{8.40}$$

$$\Sigma_V(\mathbf{x}, \mathbf{u}) \geq \Sigma_V(\mathbf{x}_0, \mathbf{u}_0). \tag{8.41}$$

An additional feature of Luyben's original definition of f_{response}, not shown in expression 8.36, is related to the maximization for the time constant τ over all possible steady states surrounding the reference steady state. In this way one looks for the worst case over all possible small scale disturbances and/or input change scenarios. This optimization-driven approach justifies Luyben's approach of including a single argument for ΔB and $\Delta\Sigma_V$.

In our approach such an maximization approach is not considered due to its inherent high computational effort. However, a rather formal definition of f_{response} is adopted (equation 8.36) together with a single input excitation. Note that by not searching all possible state trajectories, the generality of the results might be questionable and the external excitation is a fairly conservative one. However, engineering judgement can be exercised in selecting the disturbance variable $\mathbf{u}$ and the magnitude of the disturbance $\Delta\mathbf{u}$.

8.3 Integration of Volume Elements to a Column Structure

Having addressed the generalities of the GLRDVE the next step is the integration of the volume elements to a column structure. This is addressed in this section together with the re-definition of the performance criteria for the case of a RD column structure. Additionally, fundamental understanding of the effect of design decision variables on process responsiveness is discussed, using a simplified heat exchanger as the case study. Finally, this section includes the optimization approach to tackle the multiobjective problem.

8.3.1 Creating a Column Structure from the Generic Volume Element

The integration of compartments to give a column structure introduces additional degrees of freedom, which should be conveniently specified (*e.g.* reflux ratio). In the more general context of process synthesis, the issue of coupling compartments to a process unit has been frequently addressed and is not, therefore, explicitly considered in this research. Briefly speaking, the compartment integration is carried out by introducing a superstructure and finding the optimal configuration using a MINLP optimization over the superstructure. The description of the superstructure, the rules for connecting compartments with each other and with the outer world are embedded in the *structure model*. Extensive information on structure models can be found in the research work of *e.g.* Ismail *et al.* (2001); Papalexandri and Pistikopoulos (1996). In our particular case, the compartments are integrated to a column structure in such a way that the superstructure is comparable to the unit specified in table 6.2 of section §6.1.

The rules of connectivity used in the RD superstructure state that: (*i*) the outgoing

liquid at a given compartment enters the compartment located below; (*ii*) the outgoing gas at a given compartment enters the compartment located above; (*iii*) the liquid stream leaving the condenser is partially recycled back to the top compartment and withdrawn from the unit as top product; (*iv*) the liquid leaving the bottom compartment enters the reboiler; (*v*) the streams leaving the reboiler are a vapor stream, which enters the bottom compartment and a liquid stream, which is withdrawn from the unit as a bottom product; and (*vi*) side feed streams and side withdrawal streams may occur.

The connectivity rules, however, imposed some configuration limitations: (*i*) heat integration over volume elements is not considered (*i.e.* carrying heat from high temperature to low temperature elements); (*ii*) side reactors are not present; and (*iii*) no parallel structures are considered.

Note that the compartments representing the behavior of the condenser and reboiler are, in principle, identical to the GLRDVE, provided the following characteristics,

- **Condenser drum:** no chemical reaction takes place de to the absence of catalyst; a vapor phase stream enters the compartment and a liquid stream leaves it; heat exchange takes place in both phases.

- **Reboiler:** no chemical reaction takes place due to the absence of a catalyst; a liquid stream enters the compartment and liquid and vapor streams leave it; heat exchange takes place in both phases.

In addition to the specification of the reflux ratio, the compartment integration to superstructure involves the following features of the structure model: (*i*) all compartments can have a different catalyst load, but as starting point the catalyst load distribution suggested by Hauan *et al.* (1995*a*); Jacobs and Krishna (1993); Seader and Henley (1998) is used; (*ii*) the column sections can have different diameters, but initially a common value is chosen (*cf.* table 6.2 of section §6.1). The structure to be further considered during the course of this dissertation is depicted schematically in figure 8.2.

8.3.2 Development of Three Criteria for Optimization of Column Design

Having defined the superstructure to be considered for further analysis the optimization criteria have to be adapted to the new structure. Stepping out from the GLRDVE case to the integrated RD unit is intuitive for f_{econ} and f_{exergy}. The variables $\Delta \text{B}(\mathbf{x}, \mathbf{u})$ and $\Delta \Sigma_V(\mathbf{x}, \mathbf{u})$ need to be globally evaluated over all the structure for the responsiveness criterion f_{response}. The resulting performance criteria are given by the following set of

expressions,

$$f_{\text{econ}} = \sum_{k=1}^{k=n_t} \sum_{j=1}^{j=n_{st}} \sum_{i=1}^{i=n_c} [F_i^{j,k} c_i + F_{cu}^k c_{cu} + F_{hu}^k c_{hu} + c^k_{\text{unit + catalyst}}], \quad (8.42)$$

$$f_{\text{exergy}} = \frac{(W_{\text{ideal}})^{\text{total}}}{(W_{\text{ideal}})^{\text{total}} - T_0(\Sigma_V)^{\text{total}}}, \quad (8.43)$$

$$f_{\text{response}} = \frac{(\Delta \text{B}(\mathbf{x}, \mathbf{u}))^{\text{total}}}{T_0(\Delta\Sigma_V(\mathbf{x}, \mathbf{u}))^{\text{total}}}, \quad (8.44)$$

where $F_i^{j,k}$ is the externally connecting molar flow of component i ($i \in \mathbb{Z}^{n_c}$) in stream j ($j \in \mathbb{Z}^{n_{st}}$) on compartment k ($k \in \mathbb{Z}^{n_t}$), n_t is the number of compartments in the integrated structure, $(\Sigma_V(\mathbf{x}, \mathbf{u}))^{\text{total}}$ is the total rate of entropy production over all superstructure and $(\text{B}(\mathbf{x}, \mathbf{u}))^{\text{total}}$ is the total availability over all the superstructure.

The validity of an additivity property (*i.e.* the objective functions per compartment cant be added up to a corresponding objective function over the entire structure) is implicitly assumed in these definitions.

8.3.3 Responsiveness Explained Using a Heat Exchanger Example

The implications of process responsiveness for design are not totally revealed by the definition of f_{response} (equation 8.44). In this subsection the aim is to provide further foundations for the understanding and applicability of the responsiveness criterion and

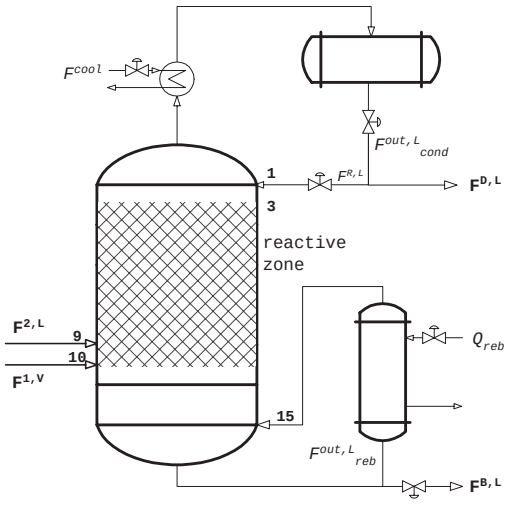

Figure 8.2. Schematic representation of a RD column as the integration of GLRDVEs. **Remark:** numbers represent tray/compartment location.

its implications for design. An ideal heat exchanger is considered in this context as the case study. The starting point of this analysis is directly derived from the definition of f_{response}. According to expression 8.44 a short responsiveness time is desired and can be attained by a large change in the entropy production rate for a given change in stored exergy.

8.3.3.1 System's Features and Model Development

The following properties of the system are considered: (*i*) two liquid-phase streams enter the heat exchange in a countercurrent set-up; (*ii*) the heat exchanger is operated at isobaric conditions; (*iii*) both liquid streams are assumed behave ideally, (*iv*) both streams have equal physical properties, excluding heat capacity, which are temperature independent; (*v*) heat transfer due to conduction is the only source of entropy production; and (*vi*) the driving force for heat transfer is computed between outlet conditions.

The last assumption is driven by two practical motivations. Firstly, it allows a simplified solution of the problem as no computations over all the unit's length are required. Secondly, the situation under consideration is the milder one in terms of entropy produced. At this condition the smallest thermal driving force is expected. If any effect on f_{response} is registered, it may occur also with a magnified intensity at any other location.

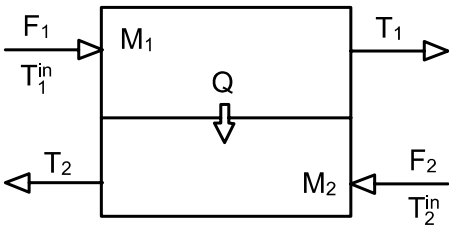

Figure 8.3. Schematic representation of an ideal countercurrent heat exchanger to assess the responsiveness index.

According to the schematic representation in figure 8.3, both liquid-phase streams enter the heat exchanger from opposite sides. Heat is transferred through the solid wall between the phases. The liquid holdup of each liquid is kept constant during the operation so that inlet and outlet flows are equal. The set of governing equations and physical properties of the system are given in tables 8.2 and 8.3, respectively. A degree of freedom analysis is now performed to estimate the number of variables to be specified to consolidate the model. All variables of this system are grouped in a column vector $\mathbb{X}$, which contains 13 elements,

$$\mathbb{X} \equiv \left[T_i^{\text{in}} \quad h_i^{\text{in}} \quad F_i \quad T_i \quad h_i \quad Q \quad \Delta T_{lm} \quad A\right]^{\text{T}}. \tag{8.45}$$

The number of governing expressions as listed in table 8.2 equals 8. Out of the five remaining variables to be specified, three are considered fixed inputs and given by the vector $\mathbb{I}$,

$$\mathbb{I} \equiv \left[F_1 \quad T_i^{\text{in}}\right]^{\text{T}}. \tag{8.46}$$

Within the two remaining degrees of freedom, one is fixed by the design target (T_1), leading to a single variable to be specified to consolidate the model. This variable could be either the outlet temperature of the cold utility or the heat transfer area. In the course of this subsection and to study the effect of varying thermal driving forces on the responsiveness index, the area A is fixed. For the sake of comparison among different units, results for additional heat transfer areas are included.

8.3.3.2 Entropy Production Rate and Stored Exergy

The entropy of the system is assumed to be exclusively generated by the heat conduction from the hot to the cold fluids. The entropy production rate, at microscopic level, can be estimated as the product of thermal driving force and heat flux. From a macroscopic stand-point the measurable heat flow is used for this computation. A better approximation can be obtained by introducing phenomenological coefficients (Hasse, 1969; Koeijer, 2002; Meeuse, 2003). For our analysis, however, we adopt an alternative approach. The overall steady state entropy equation of change is applied and the production term is related to the net change of entropy.

Therefore, for this ideal system the entropy production rate is given by the overall contributions of both streams,

$$\Delta S_i = Cp_i \times \ln \frac{T_i}{T_i^{\text{in}}}, \qquad i \in [1,2], \tag{8.47}$$

Table 8.2. Set of governing expressions for the ideal heat exchanger as depicted in figure 8.3. **Remarks:** stream 1 corresponds to the hot utility, whereas stream 2 is the cold utility.

Balance	**Governing expression**
Energy balance	$Q = F_1 \times (h_1^{\text{in}} - h_1)$
	$Q = F_2 \times (h_2 - h_2^{\text{in}})$
Enthalpy definition	$h_i^{\text{in}} = Cp_i \times (T_i^{\text{in}} - T_0)$
	$h_i = Cp_i \times (T_i - T_0)$
Heat transfer	$Q = U^{HX} \times A \times \Delta T_{lm}$
Temperature difference	$\Delta T_{lm} = \frac{T_1^{\text{in}} - T_2 - (T_1 - T_2^{\text{in}})}{\log\left(\frac{T_1^{\text{in}} - T_2}{T_1 - T_2^{\text{in}}}\right)}$

Table 8.3. Properties and operational parameters of the ideal heat exchanger system. **Remarks:** most of the operational parameters are taken from Nummedal (2001); Nummedal and Kjelstrup (2001); the nominal case results in a heat duty of Q=60 kW and a flowrate of cold utility F_2=0.286 kg $\times$s^{-1}.

Parameter	**Label**	**Value**
Flowrate hot utility	F_1	1 kg$\times$s^{-1}
Heat capacity hot utility	Cp_1	2 kJ$\times$(kg$\times$K)$^{-1}$
Heat capacity cold utility	Cp_2	4.2 kJ$\times$(kg$\times$K)$^{-1}$
Inlet temperature hot utility	T_1^{in}	400 K
Inlet temperature cold utility	T_2^{in}	300 K
Outlet temperature hot utility (target)	T_1	370 K
Heat transfer area	A	3 m^2
Heat transfer coefficient	U^{HX}	340 W$\times$(m^2 $\times$K)$^{-1}$

where Cp_i is the heat capacity of stream i evaluated in the temperature range $[T, T^{\text{in}}]$.

Summing up all the contributions leads to the overall entropy production rate of the system,

$$\Sigma_V = \sum_{i=1}^{i=2} F_i \times \Delta S_i. \tag{8.48}$$

Exergy is similarly estimated by summing up the exergy individual contributions of both liquids,

$$\Delta \mathrm{B}_i = \Delta h_i - T_0 \times \Delta S_i, \qquad i \in [1, 2], \tag{8.49}$$

which result in the overall exergy of the system,

$$\Delta \mathrm{B} = \Delta h - T_0 \times \Sigma_V, \tag{8.50}$$

where B_i is the molar exergy of stream i, Δh_i is the change of molar enthalpy of stream i and equals to $h_i - h_i^{\text{in}}$, ΔB is the change of exergy of the system.

The stored exergy function is then obtained by accounting for the holdup of liquids within the boundaries of the system,

$$\Delta \mathrm{B} = \sum_{i=1}^{i=2} (\Delta h_i - T_0 \times \Delta S_i) \times M_i, \tag{8.51}$$

where M_i denotes the liquid holdup of utility i. Note that initially the molar hold-up is not considered as design variable. This assumption is relaxed at the end of this section to study the effect of M on the responsiveness criterion.

A disturbance scenario is considered to assess the response time function τ , where the temperature target T_1 changes +/- 10K around the nominal value,

$$T_1^l < T_1(t) < T_1^u, \tag{8.52}$$

where the values of T_1^l and T_1^u are 360K and 380K, respectively.

The driving force for heat conduction from the hot to the cold utility X^{HX} is given by the simplified expression,

$$X^{HX} = \Delta\frac{1}{T} = \frac{1}{T_2} - \frac{1}{T_1}. \tag{8.53}$$

It is worth mentioning again that thermal driving force is computed between outlet conditions. The motivation behind this assumption is given in section §8.3.3.1.

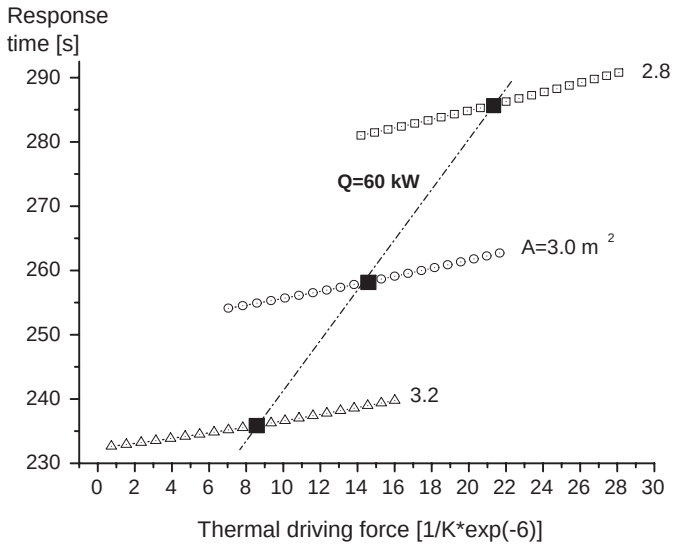

Figure 8.4. Response time as a function of the thermal driving force for an idealized heat exchanger. **Remarks:** alternative designs with different heat transfer areas are plotted and compared to the case where Q=60 $\cdot 10^3$ W (marker: ■).

The values of response time τ as a function of the thermal driving force X^{HX} are presented in figure 8.4 and for designs of different heat transfer area A. Note that from a responsiveness stand point small driving forces are desired for a given heat exchanger design and the heat exchanger with the larger transfer area copes more efficiently with the disturbance scenario. Summarizing, better process responsiveness is attained at smaller driving forces (*i.e.* larger temperature difference and larger heat exchangers).

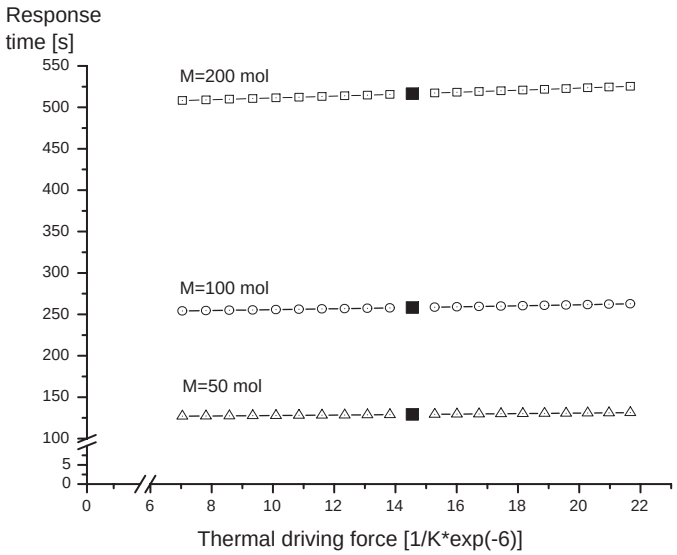

Figure 8.5. Response time as a function of the thermal driving force for an idealized heat exchanger at different hold-up values. **Remarks:** heat transfer area: A=3 m^2; heat duty of reference case: Q=60·10^3 W (marker: ■).

The effect of hold-up M on the responsiveness criterion is now analyzed. As suggested by equation 8.51, smaller hold-up decreases the exergy storage and so helps to decrease the time constant. This fact is depicted in figure 8.5, where hold-up values of 100 mol (reference value), 200 mol and 50 mol are used.

Based on the previous analysis the following practical heuristic can be suggested,

▷ **Heuristic:** maximize the exchange surface per unit of mass and keep driving force small at constant transfer duty

8.3.4 Approach to Design Optimization and References Cases

At this point we have defined the superstructure of interest, developed three performance criteria for the optimization of the superstructure and provided some fundamental insight into the impact of design variables on the responsiveness criterion. In this section the approach to solve the multiobjective optimization problem is presented together with the reference design case to be compared with the optimized designs.

Two solving approaches are adopted to solve the optimization problem involving more

Utopia point **U** in a $\mathbb{R}^{\Phi}$-space is given by the Φ-objective functions values that solve independently the Φ scalar optimization problems (Lim *et al.*, 1999). For instance, in an optimization problem involving two objective functions the mathematical formulation of the utopia point **U** is,

$$\min_{x\in\Gamma} f_1(x) = f_1^l(x^*), \quad \text{and} \quad f_2(x^*) = f_2^u(x^*), \tag{8.54}$$

$$\min_{x\in\Gamma} f_2(x) = f_2^l(x^*), \quad \text{and} \quad f_1(x^*) = f_1^u(x^*), \tag{8.55}$$

where f_i^l and f_i^u denote the lower and upper limits of the objective function f_i, respectively; Γ is the set of constraints, which define the space of design variables x.

The coordinates of the utopia point are then given by (f_1^l, f_2^l). The meaning and optimization potentiality of the utopia point is stressed using the following simple example. Let's consider the following multiobjective optimization problem,

$$\text{Function:} \qquad \min(f_1(x_1, x_2), f_2(x_1, x_2)), \tag{8.56}$$

$$\text{s.t.:} \qquad g(x_1, x_2) = 0, \tag{8.57}$$

where

$$f_1(x_1, x_2) = x_1, \tag{8.58}$$

$$f_2(x_1, x_2) = x_2, \tag{8.59}$$

$$g(x_1, x_2) = x_1 - x_2^2 - 1 = 0. \tag{8.60}$$

The solution of the optimization problem is depicted in a 2D plot of the involved objectives (figure 8.6). Each non-inferior attainable optimal solution is estimated at a given combination of objectives including constraint $g(x_1, x_2)$. All these points define a curve of non-inferior solutions, normally referred to as *Pareto curve*. For the sake of transparency a linear relation between objectives is considered (*i.e.* $F = \Sigma w_i \times f_i$), where w_i is the weighting factor of the objective function f_i and $\Sigma w_i = 1$. As expected, the utopia point is given by the coordinates

$$(f_1^l, f_2^l) = (0, -50), \tag{8.61}$$

which are the solutions of the scalar optimization problems.

Note 8.1. Utopia point in optimization problems with more than one objective function

than one objective function,

- each objective function is used independently, disregarding the other two. This approach localizes the coordinates of the *utopia point* and subsequently, reduces the computational effort by limiting the search space. For a formal definition of the utopia point, the reader is referred to the explanatory note in table 8.1,

- the second approach accounts for the interactions and trade-offs among the objectives. Thus, a multiobjective problem is formulated by using a weighted $p-$norm for the vector of objective functions, as given by Clark and Westerberg (1983),

$$\min_{\mathcal{D}\in\Gamma} F \equiv \left[\sum_i (w_i f_i)^p\right]^{\frac{1}{p}}, p \in [1, \infty), \tag{8.62}$$

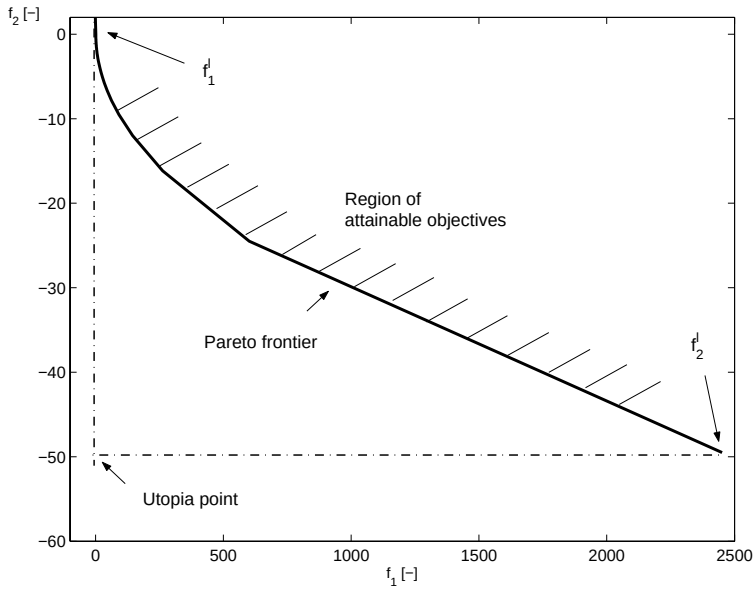

Figure 8.6. The role of utopia point in multiobjective optimization. **Remarks:** the optimization problem is formulated according to expression 8.56 given in the explanatory note of table 8.1; same note provides the mathematical definition of the utopia point.

where F is the multiobjective function, w is a vector of weighting factors, f is the vector of objective functions, $\mathcal{D}$ is the set of decision variables and constrained by the set Γ. According to Clark and Westerberg (1983) a norm of $p \leq 2$ is used to localize non-inferior points in the non-convex regions.

This theory will now be applied to the multiobjective design cases for the MTBE column. The reference design used for the sake of comparison is the structure previously introduced in chapter 7. This structure corresponds to a reactive distillation column for the synthesis of MTBE. The spatial design variables were obtained by steady-state optimization of the unit's economic performance. For background information, the reader is referred to section §6.2. The relevant parameters and schematic representation of the optimized design are given in table 8.4 and figure 8.7, respectively.

8.4 Application 1. Steady-state Entropy Production Profile in a MTBE Reactive Distillation Column

The esterification of iC_4 and methanol is used as the case study in this application. A detailed description of the system is presented in appendix B. The chemical reaction is represented by a pseudo-homogeneous kinetics. The spatial configuration of the unit is that obtained previously in section §6.2.

To prepare for the optimization task and to reduce the problem complexity we identify the dominant contributions to entropy production rate over the MTBE column. The expressions to compute all contributions to the entropy production in the GLRDVE are summarized in table 8.5. In the case of a RD column structure these expressions are applicable for all reactive and nonreactive compartments. Note that the reboiler and condenser models assume that the entropy contribution by external heat transfer is dominant.

Table 8.4. Optimized design of a RD column for MTBE synthesis based on economic performance. **Remarks:** information on this design problem is given in section §6.2; bottom section lists the operational constraints and product specifications.

	Value
Number of trays	15 [2:rectifying;8:reactive; 5:stripping]
Feed 1: location	iC_4+ nC_4: $10^{\underline{\text{th}}}$ tray (g)
Feed 1: flowrate	455 mol×s^{-1}
Feed 1: composition	iC_4: 0.37; nC_4: 0.63
Feed 1: temperature	350K
Feed 2: location	MeOH: $9^{\underline{\text{th}}}$ tray (l)
Feed 2: flowrate	168 mol×s^{-1}
Feed 2: composition	MeOH: 1.00
Feed 2: temperature	320K
Operating pressure	$11{\cdot}10^5$ Pa (top)
Reflux ratio	7
Mass of catalyst/tray	204.1 kg=1000 eq$_{[H^+]}$
Bottom flowrate	197 mol×s^{-1}
Column diameter	7.132 m
Condenser area	$1.059{\cdot}10^3$ m^2
Reboiler area	$6.93{\cdot}10^2$ m^2
Operational constraints	$P \leq P_{\text{cond}}$
	$T_{\text{reb}} < T_{c,iC_4}$
Product specifications	$x^D_{\text{MTBE}} \leq 0.1\%$
	$x^B_{\text{MTBE}} \geq 99\%$

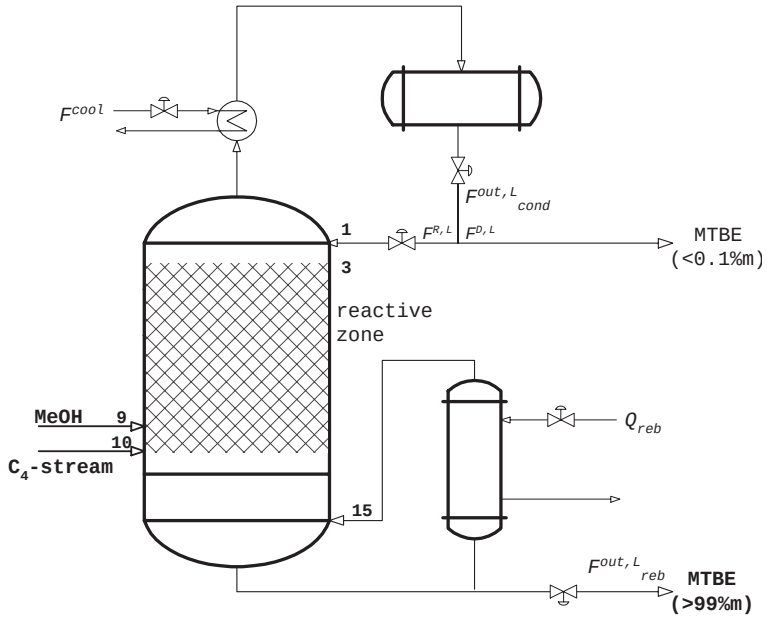

Figure 8.7. Schematic representation of a RD column in the synthesis of MTBE. **Remarks:** spatial design variables are listed in table 8.4; numbers represent tray location.

Table 8.5. Summary of expressions of all contributions to the entropy production in a GLRDVE

	Expression
mass transfer	$-\sum_{i=1}^{i=n_c} J_i \times a_\Psi \times X_{m,i}$
interface energy transfer	$J_q^L \times a_\Psi \times X_q + \sum_{i=1}^{i=n_c} J_i \times a_\Psi \times h_i \times X_e$
chemical reaction	$\frac{1}{T^L} \sum_{i=1}^{i=n_{rx}} \mathcal{A}_i^L \times \varepsilon_i^L \times V_{RX}^L$
external heat exchange	$Q \times X^{HX}$

At this point the entropy profiles along the MTBE RD column due to the different contributions are estimated. These profiles are presented in figure 8.8 and correspond to the reference design as specified in table 8.4. The following results are of interest,

- the entropy profiles show that energy transfer contributes largely to the overall entropy production and particularly in the stripping section of the column, followed by mass diffusion. In the reactive zone, however, the dominant source of entropy production is chemical reaction. In the rectifying section both mass and

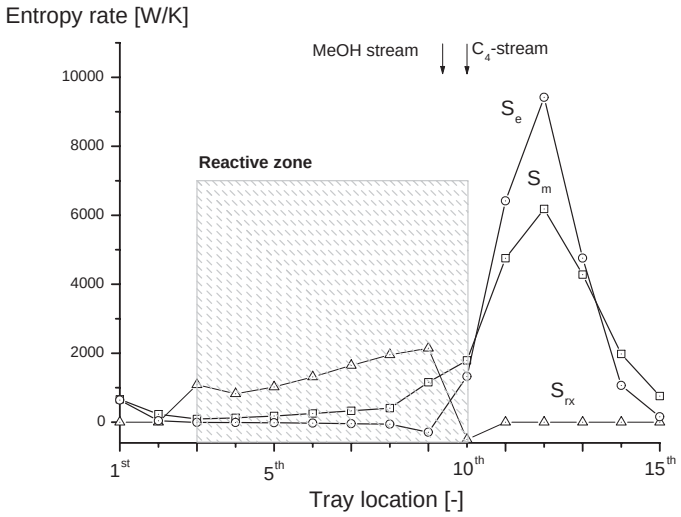

Figure 8.8. Entropy production rate profile for a 15 stage RD column for MTBE synthesis. **Legend:** S_m: entropy produced by interfacial mass diffusion; S_e: entropy produced by interfacial energy transfer; S_{rx}: entropy produced by chemical reaction; **Remarks:** stages are numbered from top to bottom; reboiler and condenser drum are not depicted; MeOH feed stream is fed at $9^{\underline{\text{th}}}$ tray and $i\text{C}_4$ stream at $10^{\underline{\text{th}}}$ tray. The operational and design variables are listed in table 8.4.

energy transfer contributions are equally important,

- the entropy contribution originated from chemical reaction shows negative values at the bottom of the reactive section. This fact may be explained by possible inconsistency between the reaction kinetics model and the affinity expression. Although MTBE decomposition takes place at that column location, due to high MTBE concentration, the reaction affinity is excepted also to change sign exactly at the same point in the (P, T, x) space. These facts result always in a nonnegative entropy production contribution,

- at the feed stages ($9^{\underline{\text{th}}}$ -$10^{\underline{\text{th}}}$) the conjugated driving forces are considerably larger than elsewhere due to the difference of chemical potential and the temperature between the entering streams and the mixture coexisting on the tray,

- external heat transfer plays a dominant role in the reboiler and condenser, exclusively.

In terms of entropy production, summarizing, the separation function dominates over the reaction function for this MTBE RD column configuration.

8.5 Application 2. Bi-Objective Optimization of a MTBE Reactive Distillation Column

A multiobjective optimization problem is formulated for the MTBE RD column with respect to economic performance and exergy efficiency. The formulation includes the balance equations 8.1-8.5 and 8.29, the criteria definitions 8.42 and the optimization formulation 8.62. Constraints imposed by operating conditions and product specifications are included. For the sake of controlled built-up of optimization complexity the first approximation of this approach omits the response time constant as objective function.

The resulting optimization problem is formulated as follows and is implemented and solved in gPROMS©/gOPT©,

$$\begin{aligned} \min_{\mathbf{x}\in\Gamma} \quad & J(f_{\text{econ}}(x), f_{\text{exergy}}(x), w), \\ \text{s.t.} \quad & f(\cdot) = 0, \\ & h(\cdot) \leq 0, \end{aligned} \tag{8.63}$$

where $\mathbf{x}$ denotes the set of design variables $([m_{\text{cat}}\ Q\ a_{\Psi}])$[‡], $f(\cdot)$ is the set of algebraic expressions that describe the system and $h(\cdot)$ is the set of inequalities defined by operating conditions and product specifications (*cf.* bottom section of table 8.4).

The planar view of the two normalized objective functions at different weighting factors is depicted in figure 8.9. The normalization of the objectives requires a priori knowledge of the minimum ($f^{\min}$) and maximum ($f^{\max}$) values for each objective. These values are found by solving the optimization problem at different weighting factors. Each objective value is then scaled based on the corresponding utopia coordinate and for a given weighting factor Thus, the normalized objective functions (f') are computed according to the expression,

$$f'_i = \frac{\overline{f_i} - \overline{f_i^{\min}}}{\overline{f_i^{\max}} - \overline{f_i^{\min}}}, \tag{8.64}$$

where the objective function $\overline{f_i}$ is scaled with respect to the corresponding coordinates of the utopia point,

$$\overline{f}_i = \left(w_i \times \frac{f_i}{f_i^{\text{U}}} \right)^p, \qquad i \in \mathbb{Z}^{n_o}, \tag{8.65}$$

where n_o denotes the number of objective functions.

[‡]Operational variables such as reflux ratio and condenser pressure have been fixed to appropriate reference values. Table 8.4 lists the actual values.

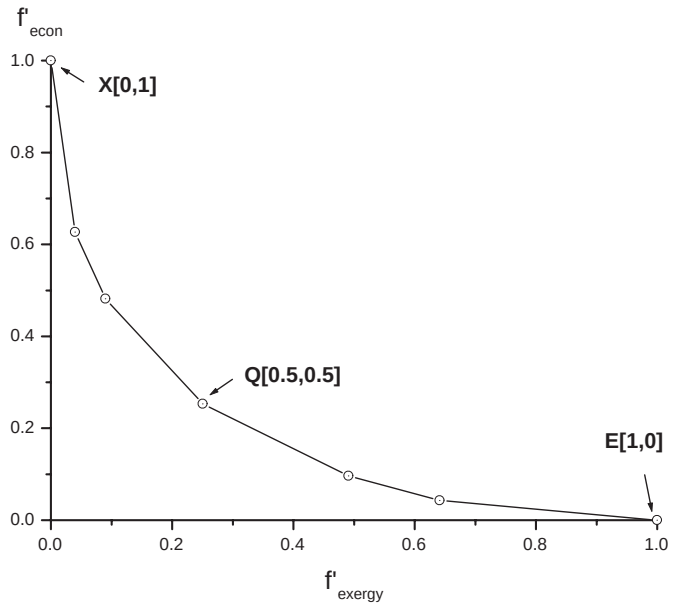

Figure 8.9. Pareto optimal curve f_{econ} versus f_{exergy}. **Legend: E:** economic-based optimal design; **X:** exergy-based optimal design; **Q:** optimal design based equally on economic performance and exergy efficiency; **Remarks:** each point of the curve represents an optimal solution in terms of the design variables $[m_{\text{cat}}, Q, a_{\Psi}]$ and weighting factors w; axes are normalized so that utopia point coordinates are: **U**=(0,0); original coordinates of **U** are: $\mathbf{U}_0$=($5.247{\cdot}10^4$ J$\times$(s$\times$K)$^{-1}$,$2.082\ {\cdot}10^8$ euro$\times$y^{-1}).

This curve is termed *Pareto curve* (*cf.* explanatory note 8.1) and clearly shows that one objective function can only be improved at the expense of the other objective function. This trade-off leads to significant deviations between optimal designs and the utopia point (up to 60%) for the pair $f'_{\text{econ}} - f'_{\text{exergy}}$. The decision maker should have in mind the importance of compromising both objectives at early stages of the design cycle.

Significant structural differences are noticed between the economic-driven (**E**; $w = [1 \quad 0]^{\text{T}}$) and exergy-driven (**X**; $w = [0 \quad 1]^{\text{T}}$) designs.

As depicted in figure 8.10, for instance, the catalyst load along the reactive trays differs among the proposed designs when compared to the reference case (**R**[†]). The catalyst load of the reference case is used to normalize the plot. When exergy is fully considered

[†]It is worth mentioning that, as expected, the optimal design based on economic performance (**E**) coincides with the reference case (**R**).

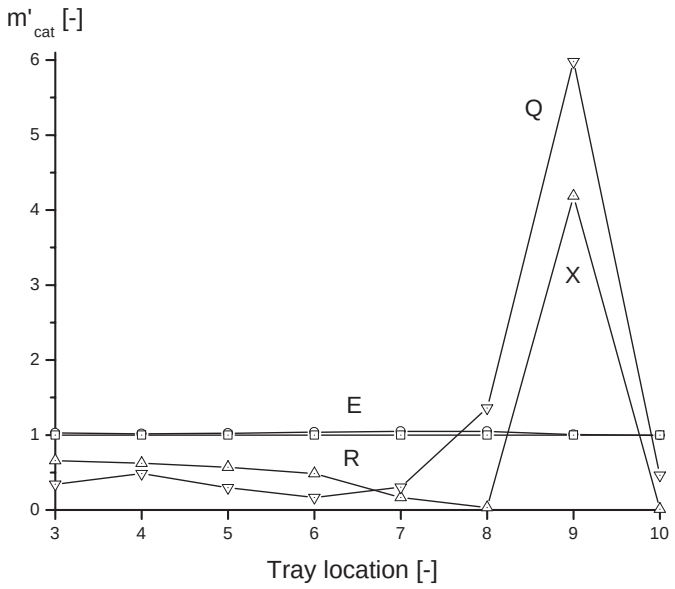

Figure 8.10. Normalized catalyst distribution in the synthesis of MTBE with respect to economic performance and exergy efficiency. **Legend: R:** reference design, whose catalyst distribution is used for normalization; **E:** optimal design based only on economic performance; **X:** optimal design based only on exergy efficiency; **Q:** optimal design based equally on economic performance and exergy efficiency.

as an objective function the last reactive tray vanishes together with the sixth reactive tray. Furthermore, the catalyst load of the seventh reactive tray is considerably higher than that of the nominal cases. This output suggest an alternative design, where a side reactor with high catalyst load is placed at the $7^{\underline{\text{th}}}$ tray. The catalyst load on the remaining reactive trays decreases when exergy is taken into account. The design with equally weighted objectives (**Q**; $w = [0.5 \quad 0.5]^{\mathrm{T}}$) presents an interesting catalyst load profile, specially at the $9^{\underline{\text{th}}}$ tray. The rather large catalyst load might be explained by the reduced catalyst load on the last reactive tray and the constraint of targeting the product specifications. The reduced catalyst load on the $9^{\underline{\text{th}}}$ tray diminishes the MTBE decomposition, at high MTBE composition and the product synthesis, at low MTBE composition. As a constraint in the product specification is included in the problem formulation, the required extent of reaction is accommodated only by having the $9^{\underline{\text{th}}}$ tray fully loaded with catalyst. Since MeOH is fed at the $9^{\underline{\text{th}}}$ tray, larger holdup of reactant is present and only converted into products by an increased amount of catalyst.

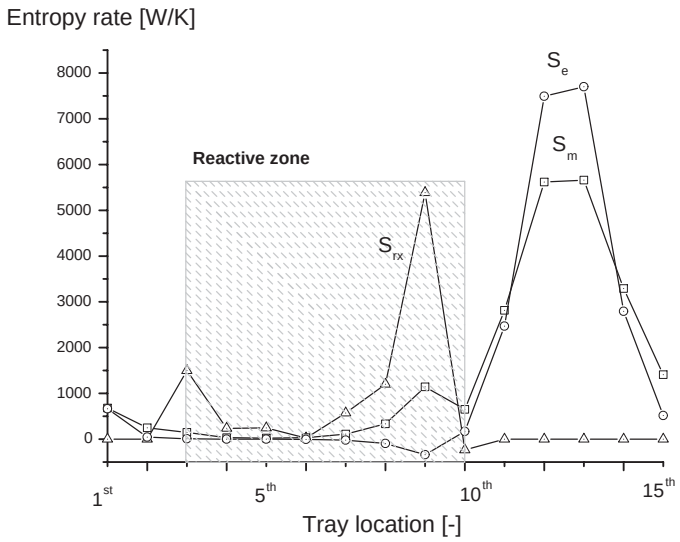

Figure 8.11. Entropy production rate profile for an optimal design of a MTBE RD column based on exergy efficiency (**X**-design). **Legend:** S_m: entropy produced by interfacial mass diffusion; S_e: entropy produced by interfacial energy transfer; S_{rx}: entropy produced by chemical reaction; **Remarks:** stages are numbered from top to bottom; MeOH feed stream is fed at $9^{\underline{\text{th}}}$ tray and $i\text{C}_4$ stream at $10^{\underline{\text{th}}}$ tray.

When the entropy profiles of the **X**-design (*cf.* figure 8.11) are compared with those of the **E**-design, it can be realized that the mayor contribution of entropy is still coming from the heat transfer process in the stripping section. However, mass diffusion becomes more relevant than in the **E**-design. In the reactive zone and in contrast to the results of figure 8.8, the exergy by chemical reaction is unevenly produced along the reactive trays. Thus, the $9^{\underline{\text{th}}}$ tray largely contributes to the overall exergy produced within the reactive section. A fully catalyst load on that tray intuitively explains this behavior.

According to these last results, it seems more attractive to reach high conversions on one or a few trays and low conversion on surrounding trays. Apparently, this finding seems to *violate* the equipartition principle of driving forces, under idealized conditions. Note that here we focus on the performance of RD process designs, paying less explicit attention to the industrial conventional processing route (see figure B.1). Therefore, a comparison between RD and non-RD processes with regard to entropy production and the design implications for the principle of equipartition of forces are recommended topics to be further researched.

8.6 Application 3. Tri-Objective Optimization of a MTBE Reactive Distillation Column: A Sensitivity-Based Approach

Based on the insight gathered in the previous applications, we are now ready to assess the optimal design of a MTBE RD column with respect to f_{econ}, f_{exergy} and f_{response}. For the sake of simplification, the following strategy is adopted: (*i*) an optimized design based in economics and exergy efficiency is considered; (*ii*) a disturbance scenario is defined; and (*iii*) the responsiveness index of the optimized design is estimated at the given disturbance scenario.

Optimized design. According to applications 1 (section §8.4) and 2 (section §8.5), the optimized designs based on f_{econ} and f_{exergy} present an important tradeoff between both objectives. This tradeoff depends on the vector of weighting factors, w. The ultimate decision on w is made by the designer according to the requirements of the design problem. In our case and only for tutorial purposes, we choose the vector $w = [0.3 \quad 0.7]^{\text{T}}$ over all available designs. The optimized design variables for this case are listed in table 8.6.

Disturbance scenario. The selection of a disturbance scenario is carried out by analyzing qualitatively the entropy profiles of figures 8.8 (**E**-design) and (**X**-design) 8.11 and by focussing on process disturbances occurring in industrial practice. An upstream variation of the MeOH feed flowrate up to -10% is chosen as disturbance scenario.

$$F_{\text{MeOH}} = F^{SS}_{\text{MeOH}} \times (1 - \alpha_\tau(t)), \qquad 0 \leq \alpha_\tau(t) \leq 0.1, \quad t \in [0, t_f]. \tag{8.66}$$

Note that the disturbance scenario is chosen so that any steady-state transition is avoided. Further supporting arguments are given in section §7.3.2.

Responsiveness index. For each MeOH feed rate the variables $\text{B}(\mathbf{x}, \mathbf{u})$ and $\Sigma_V(\mathbf{x}, \mathbf{u})$ are estimated in the corresponding steady state and the responsiveness index is computed. Note that the responsiveness index is treated as a function of the magnitude of the MeOH feed perturbation, $f_{\text{response}}(F_{\text{MeOH}})$.

Specifically, this MeOH flowrate disturbance results in a variation of the mass transfer driving forces for each component along the unit. From this point on, the analysis is focused on the top tray ($1^{\underline{\text{st}}}$), the $9^{\underline{\text{th}}}$ tray and the bottom tray ($15^{\underline{\text{th}}}$) of the RD column specified in table 8.6. Considering these tray locations, we provide a generalized overview on the unit's responsiveness in the rectifying, reactive and stripping sections. The $9^{\underline{\text{th}}}$ tray is chosen because it is on that particular feeding tray where MeOH is fed to the column and, therefore, where a more pronounced effect of feed flowrate disturbance is expected. The corresponding mass transfer and chemical reaction driving forces are

Table 8.6. Optimized design of a RD column for MTBE synthesis based on economic performance and exergy efficiency. **Remark:** $w = [0.3 \quad 0.7]^{\mathrm{T}}$.

	Value
Number of trays	15 [2:rectifying;8:reactive; 5:stripping]
Feed 1: location	iC$_4$+ nC$_4$: 10$^{\underline{\text{th}}}$ tray (g)
Feed 1: flowrate	455 mol×s^{-1}
Feed 1: composition	iC$_4$: 0.37; nC$_4$: 0.63
Feed 1: temperature	350K
Feed 2: location	MeOH: 9$^{\underline{\text{th}}}$ tray (l)
Feed 2: flowrate	168 mol×s^{-1}
Feed 2: composition	MeOH: 1.00
Feed 2: temperature	320K
Operating pressure	11·10^5 Pa (top)
Reflux ratio	7
Mass of catalyst [eq$_{[H^+]}$]	m$_{1:2}$=0; m$_3$=771.9 m$_4$=826.122; m$_5$=762.405 m$_6$=688.412; m$_7$=652.292 m$_8$=785.991; m$_9$=1359.42 m$_{10}$=982.448; m$_{11:15}$=0
Bottom flowrate	197 mol×s^{-1}
Column diameter	rectifying: 6.95 m reactive: 6.95 m stripping: 6.33 m
Condenser area	1.059·10^3 m^2
Reboiler area	6.93·10^2 m^2

plotted for trays 1, 15 and 9 in figure 8.12. It can be seen from these plots that both MeOH mass transfer driving forces increase with larger disturbances, whereas chemical reaction driving force decreases.

The response time of the MTBE RD column as a function of $X_{i,\mathrm{MeOH}}$ (1$^{\underline{\text{st}}}$ and 15$^{\underline{\text{th}}}$ tray) and X_{rx} (9$^{\underline{\text{th}}}$ tray) is depicted in figure 8.13. The variation of $\mathrm{B}(\mathbf{x},\mathbf{u})$ and $\Sigma_V(\mathbf{x},\mathbf{u})$ are computed between the initial reference state and between consecutive states. Note that the response time becomes larger at small $X_{i,\mathrm{MeOH}}$-values in the rectifying and stripping sections, whereas small driving forces lead to short response times in the reactive section. From a responsiveness perspective, therefore, small driving forces are desirable for reactive sections and large driving forces are desirable for separation (nonreactive) sections.

The first statement suggests that in the case of reactive sections driving forces should be manipulated to control the unit while flux is specified (*i.e.* a certain conversion rate).

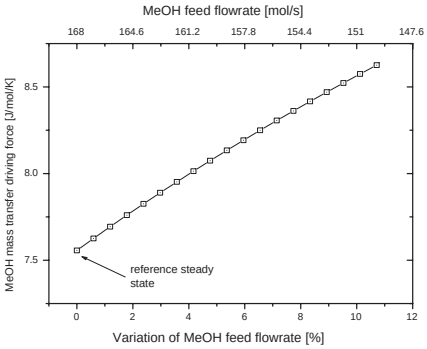

(a) Rectifying section, $1^{\underline{\text{st}}}$ tray.

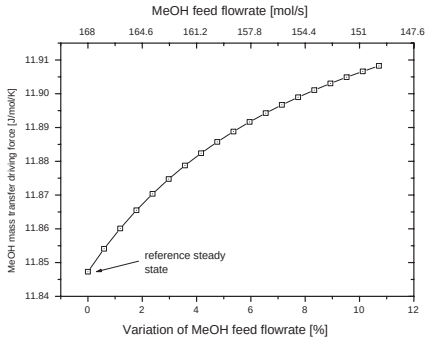

(b) Stripping section, $15^{\underline{\text{th}}}$ tray.

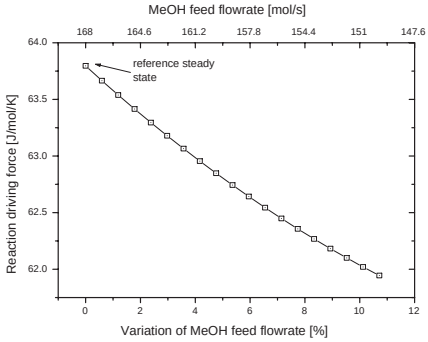

(c) Reactive section, $9^{\underline{\text{th}}}$ tray.

Figure 8.12. Driving forces as a function of the MeOH feed flowrate. **Remarks:** MeOH feed flowrate varies from the nominal value (168 mol $\times s^{-1}$) to 150 mol $\times s^{-1}$; the optimal design variables and sizing parameters corresponds to a $f_{\text{econ}} - f_{\text{exergy}}$ design, with $w = [0.3 \quad 0.7]^{\text{T}}$.

Explaining this requires the introduction of an approximated relation between fluxes and forces (Luyben *et al.*, 1999; Hasse, 1969),

$$J_k \approx \alpha \times X_k, \tag{8.67}$$

$$T_0 \times \Delta\Sigma_V \approx 2 \times T_0 \int_V dV \sum_k \alpha \times X_k \times \Delta X_k, \tag{8.68}$$

where α is a design factor, called *thermodynamic design factor* by Meeuse (2003).

At small gradient X the design factor α should be large enough to obtain the required flux. In the reactive section small reaction driving forces requires a large reaction volume on the tray. Small variations in the MeOH feed flowrate produce large changes in the affinity and subsequently large entropy production rate values. As the stored exergy

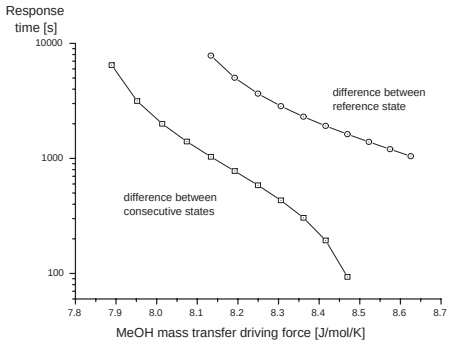

(a) Rectifying section, $1^{\underline{\text{st}}}$ tray.

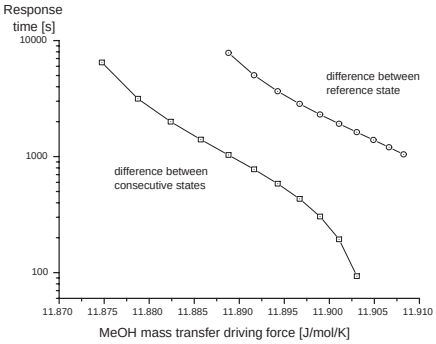

(b) Stripping section, $15^{\underline{\text{th}}}$ tray.

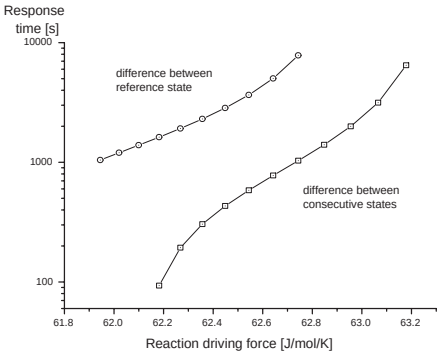

(c) Reactive section, $9^{\underline{\text{th}}}$ tray.

Figure 8.13. Response time as a function of the MeOH feed flowrate. **Remarks:** MeOH feed flowrate varies from the nominal value (168 mol $\times \text{s}^{-1}$) to 150 mol $\times \text{s}^{-1}$; the optimal design variables and sizing parameters corresponds to a $f_{\text{econ}} - f_{\text{exergy}}$ design, with $w = [0.3 \quad 0.7]^{\text{T}}$.

changes only modestly with a small flow disturbance, the overall effect enhances the process responsiveness (*i.e.* small response times).

The second statement can be explained by following the same reasoning. In a distillation (separation) process the driving force (top-bottom) is specified and the flux remains to influence. Thus, in nonreactive sections flux should be manipulated to control the unit. The results of these observations fully agrees with the analysis given by Luyben *et al.* (1999) and Meeuse (2003) for a reactor and distillation column.

Meaningfulness and validity of results. Note that in the current approach a continuous range of disturbances for one input variable is considered for the computation of the responsiveness time constant. In comparison with the generalized definition of

Table 8.7. Entropy produced in classical and green designs. **Remarks:** classical design corresponds to $w = [1 \quad 0]^{\mathrm{T}}$; green design corresponds to $w = [0.3 \quad 0.7]^{\mathrm{T}}$.

w	$f_{\mathrm{econ}}[\mathrm{euro}\times \mathrm{y}^{-1}]$	f_{exergy} $[\mathrm{J}\times(\mathrm{s}\times\mathrm{K})^{-1}]$
$[1.0 \quad 0.0]^{\mathrm{T}}$	$2.082{\cdot}10^{8}$	$5.604{\cdot}10^{4}$
$[0.3 \quad 0.7]^{\mathrm{T}}$	$2.085{\cdot}10^{8}$	$5.305{\cdot}10^{4}$
$[0.0 \quad 1.0]^{\mathrm{T}}$	$2.086{\cdot}10^{8}$	$5.251{\cdot}10^{4}$

f_{response} by Luyben *et al.* (1999), this is a very specific case. Their (Luyben's *et al.*) definition demands an optimization of the states $\mathbf{x}$ to find the worst case situation over a domain of states. Therefore, there is a latent risk that the presented results are not optimized over the feasible domain of states for normal operation. Our approach might be locally optimized for the given operational window, but might have a low degree of validity to other cases.

8.7 Comparison Between Classical and Green Designs

In the course of this chapter the economic-driven design (classical design) was implicitly compared with a new bi-optimized design (green design) for the case of a MTBE RD column. A set of indicators can be used to compare both designs: (*i*) exergy loss; and (*ii*) closed loop control performance.

The exergy loss (or entropy produced) can be extracted from the Pareto curve presented in figure 8.9. The relevant data for the classical and green designs and for the fully exergy-driven design (*i.e.* $w = [0 \quad 1]^{\mathrm{T}}$) are listed in table 8.7.

As it was expected, the green design produces less entropy than the classical one, however, economically it is less attractive than the conventional design, as it presents a higher f_{econ} value. It is worth mentioning that the increase in costs is rather marginal ($\sim$2%) and within the uncertainty range of the correlation to predict investments costs for units and catalyst. Nevertheless, a tendency towards increased cost can be suggested, but is not significant for this particular case.

A more significant change is observed for f_{exergy} ($\sim$8%). A more revealing concept to asses the impact of making a process greener is the shadow price λ_p. It is a cost penalty function for changing entropy production and given by,

$$\lambda_p = \frac{\partial f_{\mathrm{econ}}}{\partial f_{\mathrm{exergy}}}. \tag{8.69}$$

The shadow prices can be computed directly out from the data in table 8.7 or from the Pareto curve in figure 8.9. It was found that, when compared to the classical case,

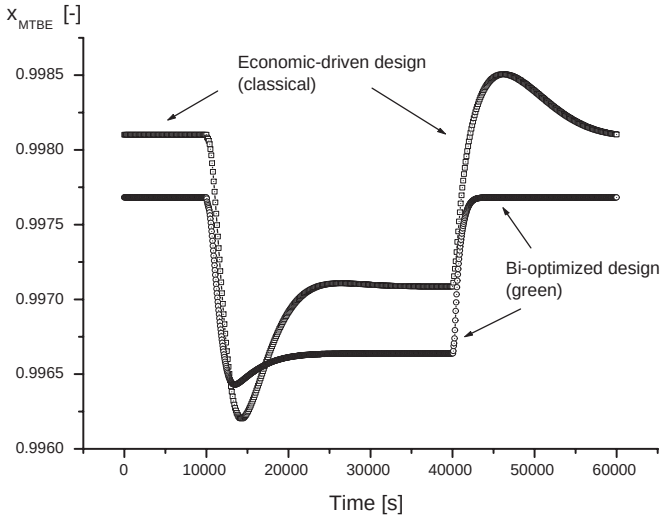

Figure 8.14. Time variation of MTBE product stream for the classic and green designs in the presence of a MeOH feed flowrate disturbance. **Remarks:** green design corresponds to $w = [0.3 \quad 0.7]^{\mathrm{T}}$; column specifications for classic and green designs are given in tables 8.4 and 8.6, respectively.

the green design presents a cost penalty of $\sim$ -2.02, whereas the **X**-design a value of $\sim$ -4.37 [euro $\times$K $\times$MJ^{-1}]. These values confirm the trade-off between both objectives and suggest that the greener the design the larger the involved cost penalty.

The closed loop control performance of both designs is now analyzed. The disturbance scenario under consideration is the one used previously in section §7.3. Thus, a step variation in the flowrate of methanol during the time horizon of $6{\cdot}10^4$ s is given by,

$$F_{\mathrm{MeOH}} = \begin{cases} F^{SS}_{\mathrm{MeOH}} & \text{if } t < 1 \cdot 10^4 \text{ s or } t > 4 \cdot 10^4 \text{ s}, \\ 1.1 \times F^{SS}_{\mathrm{MeOH}} & \text{if } 4 \cdot 10^4 \text{ s} > t > 1 \cdot 10^4 \text{ s}. \end{cases} \tag{8.70}$$

The dynamic response of the classic and green designs are depicted in figure 8.14. In this figure the MTBE composition at the bottom stream is presented as a function of time in the presence of the MeOH feed disturbance. Note that the bi-optimized design (*i.e.* green) has an improved closed loop performance compared with the classical design. The deviation from x_{MTBE} set-point are less pronounced in the green design, which smoothly returns back to the initial steady state when the disturbance disappears. Note that the set-point of the green design is slightly lower (0.05%) than the one of the classic design. This negligible variation in set-points does not affect the quality of

the analysis results. It is suggested from our results that incorporating both economic and exergy-related objectives in the unit design results in a process with better closed loop performance, provided that control structure and tuning are kept invariant. It is worth clarifying that a well-tuned control can compensate for any change in the process operability feature.

8.8 Concluding Remarks

The starting point of this chapter was the definition of a generic building block for process synthesis (GLRDVE). The sources and the distribution of the entropy production rate in a complete MTBE column were then determined and analyzed. It is believed that insight into such a distribution is helpful for assessing which column related design decision variables (*e.g.* feed tray location, reflux ratio, heat load distribution using diabatic operation, catalyst load and mass/heat transfer area) are key to optimize the column performance. The perspective adopted for selecting the design decision variables was task-oriented rather than the conventionally used equipment-oriented design approach. The chosen design decision variables included the reaction volume, the amount of heat to be added or removed and the interfacial areas for species mass and heat transfer. Operational variables such as reflux ratio and condenser pressure were fixed at appropriate reference values. Analyzing the steady state entropy production profiles in a MTBE RD column showed that, in terms of entropy production, the separation function dominates over the reaction function. A bi-objective function was then studied regarding economic and exergy performance. It is suggested that designs based exclusively on economic or exergy performances differ significantly in their structure, showing an existing trade-off. The Pareto curve provides sensitivity information on the cost effects of improving the exergy efficiency. In addition to economics and exergy objectives, this optimization-based approach covers responsiveness aspects. To define a responsiveness criteria, the availability and entropy production rate are regarded as functions of an internal state vector $\mathbf{x}$ and a vector of disturbances and/or manipulated external excitations $\mathbf{u}$. In our approach the maximization approach suggested by Luyben *et al.* (1999) is not considered due to its inherent need for high computational effort. However, a rather formal definition of f_{response} was adopted together with a single input excitation. Note that by not searching over all possible state trajectories, the generality of the results might be questionable and the external excitation is a fairly conservative one. Analyzing the responsiveness criteria of the bi-optimized design it reconfirmed that small driving forces are desirable for reactive sections and large driving forces are desirable for separation (nonreactive) sections (Luyben *et al.*, 1999; Meeuse, 2003). The first statement suggests that, in the case of reactive sections, driving forces should be manipulated to control the unit. The second statement suggests that in nonreactive

sections flux should be manipulated to control the unit. Finally, the economic-driven design (classical design) was compared with the new bi-optimized design (green design) for the case of the MTBE RD column. The green design produces less entropy than the classical one, while being economically less attractive (marginal). The bi-optimized design has an improved closed loop performance compared to the classical design, keeping the same control structure and settings. It is concluded that incorporating both economic and exergy-related objectives in the unit design results in a process with better closed loop performance and reduced exergy loss.

Mind journey to the scientific questions.

In this chapter three performance criteria were introduced in the RD design problem derived from a life-span perspective. The incorporation of those performance criteria resulted in designs with structural differences and with balanced economic-performance, thermodynamic efficiency and that are capable of coping with a realistic disturbance scenario. Thus, the material presented in this chapter effectively answers Question 7.

"It is through science that we prove, but through intuition that we discover."

Henri Poincare, mathematician (1854-1912)

9

Conclusions and Outlook

This dissertation covers the design of grassroots reactive distillation processes. In this concluding chapter we attempt to highlight the key contributions of this research to the scientific knowledge domain of reactive distillation process design. Here we pay special attention to the answers of the goal-oriented and engineering questions posted at the end of chapter 1. Additionally, we discuss various paths for further research and give some recommendations for future endeavors.

9.1 Introduction

The design and operation of reactive distillation processes has received increasing attention within academia and industrial spheres over the last decades (*cf.* figure 1 in Malone and Doherty (2000)). From a process intensified perspective and because of its inherent complexity, addressing RD is a challenging task. In the course of this dissertation we have present the relevant results and approach that can be used to produce a life-span inspired design for reactive distillation processes. In this regard, after having covered the fundamentals of RD and current design approaches (chapters 2 and 3), we suggest a novel methodology for RD process design (chapter 4), which then becomes the focus of chapters 5-8. Each chapter covers a specific aspect of the LiSp-IDM, *i.e.* life-span inspired design methodology) and answers to the engineering questions (questions 4-7) posted in chapter 1 are provided. Taking a broader perspective these engineering answers will now be used to address the goal-oriented questions (questions 1-3), either qualitatively or quantitatively.

This chapter is organized as follows: in section §9.2 we recall the specific design questions and provide the supporting scientific argumentation for the answers. In section §9.3, we infer the answers to the goal-oriented engineering questions. We adopted this ordering based on the assumption that the material presented in the previous chapters remains in the reader's memory, or at least it is easily retrieved. We address the novelty aspects of this research in section §9.4. The open opportunities identified in the course of this work are discussed along with recommendations for further research in section §9.5.

9.2 Conclusions Regarding Specific Scientific Design Questions

Recalling the specific scientific design questions formulated at the beginning of this thesis, we can draw the following conclusions.

Question 4. What is the domain knowledge required and which new echelons are needed for process synthesis?

▶ **Answer.** *Temporal domain knowledge, physical and operational knowledge and spatial-related knowledge; a multiechelon approach: formulation, feasibility analysis, temporal structure, generation of separation sequences, internal spatial structure, behavior analysis, evaluation.*

In the case of RD, the design issues are far more complex than those relating to conventional distillation and they may differ significantly from case to case. Thus, we suggest that the domain knowledge required for any (integrated) design methodology should be classified into three key areas: (*i*) temporal considerations, (*ii*) physical and opera-

tional conditions and (*iii*) spatial parameters. In terms of priority of decision the first class of key design decision variables involves *temporal considerations*. The variables of interest relate to the mode of operation of the system, namely batch, fed batch or continuous operation, together with the time horizon. The second class of design variables includes the *physical and operational conditions of the system*. These are aimed at the favorable creation of enough reaction and separation driving forces and mutual synergy. In this class design variables such as operation pressure, temperature, reflux ratio and phase velocity are of utmost importance. Moreover, the chemical reaction regime and mass/heat transfer regime should be specified. The third and last class of decision class embraces all key *spatial parameters*, ranging from establishing section with different functionalities, packing parameters, number of trays or length of sections, feeding and withdrawal points, energy exchange, section diameters, column flowsheet configuration with recycle structures and heat integration.

Both graphical and optimization-based design methods have already shown proven potential in RD process design, but some significant limitations have also been found. Graphical methods are fairly flexible for generating alternative designs at various design parameters, allowing the designer to define realistic bounds. Furthermore, the graphical nature of the methods helps us to clarify our understanding of these fundamental issues in RD, which might be disguised by other approaches. However, graphical methods are strongly limited by their graphical nature.

Optimization-based methods overcome this last limitation and can be used to solve successfully design problems that involve multicomponent mixtures, multiple chemical reactions and multiple units. However, additional caution is required during problem formulation and inappropriate initial guesses made for the optimization variables may lead to convergence difficulties. Evolutionary methods are used to cover, in more detail, some of the physical aspects of the design of RD columns. However, this approach requires a pre-defined structure and accordingly, an optimum design is not guaranteed.

Due to the size and conceptual/computational complexity of the RD design problem, a single comprehensive design strategy might not be available for some years to come. In this research, however, we propose an integrated design approach, termed *multiechelon design approach*. This strategy allows the designer to combine, in a systematic way, the capabilities and complementary strengths of the available graphical and optimization-based methods. Decomposition to give a hierarchy of imbedded design spaces of increasing refinement is used to support this approach. Moreover, it constitutes the framework of a highly aggregated design methodology, which focuses on the RD design problem from a life-span perspective (LiSp-IDM in chapter 4). The following building blocks constitute the body of the *multiechelon design approach*:

Formulation. Sustainability issue are considered and the basis of design are defined,

i.e. product and feedstock purities ranges, production modes, operating window and economics, and appropriate building model blocks are developed (*e.g.* thermodynamic, kinetic and hydrodynamic).

Feasibility analysis. Using graphical methods the feasible product compositions for a given set of input variables are determined (*e.g.* feed composition and Damköhler number) incorporating all occurring phenomena (*e.g.* distillation boundaries, (non)-reactive azeotropy).

Temporal structure. The operation mode is selected, *i.e.* batch, continuous or semi-batch, based on operational skills, production requirements and supply chain dynamics.

Generation of separation sequences. The use of rigorous graphical methods allows us to identify and organize feasible column sequences. It is necessary to estimate their type of task, *i.e.* fully reactive, hybrid and nonreactive columns, together with the number of units and their connectivity.

Internal spatial structure. The process structure obtained from the previous level is used as starting point for this stage. Using optimization-based methods we can obtain continuous variables (*e.g.* column diameter, heat exchange areas, contacting area, catalyst concentration, reboil and reflux ratios) and discrete variables (*e.g.* feed staging, reactive and nonreactive stages, withdrawal staging).

Behavior analysis. Steady-state simulations are used to explore the kinetics, G/L mass transfer, hydrodynamics and multiplicities inside the units. Additionally, dynamic simulations are performed to check the robustness of the design, in terms of the ability to maintain product purities and conversion within a desired range when disturbances occur.

Evaluation. The design options are checked with respect to their performance. Taking the wide range of criteria in the safety, health, economics, environment and technology (SHEET) aspects specific choices are made for economic performance, sustainability and technology. With respect to economics, we calculate the capital and operational costs of a process for its time horizon. We use exergy efficiency as a sustainability metric, while a systems response time is used to define the responsiveness of the process.

Question 5. What are the (performance) criteria that need to be considered from a life-span perspective when specifying a reactive distillation design problem?

▶ **Answer.** *Safety, health, environment, economics and technology (SHEET)-related metrics; in particular TAC, entropy production rate and response time.*
Aiming at a design methodology that addresses the problem from a life-span perspective, we suggested a set of performance criteria. The motivation behind our perspective relies

on the relevance of economic performance and potential losses over the process life span. Specifically, we took into consideration exergy-efficiency and responsiveness issues.

We considered a set of criteria embracing issues related to safety, health, environment, economics and technology (SHEET). Provided that safety and health issues are inherent in a responsible design approach, the remaining issues can be used to define a novel performance space. Environmental considerations are directly linked to the minimization of mass, energy and exergy losses. Economic performance is translated quantitatively to the capital and operational costs of the design. We used the total annualized cost (TAC) as a convenient index. Additionally, we considered exergy efficiency to be an environment-based metric, more specifically the entropy production rate. We completed the performance criteria set by appending a technology-based index. In this work we suggested that the responsiveness of the process can be used as an adequate metric and more specifically the response time as defined in Luyben *et al.* (1999). Using this metric we get a measure for prevention of loss of material and energy.

Question 6. What (new) methods and tools are needed for reactive distillation process synthesis, analysis and evaluation?

► **Answer.** *Improved residue curve mapping technique, multilevel modeling approach, dynamic optimization of spatial and control structures, steady-state and dynamic behavior analysis, generic lumped reactive distillation volume element, multiobjective optimization criteria.*
In the course of this thesis we have covered novel tools and methods that can be used to assist the design of reactive distillation processes (see chapters 5 to 7). A brief description of the highlights of the chapters is given below.

We showed that residue curve maps provide valuable insights and design assistance for nonideal systems, particularly for RD. Transforming the composition variables according to Doherty's approach allows us to define a *reaction invariant space* of lower dimension, formed by attainable product compositions and where the conventional concepts for residue curves can be applied. For the MTBE synthesis we defined two main subregions in the modified composition simplex, each of which were characterized by singular points and delimited by separation boundaries. We generated two different separation sequences, covering **all** the possible reacting mixture compositions.

We proposed a multilevel modeling approach, regarded as an easy-to-handle tool in the early stages of design. We derived two model levels of different degree of complexity to model the processes taking place in a RD column. Additionally, we performed rigorous and reliable degree of freedom analysis at each level, where appropriate business-related decision variables are included. These levels involve an outer (input-output) view and an inner (physical task) view. These models are linked by the extent of reaction vector,

which allows us to establish whether or not the models are well specified and mutually consistent. Additionally, the approach allows one to determine whether or not the business-related decision variables cope with the operational constraints imposed by the problem formulation (*e.g.* the SHE issues, reactants availability and market demand).

Formulating design as a dynamic optimization problem, we found that for the synthesis of MTBE, a tradeoff between control and economic performances exists. We solved this multiobjective optimization problem by incorporating appropriate time-invariant parameters (*e.g.* column diameter, heat transfer areas and controllers' parameters) in the frame of a dynamic optimization problem in the presence of deterministic disturbances. The design optimized sequentially with respect to dynamic behavior leads to a RD process with a total annualized cost higher than that obtained using simultaneous optimization of spatial and control structures.

The nonlinear coupling of reactions, transport phenomena, phase equilibria and hardware hydraulics arises as a result of the highly complicated dynamic behavior of the system. We showed that, even for a simplified reactive flash and an idealized system, a large number of bifurcation diagrams could be identified. We suggest that the main source of multiplicity is the strong nonlinear coupling of reactions, transport phenomena and phase equilibria. We used singularity to study the steady-state behavior in RD, with a particular focus on a reactive flash with a rather ideal system undergoing a mildly exothermic isomerization reaction using a light-boiling reactant. For this case the number and relative location of the turning points and feasibility boundaries corresponding to no-liquid or no-vapor products determined the qualitative nature of the bifurcation diagram. State multiplicity is present in a large area of the parameter space, for the case under consideration. We identified a large number (25) of qualitatively different bifurcation diagrams for the system. The feasibility boundaries played an important role in the classification of the reactive flash. Up to five feasibility boundaries and a maximum of 3 steady states were found in a single bifurcation diagram. Bifurcation diagrams exhibiting more then two feasibility boundaries are common for liquid or vapor feed. Increasing the heat of reaction, activation energy or relative volatility enlarges the area of multiplicity. Furthermore, a large heat of reaction can create regions in parameter space with 5 feasibility boundaries in a single bifurcation diagram.

Moreover, we explored the process dynamics of a full RD unit using a rather conventional approach. The scope of this analysis was restricted to a limited version of control system design, as a single input-single output structure and proportional-integral controllers were selected *a priori* selected. The outcome of this approach was used to set a reference performance for the next novel contribution involving the trade-off between design, responsiveness and sustainability aspects. We developed a generic dynamic model for a complete RD column. This model is composed of instances of (non-) reactive trays, condenser, reflux drum, reboiler and controllers. Based on a rigorous degree of freedom

analysis and some engineering judgment a control structure was defined. Using the synthesis of MTBE as our case study, we simulated dynamically the unit behavior in the presence of realistic disturbances scenarios. Using comparison with published work, we found a satisfactory degree of agreement between our unit output and literature data. Moreover, our proposed control structure led to minor variations in the MTBE bottom fraction in the presence of disturbances.

Question 7. Are there structural differences and significant improvements in designs derived using conventional methodologies from those obtained using an integrated design methodology?

► **Answer.** *Reduction in the number of reactive trays, more uneven distribution of catalyst and identification of suitable spots for side reactors.*
We defined a generic building block for process synthesis: the generic lumped reactive distillation volume element. We then determined and analyzed the sources and distribution of the entropy production rate in a complete MTBE column. We strongly believe that insight into such a distribution is helpful for assessing which column related design decision variables are key to optimize column performance. The perspective adopted for selecting the design decision variables was task-oriented rather than the conventionally used equipment-oriented design approach. Analyzing the steady state entropy production profiles in a MTBE RD column we found that, in terms of entropy production, the separation function dominates over the reaction function. Afterwards, we studied a bi-objective function with respect to economic and exergy performance. We found that designs based on economic or exergy performances differed significantly in their structure, showing an existing trade-off. For instance, the catalyst load along the reactive trays differed among bi-optimized designs ('green') when compared to the reference 'conventional' case. Hence, the number of reactive trays and catalyst load diminishes when exergy is optimized. Trays with high catalyst loading could be candidate spots for placing a side reactor. In addition to the economics and exergy objectives, we analyzed responsiveness aspects in this optimization-based approach. To define a responsiveness criterion we adopted a rather specific definition of response time, it being the change in availability over the change in entropy production rate due to a single input excitation. Analyzing the responsiveness criteria of the bi-optimized design we reconfirmed that small driving forces are desirable for reactive sections and large driving forces are desirable for separation (nonreactive) sections. Finally, we compared the economic-driven design (classical design) with the green design for the case of the MTBE RD column. We found that the green design produced less entropy than the classical one, while being marginally less attractive from an economics standpoint. Moreover, the green design had an improved closed loop performance compared to the classical design, keeping the same control structure and settings. We concluded that incorporating both eco-

nomic and exergy-related objectives in the unit design results in a process with better closed loop performance and reduced exergy loss for this specific case study. These facts provided the motivation for our life-span inspired perspective.

9.3 Conclusions Regarding Goal-Oriented Questions

After having addressed the engineering specific questions we propose the following answers to the goal-oriented questions.

Question 1. What benefits can be gained from having a more integrated design methodology?

In this thesis we proposed and addressed, at a certain degree of detail, a life-span inspired design methodology (LiSp-IDM, see chapter 4). The framework of our approach was derived from an extensive analysis of current design methodologies in RD. Thus, the suggested multiechelon approach combines, in a systematic way, the capabilities and complementary strengths of the available graphical and optimization-based design methodologies. The multiechelon approach is also supported by decomposition to give a hierarchy of imbedded design spaces of increasing refinement. As a design progresses the level of design resolution can be increased, while constraints on the physical feasibility of structures and operating conditions derived from first principles analysis can be propagated to limit the searches in the expanded design space.

The benefits of adopting such an integrated methodology are of different nature, ranging from responsible use of resources (via minimization of entropy production rate), economical attractiveness (via minimization of total annualized costs) and improved process responsiveness (via minimization of response time metric). Using gradual refinement of the design spaces we introduced a beneficial understanding of the ongoing physical and chemical phenomena and guaranteed a more efficient conceptual design with respect to the SHEET criteria.

The successful application of the integrated design methodology relies on considering the output of the graphical methods as an initial structure on which to base the optimization-driven design approaches. In this way, the optimized design is likely to be embedded within the feasible space and the computational effort becomes less demanding due to the reduced number of design variables. This approach is intended as a means to decompose the complexity of the design problem and it should not be considered as a mechanistic recipe.

Question 2. What are the practical constraints that need to be considered from a resources point of view, *i.e.* time, costs, tools and skill levels, when developing and applying a design methodology in a work process?

The design task is often regarded as a difficult to master activity, due to the high number of design decision variables and combinatorial complexity. For the RD case this aspect is magnified due to the large number of additional design variables that have to be considered and the presence of more interacting phenomena, when compared to conventional nonreactive separation.

This research has shown that the integrated design methodology, more specifically the multiechelon design approach, while it is a way to beat design complexity by decomposition, requires the mastery of many tools (*e.g.* RCM, MINLP and rigorous dynamic modeling) and many concepts (*e.g.* bifurcation, singulary theory and dynamic optimization). A schematic representation of the tools and concepts required for each design echelon is given in figure 9.1. This amazing complexity means that the required skill level is even higher than was initially assumed.

Question 3. What are the essential ingredients for such a design methodology?

Our integrated design methodology is composed of various design spaces, as described in chapter 4. These design spaces are the essential ingredients for a life-span approach and are characterized by the flow of information and knowledge domain. In the course of this thesis, we have addressed each space and, moreover, we have discussed the input-output information flow. These information aspects and the knowledge domains involved in each design space are summarized in table 9.1. Each design space (or echelon) is supported by a tool-kit, which includes techniques and concepts such as RCM, MINLP, dynamic modeling, dynamic optimization, irreversible thermodynamics-based and singularity theory.

9.4 Scientific Novelty of this Work

In this dissertation we addressed the fundamentals of reactive distillation process design and attempt to generate scientific novelty. These contributions to the knowledge domain are grouped in the following categories.

Formulation of an extended design problem. We formulated a refreshed and more comprehensive RD design problem in the wider context of process development and engineering and in a more relevant way regarding sustainability. The nature of the extension is given by the identification of the design decision variables and their grouping into three categories: (*i*) those related to temporal considerations; (*ii*) those

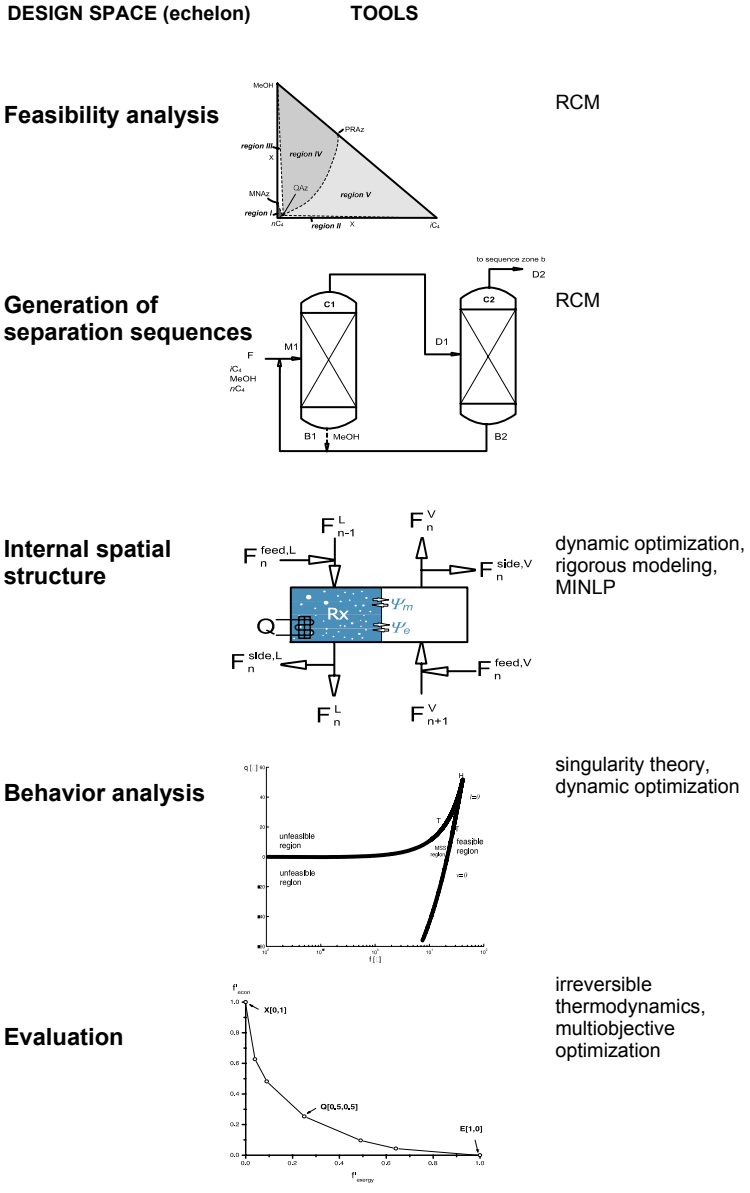

Figure 9.1. Schematic representation of the tools and concepts required at each design echelon

Table 9.1. Summary of input-output information flow

Design specifications	**Design/operational variables**	**Domain knowledge**
	Feasibility analysis	
Process:	Discrete:	- thermodynamics
- set of components	- distillation boundaries	- kinetics
- set of chemical reactions	- (non-) reactive azeotropes	- overall balances
- feed composition	Continuous:	
- operational pressure	- product feasible compositions	
Product:		
- composition target(s)		
- SHE constraints		
	Column sequencing	
Process:	Discrete:	- operational skill
- mode of operation	- type of task, separation and/or reactive	- component balances
	- number of columns	
	- columns connectivity	
	Continuous:	
	- feed ratio of reactant streams	
	Spatial structure	
Process:	Continuous:	- overall balances
- type of task	- column diameter	- component balances
- number of columns	- heat exchange/contacting areas	- dynamic behavior
- columns connectivity	- catalyst concentration	
- feed ratio of reactants	- reboil and reflux ratios	
	- controllers' parameters	
	Discrete:	
	- feed staging/withdrawal	
	- reactive and nonreactive stages	
	- control configuration	
	Behavior analysis	
Process:	Continuous:	- steady-state behavior
- unit structure	- controllability index	- dynamic behavior
- control structure	- operating conditions	
	Irreversible thermodynamics-based evaluation minimization of life-span oriented loss prevention	
Process:	Continuous:	- NEQ thermodynamics
- spatial configuration	- optimal design variables	- steady-state simulation
- control structure and settings	- performance criteria	- dynamic simulation
- operational parameters		- multiobjective optimization
- disturbance scenario		

related to physical and operational considerations and (*iii*) those related to spatial issues.

Integrated design methodology. Based on a detailed analysis of the current design methodologies in RD we presented an integrated design, *i.e.* LiSp-IDM. As industrial relevance requires design issues not to be separated from the context of process development and plant operations, we adopted a life-span inspired perspective. The framework of this methodology was structured using the *multiechelon approach*, which combines in a systematic way the capabilities and complementary strengths of the available graphical and optimization-based design methodologies. A decomposition into a hierarchy of imbedded design spaces of increasing refinement supports this approach. As a design progresses the level of design resolution can be increased, while constraints on the physical feasibility of structures and operating conditions derived from first principles analysis can be propagated to limit the searches in the expanded design space. Moreover, we considered a multilevel approach for classifying the phenomena occurring in a RD element. We approached the levels top to bottom: from process to unit and from unit to compartment.

Improvement in design tools. We supported the proposed design methodology using improved design tools. Firstly, we extended the residue curve mapping technique to the RD case and systematically applied it to reactive mixtures outside conventional composition ranges. We found this technique to be particularly useful for the sequencing of (non-) reactive separation trains. Secondly, we refined the models of the process synthesis building blocks leading to the following sub-improvements: (*i*) a refined modular representation of the building blocks; (*ii*) changes/improvements in the models of the building blocks; and (*iii*) enhancements in synthesis/analysis tools. Regarding the last item, we introduced a multilevel modeling approach with the aim of facilitating the decision-making task in the design of RD spatial structures. Moreover, we formulated our rigorous behavioral model as a dynamic optimization problem and used this technique as a design tool.

Performance criteria. To account for the process performance from a life-span inspired perspective, we defined criteria related to economic, sustainability and responsiveness aspects and embraced them in the proposed design methodology. For the first time, the interactions between economic performance, thermodynamic efficiency and responsiveness in RD process design were explored and possible trade-offs were identified. This research suggests that incorporating a sustainability-related objective in the design problem formulation might lead to promising benefits from a life-span inspired perspective. On one hand, we accounted for the exergy losses, aiming at their minimization and, on the other hand, the process responsiveness was positively enhanced.

9.5 Outlook and Further Research

In the course of this thesis we mentioned various opportunities for further research. In this section we briefly mention these possible paths for future work.

Sustainability and supply chain considerations in design problems. We used loss prevention concepts like entropy production rate as a metric for sustainability. We disregarded any other sustainability aspects like proper choice of feedstocks and products' supply chain. We strongly believe that these aspects should be explored in future work. It is important to realize, however, that incorporating supply chain motivated temporal features within the design task (*e.g.* operation and switching modes) might tremendously increase the degrees of freedom and the problem complexity.

Extended design methodology. In our integrated design methodology we considered exclusively buildings blocks with behavioral models and paid less explicit attention to structural models. Thus, in our description of the GLRDVE building block we defined a set of connectivity rules, which could be further elaborated. Our connectivity rules imposed configuration limitations, such as: (*i*) heat integration over volume elements was not considered, *i.e.* carrying heat from high temperature to low temperature elements; (*ii*) side reactors were not present; and (*iii*) no parallel structures were considered. Our design approach could be effectively complemented by building blocks with structural models, allowing for superstructure generation. The work of Pistikopoulos and co-workers (Papalexandri and Pistikopoulos, 1996; Proios and Pistikopoulos, 2005) can be used to provide the theoretical background for this task.

More refined simulation models. The challenges in the design of RD are numerous and exciting. The drive for process intensification and more sustainable plant operations can lead to more intricate geometric structures (*e.g.* packings, dividing walls and distributed heat exchange). These structures require new generation of behavioral and structural models, which couple, in a more realistic way, mass and energy transfer phenomena.

Steady-state and dynamic behavioral analysis over extended systems. Addressing a single reactive tray we aimed to explore exclusively the interaction between phase equilibrium and chemical reaction. Therefore, we consider any effect related to unit configuration outside the scope of the analysis. The possibilities for extending the steady-state analysis to a more realistic and full-scale RD system are numerous. Further research should focus on the effect of different model assumptions (*e.g.* a more refined behavioral model that includes rate limitations) and different systems (*e.g.* a full column with control structure). Thus, the effect of mass transfer would be interesting to explore, together with the behavior of systems with inert components and side reactions. Finally, the model of the reactive flash could be extended with nonreactive trays including a condenser and reboiler. Regarding dynamic behavioral analysis, we

did not address any interaction between column design and control design, this aspect is worth researching. Moreover, in this research we did not address operational aspects like flexibility. As these operational aspects could become more important than the cost aspect, we recommend that they are explored in the future.

More rigorous responsiveness index. The responsiveness index, as defined by Luyben *et al.* (1999), is a truly system feature with optimization over all possible states. In our approach we did not consider the maximization approach suggested by Luyben *et al.* (1999), due to its inherent computational effort. It is worth mentioning, therefore, that having not searched over all possible state trajectories, the generality of the results might be questionable and the external excitation given is a fairly conservative. In designing a process from a control perspective we want a process that is fast with respect to responding to changes of manipulated variables towards controlled outputs. Yet we aim for low sensitivity and slow response to disturbances acting on the process. The Luyben *et al.* responsiveness criterion does not make this kind of distinction and might require a more detailed description.

Non-equilibrium thermodynamics-based analysis. Our analysis based on multiobjective optimization of economics and exergy objective functions revealed that a beneficial design, from an economic and sustainability perspective, is obtained when high conversion rates occur in a few reaction compartments. Apparently, this finding seems to *violate* the equipartition principle of driving forces, under idealized conditions and for a single driving force. A detailed analysis of this aspect is a relevant topic for further exploration. Moreover, from a modeling perspective, more accurate approaches are required when it comes to predicting thermodynamic variables. In particular, estimation of the gradient in chemical potential for multiphase systems in turbulent mixed systems needs to be explored further.

Testing and validation of the proposed design methodology. We suggest as further activity, that our LiSp-IDM should be tested and validated. The design method is similar to a scientific hypothesis that must be tested with regard its *truth* using some experiments. The outcome of the experiments, when properly conducted, will give us the necessary information as which to extent the hypothesis can be maintained or be rejected. The approach presented by Ajah *et al.* (2004) provides an adequate theoretical background for achieving this validation. They suggest that a reliable approach for the testing and validation of a design framework (including our LiSp-IDM) might be composed of a sequence of activities: (*i*) specification of design performance criteria; (*ii*) selection of design teams and cases; (*iii*) testing and monitoring of design process and (*iv*) evaluation of design outputs. Each activity could be constrained by the quantity and quality of the resources allocated, in terms of time, costs, tools and skill levels. Thus, we should not fail to realize that, in the industrial sphere, it may rather difficult to endorse tentative design frameworks on any real scenario (Ajah *et al.*, 2004). Moreover,

a high-pressure work environment reduces the availability of experienced practicing designers who are able to adopt novel design methodologies. Nevertheless, we should not forget that historical breakthroughs in technology have all originated from human curiosity rather than from an intimate marriage with society.

A

Model Description and Degree of Freedom Analysis of a Reactive Distillation Unit

A.1 Mathematical Models

A.1.1 (Non)Reactive Tray

Component molar balance:

$$\begin{aligned}\frac{dM_i}{dt} &= F^{\text{feed,L}} \times z_i^{\text{feed,L}} + F^{\text{in},L} \times x_i^{\text{in}} + F^{\text{in},V} \times y_i^{\text{in}} - \\ & F^{\text{out},L} \times x_i - F^{\text{out},V} \times y_i + \sum_{j=1}^{j=n_{rx}} f_{rx,j} \times r_{i,j}, \quad i \in \mathbb{Z}^{n_c} \end{aligned} \tag{A.1}$$

where M in mol, F in mol$\times$s^{-1}, r in mol$\times$s^{-1}.

Appendix A

Energy balance[†]**:**

$$\begin{aligned}\frac{d\mathrm{U}}{dt} &= F^{\mathrm{feed}} \times h^{\mathrm{feed,L}} + F^{\mathrm{in},L} \times h^{\mathrm{in},L} + F^{\mathrm{in},V} \times h^{\mathrm{in},V} - \\ & F^{\mathrm{out},L} \times h^{\mathrm{out},L} - F^{\mathrm{out},V} \times h^{\mathrm{out},V} + Q - \\ & \sum_{j=1}^{j=n_{rx}} f_{rx,j} \times \sum_{i=1}^{i=n_c} r_{i,j} \times \Delta^r H_j \end{aligned} \tag{A.2}$$

where U in J, h in J×mol^{-1}, Q in W, $\Delta^r H$ in J×mol^{-1}.

Molar holdup:

$$M_i = M^L \times x_i + M^V \times y_i, \qquad i \in \mathbb{Z}^{n_c} \tag{A.3}$$

Internal energy:

$$\mathrm{U} = M^L \times h^L + M^V \times h^V - P \times V_{\mathrm{tray}} \tag{A.4}$$

where V in m^3, P in Pa.

Heat duty:

$$Q = 0 \tag{A.5}$$

Normalization expressions:

$$\sum_{i=1}^{i=n_c} x_i = y_i = 1 \tag{A.6}$$

Phase equilibrium:

$$\Phi^L(T,P,x)_i \times x_i = \Phi^V(T,P,y)_i \times y_i, \qquad i \in \mathbb{Z}^{n_c} \tag{A.7}$$

Chemical reaction driving force:

$$g_j = f_g(\mathbf{x},T,P), \qquad j \in \mathbb{Z}^{n_{rx}} \tag{A.8}$$

Chemical reaction constant:

$$k_{f,j} = k_{0,j} \times e^{-\frac{E_a}{\mathcal{R}\times T}}, \qquad j \in \mathbb{Z}^{n_{rx}} \tag{A.9}$$

where k_f in mol×(s×eq$_{[H^+]}$)$^{-1}$, E_a in J×mol^{-1}, $\mathcal{R}$ is 8.31 J×(mol×K)$^{-1}$, T in K.

Chemical equilibrium constant:

$$\ln(K_{\mathrm{eq},j}) = c_1 + \frac{c_2}{T} + c_3 \times \ln(T) + c_4 \times T + c_5 \times T^2 + c_6 \times T^3, \qquad j \in \mathbb{Z}^{n_{rx}} \tag{A.10}$$

[†]The heat of reaction in the energy balance can be omitted if the standard heat of formation is used as reference value for the enthalpy computations.

Chemical reaction rate:

$$r_{i,j} = \nu_{i,j} \times k_{f,j} \times g_j \times m_{\text{cat}}, \qquad i \in \mathbb{Z}^{n_c}, j \in \mathbb{Z}^{n_{rx}} \tag{A.11}$$

where m_{cat} in $\text{eq}_{[H^+]}$.

Tray reactivity:

$$f_{rx,j} = \begin{cases} 1 & : \quad \text{if reactive tray,} \quad j \in \mathbb{Z}^{n_{rx}} \\ 0 & : \quad \text{if nonreactive tray,} \quad j \in \mathbb{Z}^{n_{rx}} \end{cases} \tag{A.12}$$

Liquid outflow (Francis weir formula)

$$F^{\text{out},L} = 1.54 \times \text{level}_{\text{downc}} \times \max((\text{level}_{\text{tray}} - \beta_w \times ht_{\text{weir}}), 0)^{1.5} \times \rho_m^L, \quad \beta_w \in [0,1] \tag{A.13}$$

where $\text{level}_{\text{downc}}$, $\text{level}_{\text{tray}}$, ht_{weir} in m, ρ_m in $\text{kg} \times \text{m}^{-3}$.

Vapor inflow:

$$F^{\text{in},V} = \alpha_v \times \rho^V \times \sqrt{\max(\psi, 0) \frac{\rho_m^L}{\rho_m^V}} \tag{A.14}$$

$$\psi = \frac{\Delta P}{\rho_m^L \times g \times 1 \cdot 10^{-3}} - \text{level}_{\text{tray}} \times 1 \cdot 10^3 - \frac{12.5 \times 1 \cdot 10^3}{{\rho_m}^L} \tag{A.15}$$

$$\alpha_v = \frac{c_0 \times A_{\text{holes}}}{\sqrt{51}} \tag{A.16}$$

where ΔP in Pa, ρ in $\text{mol} \times \text{m}^{-3}$, $\text{level}_{\text{tray}}$ in mm, A_{holes} in m^2, $c_0 \approx 0.8$.

Pressure drop:

$$P^{\text{in},V} - P = (-\Delta P) \tag{A.17}$$

Geometry constraints:

$$V_{\text{tray}} = \frac{M^L}{\rho^L} + \frac{M^V}{\rho^V} \tag{A.18}$$

$$\text{level}_{\text{tray}} = \frac{M^L}{\rho^L \times A_{\text{tray}}} \tag{A.19}$$

where $\text{level}_{\text{tray}}$ in m, A_{tray} in m^2.

A.1.2 Block Model: PI Controller

Controller input:

$$InS = SP - e \tag{A.20}$$

Controller output:

$$OuS = Bias + K(e + \frac{\int_0^t e \times dt}{\tau_c}) \tag{A.21}$$

A.1.3 Block Model: Condenser

Component molar balance:

$$\frac{dM_i}{dt} = F^{\text{in},V} \times y_i^{\text{in}} - (F^{D,L} + F^{R,L}) \times x_i, \qquad i \in \mathbb{Z}^{n_c} \tag{A.22}$$

Energy balance:

$$\frac{d\text{U}}{dt} = F^{\text{in},V} \times h^{\text{in},V} - (F^{D,L} \times h^{D,L} + F^{R,L} \times h^{R,L}) - Q_{\text{cond}} \tag{A.23}$$

Molar holdup:

$$M_i = M^L \times x_i + M^V \times y_i, \qquad i \in \mathbb{Z}^{n_c} \tag{A.24}$$

Internal energy:

$$\text{U} = M^L \times h^L + M^V \times h^V - P \times V_{\text{cond}} \tag{A.25}$$

Reflux ratio:

$$RR = \frac{F^{R,L}}{F^{D,L}} \tag{A.26}$$

Heat duty:

$$Q_{\text{cond}} = F^{\text{cool}} \times Cp^{\text{cool}} \times MW^{\text{cool}} \times (T^{\text{out,cool}} - T^{\text{in,cool}}) \tag{A.27}$$

where Cp in $\text{J}\times(\text{g}\times\text{K})^{-1}$, MW in $\text{g}\times\text{mol}^{-1}$.

Heat transfer:

$$Q_{\text{cond}} = U_{\text{cond}}^{HX} \times A_{\text{cond}} \times \Delta T_{lm,\text{cond}} \tag{A.28}$$

where U^{HX} in $\text{W}\times(\text{m}^2\times\text{K})^{-1}$, A in m^2, ΔT_{lm} in K.

Logarithmic mean temperature difference:

$$\Delta T_{lm,\text{cond}} = \frac{(T^{\text{in}} - T^{\text{out,cool}}) - (T - T^{\text{in,cool}})}{\ln \frac{T^{\text{in}} - T^{\text{out,cool}}}{T - T^{\text{in,cool}}}} \tag{A.29}$$

Normalization expressions:

$$\sum_{i=1}^{i=n_c} x_i = y_i = 1 \tag{A.30}$$

Phase equilibrium:

$$\Phi^L(T, P, x)_i \times x_i = \Phi^V(T, P, y)_i \times y_i, \qquad i \in \mathbb{Z}^{n_c} \tag{A.31}$$

Pressure drop:

$$(-\Delta P) = \frac{f_{fr} \times \times MW^{\text{feed}} \times (F^{\text{in},V})^2}{\rho^{\text{feed}} \times A^2_{\text{total-tube,cond}}} \tag{A.32}$$

$$P^{\text{in}} = P + (-\Delta P) \tag{A.33}$$

$$f_{fr} = 8 \times f_{pd} \times (\text{length}_{\text{tube}}/d_i) + 2.5 \tag{A.34}$$

where $A_{\text{total-tube,cond}}$ equals $n_{\text{tubes}}(\pi \times d_i^2 \times 4^{-1})$, d_i in m, $\text{length}_{\text{tube}}$ in m, $f_{pd} \approx 3.5{\cdot}10^{-3}$.

Geometry constraints:

$$V_{\text{cond}} = \frac{M^L}{\rho^L} + \frac{M^V}{\rho^V} \tag{A.35}$$

$$\text{level}_{\text{cond}} = \frac{M^L}{\rho^L \times A_{\text{cond}}} \tag{A.36}$$

A.1.4 Block Model: Reboiler

Component molar balance:

$$\frac{dM_i}{dt} = F^{\text{in},L} \times x_i^{\text{in}} - (F^{\text{out},L} \times x_i + F^{\text{out},V} \times y_i), \qquad i \in \mathbb{Z}^{n_c} \tag{A.37}$$

Energy balance:

$$\frac{d\text{U}}{dt} = F^{\text{in},L} \times h^{\text{in},L} - (F^{\text{out},L} \times h^L + F^{\text{out},V} \times h^V) + Q_{\text{reb}} \tag{A.38}$$

Molar holdup:

$$M_i = M^L \times x_i + M^V \times y_i, \qquad i \in \mathbb{Z}^{n_c} \tag{A.39}$$

Internal energy:

$$\text{U} = M^L \times h^L + M^V \times h^V - P \times V_{\text{reb}} \tag{A.40}$$

Heat duty:

$$Q_{\text{reb}} = F^{\text{heat}} \times (h^{\text{in,heat}} - h^{\text{heat}}) \tag{A.41}$$

Heat transfer:

$$Q_{\text{reb}} = U_{\text{reb}}^{HX} \times A_{\text{reb}} \times \Delta T_{lm,\text{reb}} \tag{A.42}$$

Logarithmic mean temperature difference:

$$\Delta T_{lm,\text{reb}} = \frac{T^{\text{in,heat}} - T^{\text{heat}}}{\ln \frac{|T^{\text{in,heat}} - T|}{|T^{\text{heat}} - T| + \varepsilon_{\Delta T_{lm}}}} \tag{A.43}$$

where $\varepsilon_{\Delta T_{lm}}$ in K.

Normalization expressions:

$$\sum_{i=1}^{i=n_c} x_i = y_i = 1 \tag{A.44}$$

Phase equilibrium:

$$\Phi^L(T,P,x)_i \times x_i = \Phi^V(T,P,y)_i \times y_i, \qquad i \in \mathbb{Z}^{n_c} \tag{A.45}$$

Geometry constraints:

$$V_{\text{reb}} = \frac{M^L}{\rho^L} + \frac{M^V}{\rho^V} \tag{A.46}$$

$$\text{level}_{\text{reb}} = \frac{M^L}{\rho^L \times A_{\text{reb}}} \tag{A.47}$$

A.1.5 Block Model: Physical Properties

A detailed description of the calculation of physical properties and thermodynamic model is given in tables B.3 and B.1 in appendix B.

Molar enthalpy:

$$h^{(\alpha)} = f_h(T,P,\mathbf{z}^{(\alpha)}) \tag{A.48}$$

Thermodynamic model:

$$\Phi^{(\alpha)} = f_\Phi(T,P,\mathbf{z}^{(\alpha)}), \qquad i \in \mathbb{Z}^{n_c} \tag{A.49}$$

Molar density:

$$\rho^{(\alpha)} = f_\rho(T,P,\mathbf{z}^{(\alpha)}) \tag{A.50}$$

Mass density:

$${\rho_m}^{(\alpha)} = f_{\rho_m}(T,P,\mathbf{z}^{(\alpha)}) \tag{A.51}$$

Molecular weight:

$$MW^{(\alpha)} = f_{MW}(\mathbf{z}^{(\alpha)}) \tag{A.52}$$

Component vapor pressure:

$$p_i^0 = f_{p_i}(T), \qquad i \in \mathbb{Z}^{n_c} \tag{A.53}$$

where p_i^0 in Pa.

A.1.6 Block Connectivities

Trays connections:

$$(F,x,P,T,h)_{j}^{\text{out},L} = (F,x,P,T,h)_{j+1}^{\text{in},L}, \qquad j \in [1, n_t - 1] \tag{A.54}$$

$$(F,y,P,T,h)_{j-1}^{\text{out},V} = (F,y,P,T,h)_{j}^{\text{in},V}, \qquad j \in [2, n_t] \tag{A.55}$$

$$(F,z,P,T,h)_{j}^{\text{feed}} = (F,z,P,T,h)^{\text{in}}, \qquad j \in \mathbb{Z}^{n_t} \tag{A.56}$$

$$\tag{A.57}$$

Internal connections:

$$(F,x,P,T,h)_{n_t}^{\text{out},L} = (F,x,P,T,h)_{\text{reb}}^{\text{in},L} \tag{A.58}$$

$$(F,x,P,T,h)_{\text{reb}}^{\text{out},L} = (F,x,P,T,h)^{B,L} \tag{A.59}$$

$$(F,y,P,T,h)_{\text{reb}}^{\text{out},V} = (F,y,P,T,h)_{n_t}^{\text{in},V} \tag{A.60}$$

$$(F,y,P,T,h)_{1}^{\text{out},V} = (F,y,P,T,h)_{\text{cond}}^{\text{in},V} \tag{A.61}$$

$$(F,x,P,T,h)_{\text{cond}}^{D,L} = (F,x,P,T,h)^{D,L} \tag{A.62}$$

$$(F,x,P,T,h)_{\text{cond}}^{R,L} = (F,x,P,T,h)_{1}^{\text{in},L} \tag{A.63}$$

A.1.7 Design Block

Column area:

$$4 \times A_{\text{col}} = \pi \times D_{\text{col}}^2 \tag{A.64}$$

where D_{col} in m.

Active area:

$$A_{active} = 0.9 \times A_{\text{col}} \tag{A.65}$$

Holes area:

$$A_{\text{holes}} = 0.1 \times A_{\text{active}} \tag{A.66}$$

Downcomer length:

$$\text{level}_{\text{downc}} = 0.6 \times D_{\text{col}} \tag{A.67}$$

Flooding velocity:

$$K_{\text{flood}} = -0.171 \times ht_{\text{space}}^2 + 0.27 \times ht_{\text{space}} - 0.047 \tag{A.68}$$

$$u_{\text{flood}} = K_{\text{flood}} \times \sqrt{\frac{\rho^L - \rho^V}{\rho^V}} \tag{A.69}$$

where ht_{space} in m, u in m $\times \text{s}^{-1}$.

Minimum column diameter:

$$D_{\text{col}} = \sqrt{\frac{4 \times F^V}{\pi \times u_{\text{flood}} \times f_{\text{flood}} \times \rho^V}} \times \frac{1}{\sqrt{0.9}} \tag{A.70}$$

where $f_{\text{flood}} \approx 0.8 - 0.85$.

A.1.8 Economics Block

Capital costs:

$$c_{\text{shell}} = \frac{\text{MSI} \times 101.9}{280 \times \text{POT}_{\text{shell}}} \times (D_{\text{col}} \times f_{m2ft})^{1.066} \times (ht_{\text{col}} \times f_{m2ft})^{0.802} \times (218 + F_c) \times F_{fac} \tag{A.71}$$

$$c_{\text{trays}} = \frac{\text{MSI} \times 4.7}{280 \times \text{POT}_{\text{trays}}} \times (D_{\text{col}} \times f_{m2ft})^{1.55} \times (ht_{\text{stack}} \times f_{m2ft}) \times F_c \times F_{ac} \tag{A.72}$$

$$c_{\text{cond}} = \frac{\text{MSI} \times 101.3}{280 \times \text{POT}_{\text{cond}}} \times (A_{\text{cond}} \times f_{m2ft}^2)^{0.65} \times F_c \times F_{fac} \tag{A.73}$$

$$c_{\text{reb}} = \frac{\text{MSI} \times 101.3}{280 \times \text{POT}_{\text{reb}}} \times (A_{\text{reb}} \times f_{m2ft}^2)^{0.65} \times F_c \times F_{fac} \tag{A.74}$$

where c in euros$\times$y^{-1}, POT in years, ht in m.

Utility costs:

$$c_{\text{heat}} = F^{\text{heat}} \times PU_{\text{heat}} \times f_{s2y} \times f_{mol2kg} \tag{A.75}$$

$$c_{\text{cool}} = F^{\text{cool}} \times PU_{\text{cool}} \times f_{s2y} \times f_{mol2kg} \tag{A.76}$$

$$c_{\text{cat}} = \frac{m_{\text{cat}} \times PU_{\text{cat}}}{\text{POT}_{\text{cat}}} \tag{A.77}$$

$$c_{\text{raw-materials},i} = F^{\text{feed}} \times z_i^{\text{feed}} \times PU_{\text{raw-materials},i} \times f_{s2y} \times f_{mol2kg} \tag{A.78}$$

where PU in euros$\times$unit^{-1}, $i \in \mathbb{Z}^{n_c}$.

Total cost:

$$c_{\text{capital}} = c_{\text{shell}} + c_{\text{trays}} + c_{\text{cond}} + c_{\text{reb}} \tag{A.79}$$

$$c_{\text{operational}} = c_{\text{heat}} + c_{\text{cool}} + c_{\text{cat}} + \sum_{i=1}^{i=n_c} c_{\text{raw-materials},i} \tag{A.80}$$

$$c_{\text{total}} = \text{TAC} = c_{\text{capital}} + c_{\text{operational}} \tag{A.81}$$

A.2 Degree of Freedom Analysis

Table A.1. Degree of freedom analysis for the spatial and control design of a RD unit: relevant variables.

Variable	**Tray**	**Condenser**	**Reboiler**	**Column**
F^{feed}	n_t	-	-	-
z_i^{feed}	$n_t \times n_c$	-	-	-
P^{feed}	n_t	-	-	-
T^{feed}	n_t	-	-	-
h^{feed}	n_t	-	-	-
$F^{\text{in},(\alpha)}$	$2 \times n_t$	1	1	-
x_i^{in}	$n_t \times n_c$	-	n_c	-
y_i^{in}	$n_t \times n_c$	n_c	-	-
$T^{\text{in},(\alpha)}$	$2 \times n_t$	1	1	-
$P^{\text{in},(\alpha)}$	$2 \times n_t$	1	1	-
$h^{\text{in},(\alpha)}$	$2 \times n_t$	1	1	-
M_i	$n_t \times n_c$	n_c	n_c	-
$M^{(\alpha)}$	$2 \times n_t$	2	2	-
U	n_t	1	1	-
$F^{\text{out},(\alpha)}$	$2 \times n_t$	1	2	-
x_i	$n_t \times n_c$	n_c	n_c	-
y_i	$n_t \times n_c$	n_c	n_c	-
T	n_t	1	1	-
P	n_t	1	1	-
$h^{(\alpha)}$	$2 \times n_t$	2	2	-
ΔP	n_t	1	-	-
$r_{i,j}$	$n_t \times n_c \times n_{rx}$	-	-	-
g_j	$n_{rx} \times n_t$	-	-	-
$k_{eq,j}$	$n_{rx} \times n_t$	-	-	-
$k_{f,j}$	$n_{rx} \times n_t$	-	-	-
level	n_t	1	1	-
D_{col}	n_t	-	-	-
RR	-	1	-	-
A	-	1	1	-
$F^{utility}$	-	1	1	-
$LMTD$	-	1	1	-
$T^{\text{out,utility}}$	-	1	1	-
Q	n_t	1	1	-
c_{capital}	-	-	-	1
$c_{\text{operationa}}$	-	-	-	1
c_{total}	-	-	-	1
TOTAL	$\mathcal{A}$	$\mathcal{B}$	$\mathcal{C}$	$\mathcal{D}$

$\mathcal{A} = \mathbf{n_t(25 + 3n_{rx} + 6n_c + n_c \times n_{rx})}$
$\mathcal{B} = \mathbf{4n_c + 20}$
$\mathcal{C} = \mathbf{4n_c + 19}$
$\mathcal{D} = \mathbf{3}$

Appendix A

Table A.2. Degree of freedom analysis for the spatial and control design: relevant expressions. **Remarks:** figures in square brackets refer to the corresponding expression listed in the mathematical model (*cf.* section §A.1); the number of phases (α) is set to a value of 2.

Expression	**Tray**	**Condenser**	**Reboiler**	**Column**
Component molar balance	$n_t \times n_c$ [A.1]	n_c [A.22]	n_c [A.37]	-
Energy balance	n_t [A.2]	1 [A.23]	1 [A.38]	-
Molar holdup	$n_t \times n_c$ [A.3]	n_c [A.24]	n_c [A.39]	-
Internal energy	n_t [A.4]	1 [A.25]	1 [A.40]	-
Heat duty	n_t [A.5]	1 [A.27]	1 [A.41]	-
Heat transfer	-	1 [A.28]	1 [A.42]	-
LMTD	-	1 [A.29]	1 [A.43]	-
Normalization	$2 \times n_t$ [A.6]	2 [A.30]	2 [A.44]	-
Phase equilibrium	$n_t \times n_c$ [A.7]	n_c [A.31]	n_c [A.45]	-
Enthalpy	$2 \times n_t$ [A.48]	2 [A.48]	2 [A.48]	-
Chem. driving force	$n_{rx} \times n_t$ [A.8]	-	-	-
Chem. rx. constant	$n_{rx} \times n_t$ [A.9]	-	-	-
Chem. equi. constant	$n_{rx} \times n_t$ [A.10]	-	-	-
Chem. rx. rate	$n_t \times n_c \times n_{rx}$ [A.11]	-	-	-
Liquid outflow	n_t [A.13]	-	-	-
Vapor inflow	n_t [A.14]	1[A.32]	-	-
Pressure drop	n_t [A.17]	1 [A.32]	-	-
Geometry: volume	n_t [A.18]	1 [A.35]	1 [A.46]	-
Geometry: level	n_t [A.19]	1 [A.36]	1 [A.47]	-
Tray connectivity	$2(n_t - 1)(n_c + 4)$[A.54]	-	-	-
Internal connectivity	-	-	-	$4(n_c + 4)$[A.58]
Costs	-	-	-	3[A.79]
TOTAL	$\mathcal{F}$	$\mathcal{G}$	$\mathcal{H}$	$\mathcal{I}$

$F = \mathbf{n_t(20 + 5n_c) + 3n_{rx} \times n_t - 2n_c + n_{rx} \times n_c \times n_t - 8}$
$\mathcal{G} = \mathbf{3n_c + 13}$
$\mathcal{H} = \mathbf{3n_c + 11}$
$\mathcal{I} = \mathbf{4n_c + 19}$

Table A.3. Degree of freedom analysis: results

Parameter	**Number of variables or equations**
Relevant variables	$n_t(25 + 6n_c + 3n_{rx} + n_{rx} \times n_c) + 8n_c + 42$
$\mathcal{X} = \mathcal{A} + \mathcal{B} + \mathcal{C} + \mathcal{D}$	
Model equations	$n_t(20 + 5n_c + 3n_{rx} + +n_{rx} \times n_c) + 8n_c + 35$
$\mathcal{Y} = \mathcal{F} + \mathcal{G} + \mathcal{H} + \mathcal{I}$	
Degrees of freedom	$5n_t + n_t \times n_c + 7$
$\mathcal{DF} = \mathcal{X} - \mathcal{Y}$	
Input variables	$n_t \times F^{\text{feed,L}}$
	$n_t \times P^{\text{feed}}$
	$n_t \times T^{\text{feed}}$
	$n_t \times h^{\text{feed,L}}$
	$n_t \times n_c \times z_i^{\text{feed,L}}$
Degrees of freedom left	$n_t + 7$
Remaining variables to fix	
Spatial variables	$n_t \times D_{\text{col}}$
	A_{cond}
	A_{reb}
Operational variable	RR
Manipulated variables	$F_{\text{cond}}^{\text{out},L}$
	$F_{\text{reb}}^{\text{out},L}$
	F^{cool}
	F^{heat}

B

Synthesis of Methyl *t*-butyl ether Features of the System

B.1 Motivation

Although methyl *t*-butyl ether (MTBE) was first synthesized in 1904, it was only during the World War II that studies revealed its outstanding qualities as a high-octane fuel enhancer (Peters *et al.*, 2000). Hence in the early 1990s MTBE was considered one of the most promising clean burning octane enhancers, being expected to be the second largest organic chemical produced in United States by the beginning of the second millennium (Kirk-Othmer, 1994). Furthermore, its interested was promoted even further by the increased demand for premium-grade fuels and the elimination of lead gasolines.

Lately, however, MTBE harmlessness has been questioned as it has been found in drinking water supplies in several American states. In the state of California, for instance, MTBE addition in reformulated gasolines has been already banned since the late 90s. Although similar phase-out scenarios are expected in the USA during the years to come, a growth in the outside-USA markets could offset lost market demand. This fact is evident by recent joint ventures and capacity acquisitions. Roughly speaking, nowadays more than 140 MTBE plants are operating, representing a total installed capacity of $\sim 20{\cdot}10^6$ t/y (Peters *et al.*, 2000).

Table B.1. Typical compositions of C_4 streams from FCC (Peters *et al.*, 2000)

	Weight fraction
Isobutane	0.36
nC_4	0.13
iC_4	0.15
1-butene	0.12
cis-2-butene	0.09
trans-2-butene	0.14
1,3-butadiene	0.003
balance	0.007

From a research point of view, MTBE synthesis via reactive distillation still represents a major development in the field and an open door to novel and innovative processes.

B.2 Description of the System

MTBE is produced from methanol (MeOH) and isobutene (iC_4) in an equilibrium-limited liquid-phase reaction (Jimenez *et al.*, 2001) catalyzed heterogeneously by bentonites, zeolites or strong acidic macroporous ion-exchange resins (*e.g.* Amberlyst 15), or homogeneously by sulfuric acid according to the following stoichiometry,

$$\underset{\text{isobutene}}{C_4H_8} + \underset{\text{methanol}}{CH_3OH} \rightleftharpoons \underset{\text{MTBE}}{C_5H_{12}O} \tag{B.1}$$

The iC_4 stream can be originated from several sources (Peters *et al.*, 2000): (*i*) as coproduct of butadiene production from steam cracker C_4 fractions, (*ii*) as product of selective hydrogenation of butadiene in mixed C_4 fractions from steam crackers (*iii*) as iC_4 in the C_4 fraction of FCC units (*iv*) as coproduct of the dehydrogenation of isobutane, and (*v*) as coproduct of dehydration of *t*-butanol.

In this research, the FCC source has been considered as feedstock for the MTBE production. This stream, which represents 29% of the MTBE production worldwide, contains a complete range of butanes and butenes, as can be seen in table B.1. For the sake of simplifying the study and provided that the reaction is highly selective for iC_4 all the organic components in the iC_4 stream are lumped together as inert nC_4 (Güttinger, 1998).

Conventional process. The conventional route in the synthesis of MTBE is described in detail in Kirk-Othmer (1994) and Peters *et al.* (2000). For instance, the Hüls-MTBE process (figure B.1) operates with a given molar excess of methanol on

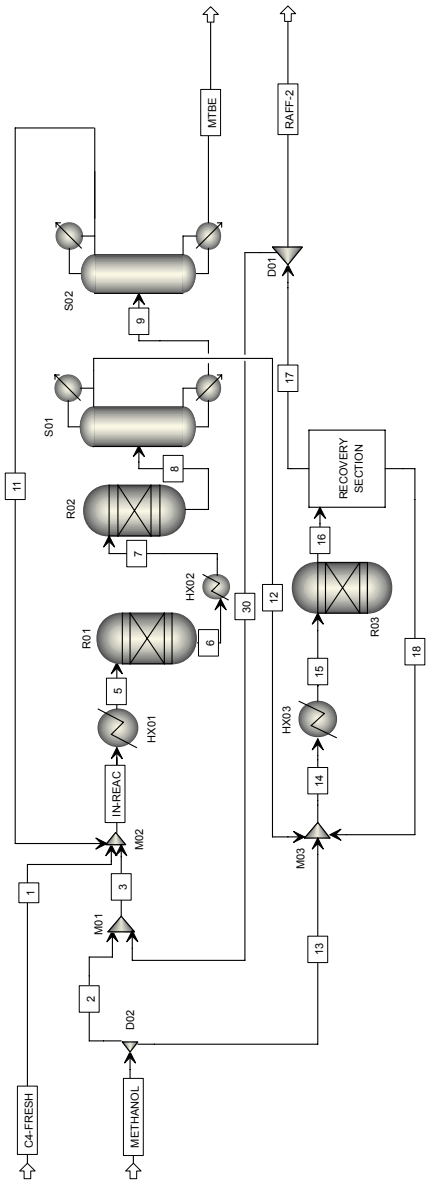

Figure B.1. Conventional route for the synthesis of MTBE: two-stage Hüls -MTBE process. **Legend:** R01: tubular reactor; R02-R03: adiabatic reactors; HX: heat exchanger; M: mixer; D: divider; S01-S02: distillation towers (adapted from Peters *et al.* (2000)).

a macroporous acidic ion exchanger (50-90 °C, 1-1.5·10^5 Pa). The reaction section is equipped with adiabatic reactors for the chosen FCC-C_4 feedstock. The iC_4 conversion reaches 85%. By simultaneous C_4 evaporation a final iC_4 conversion of $\sim$ 97% is achieved. The separation train can involve RD units, where the partly reacted mixture from the reaction section enters the RD column below the catalyst packing zone to ensure the separation of the high-boiling component MTBE from the feed stream. The catalyst packing is installed in the upper mid portion of the column with nonreactive separation sections above and below. The separation of the C_4 stream from the MTBE is affected by the azeotropy between MeOH and nC_4 (*cf.* section §2.4). An extraction train with water wash is required to completely remove the methanol from the C_4 stream. The recovered methanol is recycled to the reaction section.

B.3 Thermodynamic Model

In this study the $\gamma - \phi$ formulation (see explanatory note B.1) is used, in which the fugacities of each component in the vapor phase equal those in the liquid phase. This results is the following expression,

$$y_i \times \Phi_i \times P = x_i \times \gamma_i \times p_i^0, \qquad i \in [1, n]. \tag{B.2}$$

The vapor phase is assumed to behave ideally ($\Phi_i = 1$), whereas the liquid-phase is modelled using Wilson activity coefficient equation. This thermodynamic method is particularly accurate for multicomponent mixtures that do not form two liquids (Kooijman and Taylor, 2000) and is given by the following set of algebraic equations,

$$\ln(\Lambda_{ij}) = a_{ij} + b_{ij}/T, \tag{B.9}$$

$$S_{W,i} = \sum_{j=1}^{j=n_c} x_j \times \Lambda_{ij}, \tag{B.10}$$

$$\ln(\gamma_i) = 1 - \ln(S_{W,i}) - \sum_{k=1}^{k=n_c} \frac{x_k \times \Lambda_{ki}}{S_{W,k}}, \tag{B.11}$$

where Λ_{ij} is the binary interaction parameter for the pair $i, j \in \mathbb{Z}^{n_c}$ and a_{ij} and b_{ij} are model parameters (table B.2).

B.4 Physical Properties, Reaction Equilibrium and Kinetics

The models that predict the physical properties of the iC_4-MeOH-MTBE-inert system are given in tables B.3 and B.4. The reaction equilibrium and kinetics of MTBE synthesis have been subject of intensive research during the last decade (Colombo *et al.*, 1983;

$\gamma - \phi$ **thermodynamic model.** This method uses the definition of the fugacity coefficient (ϕ) and activity coefficient (γ) to describe the properties of the gas and liquid phase(s), respectively (Malanowski and Anderko, 1992). The computation of VL-equilibria is based on the condition of equality of intensive properties in the coexisting phases. In terms of fugacities, the equality is given by,

$$f_i^L = f_i^V, \tag{B.3}$$

where $f_i^{(\alpha)}$ is the fugacity of component i in phase (α).

The vapor fugacity can be written in terms of the fugacity coefficient *phi*,

$$f_i^V = P \times y_i \times \phi_i. \tag{B.4}$$

Taking as reference state the pure liquid i at equilibrium temperature T and pressure P, the liquid phase fugacity f_i^L can be related to the activity coefficient γ_i by,

$$f_i^L = f_i^0(P) \times x_i \times \gamma_i, \tag{B.5}$$

where f_i^0 is the fugacity of the pure substance at pressure P, which can be expressed in terms of the fugacity coefficients of pure substances, ϕ_i^0 and the *Poynting correction factor*,

$$f_i^0(P) = p_i^0 \times \phi_i^0 \times e^{-\int_{p_i^0}^{P} \frac{v_i}{R \times T} dP}. \tag{B.6}$$

Replacing B.4 and B.5 into B.6 leads to the general VL-equilibrium condition,

$$P \times y_i \times \Phi_i = x_i \times \gamma_i \times p_i^0, \tag{B.7}$$

where the correction factor Φ_i accounts for the vapor phase nonideality and the difference between the equilibrium pressure and the pure component vapor pressure, p_i^0,

$$\Phi_i = \frac{\phi_i}{\phi_i^0} \times e^{\int_{p_i^0}^{P} \frac{v_i}{R \times T} dP}. \tag{B.8}$$

Note B.1. Phase equilibrium intermezzo: the $\gamma - \phi$ thermodynamic model

Table B.2. Wilson interaction parameters for the system iC$_4$-MeOH-MTBE-nC$_4$ at 11·10^5 Pa (Ung and Doherty, 1995*c*; Güttinger, 1998)

	iC$_4$	MeOH	MTBE	nC$_4$
		a_{ij} [-]		
iC$_4$	0.00000	-0.74200	0.24130	0.00000
MeOH	0.74200	0.00000	0.98330	0.81492
MTBE	-0.2413	-0.98330	0.0000	0.00000
nC$_4$	0.00000	-0.81492	0.00000	0.00000
		b_{ij} [K]		
iC$_4$	0.0000	-85.5447	30.2477	0.0000
MeOH	-1296.719	0.0000	-746.3971	-1149.280
MTBE	-136.6574	204.5029	0.0000	0.0000
nC$_4$	0.0000	-192.4019	0.0000	0.0000

Rehfinger and Hoffmann, 1990; Zhang and Datta, 1995; Izquierdo *et al.*, 1992; Thiel *et al.*, 2002). A brief description of the reported models for equilibrium and kinetics constants is given in tables B.5 and B.6, respectively.

Table B.3. Set of expressions used to predict relevant physical properties

Property	**Expression and nomenclature**
Molecular weight	$MW^{(\alpha)} = \sum_{i=1}^{i=n_c} MW_i \times z_i^{(\alpha)}$ MW is in g×mol^{-1} and $z^{(\alpha)}$ denotes molar fraction in the corresponding phase (α)
Vapour pressure	$\ln(p_i^0) = A_i + B_i/(T + C_i)$ p_i^0 is in Pa and A_i, B_i and C_i are model parameters of component $i \in \mathbb{Z}^{n_c}$, taken from (Güttinger, 1998) and listed in table B.4
Component enthalpy	$\Delta^v H_i = \mathcal{R} \times T_{c,i} \times (7.08 \times (1 - \frac{T}{T_{c,i}})^{0.354} + \cdots$ $\cdots + 10.95 \times \omega_i \times (1 - \frac{T}{T_{c,i}})^{0.456})$ $h_i^V = h_{f,i}^V + c_{pai} \times (T - T_{\text{ref}}) + \cdots$ $\cdots + \frac{c_{pbi}}{2} \times (T^2 - T_{\text{ref}}^2) + \cdots$ $\cdots + \frac{c_{pci}}{3} \times (T^3 - T_{\text{ref}}^3) + \cdots$ $\cdots + \frac{c_{pdi}}{4} \times (T^4 - T_{\text{ref}}^4)$ $h_i^L = h_i^V - \Delta^v H_i$ h is in J×mol^{-1}, T_c is the critical temperature, ω is the acentric factor and c_{pa}, c_{pb}, c_{pc} and c_{pd} are parameters listed in table B.4
Mixture enthalpy	$h^{(\alpha)} = \sum_{i=1}^{i=n_c} h_i^{(\alpha)} \times z_i^{(\alpha)}$ h is given in J×mol^{-1} and $z^{(\alpha)}$ denotes the corresponding molar fraction in phase (α)
Component molar density	$\rho_i^L \times T_{c,i} \times zr_i^{1+(1-\frac{T}{T_{c,i}})^{0.2857}} = \frac{P_{c,i}}{\mathcal{R}}$ $\frac{P}{\mathcal{R}} = \rho_i^V \times T$ ρ is given in mol×m^{-3}
Mixture molar density	$\rho^V = \sum_{i=1}^{i=n_c} \rho_i^V \times y_i$ $\frac{1}{\rho^L} = \sum_{i=1}^{i=n_c} \frac{x_i}{\rho_i^L}$ $\rho^{\text{feed}} = \sum_{i=1}^{i=n_c} \rho_i^{\text{feed}} \times z_i^{\text{feed}}$
Mixture mass density	$1000 \times \rho_m{}^{(\alpha)} = \rho^{(\alpha)} \times MW^{(\alpha)}$ ρ_m is in kg×m^{-3} and (α) denotes the corresponding phase

Table B.4. Parameters used for the estimation of physical properties in the synthesis of MTBE

Parameter	**Unit**	iC$_4$	MeOH	nC$_4$	MTBE
MW	g×mol^{-1}	56.11	32.01	58.12	88.15
P_c	Pa	40·10^5	80.9·10^5	38·10^5	33.7·10^5
T_c	K	417.9	513.15	425.18	497.14
ω	-	0.194	0.556	0.199	0.266059
c_{pa}	J×mol^{-1}×K^{-1}	16.05	21.15	9.487	2.534
c_{pb}	J×mol^{-1}×K^{-2}	0.2804	0.07092	0.3313	0.5136
c_{pc}	J×mol^{-1}×K^{-3}	-1.091·10^{-4}	2.587·10^{-5}	-1.1408·10^{-4}	-2.596·10^{-4}
c_{pd}	J×mol^{-1}×K^{-4}	9.098·10^{-9}	-2.852·10^{-8}	-2.822·10^{-9}	4.303·10^{-8}
h_f^V	J×mol^{-1}	-1.691·10^4	-2.013·10^5	-1.262·10^5	-2.931·10^5
zr	-	0.2728	001224	0.2730	0.26721
A	-	20.6556	23.49989	20.57070	20.71616
B	K	-2125.74886	-3643.31362	-2154.8973	-2571.58460
C	K	-33.16000	-33.43400	-34.42000	-48.40600

Table B.5. Temperature dependence of equilibrium constant in MTBE synthesis

$$\begin{aligned} \ln(K_{\text{eq}}) &= \alpha + \frac{\beta}{T} + \delta \times \ln(T) \\ \alpha &= -10.0982 \\ \beta &= 4254.0500 \\ \delta &= 0.2667 \end{aligned} \tag{B.12}$$

Source:
Güttinger (1998); Colombo *et al.* (1983)
Validity: homogeneous catalyst (*e.g.* sulfuric acid); UNIFAC model

---

$$\begin{aligned} \ln K_{\text{eq}} &= \ln K_{\text{eq},0} + \alpha(\frac{1}{T} - \frac{1}{T_0}) + \beta \times \ln(\frac{T}{T_0}) + \dot{\gamma} \times (T - T_0) + \\ &\quad +\delta \times (T^2 - T_0^2) + \epsilon \times (T^3 - T_0^3) + \phi \times (T^4 - T_0^4) \\ \alpha &= -1.49277 \cdot 10^3 \\ \beta &= -7.74002 \cdot 10^1 \\ \dot{\gamma} &= 5.07563 \cdot 10^{-1} \\ \delta &= -9.12739 \cdot 10^{-4} \\ \epsilon &= 1.10649 \cdot 10^{-6} \\ \phi &= -6.27996 \cdot 10^{-10} \\ T_0 &= 298.15\text{K} \\ K_{\text{eq},0} &= 284 \end{aligned} \tag{B.13}$$

Source:
Rehfinger and Hoffmann (1990); Thiel *et al.* (2002)
Validity: heterogeneous catalyst (Amberlyst 15)

$$\begin{aligned} \ln K_{\text{eq}} &= \ln k_{eq,0} + \alpha \times \frac{1}{T} + \beta \times \ln(T) + \gamma \times T + \\ &\quad \delta \times T^2 + \epsilon \times T^3 \\ \alpha &= -14634 \\ \beta &= -233 \\ \gamma &= 1.066 \\ \delta &= -1.077 \cdot 10^{-3} \\ \epsilon &= -5.306 \cdot 10^{-7} \\ \ln K_{\text{eq},0} &= 1144 \end{aligned} \tag{B.14}$$

Source:
Izquierdo *et al.* (1992)
Validity: heterogeneous catalyst (ion exchange resin Lewatit SPC 118 BG); low temperature (313K<T<353K)

Table B.6. Temperature dependence of kinetic constant in MTBE synthesis

$$
\begin{aligned}
k_f(T) &= k_f(T^*) \times e^{-\frac{E_a}{\mathcal{R}}\left(\frac{1}{T}-\frac{1}{T^*}\right)} \\
k_f(T^*) &= 243.8 \cdot 10^{-3}\ \text{mol} \times (\text{s} \times \text{eq}_{[H+]})^{-1} \\
E_a &= 92400\ \text{J} \times \text{mol}^{-1} \\
T^* &= 363\text{K}
\end{aligned}
\tag{B.15}
$$

Source: Rehfinger and Hoffmann (1990)
Validity: heterogeneous catalyst (Amberlyst 15)

$$
\begin{aligned}
k_f(T) &= k_f(T^*) \times e^{-\frac{E_a}{\mathcal{R}}\left(\frac{1}{T}-\frac{1}{T^*}\right)} \\
k_f(T^*) &= 15.5 \cdot 10^{-3}\ \text{mol} \times (\text{s} \times \text{eq}_{[H+]})^{-1} \\
E_a &= 92400\ \text{J} \times \text{mol}^{-1} \\
T^* &= 333.15\text{K}
\end{aligned}
\tag{B.16}
$$

Source: Thiel *et al.* (2002)
Validity: heterogeneous catalyst (Amberlyst 15)

$$
\begin{aligned}
k_f(T) &= k_f(T^*) \times e^{-\frac{E_a}{\mathcal{R}\times T}} \\
k_{f,0} &= 3.5714 \cdot 10^{12}\ \text{mol} \times (\text{s} \times \text{eq}_{[H+]})^{-1} \\
E_a &= 85400\ \text{J} \times \text{mol}^{-1}
\end{aligned}
\tag{B.17}
$$

Source: Izquierdo *et al.* (1992)
Validity: heterogeneous catalyst (ion exchange resin Lewatit SPC 118 BG); low temperature (313K$< T <$353K)

References

Agreda V. and Partin L. (1984). Reactive distillation process for the production of methyl acetate (US4435595). Patent. 1.2.1

Ajah A., Swinkels P.L.J. and Grievink J. (2004). Towards testing and validation of novel conceptual process design frameworks. *AIChE Symposium Series* 2004, 231–235. 9.5, B.4, B.4

Al-Arfaj M. and Luyben W. (2002*a*). Comparative control study of ideal and methyl acetate reactive distillation. *Chemical Engineering Science* 57, 5039–5050. 2.9.1.2, 2.9.1.2, 2.9.2

Al-Arfaj M. and Luyben W. (2002*b*). Design and control of an olefin metathesis reactive distillation column. *Chemical Engineering Science* 57 (2002), 715–733. 2.9.1.2

Alejski K. and Duprat F. (1996). Dynamic simulation of the multicomponent reactive distillation. *Chemical Engineering Science* 51 (18), 4237–4252. 7.3.1

Almeida-Rivera C.P. and Grievink J. (2001). Reactive distillation: On the development of an integrated design methodology. *Chemie Ingenieur Technik* 73 (6), 777–777. 3.5, †, 4.1, 4.5

Almeida-Rivera C.P. and Grievink J. (2002). Feasibility of equilibrium-controlled reactive distillation process: application of residue curve mapping. *Computer-Aided Chemical Engineering* 10, 151–156. 3.2.2, †

Almeida-Rivera C.P. and Grievink J. (2004). Feasibility of equilibrium-controlled reactive distillation process: application of residue curve mapping. *Computers and Chemical Engineering* 28 (1-2), 17–25. 3.2.2, †

Almeida-Rivera C.P., Swinkels P.L.J. and Grievink J. (2003). Multilevel modelling of spatial structures in reactive distillation units. *Computer-Aided Chemical Engineering* 15, 696–701. †

Almeida-Rivera C.P., Swinkels P.L.J. and Grievink J. (2004*a*). Designing reactive distillation processes: present and future. *Computers and Chemical Engineering* 28 (10), 1997–2020. †, 3.5, †, 4.1, 4.5, 5.1

Almeida-Rivera C.P., Swinkels P.L.J. and Grievink J. (2004*b*). Economics and exergy efficiency in the conceptual design of reactive distillation processes. *AIChE Symposium Series* 2004, 237–240. 1.3.2, †

Backhaus A.A. (1921*a*). Apparatus for the manufacture of esters (US1.400.849.20.12). Patent. 1.2.1

Backhaus A.A. (1921*b*). Apparatus for the manufacture of esters (US1.400.850.20.12). Patent. 1.2.1

Backhaus A.A. (1921*c*). Apparatus for the manufacture of esters (US1.400.851.20.12). Patent. 1.2.1

References

Balakotaiah V. and Luss D. (1984). Global analysis of the multiplicity features of multi-reaction lumped-parameter systems. *Chemical Engineering Science* 39, 865–881. 7.2.3

Bansal V. (2000). *Analysis, design and control optimization of process systems under uncertainty*. Thesis/dissertation, University of London, Imperial College of Science, Technology and Medicine. 3.3, 3.3.3, 3.3.3, 3.3, 6.2, 6.2.1, 6.2.2

Bansal V., Perkins J., Pistikopoulos E., Ross R. and van Schijndel J. (2000). Simultaneous design and control optimisation under uncertainty. *Computers and Chemical Engineering* 24, 261–266. 3.3, 3.3.3, 3.3.3, 3.3, 6.2, 6.2.1, 6.2.2, 6.2.2, 6.2.3.1, 6.3

Bansal V., Sakizlis V., Ross R., Perkins J. and Pistikopoulos E. (2003). New algorithms for mixed-integer dynamic optimization. *Computers and Chemical Engineering* 27, 647–668. 6.3

Barbosa D. and Doherty M. (1988*a*). Design and minimum-reflux calculations for single-feed multicomponent reactive distillation columns. *Chemical Engineering Science* 43 (7), 1523–1537. 2.4, 2.4, 2.4, 3.2.2, 3.2.4, 3.2.4

Barbosa D. and Doherty M.F. (1987*a*). A new set of composition variables for the representation of reactive-phase diagrams. *Proceedings of the Royal Society of London Series A Mathematical Physical and Engineering Sciences* 413, 459–464. 2.4, 3.2.4, 3.2.4, 3.2.4

Barbosa D. and Doherty M.F. (1987*b*). Theory of phase diagrams and azeotropic conditions for two-phase reactive systems. *Proceedings of the Royal Society of London Series A Mathematical Physical and Engineering Sciences* 413, 443–458. 2.4, 2.4, 3.2.4, 3.2.4

Barbosa D. and Doherty M.F. (1988*b*). The simple distillation of homogeneous reactive mixtures. *Chemical Engineering Science* 43 (3), 541–550. 3.2.2, 3.2.4, 3.2.4

Baur R., Higler A., Taylor R. and Krishna R. (2000). Comparison of equilibrium stage and nonequilibrium stage models for reactive distillation. *Chemical Engineering Journal* 76, 33–47. 2.1, 2.6, 2.9.3, 4.3

Baur R. and Krishna R. (2002). Hardware selection and design aspects for reactive distillation columns. A case study on synthesis of TAME. *Chemical Engineering and Processing* 41, 445–462. 2.6, 2.9.3, 4.3

Baur R. and Krishna R. (2003). Distillation column with reactive pump arounds: an alternative to reactive distillation. *Catalysis Today* 79-80, 113–123. 4.2, 4.3

Baur R., Taylor R. and Krishna R. (2001*a*). Dynamic behaviour of reactive distillation columns described by a nonequilibrium stage model. *Chemical Engineering Science* 56, 2085–2102. 2.9.1.2, 2.9.1.2, 2.9.3, 4.3

Baur R., Taylor R. and Krishna R. (2001*b*). Dynamic behaviour of reactive distillation tray columns described with a nonequilibrium cell model. *Chemical Engineering Science* 56, 1721–1729. 2.9.3, 4.3, 7.2.1

Baur R., Taylor R. and Krishna R. (2001*c*). Dynamics of a reactive distillation column for TAME synthesis described by a nonequilibrium stage model. *Computer-Aided Chemical Engineering* 9, 93–98. 2.9.3, 4.3, 7.2.9, 7.4

Baur R., Taylor R. and Krishna R. (2001*d*). Influence of column hardware on the performance of reactive distillation columns. *Catalysis Today* 66, 225–232. 2.6, 2.9.3

References

Baur R., Taylor R. and Krishna R. (2003). Bifurcation analysis for TAME synthesis in a reactive distillation column: Comparison of pseudo-homogeneous and heterogeneous reaction kinetics models. *Chemical Engineering and Processing* 42, 211–221. 2.9, 2.9.1.2, 2.9.1.2, 2.9.2, 2.9.3

Bedeaux D. and Kjelstrup S. (2004). Irreversible thermodynamics - a tool to describe phase transitions far from global equilibrium. *Chemical Engineering Science* 59, 109–118. 8.2.1

Bedenik M.I., Pahor B. and Kravanja Z. (2001). Synthesis of reactor/separator networks by the combined MINLP/analysis approach. *Computer-Aided Chemical Engineering* 9, 59–64. 3.3

Bermingham S. (2003). *A design procedure and predictive models for solution crystallisation processes*. Thesis/dissertation, Delft University of Technology. 4.2

Bessling B., Loning J.M., Ohligschlager A., Schembecker G. and Sundmacher K. (1998). Investigations on the synthesis of methyl acetate in a heterogeneous reactive distillation process. *Chemical Engineering and Technology* 21 (5), 393–400. 3.2.6, 3.6

Bessling B., Schembecker G. and Simmrock K.H. (1997). Design of processes with reactive distillation line diagrams. *Industrial and Engineering Chemistry Research* 36, 3032–3042. 2.6, 2.6, 3.2.6, 3.1, 3.3, 3.8

Biegler L., Grossman I. and Westerberg A. (1997). *Systematic methods of chemical process design*. Prentice Hall, New York. 2.2, 4.3, 4.2

Bildea C.S. and Dimian A. (1999). Singularity theory approach to ideal binary distillation. *AIChE Journal* 45 (12), 2662–2666. 2.9, 2.9.1.1, 7.2.3

Bird B., Stewart W. and Lightfoot E. (2003). *Transport phenomena*. John Wiley and Sons, Inc., New York. 8.2.1, 8.2.1, 8.2.1

Bisowarno B.H. and Tade M.O. (2000). Dynamic simulation of startup in ethyl tert-butyl ether reactive distillation with input multiplicity. *Process Design and Control* 39, 1950–1954. 2.9.1.2, 2.9.1.2, 2.9.2

Buzad G. and Doherty M. (1994). Design of three-component kinetically controlled reactive distillation columns using fixed-point methods. *Chemical Engineering Science* 49 (12), 1947–1963. 3.2.4, 3.2.4, 3.2.4, 3.2.4

Buzad G. and Doherty M. (1995). New tools for the design of kinetically controlled reactive distillation columns for ternary mixtures. *Computers and Chemical Engineering* 19 (4), 395–408. 1.3.1, 3.2.4, 3.2.4, 4.2, 5.1

Cardoso M.F., Salcedo R.L., de Azevedo S.F. and Barbosa D. (2000). Optimization of reactive distillation processes with simulated annealing. *Chemical Engineering Science* 55, 5059–5078. 3.3, 3.3.1

Chadda N., Malone M.F. and Doherty M. (2003). Feasibility and synthesis of hybrid reactive distillation systems. *AIChE Journal* 48 (12), 2754–2768. 3.2.5

Chen F., Huss R.S., Doherty M. and Malone M.F. (2002). Multiple steady states in reactive distillation: kinetic effects. *Computers and Chemical Engineering* 26, 81–93. 2.1, 2.5, 2.9, 2.9.1.1, 2.9.1.2, 2.9.1.2, 7.2.1

Ciric A. and Gu D. (1994). Synthesis of nonequilibrium reactive distillation processes by MINLP optimization. *AIChE Journal* 40 (9), 1479–1487. 2.9.3, 2.10, 3.2.4, 3.2.4, 3.3, 3.3.1, 4.3

References

Ciric A. and Miao P. (1994). Steady state multiplicites in a ethylene glycol reactive distillation column. *Industrial and Engineering Chemistry Research* 33, 2738–2748. 2.9, 2.9.1.1, 2.9.2, 2.9.3, 3.3, 7.2.1, 7.2.8

Clark P. and Westerberg A. (1983). Optimization for design problems having more than one objective. *Computers and Chemical Engineering* 7 (4), 259–278. 1.3.2, 4.4, 8.3.4, 8.3.4

Colombo F., Cori L., Dalioro L. and Delogu P. (1983). Equilibrium constant for the methyl tert-butyl ether liquid phase synthesis by use of UNIFAC. *Industrial Engineering Chemistry Fundamentals* 22 (2), 219–223. B.4, B.5

Costa L. and Oliveira P. (2001). Evolutionary algorithms apporach to the solution of mixed integer non-linear programming problems. *Computers and Chemical Engineering* 25, 257–266. 3.3.1

Coulson J.M. and Richardson J.F. (1991). *Chemical engineering. Volume 6. Design*. BPCC Wheatons Ltd., London. 7.3.2.1

Dhooge A., Govaerts W., Kuznetsov Y., Mestrom W. and Riet A.M. (2003). cl-matcont: a continuation toolbox in Matlab. In: *Proceedings of the 2003 ACM symposium on Applied computing*, (161–166), ACM Press. 7.2.3

Doherty M. and Malone M.F. (2001). *Conceptual design of distillation systems*. McGraw-Hill, USA. 1.2.1, 2.1, 2.5

Doherty M.F. and Buzad G. (1992). Reactive distillation by design. *Trans. Institution of Chemical Engineers - Part A* 70, 448–458. 1.3.1, 2.4, 2.4, 2.4, 3.2.2, 3.2.4, 3.2.4, 3.2.4, 4.2, 4.3, 5.1

Douglas J. (1988). *Conceptual design of chemical process*. McGraw-Hill, USA. 1.3.1

Eldarsi H.S. and Douglas P.L. (1998). Methyl-tert butyl ether catalytic distillation column. Part I: multiple steady states. *Chemical Engineering Research and Design* 76, 509–516. 2.9.1.2

Espinosa J., Aguirre P., Frey T. and Stichlmair J. (1999). Analysis of finishing reactive distillation columns. *Industrial and Engineering Chemistry Research* 38 (1), 187–196. 3.2.2

Espinosa J., Aguirre P. and Perez G. (1996). Some aspects in the design of multicumponent reactive distillation columns with a reacting core: mixtures containing inerts. *Industrial and Engineering Chemistry Research* 35 (12), 4537–4549. 2.9.3, 3.2.2, 3.2.4, 3.2.4, 3.2.4

Fair J., Seibert F., Behrens M., Saraber P. and Olujic Z. (2000). Structured packing performance - experimental evaluation of two predictive models. *Industrial and Engineering Chemistry Research* 39, 1788–1796. 2.7.1, 2.7.1

Feinberg M. (1999). Recent results in optimal reactor synthesis via attainable theory. *Chemical Engineering Science* 54, 2535–2543. 3.2.3, 4.2

Fien G. and Liu Y. (1994). Heuristic synthesis and shortcut design of separation processes using residue curve maps: a review. *Industrial and Engineering Chemistry Research* 33, 2505–2522. 2.3, 3.2.2, 4.2, 5.3, 5.3, 5.3, 5.4, 5.4, 5.5.3, 5.6

Frass M. (2005). Begriffe der DIN 19226 - Regelung und Steuerung. Data File. 1.3.1

Frey T. and Stichlmair J. (1999*a*). Reactive azeotropes in kinetically controlled reactive distillation. *Trans. Institution of Chemical Engineers - Part A* 77 (7), 613–618. 2.3, 2.4, 2.4, 2.6

References

Frey T. and Stichlmair J. (1999*b*). Thermodynamic fundamentals of reactive distillation. *Chemical Engineering and Technology* 22 (1), 11–18. 2.3, 2.3, 2.2, 2.4, 2.3, 3.2.4, 3.3, 3.2.6

Frey T. and Stichlmair J. (2001). MINLP Optimization of reactive distillation columns. *Computer-Aided Chemical Engineering* 8, 115–120. 3.3, 3.3.1

Gadewar S.B., Chadda N., Malone M.F. and Doherty M. (2003). Feasibility and process alternatives for reactive distillation. In: *Reactive distillation. Status and future directions* (K. Sundmacher and A. Kienle, eds.), book chapter 6, (145–168), Wiley-VCH. 3.2.3, 3.2.5

Gehrke V. and Marquardt W. (1997). A singularity theory approach to the study of reactive distillation. *Computers and Chemical Engineering* 21 (SS), S1001–S1006. 2.9, 2.9.1.1, 7.2.3

Georgiadis M., Schenk M., Pistikopoulos E. and Gani R. (2002). The interactions of design, control and operability in reactive distillation systems. *Computers and Chemical Engineering* 26, 735–746. 3.3, 3.3.3, 3.3.3, 4.3, 6.2, 6.2.1, 6.2.3.1, 6.2.3.2

Giessler S., Danilov R.Y., Pisarenko R.Y., Serafimov L.A., Hasebe S. and Hashimoto I. (1998). Feasibility study of reactive distillation using the analysis of the statics. *Industrial and Engineering Chemistry Research* 37, 4375–4382. 2.9.3, 3.2.1, 3.2.1, 3.3

Giessler S., Danilov R.Y., Pisarenko R.Y., Serafimov L.A., Hasebe S. and Hashimoto I. (2001). Systematic structure generation for reactive distillation processes. *Computers and Chemical Engineering* 25, 49–60. 3.2.1

Giessler S., Danilov R.Y., Serafimov L.A., Hasebe S. and Hashimoto I. (1999). Feasible separation modes for various reactive distillation systems. *Industrial and Engineering Chemistry Research* 38, 4060–4067. 3.2.1, 3.1, 3.2.1

Goel H. (2004). *Integrating Reliability, Availability and Maintainability (RAM) in conceptual process design*. Thesis/dissertation, Delft University of Technology. 1.3.1

Golubitsky M. and Schaeffer D.G. (1985). *Singularities and groups in bifurcation theory*. Springer-Verslag, New York. 7.2.3

Gorissen H.J. (2003). A general approach for the conceptual design of counter-current reactive separations. *Chemical Engineering Science* 58, 809–814. 4.3

Grievink J. (2003). Lecture notes on Process Systems Design. Unpublished Work. 1.3.1

Grievink J. (2005). SHEET performance criteria. Personal Communication. 4.4

Grossman I. and Westerberg A. (2000). Research challenges in Process Systems Engineering. *AIChE Journal* 46 (9), 1700–1703. 1.1, 1.3.1, 1.3.2, 1.3.3

Grüner S. and Kienle A. (2004). Equilibrium theory and nonlinear waves for reactive distillation columns and chromatographic reactors. *Chemical Engineering Science* 59, 901–918. 2.9

Gumus Z. and Ciric A. (1997). Reactive distillation column design with vapour/liquid/liquid equilibria. *Computers and Chemical Engineering* 21 (SS), S983–S988. 3.3, 3.3.1

Güttinger T.E. (1998). *Multiple steady states in azeotropic and reactive distillation*. Thesis/dissertation, Swiss Federal Institute of Technology. 2.8, 2.9, 2.9.1, 2.9.1.1, 2.9.2, 3.2.4, 4.2, 5.5.2, B.2, B.2, B.3, B.5

Güttinger T.E. and Morari M. (1997). Predicting multiple steady states in distillation: singularity analysis and reactive systems. *Computers and Chemical Engineering* 21 (SS), S995–S1000. 2.9, 2.9.1.1, 2.9.1.1, 2.9.1.2, 2.9.2, 4.2, 7.2.9

Güttinger T.E. and Morari M. (1999*a*). Predicting multiple steady states in equilibrium reactive distillation. 1. Analysis of non-hybrid systems. *Industrial and Engineering Chemistry Research* 38 (4), 1633–1648. 2.1, 2.9, 2.9.1.1, 2.9.2, 4.2

Güttinger T.E. and Morari M. (1999*b*). Predicting multiple steady states in equilibrium reactive distillation. 2. Analysis of hybrid systems. *Industrial and Engineering Chemistry Research* 38 (4), 1649–1665. 2.1, 2.9, 2.9.1.1, 2.9.2, 4.2

Harding S.T. and Floudas C.A. (2000). Locaring all heterogeneous and reactive azeotropes in multicomponent mixtures. *Industrial and Engineering Chemistry Research* 39, 1576–1595. 2.4

Harding S.T. and Floudas C.A. (2001). EQUISTAR: Reliable software for design of nonideal and reactive systems. *Computer-Aided Chemical Engineering* 9, 153–158. 2.4

Harding S.T., Maranas C.D., McDonald C.M. and Floudas C.A. (1997). Locating all homogeneous azeotropes in multicomponent mixtures. *Industrial and Engineering Chemistry Research* 36, 160–178. 2.4

Harmsen G.J. and Chewter L.A. (1999). Industrial applications of multi-functional, multi-phase reactors. *Chemical Engineering Science* 54, 1541–1545. 1.3.1

Harmsen G.J., Hinderink P., Sijben J., Gottschalk A. and Schembecker G. (2000). Industrially applied process synthesis method creates synergy between economy and sustainability. *AIChE Symposium Series* 96 (323), 364–366. 1.3.1, 1.3.2

Hasse R. (1969). *Thermodynamics of irreversible processes*. Addison-Wesley Publishing Company, Darmstadt. 8.3.3.2, 8.6

Hauan S. (1998). *On the behaviour of reactive distillation systems*. Thesis/dissertation, Norwegian University of Science and Technology. 3.2.8

Hauan S., Ciric A., Westerberg A. and Lien K. (2000*a*). Difference points in extractive and reactive cascades. I. Basic properties and analysis. *Chemical Engineering Science* 55, 3145–3159. 3.2.9

Hauan S., Hertzberg T. and Lien K. (1995*a*). Multiplicity in reactive distillation of MTBE. *Computers and Chemical Engineering* 19 (SS), S327–S332. 2.9, 2.9.1.2, 2.9.1.2, 2.9.2, 6.1.4, 6.2, 6.2.3.1, 7.2.1, 7.3.1, 7.3.2.1, 8.3.1

Hauan S., Hertzberg T. and Lien K. (1995*b*). Why methyl ter-butyl ether production by reactive distillation may yield multiple solutions. *Industrial and Engineering Chemistry Research* 34, 987–991. 2.9, 2.9.1.1, 2.9.1.2, 2.9.2, 2.9.3, 7.3.1

Hauan S., Lee J.W., Westerberg A. and Lien K.M. (2000*b*). Properties of sectional profiles in reactive separation cascades. *Foundations of Computer-Aided Process Design* 96 (323), 397–401. 3.2.8

Hauan S. and Lien K. (1996). Geometric visualisation of reactive fixed points. *Computers and Chemical Engineering* 20 (SS), S133–S138. 3.2.8

Heiszwolf J.J., Engelvaart L.B., van den Eijnden M.G., Kreutzer M.T., Kapteijn F. and Moulijn J. (2001). Hydrodynamic aspects of monolith loop reactor. *Chemical Engineering Science* 56 (2001), 805–812. 2.6, 2.7.1

References

Herder P. (1999). *Process Design in a changing environment*. Thesis/dissertation, Delft University of Technology. 1.1

Higler A. (1999). *A non-equilibrium model for reactive distillation*. Thesis/dissertation, Clarkson University. 2.9.3, 4.3

Higler A., Krishna R. and Taylor R. (1999*a*). Nonequilibrium cell model for packed distillation columns - the influence of maldistribution. *Industrial and Engineering Chemistry Research* 38, 3988–3999. 2.9.3, 4.3

Higler A., Krishna R. and Taylor R. (2000). Nonequilibrium modelling of reactive distillation: a dusty fluid model for heterogenously catalyzed processes. *Industrial and Engineering Chemistry Research* 39 (6), 1596–1607. 2.7, 2.9.3, 4.3

Higler A., Taylor R. and Krishna R. (1998). Modelling of a reactive separation process using a non-equilibrium stage model. *Computers and Chemical Engineering* 22 (SS), S111–S118. 2.9.3, 4.3

Higler A., Taylor R. and Krishna R. (1999*b*). Nonequilibrium modelling of reactive distillation: mutiple steady states in MTBE synthesis. *Chemical Engineering Science* 54, 1389–1395. 2.9, 2.9.1.2, 2.9.3, 4.3, 7.2.9, 7.4

Huss R.S., Chen F., Malone M.F. and Doherty M. (1999). Computer-aided tools for the design of reactive distillation systems. *Computers and Chemical Engineering* 23 (SS), S955–S962. 3.2.4

Ismail S., Proios P. and Pistikopoulos E. (2001). Modular synthesis framework for combined separation/reaction systems. *AIChE Journal* 47 (3), 629–649. 3.3.1, 8.3.1

Izquierdo J., Cunill F., Vila M., Tejero J. and Iborra M. (1992). Equilibrium constants for methyl tert-butyl ether liquid-phase synthesis. *Journal of Chemical and Engineering Data* 37, 339–343. B.4, B.5, B.6

Jacobs R. and Krishna R. (1993). Multiple solutions in reactive distillation for methyl tert-butyl ether synthesis. *Industrial and Engineering Chemistry Research* 32 (8), 1706–1709. 2.1, 2.9, 2.9.1.1, 2.9.1.1, 2.9.1.2, 2.9.1.2, 2.9.2, 6.1.4, 6.2, 6.2.3.1, 7.3.1, 7.3.2.1, 8.3.1

Jimenez L., Wanhschafft O. and Julka V. (2000). Synthesis of reactive and extractive distillation units using distillation line diagrams. *Computer-Aided Chemical Engineering* 8, 985–990. 3.2.2

Jimenez L., Wanhschafft O. and Julka V. (2001). Analysis of residue curve maps of reactive and extractive distillation units. *Computers and Chemical Engineering* 25, 635–642. 4.1, B.2

Jimenez-Gonzalez C., Curzons A.D., Constable D.J.C. and Cunningham V. (2004). Cradle-to-Gate life cycle inventory and assessment of pharmaceutical compounds. *International Journal of Life Cycle Assessment* 9 (2), 114–121. 1.4

Jimenez-Gonzalez C., Kim S. and Overcash M.R. (2000). Methodology for developing gate-to-gate life cycle inventory information. *International Journal of Life Cycle Assessment* 5 (3), 153–159. 1.4

Kenig E., Butzmann F., Kucka L. and Górak A. (2000). Comparison of numerical and analytical solutions of a multicomponent reaction-mass-transfer problem in terms of the film model. *Chemical Engineering Science* 55, 1483–1496. 2.5

Kienle A., Groebel M. and Gilles E.D. (1995). Multiple steady states in binary distillation - theoretical and experimental results. *Chemical Engineering Science* 50 (17), 2691–2703. 2.9

Kim K.J. and Smith R.L. (2004). Parallel multiobjective evolutionary algorithms for waste solvent recycling. *Industrial and Engineering Chemistry Research* 43 (11), 2669–2679. 1.3.2

Kirk-Othmer (1994). Methyl Tert-Butyl Ether. In: *Encyclopedia of Chemical Technology*, book chapter 9, (871–875), John Wiley and Sons, Inc. B.1, B.2

Kjelstrup S. (2005). Personal Communication. 8.2.1

Kjelstrup S. and Bedeaux D. (2001). *Elements of Irreversible Thermodynamics*. International Centre for Applied Thermodynamics, Istanbul. 8.2.1, 8.2.1, 8.2.1

Koeijer G. (2002). *Energy efficient operation of distillation columns and a reactor applying irreversible thermodynamics*. Thesis/dissertation, Norwegian University of Science and Technology. 8.2.1, 8.2.1, 8.2.1, 8.2.1, 8.3.3.2

Koeijer G., Kjelstrup S., vander Kooi H.J., Gros B., Knoche K.F. and Andersen T.R. (2002). Positioning heat exchangers in binary tray distillation using isoforce operation. *Energy Conversion and Management* 43, 1571–1581. 8.1, 8.2.1, 8.2.1

Koeijer G. and Rivero R. (2003). Entropy production and exergy loss in experimetal distillation columns. *Chemical Engineering Science* 58, 1587–1597. 8.2.1

Kooijman H. and Taylor R. (2000). *The ChemSep book*. Libri books on demand, USA. 2.7.1, B.3

Korevaar G. (2004). *Sustainable chemical processes and products*. Thesis/dissertation, Delft University of Technology. 1.4, 4.3

Krishna R. (2003). Hardware selection and design aspects for reactive distillation columns. In: *Reactive distillation. Status and future directions* (K. Sundmacher and A. Kienle, eds.), book chapter 7, (169–189), Wiley-VCH. 4.2, 4.3

Krishnamurthy R. and Taylor R. (1985). Nonequilibrium stage model of multicomponent separation processes. *AIChE Journal* 31 (3), 449–456. 2.9.3, 4.1, 4.3

Lakerveld R., Bildea C.S. and Almeida-Rivera C.P. (2005). Exothermic isomerization reaction in reactive flash: steady state behaviour. *Industrial and Engineering Chemistry Research* 44 (10), 3815–3822. †, 7.2.1, 7.2.5, ‡, 7.2.6, 7.2.8

Lee J.W., Hauan S., Lien K. and Westerberg A. (2000*a*). Difference points in extractive and reactive cascades. II. Generating design alternatives by the lever rule for reactive systems. *Chemical Engineering Science* 55, 3161–3174. 3.2.9

Lee J.W., Hauan S., Lien K.M. and Westerberg A. (2000*b*). A graphical method for designing reactive distillation columns I. The Ponchon-Savarit method. *Proceedings of the Royal Society of London Series A Mathematical Physical and Engineering Sciences* 456, 1953–1964. 3.2.7, 3.2.7

Lee J.W., Hauan S., Lien K.M. and Westerberg A. (2000*c*). A graphical method for designing reactive distillation columns II. The McCabe-Thiele method. *Proceedings of the Royal Society of London Series A Mathematical Physical and Engineering Sciences* 456, 1965–1978. 3.2.7, 3.2.7, 3.4

Lee J.W., Hauan S. and Westerberg A. (2000*d*). Graphical methods for reaction distribution in a reactive distillation column. *AIChE Journal* 46 (6), 1218–1233. 3.2.7

Lee J.W. and Westerberg A. (2000). Visualization of stage calculation in ternary reacting mixtures. *Computers and Chemical Engineering* 24, 639–644. 3.2.7, 3.2.9, 3.2.9

References

Leon S.J. (1998). *Linear algebra with applications*. Prentice-Hall, New Jersey. 5.4

Li X. and Kraslawski A. (2004). Conceptual design synthesis: past and current trends. *Chemical Engineering and Processing* 43, 589–600. 1.2.1, 1.3.1, 1.3.2

Lim Y.I., Floquer P., Joulia X. and Kim S.D. (1999). Multiobjective optimization in terms of economics and potential environment impact for process design and analysis in a chemical process simulator. *Industrial and Engineering Chemistry Research* 38 (12), 4729–4741. 1.3.2, 8.3.4

Luyben W. (2002). *Plantwide dynamic simulators in chemical processing and control*. Marcel Dekker Inc., USA. 6.2.3.2

Luyben W.L., Tyreus B.D. and Luyben M.L. (1999). *Plantwide process control*. McGraw-Hill, New York. 7.3.2.2, 7.3.2.2, 8.1, 8.2.2, 8.2.4, 8.2.4, 8.6, 8.6, 8.8, 9.2, 9.5, B.4, B.4

Mahajani S. (1999*a*). Design of reactive distillation columns for multicomponent kinetically controlled reactive systems. *Chemical Engineering Science* 54 (10), 1425–1430. 3.2.4, 3.2.4

Mahajani S. (1999*b*). Kinetic azeotropy and design of reactive distillation columns. *Industrial and Engineering Chemistry Research* 38 (1), 177–186. 3.2.4

Mahajani S. and Kolah A. (1996). Some design aspects of reactive distillation columns (RDC). *Industrial and Engineering Chemistry Research* 35, 4587–4596. 3.2.4, 3.2.4, 3.2.4, 3.2.4

Maier R., Brennecke J. and Stadtherr M. (2000). Reliable computation of reactive azeotropes. *Computers and Chemical Engineering* 24, 1851–1858. 2.4

Malanowski S. and Anderko A. (1992). *Modelling phase equilibria - thermodynamic background and practical tools*. John Wiley and Sons, Inc., New York. 2.2, B.3

Malone M.F. and Doherty M.F. (2000). Reactive Distillation. *Industrial and Engineering Chemistry Research* 39, 3953–3957. 1.2.1, 2.1, 2.7, 3.2.2, 3.2.2, 3.3.1, 4.1, 4.3, 8.1, 9.1, B.4, B.4

Marquardt W. (2004). Lectures on "Modeling and Analysis of Chemical Process Systems" - Delft University of Technology. Audiovisual Material. 1.3.1, 8.2.1

Meeuse M. (2003). *On the design of chemical processes with improved controllability characteristics*. Thesis/dissertation, Delft University of Technology. 1.3.1, 1.4, 8.3.3.2, 8.6, 8.8

Meeuse M. and Tousain R. (2002). Close-loop controllability analysis of process designs: Application to distillation column design. *Computers and Chemical Engineering* 26, 641–647. 6.2

Melles S., Grievink J. and Schrans S.M. (2000). Optimization of the conceptual design of reactive distillation columns. *Chemical Engineering Science* 55, 2089–2097. 3.2.4, 6.1.3

Mohl K.D., Kienle A., Gilles E.D., Rapmund P., Sundmacher K. and Hoffmann U. (1997). Nonlinear dynamics of reactive distillation process for the production of fuel ethers. *Computers and Chemical Engineering* 21 (SS), S989–S994. 2.9.1.1, 2.9.1.1, 2.9.1.2, 2.9.2

Mohl K.D., Kienle A., Gilles E.D., Rapmund P., Sundmacher K. and Hoffmann U. (1999). Steady-state multiplicities in reactive distillation columns for the production of fuel ethers MTBE and TAME: Theoretical analysis and experimental validation. *Chemical Engineering Science* 54, 1029–1043. 2.9.1.1, 2.9.1.2, 2.9.1.2, 2.9.2, 6.1.4, 7.2.1

References

Mohl K.D., Kienle A., Sundmacher K. and Gilles E.D. (2001). A theoretical study of kinetic instabilities in calatylic distillation processes: influence of transport limitations inside the catalyst. *Chemical Engineering Science* 56, 5239–5254. 2.9.1.1, 2.9.1.1, 2.9.1.2, 2.9.1.2

Monroy-Loperena R., Perez-Cisneros E. and Alvarez-Ramirez J. (2000). A robust PI control configuration for a high-purity ethylene glycol reactive distillation column. *Chemical Engineering Science* 55, 4925–4937. 2.9.1.2, 2.9.2

Moulijn J., Makkee M. and van A.D. (2001). *Chemical Process Technology*. John Wiley and Sons, Inc., London. 1.3.1

Mutalib A. and Smith R. (1998*a*). Operation and control of dividing wall distillation columns. Part I: Degrees of freedom and dynamic simulation. *Trans. Institution of Chemical Engineers - Part A* 76, 308–318. 4.2

Mutalib A. and Smith R. (1998*b*). Operation and control of diving wall distillation columns. Part II: Simulation and pilot plant studies using temperature control. *Trans. Institution of Chemical Engineers - Part A* 76, 319–334. 4.2

Nisoli A., Malone M.F. and Doherty M. (1997). Attainable regions for reaction with separation. *AIChE Journal* 43 (2), 374–387. 3.2.3, 4.2

Nummedal L. (2001). *Entropy production minimization of chemical reactors and heat exchangers*. Thesis/dissertation, Norwegian University of Science and Technology. 8.3

Nummedal L. and Kjelstrup S. (2001). Equipartition of forces as a lower bound on the entropy production in heat exchange. *International Journal of Heat and Mass Transfer* 44, 2827–2833. 8.3

Okasinski M. (1998). *Design methods for kinetically controlled, stagewise reactive distillation columns*. Thesis/dissertation, University of Massachusetts. 3.2.4

Okasinski M. and Doherty M. (1998). Design method for kinetically controlled, staged reactive distillation columns. *Industrial and Engineering Chemistry Research* 37 (7), 2821–2834. 3.2.4, 3.2.4, 3.2.4, 3.2.4, 3.2.4, 3.4, 4.3

Okasinski M. and Doherty M.F. (1997). Thermodynamic behavior of reactive azeotropes. *AIChE Journal* 43 (9), 2227–2238. 2.4, 4.3, 5.3

Omota F., Dimian A. and Bliek A. (2001). Design of reactive distillation process for fatty acid esterification. *Computer-Aided Chemical Engineering* 9, 463–468. 1.2.1

Omota F., Dimian A. and Bliek A. (2003). Fatty acid esterification by reactive distillation. Part 1: Equilibrium-based design. *Chemical Engineering Science* 58, 3159–3174. 1.2.1

Papalexandri K. and Pistikopoulos E. (1996). Generalized modular representation framework for process synthesis. *AIChE Journal* 42 (4), 1010–1032. 3.3.1, 6.1.3, 8.3.1, 9.5

Pekkanen M. (1995). A local optimization method for the design of reactive distillation. *Computers and Chemical Engineering* 19 (SS), S235–S240. 3.3, 3.3.1

Pellegrini L. and Possio C.T. (1996). A non-ideal CSTR: a hight codimension bifurcation analysis. *Chemical Engineering Science* 51 (11), 3151–3156. 2.9

Peng J., Edgar T. and Eldridge R.B. (2003). Dynamic rate-based and equilibrium models for a packed reactive distillation column. *Chemical Engineering Science* 58, 2671–2678. 2.9.3

References

Peters U., Nierlich F., Schulte-Körne E. and Sakuth M. (2000). Methyl tert-butyl ether. In: *Ullmann's Encyclopedia of Industrial Chemistry*, John Wiley and Sons, Inc. B.1, B.1, B.2, B.2, B.1

Pilavachi P.A., Schenk M., Perez-Cisneros E. and Gani R. (1997). Modeling and simulation of reactive distillation operations. *Industrial and Engineering Chemistry Research* 36, 3188–3197. 2.9.3

Podrebarac G.G., Ng F.T.T. and Rempel G.L. (1998). The production of diacetone alcohol with catalytic distillation. Part II: a rate-based catalytic distillation model for the reaction zone. *Chemical Engineering Science* 53 (5), 1077–1088. 2.9.3

Poth N., Frey T. and Stichlmair J. (2001). MINLP optimization of kinetically controlled reactive distillation processes. *Computer-Aided Chemical Engineering* 9, 79–84. 3.3, 3.3.1

Proios P. and Pistikopoulos E. (2005). Generalized modular framework for the representation and synthesis of complex distillation column sequences. *Industrial and Engineering Chemistry Research* 44 (13), 4656–4675. 6.1.3, 9.5

PSE (1999). *gPROMS advanced user guide*. Process Systems Enterprise, London. 6.2.2

Qi Z., Sundmacher K., Stein E., Kienle A. and Kolah A. (2002). Reactive separation of isobutene from C_4 crack fractions by catalytic distillation processes. *Separation and Purification Technology* 26, 147–163. 2.9.1.2

Razon L.F. and Schmitz R.A. (1987). Multiplicities and instabilities in chemically reacting systems - a review. *Chemical Engineering Science* 42 (5), 1005–1047. 7.2.3

Rehfinger A. and Hoffmann U. (1990). Kinetics of methyl tertiary butyl ether liquid phase synthesis catalyzed by ion exchange resin - I. Intrinsic rate expression in liquid phase activities. *Chemical Engineering Science* 45 (6), 1605–1617. 2.9.1.1, B.4, B.5, B.6

Rocha J.A., Bravo J.L. and Fair J. (1996). Distillation columns containing structured packings: a comprehensive model for their performance. 2. Mass-transfer model. *Industrial and Engineering Chemistry Research* 35, 1960–1967. 2.7.1

Rocha J.A., Bravo J.L. and Fair J. (2004). Distillation columns containing structured packings: A comprehensive model for their performance. 1. Hydraulic models. *Industrial and Engineering Chemistry Research* 32, 641–651. 2.7.1, 2.7.1

Rodriguez I.E., Zheng A. and Malone M.F. (2001). The stability of a reactive flash. *Chemical Engineering Science* 56, 4737–4745. 2.9, 2.9.1.1, 7.2.1, 7.3

Rodriguez I.E., Zheng A. and Malone M.F. (2004). Parametric dependence of solution multiplicity in reactive flashes. *Chemical Engineering Science* 59, 1589–1600. 2.9, 2.9.1.1, 7.2.1, 7.3

Ruiz C.A., Basualdo M.S. and Scenna N.J. (1995). Reactive distillation dynamic simulation. *Trans. Institution of Chemical Engineers - Part A* 73 (5), 363–378. 7.3.1

Russel B.M., Henriksen J.P., Jorgensen S. and Gani R. (2000). Integration of design and control through model analysis. *Computers and Chemical Engineering* 24, 967–973. 3.3.3

Scenna N.J., Ruiz C.A. and Benz S.J. (1998). Dynamic simulation of start-up procedures of reactive distillation columns. *Computers and Chemical Engineering* 22 (SS), S719–S722. 2.9.1.2, 2.9.1.2

Schembecker G. and Tlatlik S. (2003). Process synthesis for reactive separations. *Chemical Engineering and Processing* 42, 179–189. 1.2.2, 4.1

Schildhauer T., Kapteijn F. and Moulijn J. (2005). Reactive stripping in pilot plant scale monolith reactors - application to esterification. *Chemical Engineering and Processing* 44 (2005), 695–699. 2.6

Schneider R. and Marquardt W. (2002). Information technology in the chemical process design life cycle. *Chemical Engineering Science* 57, 1763–1792. 1.4

Schoenmakers H. and Bessling B. (2003*a*). Reactive and catalytic distillation from an industrial perspective. *Chemical Engineering and Processing* 42, 145–155. 2.8

Schoenmakers H. and Bessling B. (2003*b*). Reactive distillation process development in the chemical process industries. In: *Reactive Distillation. Status and future directions* (K. Sundmacher and A. Kienle, eds.), book chapter 2, (30–48), Wiley-VCH. 4.2

Schrans S.M., Wolf S. and Baur R. (1996). Dynamic simulation of reactive distillation: an MTBE case study. *Computers and Chemical Engineering* 20 (SS), S1619–S1624. 2.9.1.2, 2.9.1.2, 2.9.2, 6.1.4, 7.3.1, 7.3.2.3, 7.3.3

Seader J.D. (1985). The B.C. (Before Computers) and A.D. of equilibrium-stage operations. *Chemical Engineering Education* 19, 88–103. 2.6

Seader J.D. and Henley E.J. (1998). *Separation Process Principles*. John Wiley and Sons, Inc., New York. 6.2, 7.3.2.1, 8.3.1

Seferlis P. and Grievink J. (2001). Optimal design and sensitivity analysis of reactive distillation units using collocation models. *Industrial and Engineering Chemistry Research* 40, 1673–1685. 3.3, 3.3.2

Seider W., Seader J.D. and Lewin D. (1999). *Process design principles*. John Wiley and Sons, Inc., New York. 8.2.1, 8.2.2, 8.2.4

Serafimov L.A., Pisarenko Y.A. and Kardona K.A. (1999). Optimization of reactive distillation processes. *Theoretical Foundations of Chemical Engineering* 33 (5), 455–463. 3.2.1

Seydel R. and Hlavacek V. (1987). Role of continuation in engineering analysis. *Chemical Engineering Science* 42 (6), 1281–1295. 7.2.3

Siirola J.J. (1996*a*). Industrial applications of chemical process synthesis. In: *Advances in Chemical Engineering. Process Synthesis* (J. Anderson, ed.), book chapter 23, (1–61), Academic Press. 1.2.1, 3.2.2, 4.3, 4.5

Siirola J.J. (1996*b*). Strategic process synthesis: advances in the hierarchical approach. *Computers and Chemical Engineering* 20 (SS), S1637–S1643. 3.2.2, 4.3, 4.2, 4.5

Skogestad S. and Postlethwaite I. (1999). *Multivariable feedback control: analysis and design*. John Wiley and Sons, Inc., New York. 6.2

Smejkal Q. and Soos M. (2002). Comparison of computer simulation of reactive distillation usign ASPEN PLUS and HYSYS software. *Chemical Engineering and Technology* 41, 413–418. 4.3

Smith J.M. and van Ness H.C. (1987). *Introduction to chemical engineering thermodynamics*. McGraw-Hill, New York. 2.2

Sneesby M.G., Tade M.O. and R. S. (1998*a*). Multiplicity and pseudo-multiplicity in MTBE and ETBE reactive distillation. *Chemical Engineering Research and Design* 76 (4), 524–531. 2.9.1, 2.9.1.2, 7.2.1, 7.3.2.3, 7.3.3

Sneesby M.G., Tade M.O. and Smith T.N. (1998*b*). Steady-state transitions in the reactive distillation of MTBE. *Computers and Chemical Engineering* 22, 879–892. 2.9.1.2, 2.9.1.2, 7.2.1, 7.3.2.2, 7.3.2.3, 7.3.3

Solokhin A.V. and Blagov S.A. (1996). Reactive distillation is an advanced technique of reaction process operation. *Chemical Engineering Science* 51 (11), 2559–2564. 3.4

Song W., Huss R.S., Doherty M. and Malone M.F. (1997). Discovery of reactive azeotropes. *Nature* 388 (7), 561–563. 2.4

Stankiewicz A. (2001). Between the chip and the blast furnace. *NPT Processtechnologie* 8 (2), 18–22. 1.2.1

Stankiewicz A. (2003). Reactive separations for process intensification: an industrial perspective. *Chemical Engineering and Processing* 42, 137–144. 1.2.1, 1.2.1, 1.2.2, 1.3.1, 1.3.2

Stankiewicz A. and Moulijn J. (2002). Process intensification. *Industrial and Engineering Chemistry Research* 41 (8), 1920–1924. 1.1, 1.2.1, 1.3.1, 1.3.2

Stichlmair J. and Frey T. (1999). Review: Reactive distillation process. *Chemical Engineering and Technology* 22 (2), 95–103. 3.2.6, 4.1

Stichlmair J. and Frey T. (2001). Mixed-Integer Nonlinear Programming optimization of reactive distillation processes. *Industrial and Engineering Chemistry Research* 40 (25), 5978–5982. 2.9.1.1, 3.3, 3.3.1

Subawalla H. and Fair J. (1999). Design guidelines for solid-catalyzed reactive distillation systems. *Industrial and Engineering Chemistry Research* 38 (10), 3696–3709. 2.6, 3.4, 3.9, 3.4, 3.5, 4.1

Sundmacher K. and Hoffmann U. (1996). Development of a new catalytic distillation process for fuel ethers via a detailed nonequilibrium model. *Chemical Engineering Science* 51 (10), 2359–2368. 2.9.3

Sundmacher K. and Hoffmann U. (1999). Multiple reactions in catalytic distillation processes for the production of the fuel oxygenates MTBE and TAME: Analysis by rigourous model and experimental validation. *Chemical Engineering Science* 54, 2839–2847. 2.6, 2.9.2, 6.1.4

Taylor R. and Krishna R. (1993). *Multicomponent mass transfer*. John Wiley and Sons, Inc., New York. 2.5, 2.6, 4.1, 4.3

Taylor R. and Krishna R. (2000). Review: modelling reactive distillation. *Chemical Engineering Science* 55, 5183–5229. 2.1, 2.6, 2.9.3, 4.1, 4.3

Taylor R. and Krishna R. (2003). Modelling of homogeneous and heterogeneous reactive distillation processes. In: *Reactive distillation. status and future directions* (K. Sundmacher and A. Kienle, eds.), book chapter 9, (217–240), Wiley-VCH. 4.1, 4.3

Taylor R., Krishna R. and Kooijman H. (2003). Real-world modeling of distillation. *CEP Magazine* (7), 28–39. 2.9.3

Thiel C., Sundmacher K. and Hoffmann U. (2002). Residue curve maps for heterogeneously catalysed reactive distillation of fuel ethers MTBE and TAME. *Chemical Engineering Science* 52 (6), 993–1005. B.4, B.5, B.6

Tuchlenski A., Beckmann A., Reusch D., Dussel R., Weidlich U. and Janowsky R. (2001). Reactive distillation-industrial applications, process design and scale-up. *Chemical Engineering Science* 56, 387–394. 2.6, 2.7

References

Ung S. and Doherty M. (1995*a*). Calculation of residue curve maps for mixture with multiple equilibrium chemical reactions. *Industrial and Engineering Chemistry Research* 34, 3195–3202. 2.4, 3.2.2, 3.2.4, 4.3, 5.3, ‡

Ung S. and Doherty M. (1995*b*). Necessary and sufficient conditions for reactive azeotropes in multireaction mixtures. *AIChE Journal* 41 (11), 2383–2392. 2.4, 2.4

Ung S. and Doherty M. (1995*c*). Vapor-liquid phase equilibrium in systems with multiple chemical reactors. *Chemical Engineering Science* 50 (1), 23–48. 2.4, 3.2.4, 3.2.4, 4.3, 5.5.3, ‡, B.2

Vadapalli A. and Seader J.D. (2001). A generalized framework for computing bifurcation diagrams using process simulation programs. *Computers and Chemical Engineering* 25, 445–464. 7.2.3

Venkataraman S., Chan W. and Boston J. (1990). Reactive distillation using ASPEN PLUS. *Chemical Engineering Progress* (45–54). 4.3

Wang S.J., Wong D.S.H. and Lee E.K. (2003). Effect of interaction multiplicity on control system design for a MTBE reactive distillation column. *Journal of Process Control* 13, 503–515. (document), 2.9.1.2, 7.3.2.2, 7.16, 7.3.3, 7.3.3

Waschler R., Pushpavanam S. and Kienle A. (2003). Multiple steady states in two-phase reactors under boiling conditions. *Chemical Engineering Science* 58, 2203–2214. 2.9.1.1

Wayburn T.L. and Seader J.D. (1987). Homotopy continuation methods for computer-aided process design. *Computers and Chemical Engineering* 11 (1), 7–25. 7.2.3

Wesselingh J.A. (1997). Non-equilibrium modelling of distillation. *Transactions Institution of Chemical Engineers - Part A* 75, 529–538. 2.5, 2.6, 2.9.3, 4.3

Wesselingh J.A. and Krishna R. (2000). *Mass transfer in multicomponent mixtures*. Delft University Press, Delft. 2.5, 2.5

Westerberg A., Lee J.W. and Hauan S. (2000). Synthesis of distillation-based processes for non-ideal mixtures. *Computers and Chemical Engineering* 24, 2043–2054. 2.3, 3.2.2, 3.2.8, 5.3

Westerberg A. and Wahnschafft O. (1996). Synthesis of distillation-based separation systems. In: *Advances in Chemical Engineering. Process synthesis* (J. Anderson, ed.), book chapter 23, (63–170), Academic Press. 2.3, 4.2

Wolf-Maciel M.R., Soares C. and Barros A.A.C. (2001). Validations of the nonequilibrium stage model and of a new efficiency correlation for non ideal distillation process through simulated and experimental data. *Computer-Aided Chemical Engineering* 9, 321–326. 2.9.3

Yu S., Zhou A. and Tan Q. (1997). Simulation of multistage catalytic stripping with a nonequilibrium stage model. *Computers and Chemical Engineering* 21 (4), 409–415. 2.9.3

Yuxiang Z. and Xien X. (1992*a*). Study on catalytic distillation proceses. Part II. Simulation of catalytic distillation processes - Quasi-homogeneous and rate-based model. *Trans. Institution of Chemical Engineers - Part* 70 (A), 465–470. 2.6, 2.9.3

Yuxiang Z. and Xien X. (1992*b*). Study on catalytic distillation processes. Part I. Mass transfer characteristics in catalyst bed within the column. *Trans. Institution of Chemical Engineers - Part A* 70, 459–464. 2.6

References

Zhang T. and Datta R. (1995). Integral analysis of methyl tert-butyl ether synthesis kinetics. *Industrial and Engineering Chemistry Research* 34 (3), 730–740. 5.5.1, B.4

Zheng Y., Ng F.T.T. and Rempel G.L. (2004). A comparison of a pseudo-homogeneous non-equilibrium model and a three-phase non-equilibrium model for catalytic distillation. *Chemical Engineering Journal* 100, 119–127. 2.9.3

Summary

Designing Reactive Distillation Process with Improved Efficiency - economy, exergy loss and responsiveness
Cristhian P. Almeida-Rivera
ISBN 9-090200-37-1 / 9789090200378
November, 2005

The design and operation of reactive distillation processes have become increasingly important within academia and industrial spheres over the last few decades (*cf.* figure 1 in Malone and Doherty (2000)). Addressing reactive distillation design is a challenging task both from a process-intensified perspective and because of its inherent complexity. Reactive distillation design is far more complicated than conventional distillation because of: (*i*) the presence of additional design decision variables (*e.g.* distribution of catalyst in the reactive section); (*ii*) the nonlinear interaction between thermodynamic phases and chemical reactions; and because of (*iii*) strong coupling between heat and mass flow throughout a reactive distillation unit.

In this dissertation a life-span inspired perspective is taken on the conceptual design of grassroots reactive distillation processes. Attention was paid to the economic performance of the process and to potential losses of valuable resources over the process life span.

The research was cast in a set of goal-oriented engineering and specific scientific design questions. The scientific novelty of this work is based around four key aspects of reactive distillation process design: (*i*) the formulation of an extended design problem in reactive distillation achieved by refreshing it in the wider context of process development and engineering and in a more relevant way regarding sustainability; (*ii*) the definition of an integrated design methodology achieved by analyzing current design methodologies and bridging the gaps between them; while we suggest this methodology as a way to beat the design complexity by decomposition, it requires the mastery of many tools and many concepts; (*iii*) the improvement of design tools achieved by exploring and extending current techniques and systematically applying them to the reactive distillation case;

(*iv*) the definition of performance criteria that can be used to account for the process performance from a life-span inspired perspective, as well as applications of them.

After having covered the fundamentals of reactive distillation and current design approaches in the initial chapters of this dissertation, we suggest a novel methodology for reactive distillation process design: life-span inspired design methodology (LiSp-IDM). The framework of this design method is the *multiechelon design approach*, in which a hierarchy of embedded design spaces of increasing refinement is used and the strengths of current design methods are conjugated. A fundamental understanding of the various echelons of the proposed methodology is obtained through direct application to an industrial case study (*i.e.* the catalytic synthesis of MTBE from isobutylene and methanol in the presence of inert components).

We propose the following design echelons:

Formulation, in which sustainability issues are considered and the basis of design (*i.e.* product and feedstock purities ranges, production capacity, operating window and economics life-span accounting for sustainability aspects) are defined.

Feasibility analysis, in which, using graphical methods, the feasible product compositions for a given set of input variables incorporating all occurring phenomena are determined.

Temporal structure, in which the mode of operation based on operational skills, production requirements and supply chain dynamics is selected.

Generation of separation sequences, in which the feasible column sequences are identified and organized; and their type of task, together with the number of units and their connectivity are estimated.

Internal spatial structure, in which the process structure obtained from the previous design echelons is used as the starting point for this design space. Using a multilevel modeling approach, developing appropriate building model blocks and optimization-based methods both continuous variables and discrete variables for the process and its control structure are obtained.

Behavior analysis, in which steady-state simulations are carried out to analyze the kinetics, gas/liquid mass transfer, hydrodynamics and steady-state multiplicities inside the units. Additionally, dynamic simulations are performed to check the robustness of the design, in terms of the ability to maintain product purities and conversion in a desired range when disturbances occur. At this design echelon the amazing complexity of the reactive distillation design problem is acknowledged. Even for a simplified and idealized system (*i.e.* reactive flash), a large number of bifurcation diagrams, exhibiting up to three steady states are reported.

Evaluation, in which the design options are checked with respect to their performance. Within the wide range of criteria in safety, health, economics, environment and technology aspects specific choices are made for economic performance, sustainability and technology. The capital and operational costs of the process during the time horizon are calculated and the exergy efficiency is used as sustainability metric, while the responsiveness of the process acts as a metric for its capability to deal with disturbances. A short response time reduces losses from 'off-spec' products.

The specifics of each design echelon are described as follows. In the course of this thesis the **feasibility** of reactive distillation processes was explored using an improved residue curve mapping technique. The analysis of the behavior of singular points in a transformed composition space resulted in different reactive separation **sequences** according to the feed compositions. The **spatial and control design** of a chosen superstructure configuration was addressed using a multilevel approach and simultaneous dynamic optimization of spatial and control structures, respectively. The multilevel strategy is proposed as being an easy-to-handle tool that can be used to assist one in the early stages of the design task. Additionally, this approach allows the designer to determine whether or not the business-related decision variables cope with the operational constraints imposed by the problem formulation. Aspects of **steady-state and dynamic behavior** in reactive distillation are also covered in this thesis. We found that, even for a simplified case study, a large number of bifurcation diagrams is possible, exhibiting a maximum of three steady states. A rather conventional control design was considered, with the intention to define a reference design for new developments later in this research. In this regard, a thermodynamic-based design approach was explored aiming at incorporating life-span considerations in the design problem. Thus, for **evaluation** and **optimization** purposes, a set of performance criteria accounting for the economic performance, process sustainability and responsiveness was defined. The entropy production rate was chosen as metric for process sustainability, whereas response time, as defined by Luyben *et al.* (1999), was used as a responsiveness index. In fact we accept a simplified version of the response time, considering only one disturbance rather the worst case disturbance. In particular, process responsiveness was expressed in the framework of thermodynamics of irreversible processes. Gradually incorporating each performance criterion the design problem was reformulated as a multiobjective optimization and a suggestion is made that a trade-off exists between economic and sustainability-based aspects. **Designs** were **compared** with respect to exergy loss and closed loop control performance. The first design (conventional) was obtained by optimization of economic performance only; the second design (green) included both economic and sustainability aspects in the formulation of the optimization problem. Substantial structural differences were observed between the designs, such as a reduction in the number of reactive trays, more uneven distribution of catalyst along

the units and the identification of suitable spots for side reactors. Having analyzed the response times of the bi-optimized designs a suggestion is made that small driving forces are desirable for reactive sections, while large driving forces are desirable for separation (nonreactive) sections. It is acknowledged that the design comparison might be of limited generality as only one case study was considered.

The complexity of reactive distillation process design is amazing and even higher than initially envisaged. Although the LiSp-IDM design approach is our first attempt towards a systematic design strategy, it requires the mastery of many tools and advanced concepts. Therefore, there are numerous opportunities to extend and validate this work, these are briefly mentioned below.

Sustainability aspects like proper choice of feedstocks and a products' supply chain should be included as metrics together with a loss prevention concept. The extension of the proposed **design methodology** should include more refined behavioral models and structural models, to allow for superstructure generation. Further study is recommended on the use of the current methodology for reaction systems with more than four species and multiple reactions. Moreover, it is worth researching on how to link the outcome of graphical methods for problems of low dimensionality to optimization design methods with high dimensionality. Regarding **steady-state analysis**, further research should focus on the effect of different model assumptions (*e.g.* rate limitations) and more extended systems (*e.g.* full column with control structure). Regarding the **dynamic behavioral analysis**, it is recommended to study further operational aspects like flexibility, as they could become more important than cost aspects. One topic for further research would be the definition of a more descriptive **responsiveness criterion**. This new index should be capable of making the distinction between response on changes of manipulated variables towards controlled outputs and response to disturbances acting on the process. From a **non-equilibirum thermodynamics** angle, more accurate approaches are required when it comes to the prediction of certain thermodynamic variables. In particular, the estimation of the gradient in chemical potential for multiphase systems needs to be further explored in turbulent mixed systems.

Finally, it is suggested that the LiSp-IDM presented here should be **tested** in regard of its **practical applicability**. The approach presented by Ajah *et al.* (2004) would provide a convenient theoretical background for this work.

Sammenvatting

Designing Reactive Distillation Process with Improved Efficiency - economy, exergy loss and responsiveness
Cristhian P. Almeida-Rivera
ISBN 9-090200-37-1 / 9789090200378
November, 2005

Ontwerp en uitvoering van reactieve distillatie (RD) processen zijn belangrijker geworden in de procesindustrie over de laatste decennia (*cf.* figuur 1 in Malone and Doherty (2000)). Het ontwerpen van een RD proces is een uitdagende taak, niet alleen vanwege het bereiken van proces-intensificatie, maar ook vanwege zijn inherente complexiteit. Bijvoorbeeld, het ontwerpen van RD is veel ingewikkelder dan dat van conventionele distillatie wegens: (*i*) het voorkomen van extra ontwerpvariabelen (b.v. distributie van katalysator in de reactieve sectie); (*ii*) de niet-lineaire interactie tussen thermodynamische fasen en chemische reacties en (*iii*) sterke koppeling tussen energie- en massastromen door een RD eenheid.

Dit proefschrift presenteert resultaten van onderzoek aan het conceptueel ontwerpen van nieuwe reactieve distillatie processen. Het onderzoek houdt rekening met bepaalde aspecten van duurzaamheid over de levensduur van het proces. D.w.z., we geven niet alleen aandacht aan de economische prestaties van het proces, maar ook aan preventie van potentiële verliezen van andere waardevolle middelen over de levensduur.

Wij geven dit onderzoek vorm door middel van een reeks doelgerichte engineering vragen en vragen betreffende specifieke, wetenschappelijke aspecten van ontwerpen. De wetenschappelijke vernieuwing in dit onderzoek betreft vier sleutelaspecten van RD procesontwerp: (*i*) formulering van een uitgebreid ontwerpprobleem in RD, nieuw geplaatst in een bredere context van procesontwikkeling en -engineering en met meer relevantie voor duurzaamheid; (*ii*) presentatie van een geïntegreerde ontwerpmethodologie, verkregen door analyse van huidige ontwerpmethoden en overbrugging van de hiaten daartussen. Deze methodologie die we zien als een manier om de complexiteit van ontwerp te verslaan door decompositie, vereist de beheersing van vele concepten en hulpmiddelen die alle relevant zijn; (*iii*) verbetering van ontwerphulpmiddelen door onderzoek aan en

uitbreiding van huidige technieken met een systematische toepassing op een RD case studie; (*iv*) definitie van criteria voor prestaties van een proces, die sommige levensduuraspecten in rekening brengen, alsmede toepassing daarvan.

De grondbeginselen van RD en huidige ontwerpbenaderingen worden behandeld in de eerste hoofdstukken van dit proefschrift. Vervolgens stellen wij een nieuwe ontwerpmethodologie voor RD processen voor, genaamd LiSp-IDM (life-span inspired design methodology). De ruggraat van deze ontwerpmethode is de zogenaamde multiechelon ontwerpbenadering, die gebruik maakt van een hiërarchie van ingebedde ontwerpruimten van toenemende verfijning en tevens de sterke punten van huidige ontwerpmethodes benut. Het fundamentele begrip van de diverse echelons in de voorgestelde methodologie wordt opgebouwd door directe toepassing op een industriële case studie, namelijk de katalytische synthese van MTBE uit isobuteen en methanol in aanwezigheid van inerte componenten.

Wij benoemen de volgende ontwerpechelons:

Probleemformulering, waar wij de basis van het ontwerp vaststellen (systeemgrenzen, zuiverheidbereik van product en grondstoffen, productie capaciteit, venster van toelaatbare procescondities en proceseconomie, gewenste levensduur) rekening houdend met duurzaamheidaspecten.

'Feasibility' analyse, waar wij door middel van grafische methodes de reikwijdte aan productcomposities bepalen die mogelijk is voor een gegeven voedingsamenstelling, wanneer alle optredende fysische verschijselen worden meegenomen.

Temporele structuur, waar de wijze van procesvoering wordt gekozen, gebaseerd op operationele vaardigheden, productievereisten en de externe dynamica van de productieketen waarin het proces is opgenomen.

Volgorde van scheidingen, waar wij uitvoerbare schakelingen van processtappen identificeren en structureren. Voorts bepalen we de fysische taken in de processtappen samen met het aantal eenheden en de wijze van verbinding.

Interne ruimtelijke kolomstructuur, waar wij de processtructuur, die uit vorige ontwerpechelons is verkregen, als uitgangspunt gebruiken in deze ontwerpruimte. Door middel van een modelleringbenadering waarbij op verschillende aggregatieniveaus modellen worden ontwikkeld van de bouwstenen voor de synthese verkrijgen wij zowel continue als discrete beslissingsvariabelen voor een proceseenheid en zijn regeling. Door inbedding van de synthesemodellen in een optimalisatie raamwerk worden deze variabelen vastgelegd.

Analyse van fysisch gedrag, waar we stationaire simulaties uitvoeren om kinetiek van reacties, gas-vloeistof massaoverdracht en hydrodynamica alsmede multipliciteiten van stationaire toestanden binnen de eenheden te analyseren. Bovendien, voeren we

dynamische simulaties uit om de robuustheid van het ontwerp te controleren, in termen van het vermogen productzuiverheid en omzetting binnen de gewenste marge te handhaven wanneer zich storingen voordoen. Bij dit ontwerpechelon ondervinden we de verbazingwekkende ingewikkeldheid van het ontwerpprobleem in RD. Zelfs bij een vereenvoudigd en geïdealiseerd systeem als een reactieve flash zien we een groot aantal gevarieerde bifurcaties, waarbij tot drie stationaire toestanden kunnen optreden.

Evaluatie, waar de uitgewerkte ontwerpopties met betrekking tot hun prestaties worden bekeken. Binnen de brede waaier van criteria voor safety, health, economics, environment & technology aspecten maken we een specifieke keuze voor economische prestatie, duurzaamheid en technologie. Bij de economie berekenen wij kapitaal en operationele kosten van het proces over de levensduur. Voorts gebruiken wij de exergy efficiency als maat voor duurzaamheid, terwijl de 'response tijd' van het proces een maat is voor de snelheid waarmee het proces zich kan herstellen van de gevolgen van storingen. Een korte response tijd reduceert verliezen door 'off-spec' producten.

De resultaten op elk ontwerpechelon worden aangeduid. In dit proefschrift bepalen wij de **haalbaarheid** van RD processen door middel van een verbeterde residue curve map. De analyse van het gedrag van singuliere punten in een getransformeerde compositieruimte resulteert in verschillende **sequenties** van reactieve scheidingen afhankelijk van de voedingssamenstelling. Het ontwerpen van de **ruimtelijke indeling en de regeling** van een RD eenheid (kolom) gebeurt binnen een gekozen superstructuur door middel van een modelbeschrijving op verschillende niveaus van detail en door een simultane dynamische optimalisering van de ruimtelijke structuur en de regeling. Wij zien deze strategie van modelbeschrijving op verschillende niveaus als een gemakkelijk te hanteren aanpak voor de beginfase van het ontwerp. Bovendien, staat deze benadering de ontwerper toe te bepalen of de beslissingsvariabelen die gerelateerd zijn aan de bedrijfseconomie voldoen aan de operationele beperkingen zoals vastgelegd in de formulering van het ontwerpprobleem. De aspecten van **stationair en dynamisch gedrag** in RD zijn ook behandeld in dit proefschrift. Wij rapporteren dat zelfs voor een sterk vereenvoudigd geval een groot aantal bifurcaties mogelijk is, waarbij maximaal drie stationaire toestanden kunnen voorkomen. Bij de procesregeling is gekozen voor een conventioneel ontwerp, louter met de bedoeling een referentieontwerp te hebben voor vergelijk met nieuw te ontwikkelen procesontwerpen. Aangaande het maken van nieuwe ontwerpen is gekozen voor het uitdrukken van duurzaamheid en robuustheid in het ontwerpprobleem in fysische grootheden uit de niet-evenwicht thermodynamica, zoals exergie en entropie productie. Aldus, voor **evaluatie** en **optimalisering** doeleinden maken we gebruik van een drietal prestatiecriteria die rekenschap geven van de economie, de duurzaamheid van procesvoering en de robuustheid. Wij kiezen exergie- efficiëntie als een maat voor de procesduurzaamheid, terwijl wij een responsetijd - zoals bepaald door Luyben *et al.* (1999) - als robuustheidindex beschouwen. In feite nemen we genoe-

gen met een vereenvoudigde versie van het begrip responsetijd, waarbij we slechts een enkele dominante verstoring meenemen in plaats van de meest slechte verstoring. Door stapsgewijs deze prestatiecriteria te introduceren wordt het ontwerpprobleem vertaald in een 'multi-objective' optimalisatie probleem, waarbij een Pareto afweging kan worden gemaakt tussen economische en duurzaamheidgebaseerde prestaties. We **vergelijken procesontwerpen** met betrekking tot exergy verlies en de robuustheidprestatie van het geregelde proces. Het eerste, conventionele ontwerp wordt verkregen door alleen maar te optimaliseren naar de economische prestatie, terwijl het tweede, groene ontwerp zowel economische als duurzaamheidaspecten in de formulering van het optimaliseringprobleem omvat. We vinden wezenlijke, structurele verschillen tussen deze ontwerpen, zoals de vermindering van het aantal reactieve schotels, meer ongelijke verdeling van de katalysator over de eenheden en de andere geschikte plekken voor zijreactoren. Door de responsetijden van de bi-geoptimaliseerde ontwerpen te analyseren concluderen wij dat kleine drijvende thermodynamische krachten in de reactieve secties wenselijk zijn, terwijl grote drijvende krachten voor scheidingsecties wenselijk zijn. We tekenen hierbij aan dat de uitkomst van de vergelijking van deze ontwerpen een beperkte geldigheid kan hebben omdat we slechts n geval hebben onderzocht.

De ingewikkeldheid van RD procesontwerp is verbazend hoog; veel hoger dan aanvankelijk ingeschat. Hoewel onze LiSp-IDM ontwerpbenadering onze eerste poging is tot een systematische ontwerpstrategie, vereist het reeds de beheersing van vele hulpmiddelen en geavanceerde concepten. Daarom zijn de kansen om dit werk uit te breiden en te valideren talrijk. Ze worden kort vermeld.

Wij geloven dat **duurzaamheidaspecten** breder kunnen worden behandeld zoals de keuze van geschikte grondstoffen en de plaatsing van het RD proces in de gehele productieketen, tezamen met het concept van preventie van verliezen in het proces zelf. De voorgestelde **ontwerpmethodologie** zou bij uitbreiding niet alleen meer verfijnde gedragsmodellen moeten bevatten, maar ook de formele uitwerking van structuur modellen, passend bij een 'superstructuur' voor het ontwerp. Verder wordt aanbevolen de toepasbaarheid van de huidige methodologie op reactiesystemen met meer dan vier componenten en meerdere reacties te bestuderen. In verband hiermee is het de moeite waard na te gaan hoe het resultaat van grafische methodes voor problemen van lage dimensionaliteit kan worden verbonden met optimalisatie gebaseerde ontwerptechnieken voor problemen met hoge dimensionaliteit. Betreffende **analyse van stationair gedrag** zou het verdere onderzoek zich kunnen concentreren op het effect van verschillende modelveronderstellingen (b.v. beperkingen in overdrachtssnelheden) en op uitbreidingen van het systeem (b.v. volledige kolom met regelstructuur). Betreffende **analyse van dynamisch gedrag** adviseren wij om operationele aspecten zoals flexibiliteit verder te bestuderen, aangezien zij in belang kunnen toenemen ten opzichte van de kosten aspecten. Langs die lijn past ook verder onderzoek aan een verfijning van de definitie

van **response tijd**. Deze nieuwe index zou onderscheid moeten kunnen maken tussen reacties op veranderingen van gemanipuleerde variabelen naar geregelde output variabelen en reacties op storingen die inwerken op het proces. Binnen het kader van het gebruik van de **niet-evenwicht thermodynamica** zijn nauwkeurigere benaderingen vereist voor de voorspelling van bepaalde thermodynamische variabelen. In het bijzonder behoeft de schatting van de gradiënt in de chemisch potentiaal in een turbulent gemengd meerfasen systemen nader onderzoek.

Tot slot stellen wij voor onze ontwerpmethode, LiSp-IDM, verder te testen op praktische bruikbaarheid. De benadering die door Ajah *et al.* (2004) werd voorgesteld verschaft een geschikt theoretische raamwerk om zulke testen uit te voeren.

Acknowledgments

This research thesis compiles the upmost results of a 4-year period of intense and challenging work. Independently on the nature of their contribution (intellectual or/and emotional), many people have pushed toward the completion of this work. To all of them I am deeply and sincerely indebted.

My first words of thanks go, sincerely, to my promotor, Prof. Johan Grievink. I thank you Johan for your continuous guidance and scientific insight during these 4+ years and, on top of this, for your admirable kindness and politeness. I fully enjoyed the long hours we spent together, discussing a wide range of topics and always with the pleasant companion of sufficient quantities of loose leaves tea. Furthermore, I highly appreciate the scientific freedom you provided me, which enabled me to explore numerous topics within the technical knowledge domain. Despite of this enjoyable scientific freedom, you kindly put me back on track when my compass was functioning wrongly or when my writing was turning to be baroque and fuzzy. Your *helicopter view* was very much appreciated and valuable for the completion of this dissertation. Without all your comments and suggestions this thesis probably would have remained as a bunch of unconnected manuscripts. Additionally, I am very much thankful for allocating time in your tight agenda to discuss and repeatedly and repletely correct all the dissertation chapters.

I am in particular indebted to Peter Verheijen for always being aware of my well-being before, during and after this research. Many thanks Peter for your suggestions while I was in the midst of a PhD quest. Actually, it was in your office where all this scientific journey started. My thanks are extended to Pieter Swinkels and C. Sorin Bildea for their contributions to this research. Your scientific insight, practical expertise and fruitful discussions were successfully materialized in various publications.

I would like to express my thanks to all my PSE-colleagues for their companion, coffee-break discussions, scientific criticism and common quest for knowledge. Special thanks go to those fellows, with whom I shared the AIO-kamer at the end of the corridor: Austin Ajah, Gijsbert Korevaar, Marco van Goethem, Michiel Meeuse, Michiel van Wissen, Pieter Schmal and my reactive-corner fellow Sachin Singare. These thanks

are extended to my partly-PSE colleagues: Abilash Menon and Harish Goel. I am in particular indebted to Harish for the last-minute tips regarding the final polishing of the manuscript.

This dissertation would not have been materialized without the effort and (in-)direct contribution of several graduate students. Many thanks to Arjan van Benthem for setting-up the basis of a RD column model and for enabling my first exposure to gPROMS©/gOPT©, to Vincent van Hijkoop for the discussions on reactive azeotropy, to Tymon Vermeulen for his extremely hard work in the dynamic simulation of the MTBE RDC and professional commitment to achieve the assignment's ultimate goal, to Gilles Camaret for his enthusiasm despite a non-optimal scenario, to Richard Lakerveld for successfully mastering one of the complexities in RD (MSS) and nicely conveying the project output into a scientific article, to all the graduate students of the CPD groups 3268, 3285, 3296 and 3310 for their technical and creativity discussions.

Many thanks go to Mart Valentijn for the technical discussions we had regarding flowsheeting and continuation methods and to Caroline Monna for her assistance and keeping our agendas in good shape.

Many people provided valuable comments to this research and contributed (in-)directly towards a broader scientific added value. The following researchers are sincerely acknowledged: Prof. Michael Doherty (UCSB, USA), Prof. Jan Harmsen (TUDelft and Shell Chemicals, The Netherlands), Dr. Eugene Kenig (University of Dortmund, Germany), Prof. Signe Kjelstrup (NTNU Trondheim, Norway), Prof. Jae Woo Lee (UC-NYC, USA), Prof. Wolfgang Marquardt (RWTH-Aachen, Germany), Prof. Stratos Pistikopoulos (Imperial College, UK) for his hospitality during my stay at the CPSE-Imperial College, Dr. Tylman Schildhauer (ex TUDelft, The Netherlands), Prof. Hartmut Schoenmakers (BASF, Germany), Dr. Panos Seferlis (CPERI, Greece) and Dr. Jeff Siriola (Eastman Chemicals, USA).

Many thanks to my Ecuadorian fellows in the Netherlands for allowing the much-needed emotional balance for one in a foreign land. Thanks to you all: Fam. Guerra-Torres, Fam. LeMarie-Yepez and Maria Luisa Martinod. I shall not fail thanking all the people that -in one way or another- contributed in making life outside university boundaries so much fun. In particular, many thanks to Ana Maria Garavito, Marc de Reuver, Fabian Zhindon, Yenory Morales, Pilar Garate and Nacho Guerra, among others. Special thanks go to Fr. Ben Engelbertink for the spiritual guidance, the dot-painting and those Thursdays of webdesign.

Furthermore, I am indebted to Ann O'Brien for her unconditional and continuous support for the last 6+ years and to Miranda Aldham-Breary, Grace and Eric Eccarius for their help in improving the technical writing of this thesis.

Moreover, I would like to thank my colleagues of the Process and Supply Chain Design

group in Unilever Food and Health Research Institute (Vlaardingen, The Netherlands) for the challenging and stimulating working environment. Special thanks go to Clive Marshman, Ardjan Krijgsman and Peter Bongers for their understanding and support during the last and determining steps in this *promotie*-process.

Deep in my heart I thank my parents, brothers and sister for their everyday support and trust in me. Papi and Mami, I owe you the most valuable lesson one can receive: be responsible and work hard. But on top of this, I am fully indebted for all your prayers, blessings and tender care during the last 3+ decades. A *Thank You* goes to my siblings Fernando, Doris and Hernán for all the joyful moments that we have shared, those that in a way or another have contributed to a balanced emotional quotient. Furthermore, I would like to thank my parents- and siblings-in-law for their trust and understanding. Visiting periodically my family allowed undoubtedly a synergic enhancement of my scientific performance.

Last and not least I would like to express my most sincere acknowledgement to my wife Paty and our beloved daughter Lucia. Thanks to you, Paty, for your understanding and unconditional support during the moments of deep uncertainty, for your words of confidence when the light at the end of the tunnel seemed to vanish, for the quality of your love, for your criticism and reflection towards my sometimes awkward thoughts, for always believing in me despite my human failures, for reminding me every now and then what life is all about and for sharing with me the most precious gift of life: our daughter. My beloved Lucía, I thank you for all the joyful and cheering-up moments we spend together, for you laughing, jumping and singing in my dreams, for your first words, steps and kisses, for always receiving me with a big hug and calling me '*papito*'. But, on top of these, thank you my dearest Lucía for allowing me to experience the endless love that a father can give to his child.

Finally, I thank my God almighty for His blessings and providing me with the strength and firmness to succeed.

CPAR/October 25, 2005

Selected publications

- Almeida-Rivera C.P. and Grievink J. (2001). Reactive distillation: on the development of an integrated design methodology. *Chemie Ingenieur Technik* 73(6), 777.
- Almeida-Rivera C.P. and Grievink J. (2002). Feasibility of equilibrium controlled reactive distillation processes: application of residue curve mapping. *Computer-Aided Chemical Engineering* 10, 151-156.
- Almeida-Rivera C.P., Swinkels P.L.J. and Grievink J. (2003). Multilevel modeling of spatial structures in reactive distillation units. *Computer-Aided Chemical Engineering* 15 (Part A & B), 696-701.
- Almeida-Rivera C.P. and Grievink J. (2004). Feasibility of equilibrium controlled reactive distillation process: application of residue curve mapping. *Computers and Chemical Engineering*, 28(1-2), 17-25.
- Almeida-Rivera C.P., Swinkels P.L.J. and Grievink J. (2004). Economics and exergy efficiency in the conceptual design of reactive distillation processes. *AIChE Symposium Series* 2004, 237-240.
- Almeida-Rivera C.P., Swinkels P., Grievink J. (2004). Designing reactive distillation processes: present and future. *Computers and Chemical Engineering*, 28(10), 1997-2020.[†]
- Lakerveld R., Bildea C.S. and Almeida-Rivera C.P. (2005). Exothermic isomerization reaction in a reactive flash: steady state behavior. *Industrial Engineering Chemistry Research*, 44(10), 3815-3822.

[†]Top ranked (2nd in March 2005) in the list of TOP25 Hottest articles in Computers and Chemical Engineering (`http://top25.sciencedirect.com`); listed since March 2005 until now (November 2005)

About the author

Cristhian P. Almeida-Rivera was born in 1972 in Quito-Ecuador. In 1990 he completed his high-school studies and graduated from the German School (Quito) majoring in Physics and Mathematics, with distinction and best grade average. In the same year he started his university education in the Escuela Politécnica Nacional (Quito) and in 1997 he received a degree in chemical engineering with honors (*cum laude*) and best grade average. In 1998 he joined the Master of Science International Programme at Delft University of Technology (The Netherlands). Two years later he was awarded a degree with honors (*cum laude*) majoring in Particle Technology and Chemical Risk Management. Moreover, Cristhian was *valedictorian* of his class. During his MSc studies he spent a 3-month internship at the Process Engineering Department of the Eidgenössiche Anstalt für Wasserversorgung, Abwasserreinigung und Gewässerschutz (EAWAG) in Zürich-Switzerland. In 2000 Cristhian was appointed as PhD student for the Process Systems Engineering group at DelftChemTech, Faculty of Applied Sciences, Delft University of Technology under the supervision of Prof. Johan Grievink. In 2002 Cristhian spent a 6-week visit at the Centre for Process Systems Engineering of Imperial College of Science and Technology in London-UK under the supervision of Prof. Stratos Pistikopoulos. The results of Cristhian's PhD research have been presented locally and internationally in CACE-symposia and congresses (*e.g.* NPS2-4, NL-GUTS, IROP, DCSIP, ISMR-2, ESCAPE12, PSE2003 and FOCAPD2004) and published in refereed scientific journals. For the last four years, he was additionally involved in the supervision of undergraduate students during their graduation projects (4), 3-month Conceptual Process Design assignments (20), research assignment (1) and literature review assignments (2).

Since January 2005 Cristhian works as process/research engineer at Unilever Food and Health Research Institute in Vlaardingen (The Netherlands) in the department of Process and Supply Chain Design. Cristhian was in the dean's list (Escuela Politécnica Nacional, 1992-1997), was a UFP fellowship holder (1998-2000), has been student representative (1995-1997), is a soccer fan and dot-painter, has been married with Patricia since 1998 and in March 2003 became the father of Lucía. October 25, 2005

Index

List of Symbols

Acronyms

AR	attainable region
BD	bifurcation diagram
CME	chemical equilibrium manifold
CMO	constant molar overflow
CPD	conceptual process design
GLRDVE	generic lumped reactive distillation volume element
LiSp-IDM	life-span inspired design methodology
LMB	line of mass balance
LSS	limiting steady state
MESH	mass balance, equilibrium, summation, energy balance
MIDO	mixed integer dynamic optimization
MINLP	mixed integer nonlinear programming
MNAz	methanol-nC$_4$ azeotrope
MSE	Maxwell-Stefan equation
MSI	Marshall and Swift index
MSS	multiple steady state
MTBE	methyl t-butyl ether
NEQ	non-equilibrium
POT	pay-out time
PRAz	pseudo reactive azeotrope
PSE	process systems engineering
PU	price per unit
QAz	quaternary azeotrope
RCM	residue curve mapping
RD	reactive distillation

RTD	residence time distribution
SHEET	safety, health, environment, economics, technology criteria
SISO	single input single output
SP	set point
SS	steady state
TAC	total annualized cost
Universal constants	
$\mathcal{R}$	universal gas constant
g	gravitational acceleration
Greek symbols	
α	thermodynamic design factor
α_τ	flowrate disturbance
α_v	constant for vapor inflow
β	ratio of characteristic times in the vapor and liquid sides
β_w	geometry parameter of weir
ΔP	pressure drop
ΔT_{lm}	log-mean temperature difference
Δ	difference operator
$\delta_{R,n}^{\text{rect}}$	composition coordinate in the Ponchon-Savarit diagram for rectifying section
$\Delta^r H$	heat of chemical reaction
$\Delta^v H$	heat of vaporization
$\dot{\alpha}$	relative volatility
$\dot{\gamma}$	dimensionless activation energy
ϵ	numerical tolerance
η	scaled time
η^{II}	second law efficiency
γ	activity coefficient
λ	dimensionless heat capacity
λ_p	shadow price
Λ_{ij}	binary interaction parameter for the pair $i-j$
$\mathcal{V}_{\text{ref}}$	matrix of stoichiometric coefficients for reference components
$\mu_i^{(\alpha)}$	chemical potential of component i in phase (α)
$\nabla \cdot \varsigma$	rate of momentum gain by viscous transfer per unit volume

ν_{total}	sum of the stoichiometric coefficients
ν_i	stoichiometric coefficient of component i
ω	acentric factor
Φ_i	correction factor accounting for system nonideality
ϕ_i	fugacity coefficient of component i
ϕ_m	mass-based vapor fraction
ϕ_p	ratio between phases
$\phi_{R,j}$	fraction of feed vaporized in the unit j in a reactive cascade
$\pi^{(\alpha)}$	pressure tensor in phase (α)
Ψ_e	energy flux associated with the interface mass and heat transfer
ψ_{FR}	functions for the liquid and vapor flow regimes
ψ_{PP}	physical properties functions for the liquid and vapor phases
ρ_i	molar density of component i
$\rho_{m,i}$	mass density of component i
σ_f	fast moving disturbance
σ_s	slow moving disturbance
$\Sigma_V^{(\alpha)}$	entropy production rate in phase (α)
$\sigma_V^{(\alpha)}$	entropy production rate per unit of volume in phase (α)
τ	response time
τ_c	controller reset time
τ_w	warped time
θ	dimensionless temperature
ε	vapor fraction in reactive flash
ε_k	extent of reaction k; degree of advancement of chemical reaction k
φ_i	dimensionless flux
ξ	total friction factor
ζ_z	dimensionless height of the column
$\zeta_{i,j}$	friction coefficient between species i and j
ν_{total}	vector of total mole number change in each reaction
ν_i	vector of stoichiometric coefficients for component i
ν_i	vector of stoichiometric coefficients

Roman symbols

$\bar{x}$	deviation from specifications

List of Symbols

$\hat{\mathcal{M}}$	length of the mixing vector
$\hat{\mathcal{R}}$	scalar
$\hat{\mathcal{S}}$	matrix of average mass transfer rates
$\hat{f}$	frictional force
$\mathbb{A}$	vector of unknowns
$\mathbb{D}$	Maxwell-Stefan diffusivity
$\mathbb{N}$	species flux
$\mathbb{X}_{\text{variables}}$	set of all involved variables
$\mathbb{Y}^{\text{total}}$	set of algebraic equations
$\mathbf{g}$	vector of external forces per molar unit
$\mathbf{J_q}^{(\alpha)}$	measurable heat flux of phase (α)
$\mathbf{j}_i^{(\alpha)}$	molar diffusion flux vector
$\mathbf{Q}$	row vector of draw-off heat rates
$\mathbf{q}^{(\alpha)}$	multicomponent energy flux through the element interphase relative to the mass average velocity in phase (α)
$\mathbf{RS}(x_i, y_i)$	reaction-separation term
$\mathbf{v}^{(\alpha)}$	fluid velocity vector in phase (α)
$\mathbf{x}$	vector of liquid molar compositions
$\mathbf{z}^{\text{feed}}$, $\mathbf{p}$	molar fractions vector for feed, side draw-off streams, respectively
$\mathbf{z}^{(\alpha)}$	vector of molar fractions in phase (α)
$\mathcal{A}_i^L$	affinity of chemical reaction i
$\mathcal{D}$	normalized Damköhler number
$\mathcal{E}$	overall energy balance
$\mathcal{MC}$	component molar balances
A	availability
B	availability function
$\overline{f}$	objective function scaled with respect to utopia point
$\overline{H}_i^{(\alpha)}$	partial molar enthalpy of component i in phase (α)
Ψ_i	interfacial molar flux of component i
$\mathbf{U}$	utopia point
$\mathrm{S}^{(\alpha)}$	total entropy in phase (α)
U	total internal energy
$\tilde{y}$	integer variables
$\underline{F}^{j,V}$	total flow of stream j in the vapor phase

List of Symbols

A	heat exchange area
$A(z)$	cross sectional area at distance z
a_Ψ	interfacial area
A_{active}	active area
A_{holes}	holes area
a_i	activity of specie i
A_i, B_i, C_i	constants for component i in Antoine expression
a_{ij}, b_{ij}	constants for the pair $i-j$ in Wilson model
B	adiabatic temperature rise
B_v	volumetric bottoms flowrate
$Bias$	controller bias
c	monetary cost
$c_0 - c_6$	constants for hydrodynamic and chemical equilibrium
C_{total}	average concentration
$c_{pai} - c_{pdi}$	coefficients for heat capacity of component i
Cp	heat capacity
D	distillate flow
$d(\cdot)$	set of disturbance variables
d_i	tube internal diameter
D_v	volumetric distillate flowrate
Da	Damköhler number
dn_i	change in mole numbers of component i
E	electric field
e	controller error
E_a	activation energy
F	molar flowrate
f	dimensionless feed
f'	normalized objective function
$f(\cdot)$, $g(\cdot)$	differential and algebraic expressions respectively
F^{feed}, F^{side}	molar rates of feed and side draw-off streams, respectively
f_{econ}	economic objective function
f_{exergy}	sustainability objective function
f_{flood}	hydrodynamic constant

f_{response}	responsiveness objective function
F_c	factor related to material of construction
f_i^0	reference state fugacity of component i
$f_i^{(\alpha)}$	fugacity of component i in phase (α)
f_k	nonlinear function of the distribution coefficients
F_m	mass-based feed flow
F_{fac}	scale-up factor
f_{fr}	two-phase friction factor
$f_{m2ft}, f_{mol2kg}, f_{s2y}$	conversion factors
f_{pd}	friction constant for pressure drop
G	Gibbs free energy
$g_i^{j,(\alpha)}$	external force exerted on component i per molar unit in stream j and phase (α)
$g_j(\cdot)$	driving force of chemical reaction j based on activities
$h_{R,n}^{\text{rect}}$	enthalpy coordinate in the Ponchon-Savarit diagram for rectifying section
$h_{\text{HX}}^{(\alpha)}$	heat transfer coefficient in phase (α)
$h_{f,i}^V$	enthalpy of formation of component i in the vapor state
ht	height
ht_{space}	space between stages/compartments
InS	controller input
j	electric current density
$J_e^{i,(\alpha)}$	total flux of energy
$J_i^{(\alpha)}$	diffusion flux of component i in phase (α)
$J_m^{i,(\alpha)}$	mass flux
J_q^L	measurable heat flux into the liquid phase
$J_s^{(\alpha)}$	entropy flux in phase (α)
K	controller gain
K_{eq}	temperature-dependent chemical equilibrium constant
k_f	forward reaction rate cosntant
$k_{f,0}$	forward reaction rate constant evaluated at a reference temperature T_0
$k_{i,m}$	mass transfer coefficient of component i in mixture m
l	dimensionless liquid flowrate
l_{PFR}	length of PFR

List of Symbols

L_v	volumetric reflux flowrate
$M(\alpha)$	holdup of phase (α)
M_0^L	initial mass of liquid in the pot
MW	molecular weight; averaged molecular weight
n	total number of moles
n_{feed}	number of feed streams
n_{off}	number of side draw-off streams
n_c	number of components
$n_i^{(\alpha)}$	number of moles of component i in phase (α)
n_o	number of objective functions
n_p	number of phases in the system
n_q	number of heat streams
n_{rx}	number of chemical reactions
n_{st}	number of streams
P	absolute pressure
p^p, p^c	sets of time-varying variables
$P_{c,i}$	critical pressure of component i
q	dimensionless heat duty
$q^{(\alpha'-\alpha)}$	heat flux from phase (α') to phase (α)
Q_{cond}	condenser duty
Q_{reb}	reboiler duty
r	composition-dependent reaction rate
RR,RS	reflux and reboil ratios
S	molar entropy
$S_j^{i,(\alpha)}$	molar entropy of component j in stream i and phase (α)
S_W	auxiliary variable for phase-equilibrium model
T	temperature
T_b	boiling temperature
T_Q	temperature of the heat source/sink
$T_{c,i}$	critical temperature of component i
U	molar internal energy
u	internal energy density
$u(\cdot)$	set of input variables

U^{HX}	global heat transfer coefficient
u_{flood}	flooding velocity
u_i^{diff}	diffusive velocity of specie i
v	dimensionless vapor flowrate
V_0	initial vapor flow
v_i	molar volume of component i
V_m	mass-based vapor flow
W	work
w	vector of weighting factors
W_{cat}	amount of catalyst
x	liquid phase composition
$x(\cdot)$	set of state variables
X_i,Y_i	transformed composition variables for component i in the liquid and vapor phases, respectively
$X_{rx,j}$, X_q, X_e, $X_{m,j}$, X^{HX}	conjugated driving forces for chemical reaction, heat exchange between phases, interfacial heat diffusion, interfacial mass diffusion of component j and heat exchange with the external world, respectively
y	vapor phase composition
$y(\cdot)$	set of output variables
z	length of section
z^p, z^c	sets of time-invariant parameters
zr_i	constant of component i
h	molar enthalpy without heat of formation
$n\text{C}_4$	n-butane
$i\text{C}_4$	isobutylene
cP	product coefficient vector
cR	reactant coefficient vector
$f(\cdot)$, $g(\cdot)$, $h(\cdot)$	sets of differential, algebraic equality and inequality equations, respectively
$i(\cdot)$	set of initial conditions
$J(\cdot)$	objective function
level	level
MeOH	methanol

Subscripts and superscripts

0	standard state

cat	catalyst
col	column
ref	reference component; reference conditions
shell	shell
stack	tray stack
trays	trays
L	liquid phase
m	mass-based values
out	outlet
R	reflux stream
S	entropy-related value
V	vapor phase
in	inlet
cond	condenser
cool	cooling utility
cu	cool utility
downc	downcomer
feed	feed stream
heat	heating utility
hu	hot utility
reb	reboiler
rect	rectifying section
strip	stripping section
tubes	condenser tubes
weir	weir

Colophon

This dissertation was typeset by CPAR on a Pentium IV workstation using the latest version of LaTeX and the compiler e-TeX (`http://www.MIKTeX.org`). The input files were typed and edited using WinEdt (`http://www.WinEdt.com`) and translated into PostScript using dvips. Figures were generated with Microcal Origin and Matlab. Drawings and plots (.eps) were produced with Macromedia Flash and Visio. The postscript document was converted into portable digital file (.pdf) using Adobe Distiller with a resolution of 2400 dpi. Times package (times.sty) was used to produce the family of roman fonts. The bibliography entries were produced with Reference Manager and its bibtex.os output style. The natbib.sty package was used to produce the BibTeX bibliography file in combination with an author's customized bibliography style file (.bst). The interface makebst.tex was particularly helpful in the generation of the .bst style file. The index was generated from LaTeX .idx file using MakeIndex.

The design of the cover represents the flowsheet of a reactive distillation process for the synthesis of MTBE.

Finally, this dissertation was printed by PrintPartners Ipskamp (`http://www.ppi.nl`) in Enschede-The Netherlands with a production volume of 200 copies.